The Shade Curtain Barrier

A conceptual design for a storm surge barrier at the San Luis Pass in Galveston Bay, Texas, United States of America

M.M.J. van Schaijk

TU Delft Delft University of Technology ARCADIS TEXAS A&M UNIVERSITY

The Shade Curtain Barrier

A conceptual design for a storm surge barrier at the San Luis Pass in Galveston Bay, Texas, United States of America

by

Malou M. J. van Schaijk

to obtain the degree of Master of Science
at the Delft University of Technology,
to be defended publicly on Wednesday September 21, 2022 at 2 PM.

Faculty of Civil Engineering and Geosciences
Hydraulic Engineering

In collaboration with:

Student number:	4457218	
Project duration:	November, 2021 - September, 2022	
Thesis committee:	Prof. dr. ir. S.N. Jonkman	TU Delft
	Dr. ir. B.C. van Prooijen	TU Delft
	Dr. ir. E.C. van Berchum	Arcadis
	Dr. J. Figlus	Texas A&M University

Preface

This thesis is presented in partial fulfillment of the requirements for the degree of Master of Science in Hydraulic Engineering and has been completed at the Delft University of Technology. This report covers the study regarding a conceptual design for a storm surge barrier at the San Luis Pass in Galveston, United State of America.

I am grateful to all the people who have been involved in the process of my master thesis and especially to the members of my graduation committee. First of all, I would like to thank Bas Jonkman for being the chairman of my graduation committee, his feedback and brainstorm sessions, Bram van Prooijen for his involvement during the meetings, Erik van Berchum for his suggestions, comments and advice during this research and Jens Figlus for his participation in my thesis and guidance in Texas.

Furthermore, I would like to thank all my colleagues at Arcadis, I have always felt very welcome at the Rotterdam office during my graduation. A special thank-you goes to Piet Dircke for giving me the opportunity to visit the New Orleans storm surge barrier and to participate in a resiliency workshop in Tampa in the United States of America. I want to express my gratitude to professor Bill Merrel, Yoon-jeong Lee and the people of the research group for their hospitality and the support I received during my visit to the Texas A&M Galveston campus in the United States of America. My appreciation goes to members of the Gulf Coast Protection District and USACE Galveston District for their contribution. Additionally, I would like to thank BACPA for their financial support to make my visit to Galveston possible. I also want to thank Baukje Kothuis for making me feel at home in Galveston and for her inspiring front porch where the shade curtain barrier was first invented.

As this report not only marks the end of my graduation but also my study period, I also want to thank all my friends, (ex-)roommates and everyone I have gotten to know throughout my study time for the great time I had. Lastly, I want to thank my family, who always supported me.

I hope you will enjoy reading this report.

"Research is to see what everybody else has seen, and to think what nobody else has thought"
Albert Szent-Gyorgyi

Malou van Schaijk

Delft, September 2022

Abstract

Low-lying, densely-populated coastal areas across the world are under threat of hurricane-induced floods. This is the case in, among others, the Galveston Bay Area. In response to this threat the USACE (United States Corps of Engineers) recommended a plan to reduce the risk of flooding, through a range of measures to form a resilient coast of Texas. This plan includes a storm surge barrier at Bolivar Roads in Galveston Bay, whilst the other inlet at San Luis Pass remains open for environmental reasons. Leaving the San Luis Pass open still results in a significant rise in the water level of Galveston Bay, so finding a way to close the San Luis Pass is preferred. Therefore, this thesis researches a barrier for the San Luis Pass to contribute to a resilient Texan coast whilst also taking the local natural habitat into account. The methodology combines the concept of 'Building with Nature' and the civil engineering design method. The methodology incorporates the flood safety, ecological values, and socio-economic aspect into the design process. A conventional storm surge barrier does not fulfill all the requirements and criteria for the San Luis Pass. This research thus proposes a new, innovative type of storm surge barrier: The Shade Curtain Barrier. The shade curtain barrier functions by being rolled down in extreme conditions and stored under the bridge under normal conditions. The two main advantages are that no bottom protection is required and the view is hardly disrupted. Concluding, the shade curtain barrier is a promising solution for a storm surge barrier at the San Luis Pass to contribute to a resilient Texas coast.

Keywords: Storm Surge Barrier, Building with Nature, San Luis Pass, Resilient Solution, Shade Curtain Barrier, Flood Risk Reduction.

Summary

Many of the world's coasts have long been subject to the risk of severe storms and subsidence. In the future, coastal flood risk will likely increase further due to urban development, sea-level rise, and potential change of storm surge climatology. This research focuses on one of these areas that is at risk, specifically the Galveston Bay Area in Texas, United States of America, which is located in a hurricane-prone area, and has experienced several major hurricanes. In an effort to reduce hurricane-induced flooding around Galveston Bay, the USACE (United States Corps of Engineers) has recommended a plan to form a resilient Texas coast. In their design, the San Luis Pass remains open for environmental reasons. However, leaving this pass open could still result in a significant increase in the water level in Galveston Bay during storm surge (Texas A&M University Galveston, 2021), and thus contribute to flooding. Therefore, the main goal of this thesis is to develop a conceptual design for the storm surge barrier at the San Luis Pass in Texas, United States of America whilst also taking the local natural habitat into account.

The Galveston Bay is a semi-enclosed basin that contains both fresh and salt water, and is a micro-tidal region. The exchange of water between the Gulf of Mexico and Galveston Bay is primarily (80%) through the Bolivar Roads. As a result, most research and design regarding local flood risk has been focusing on this inlet. The water exchange through the Rollover Pass is negligible, meaning the San Luis Pass contributes the resulting 20%. Surprisingly, a storm surge barrier for the San Luis Pass has not yet been investigated, even though previous research showed that leaving the San Luis Pass open still results in a significant rise in the water level of Galveston Bay (Texas A&M University Galveston, 2021). The location of the San Luis Pass is west of Galveston Island. A bridge connects Galveston Island to Follets Island and functions as an evacuation route. This bridge over the San Luis Pass is in a poor state and needs to be replaced in the near future. Inland of the San Luis Pass is the Brazoria National Wildlife Refuge, home to species of birds and fish, and vegetation. The San Luis Pass itself is an extremely dynamic pass in terms of sediment transport, and includes areas of quicksand. Therefore, swimming is prohibited.

Figure 1: Galveston Bay Area, including key inlets and locations (after (TSHA Texas State Historical Association, 2017))

In the case of a hurricane, the hurricane path determines the effects of leaving the San Luis Pass open. In fact, it depends on the landfall location of the hurricane eye. During a hurricane, wind directions can change rapidly. As the storm surge height and flow direction depend on the wind direction, this can also change rapidly. Closing the San Luis Pass in addition to the proposed plan of the USACE could lead to extra reduction of the water level in Galveston Bay. For a hurricane similar to Hurricane Ike, the reduction of peak surge elevation is around 1.6 m (5.2 ft) at the west end of Galveston bay, 0.5 m (1.5 ft) at the City of Galveston, and 0.4 m (1.3 ft) at Galveston Bay. Note that the sea level in the area is expected to rise 75 cm (2.5 ft) by 2060 (in the scenario of the upper bound of the observation-based extrapolations), this is relatively high compared to other parts of the United States of America (Sweet et al., 2022). Therefore, a storm surge barrier at San Luis Pass contributes to the resilient Texas coast plan of the USACE and could be an integral part of a coastal spine.

A new methodology is used for the design of this storm surge barrier at the San Luis Pass. This methodology combines the civil engineering design method and the 'Building with Nature' concept. This resulted in adding an analysis of the integrated system before the functional specification, leading to flood safety, ecological values, and socio-economic aspects in the requirements of the storm surge barrier. Regarding flood safety, the design storm is a 1/100 year storm. In normal conditions, the sandy bottom surface is at 1 m (3.3 ft) below the mean sea level, with a tidal amplitude of 0.35 m (1 ft), and a significant wave height of 0.5 m (1.6 ft). The five influencing factors of the environment are the tidal range, tidal prism, change in intertidal area, salinity, and sediment transport. Each influence factor is linked to the reduction in flow area in the San Luis Pass. The tidal range reduction is approximately $\frac{2}{3}$ of the reduction in flow area at the San Luis Pass. The tidal prism reduction is proportional to the reduction in flow area at the San Luis Pass. A 60% reduction of the flow area at the San Luis Pass results in a 35% reduction of intertidal area. The salinity is not effected by a reduction in flow area at the San Luis Pass. There is no net sediment transport through the San Luis Pass. The socio-economic requirement for the San Luis Pass is that it creates no bigger view-disruption than the disruption already present as a result of the bridge. This makes a combined design of the barrier and the bridge preferable.

Next, a solution is developed for the San Luis Pass. A storm surge barrier is preferred in this area to keep the exchange of water under normal conditions for environmental reasons, whilst being able to close the inlet during a hurricane. Around the world, several storm surge barriers are in use, which can be divided into seventeen concepts. The functional requirements in this case leave only six potential concepts for a storm surge barrier at the San Luis Pass, mostly due to remaining flow area and large water level difference. The position of the storm surge barrier under normal conditions is an important aspect that determines whether there is an open view. To avoid visual disruption the barrier can be stored above or below water. The remaining six options are divided into four stored above water and two stored below. The four options stored above water (vertical lifting gate, visor gate, caisson structure and segment gate), require a fixed bottom and disrupt the view. The two options stored below water (bear trap gate and parachute barrier) are sensitive to sedimentation and difficult in maintenance. In conclusion, no optimal solution is found for the San Luis Pass within the conventional storm surge barrier designs.

Therefore, this research proposes a new type of storm surge barrier: The Shade Curtain Barrier. The shade curtain barrier operates as a window shade curtain (much like a roller blind), it is connected to the bridge deck, rolls down during a hurricane, and can be stored under the bridge in normal conditions. Two possible variations of this idea resulted in the design of the shade curtain barrier. This design would be optimal for the San Luis Pass, the final design is illustrated in Figure 2. The design has a minimum impact on the ecosystem, sedimentation, and landscape at the San Luis Pass. Because under normal conditions, it does not affect the flow area. The two main advantages are that no bottom protection is required, and the view is hardly disrupted in normal conditions. The shade curtain barrier consists of a flexible membrane fabric, sinker, cable, and rotating axis. The flexible membrane fabric has two functions: it prevents the water from flowing into the Galveston Bay, and it protects against piping as it functions as geotextile that increases the seepage length. The flexible membrane fabric is already available, can withstand the forces during a design storm, and can be opened under negative head. The sinker keeps the flexible membrane fabric at the bottom surface, and the cables prevent it from moving. The rotating axis stores the flexible membrane fabric beneath the bridge under normal conditions and can adjust the required length under hurricane conditions.

The structural verification identified and analyzed several potential failure mechanisms for this barrier. The possible failure mechanisms for the shade curtain barrier include piping, sinker uplift, flexible membrane fabric damage/uplift/erosion, rotational axis failure, bridge failure, gate failure, and connection failure. Due to the early design stage, the failure mechanisms (damage to the flexible membrane fabric, failure of the rotational axis, failure of the bridge, and failure of one of the shade curtain barrier gates) are not elaborated upon further. However, the forces on the bridge under the governing hurricane can already be estimated. The governing hurricane is a 1/100-year hurricane. Resulting in a force of 470 kN/m at 45 degrees at the West Bay side bridge deck. The anchor must withstand 470 kN/m of horizontal force. The horizontal length of the flexible membrane fabric prevents piping. The laboratory experiment shows that the flexible membrane fabric and bridge piles must be waterproofed. Otherwise, the probability that scour and piping causes structural failure is significant. Laboratory experiments reveal that horizontal cables reduce the probability of structure failure due to uplift and erosion under the flexible membrane fabric. Compared to an angled cable, the sinker's weight (and size) is reduced as well. Therefore, the final design for the storm surge barrier at the San Luis Pass consists of horizontal cables and a minimum 12 m length of flexible membrane on the bottom, illustrated in Figure 2.

The shade curtain barrier minimizes the unwanted effects regarding a storm surge barrier at the San Luis Pass because, under normal conditions, it does not affect the flow area. Therefore, neither the tidal range nor the intertidal area will be effected. In addition, sediment can move freely because there is no requirement for bottom protection or a rigid closure structure. The shade curtain barrier is not visible under normal conditions because it is stored beneath the bridge and it decreases the risk of flooding during a hurricane. Therefore, this design has a minimal impact on the ecosystem, sedimentation, and landscape at the San Luis Pass.

At this moment additional research is recommended regarding the exact connection between the vertical piles and flexible membrane fabric, the ideal curvature and the load distribution of the shade curtain barrier under hurricane conditions. Overall, the shade curtain barrier is a promising solution for a storm surge barrier at the San Luis Pass to contribute to a resilient Texas coast.

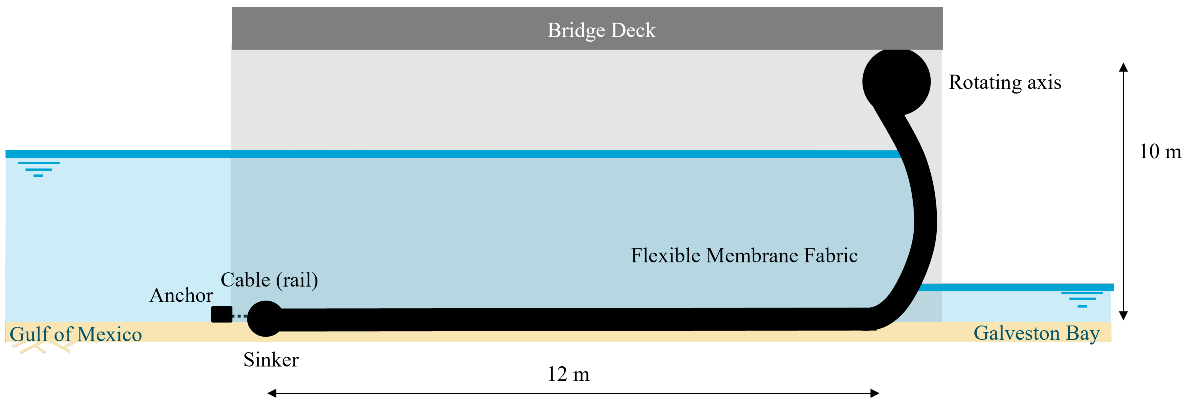

Figure 2: The Shade Curtain Barrier

Table of content

1 Introduction

1.1 Motivation of Research

Many of the world's coasts have long been subject to the risk of severe storms and subsidence. In the future, coastal flood risk will likely increase due to urban development, sea-level rise, and potential change of storm surge climatology. Houston is a metropolitan area in the Galveston Bay region along the upper coast of Texas in the United States of America, shown in Figure 1.1. This is a hurricane-prone area. The Houston metropolitan area is the fifth most populous in the United States of America, with a population of 7.15 million in 2020 (Duran et al., 2021). The Houston metropolitan region is economically important, with a nominal gross area product of $512.2 billion in 2019 (Duran et al., 2021). According to the International Monetary Fund, Houston's GDP would rank 24th in the world if it was a country, even larger than Poland and Nigeria (Greater Houston Partnership Research, 2017).

The Galveston Bay Area is vulnerable to coastal and pluvial floods due to its large population, economic importance, and low-laying location. In the past, hurricanes caused extreme storm surge at Galveston Bay, resulting in extensive damage. For example, in 2008 Hurricane Ike caused a storm surge of 3-4 m in Galveston Bay, resulting in roughly $100 billion dollars worth of damage and over 100 deaths (Rego and Li, 2010). In 2017 Hurricane Harvey caused 150-180 billion dollars in economic damage and over 75 deaths due to heavy rainfall induced flooding (Sebastian et al., 2017). Figure 1.2 shows the physical factors directly contributing to coastal flood exposure. During this research, these physical factors must be considered. By 2050, the expected relative sea level will cause tide and storm surge heights to increase and will lead to a shift in U.S. coastal flood regimes, with moderate and major high tide flood events occurring as frequently as minor and moderate high tide flood events occur today. Without additional risk-reduction measures, U.S. coastal infrastructure, communities, and ecosystems will face significant consequences (Sweet et al., 2022).

Figure 1.1: Galveston Bay Area, including key inlets and locations (after (TSHA Texas State Historical Association, 2017))

In an effort to reduce hurricane-induced coastal flooding in the densely populated areas surrounding Galveston Bay, much time and effort is put into researching, developing, and comparing bay-wide flood risk reduction strategies, including a variety of levees, storm surge barriers, nature-based solutions, and smaller inland measures. Storm surge barriers are normally used to protect urban settlements and infrastructure that are heavily affected by storm surges and sea flooding. When it comes to a potential coastal storm surge barrier at the Galveston Bay Area, most attention is on the large inlet, Bolivar Roads, which should remain a crucial shipping lane. The shipping lane is a channel from the Gulf of Mexico to the port of Houston. The port of Houston is the largest on the Gulf Coast and the world's second-largest petrochemical complex (Port of Houston, 2021).

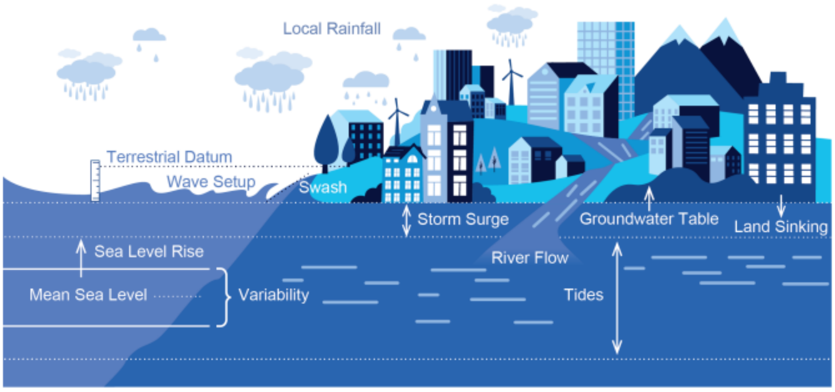

Figure 1.2: Physical factors directly contributing to coastal flood exposure (Sweet et al., 2022)

A smaller entrance, San Luis Pass, is located on the west side of Galveston Island, illustrated in Figure 1.1. This inlet connects the Gulf of Mexico to Galveston Bay through the West Bay. The San Luis Pass is responsible for 20% of Galveston Bay's tidal exchange (Lester and Gonzalez, 2011). The San Luis Pass has an essential ecological role in the West Bay's wetlands preservation. Furthermore, an important highway and evacuation route runs across the San Luis Pass that connects Galveston and Follets Island. A lot of research has already been done on how to protect the Galveston Bay Area against coastal floods. These previous studies focused mostly on the east of the area, particularly Bolivar Roads, as depicted in Figure 1.1. This study focuses on the San Luis Pass, which is located to the west of Galveston Island.

In order to be resilient for the future and keep the important ecological function of the wetlands whilst aiming to introduce a storm surge barrier at the San Luis Pass, the building with nature philosophy is introduced. The building with nature philosophy is the result of a changed perspective from building in nature through building of nature to building with nature (Van Koningsveld and Van Raalte, n.d.). Building with Nature for this thesis is defined as: *'Shifting from focusing on a single object to looking at the entire system, and working to design an object that becomes a part of the system'*, explained in Appendix B.1.

1.2 Previous Research

The United States Army Corps of Engineers (USACE), Texas A&M University, and Delft University of Technology, among others, conducted extensive flood protection research in the Houston-Galveston Bay Area. Many alternative barriers are investigated, but all research focused on the Bolivar Roads, whilst the San Luis Pass has yet to be looked at. The USACE recently released a recommended plan for the Galveston Bay coast. This plan consists of a barrier at Bolivar Roads, whilst leaving the San Luis Pass open (Army Corps of Engineers - Galveston District (US), 2021). Following, Texas A&M University investigated the consequences of closing Bolivar Roads whilst leaving the San Luis Pass open during an extreme event (Texas A&M University Galveston, n.d.), described in Section 1.3.

De Boer (2015) investigated integrating building with nature to flood risk reduction solutions in Galveston Bay. According to his findings, building with nature solutions and hard flood protection structures should be built alongside each other to significantly reduce flood risk (de Boer, 2015). That these two disciplines can be combined in a single flood protection structure was already touched upon in the Eastern Scheldt Barrier design. The Eastern Scheldt Barrier was built with vertical lifting gates instead of a dam as part of the Delta Works in the Netherlands for environmental reasons. Previous research of the Eastern Scheldt Barrier's effects still revealed that the estuary developed 'sand hunger,' and large scour holes. A more optimal combination of hard flood protection and building with nature is thus desired.

1.3 Problem Analysis

The USACE plan for a more resilient Texas coast includes multiple coastal storm risk management and ecosystem restoration features (Army Corps of Engineers - Galveston District (US), 2021). The plan includes a storm surge barrier at Bolivar Roads, east of Galveston, and an open San Luis Pass. The Bolivar Roads storm surge barrier consists of two double floating sector gates at the location of the shipping lane, a number of vertical lift gates for environmental reasons, a flood wall, and smaller locks for recreational vessels. According to the USACE's recommended plan, the San Luis Pass will remain open because the relatively low importance of developed areas to the west of Galveston Bay do not justify the environmental impacts of constructing a barrier in the pass, and it does not contribute to adequate storm surge reduction.

However, leaving the San Luis Pass open results in a higher peak surge (Texas A&M University Galveston, n.d.), which can lead to more damages in the western part of the Galveston Bay. Specifically, an open San Luis Pass would result in an increased peak surge elevation of 1.50-1.65 m at the west end of Galveston bay, 0.45-0.6 m at the City of Galveston, and 0.3-0.45 m at most places in Galveston bay for a hurricane similar to Hurricane Ike. The impact would be even greater if the hurricane's path was more to the west, even with a storm surge barrier present at Bolivar Roads in both cases. Figure 1.3 and 1.4 respectively show the peak surge height in Galveston Bay with and without a barrier at the San Luis Pass for a hurricane similar to Hurricane Ike. Note that both figures provide the peak surge elevation in feet.

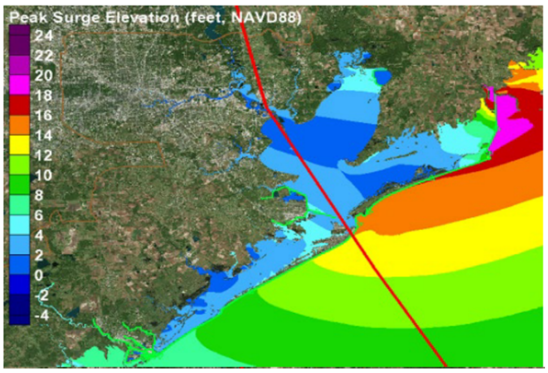

Figure 1.3: Peak Surge height of Hurricane Ike, with a barrier at Bolivar Roads and San Luis Pass (Texas A&M University Galveston, n.d.)

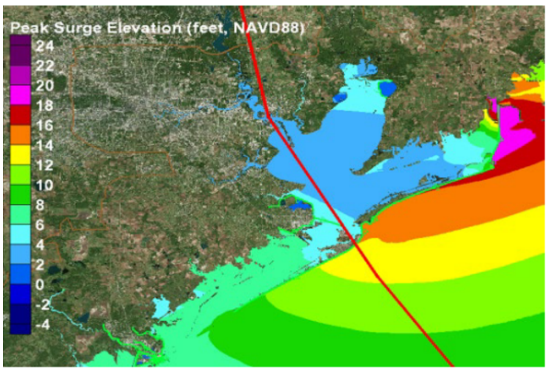

Figure 1.4: Peak Surge height of Hurricane Ike, with a barrier at Bolivar Roads and without a barrier at San Luis Pass (Texas A&M University Galveston, n.d.)

The water level in Galveston Bay rises days before a hurricane eye makes landfall due to a forerunner, leading to a gradual rise of the water surface elevation in the days leading up to the hurricane eye making landfall (Texas A&M University Galveston, n.d.). This process results in a water level elevation of 1 m higher in the West Bay and 0.2 m higher in Galveston Bay 12 hours before landfall of the hurricane

eye without a barrier at San Luis Pass for a hurricane similar to Hurricane Ike (Texas A&M University Galveston, n.d.).
In addition, sea level rise and subsidence predictions for the future result in a larger difference between the peak surge height with and without a barrier at San Luis Pass than shown respectively in Figures 2.15 and 2.16. In the case of SLR RCP8.5, Galveston and Texas City will already be flooded with a storm surge of 0.5 m in 2100 if no changes are made to the current coastline protection (Miller and Shirzaei, 2021). As a result, leaving the San Luis Pass open undermines the effectiveness of the coastal protection of the USACE (Texas A&M University Galveston, 2021), one of the potential solutions is to close the San Luis Pass as well.

However, the San Luis Pass serves an important ecological purpose in preserving the wetlands that surround the West Bay. Furthermore, a major highway that connects Galveston Island to the mainland currently runs across the San Luis Pass, making it a vital evacuation route. The building with nature philosophy is being implemented in order to be future-proof and maintain the important ecological function of the wetlands. The building with nature philosophy means that the requirements of the local ecology are considered in all aspects of the design.

Closing the San Luis Pass directly benefits the reduction in damage and cost avoidance that result from the ability to reduce design water levels and wave conditions for all in-bay second lines of defense and non-structural measures, which reduces the required extent of strength, height, and cost of all in-bay measures (Texas A&M University Galveston, 2021). Another aspect considered is the need for the State of Texas to replace the bridge over San Luis Pass. This could be an excellent time to investigate the feasibility of combining a bridge and a storm surge barrier at San Luis Pass. In summary, the Galveston Bay Area faces the challenge of implementing optimal flood risk reduction measures whilst minimizing the corresponding unwanted effects of these measures on the area.

1.4 Research Objective and Question

The main objective of this research is to develop a conceptual design for a storm surge barrier at the San Luis Pass that is designed in accordance to the building with nature philosophy in order to minimize the associated environmental impacts. In normal conditions, a storm surge barrier is open; however, in the event of a storm surge, it is closed. The design should be a storm surge barrier that minimizes the corresponding unwanted effects on the ecosystem, sedimentation, and landscape under normal conditions. And maximizes flood risk safety under hurricane conditions. In order to obtain the research objective of this thesis, the research question is:

How can a storm surge barrier be designed such that it is connected to the San Luis Pass bridge and has minimal impact on the ecosystem, sedimentation, and landscape?

1.5 Methodology and Report Structure

The methodology of this research is the 'Building with Nature' method adjusted with the traditional civil engineering design method. These adjustments are starting with the exploration of the problem and specify the program of requirements and boundary conditions. These adjustments are made to incorporate the specific aspects of hydraulic structures into the 'Building with Nature' method. Figure 1.5 shows the design steps of this thesis. The colored circles represent Building with Nature design steps, explained in Appendix A.3. The gray circles represent the civil engineering design method, explained in Appendix A.1 and A.2.

This research's methodology consists of seven steps, each of which is described briefly. The first step of this methodology is to investigate the problem. The second step is to understand the system (physical, ecological, and societal) under both normal and extreme conditions, in addition to an exploration of the problem. The third step is the functional specifications. This includes the boundary conditions and requirements, which lead to criteria for the storm surge barrier that include both nature and human values. The fourth step is to identify the alternatives that use or provides values for nature and human. The fifth step is the evaluation of each alternative to select an integral solution. The sixth step is the refinement of the solution. The evaluation has identified areas where the solution could be refined to become more integrated into the environment. The seventh and final step is preparation for implementation of the concept.

The structure of the report is as follows, Chapter 1 is the introduction, aligned with step 1 of the methodology, the problem analyses. Chapter 2 is the system analyses, which is formed by the execution of step 2 of the methodology. Chapter 3 provides the program of requirements and boundary conditions, which is formed by the execution of step 3 of the methodology. Chapter 4 is the generation, verification, and evaluation of the conventional storm surge barriers, which is the result of the implementation of step 4 and 5 of the methodology. Resulting in Chapter 5, the introduction of a new concept for a storm surge barrier. This chapter generates, evaluates and discusses the new concepts, which is the result of the implementation of step 4 and 5 of the methodology. Chapter 6 provides an optimized concept of the new storm surge barrier. This chapter is the implementation of steps 5 until 7 of the methodology. Resulting in the final design for the storm surge barrier at the San Luis Pass. Chapter 7 discusses this research design approach. Finally, Chapter 8 provides the conclusion and recommendation of this research. This is illustrated in Figure 1.5.

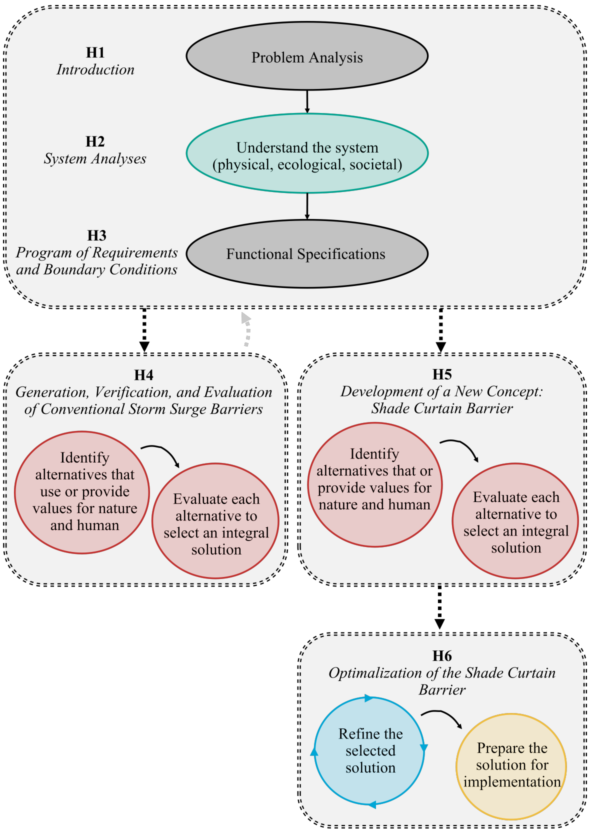

Figure 1.5: Methodology and structure of the report. The colored circles represent the corresponding Building with Nature design steps and the gray circles represent the civil engineering design method.

2
System Analysis

The San Luis Pass is located in the Galveston Bay Area in Texas, United States of America. More precisely it is located at the east side of Galveston Island. The Galveston Bay system is the seventh-largest estuary in the US, with about 153,000 ha of open water and 44,000 ha of estuaries, salt and brackish marshes. The bay is close to the Houston metropolitan area. As a result, industrial and municipal development, pollution, and wastewater effluent discharge, channelization and dredging projects, subsidence, and changes in bay-water circulation dynamics have all had a significant impact on the estuary. This region is particularly well-known as a global hub for the shipping and petrochemical-refining industries (Warren Pulich, 2007).

This chapter is structured as follows, Section 2.1 describes the history of Galveston Bay, including previous hurricanes. Section 2.2 describes the present system under normal and extreme conditions. Section 2.3 describes the future of Galveston Bay regarding flood protection, including the sea level rise and subsidence. Section 2.4 describes the consequences of leaving the San Luis Pass open, including water level height and economics. Section 2.5 explains the politics in the United States of America regarding flood defenses. Section 2.6 points out the main stakeholders for the San Luis Pass area. Section 2.7 summarizes the main values of the San Luis Pass system. This chapter corresponds to the second step in the methodology.

2.1 History of Galveston Bay

Galveston Island was created 5,000 years ago by a long-shore current that deposited sediments and generated a sandbar. Another sandbar, now known as the Bolivar Peninsula, was created 2,500 year ago. Galveston Bay developed behind these barrier islands. The first known map of Galveston Bay is a French map from 1721. Around 1800 the Galveston Bay Area made the transition from a food source to a place of settlement and colonization. In 1822 Galveston Bay became an important strategic place to trade goods, due to the easy water transport for steamboats. Therefore, Galveston and Houston became prominent cities in 1836. In 1880 Galveston was the largest city in Texas with 22,248 inhabitants. For reference, Houston had 16,513 inhabitants and was the third-largest city (Galveston Bay Foundation, 2013).

In 1900 many of the Galveston Island businesses relocated inland due to a major hurricane devastating Galveston, leading to an estimated 6,000 casualties. In 1908 the Houston Ship Channel was completed, a 5.5 m deep channel and a turning circle. As ships became bigger and bigger, the channel was deepened to 7.5 meters in 1914. Additionally, a dike was constructed to protect the channel. This dike had a significant impact on the ecology of the West Bay. In 1919 the first oil refinery was constructed on Goose Creek. The start of various oil and chemical companies around Galveston Bay. The area was very popular because of the deep water channels and ports, wide open spaces, underground sources of fresh water and general lack of regulations. Around 1919 the water quality in Galveston Bay dropped, the water became increasingly oily and fish died. In 1969 a National Environmental Policy Act and together environmental impact statements (EIS) for large projects were made. In 1987, forty individuals became the charter members and incorporates of the Galveston Bay Foundation, a new environmental nonprofit corporation focused on the interests of Galveston Bay (Galveston Bay Foundation, 2013). Figure 2.1 illustrates the Galveston Bay Area and highlights the most significant historical landmarks.

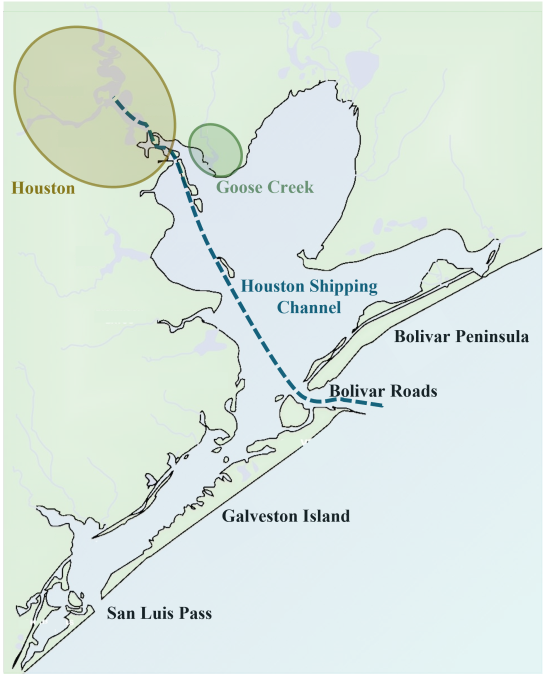

Figure 2.1: Galveston Bay Area

Previous events and consequences

Galveston Bay has experienced a lot of hurricanes in its history. In the past years, there were two hurricanes that had a large impact on the surrounding of Galveston Bay. These hurricanes are: Hurricane Ike (2008) and Hurricane Harvey (2017), respectively, described below. The causes of the large impact both hurricanes had are distinct. Hurricane Ike due to a high storm surge along the coast, and Hurricane Harvey due to extreme rainfall.

Hurricane Ike (2008)

In September 2008 Hurricane Ike made landfall as a strong category 2 hurricane, with a storm surge of 3-4 m around Galveston Bay (Rego and Li, 2010). Hurricane Ike severely damaged the San Luis Pass. The maximum recorded high watermarks at Galveston Bay were nearly 6 m high (Irish et al., 2011). Hurricane Ike caused extensive damage (around $100 Billion dollars) and over 100 deaths and at the coasts of Texas and Louisiana, wind speeds of 230 km/h were recorded (Rego and Li, 2010). Hurricane Ike also had major impact on the wetlands in Brazoria National Wildlife Refuge. After Hurricane Ike, vegetated wetland areas decreased ("Wetlands Communities in the Galveston Bay area", n.d.).

Hurricane Harvey (2017)

In August 2017 Hurricane Harvey made landfall at San Jose Island, Texas. Hurricane Harvey was a category 4 hurricane with maximum winds speeds op 209 km/h (Sebastian et al., 2017). The highest total water level was 3.7 m at Aransas Wildlife Refuge (Sebastian et al., 2017). Hurricane Harvey caused heavy rainfall in the Houston Galveston Bay Area, 1016 mm in 48 hours (Sebastian et al., 2017). The damage of Hurricane Harvey was between 150-180 billion dollars in addition to over 75 deaths (Sebastian et al., 2017). After Hurricane Harvey, homes in Houston damaged by water suffered losses of $65,000 per home (American Flood Coalition et al., 2020). Hurricane Harvey also had an effect on the estuaries' salinity. The estuary salinity had a recovery time of 2 months after Hurricane Harvey (Du and Park, 2019).

2.2 Present System

2.2.1 Galveston Bay under Normal Conditions

This section describes the current system of the Galveston Bay and San Luis Pass. The Galveston Bay Area is located at the upper Texas coast. Figure 1.1 shows the Galveston Bay Area, this is a coastal barrier system. A coastal barrier system consists of bays, barrier islands and tidal inlets and deltas fringing the mainland coast (Oertel, 1985). Galveston Bay is a bay that is connected to the Gulf of Mexico and has three rivers ending in the bay. These rivers are: San Jacinto River, Trinity River and Buffalo Bayou/Houston Ship Channel. The San Jacinto river contributes a median annual fresh water flow into the bay of about 616.5 m^3 and the Trinity River of 9,247.5 m^3 (Warren Pulich, 2007). The estuary is a semi-enclosed basin that contains both fresh and salt water.

Between Galveston Bay and the Gulf of Mexico, two barrier islands are located: Galveston Island and Bolivar Peninsula. Galveston Island is a significant tourist and commercial area on the Gulf of Mexico. On the east side of Galveston Island is the Bolivar Roads Pass, and on the west side is the San Luis Pass. Bolivar Peninsula is a smaller community, that until 1930 used the beach as a highway.

Three inlets connect the Galveston Bay with the Gulf of Mexico between the barrier islands, namely: Rollover Pass, Bolivar Roads and San Luis Pass. The Rollover Pass has a width of approximately 60 m and the influence on the tidal range in Galveston Bay is negligible (Lester and Gonzalez, 2011). The Bolivar Roads has a width of approximately 3 km and has an 80% tidal influence on Galveston Bay (Lester and Gonzalez, 2011). The Bolivar Roads is the main shipping lane for the Port of Houston. The San Luis Pass has a width of approximately 1 km and has a 20% tidal influence on Galveston Bay (Lester and Gonzalez, 2011). More recent research shows that the San Luis Pass is responsible for 18% of the inflow-outflow transport. (Salas-Monreal et al., 2018). Tidal inlets facilitate the flow of water between bays and the ocean. Therefore, the inlets often have complex dynamics with strong varying parameters, like sediment grain size and water velocity (Ramon-Duenas et al., 2021). Friction and inertia in the Galveston Bay can be neglected, so the water levels inside the Galveston Bay are roughly equal at a single moment in time (Jonkman et al., 2013). Therefore, the small-basin approximation holds.

The San Luis Pass is a tidal inlet at the west end of the West Bay, shown in Figure 1.1. As mentioned, the inlet is extremely dynamic. The strong tidal current has several victims each year, including fishermen and kayakers (Chen, 2015). As a result, it is prohibited to swim. The Galveston West Bay behind is a very shallow area, so much so you can walk across. It is largely made up of mud flats and sandbanks that migrate though the bay. This part of the system consists of a lot of loose sediments. The area around the San Luis Pass is a quicksand area. Quicksand is ordinary sand that is so saturated with water that the friction between sand particles is reduced, making them unable to support any weight. The real danger of quicksand is that you can get stuck in it when the high tides come up (Khaldoun et al., 2005).

2.2.2 Galveston Bay under Extreme Conditions

Hurricanes are the main cause of extreme storm surges in Galveston Bay. The location of landfall of the hurricane influences the local wind set-up within a semi-enclosed basin (which is representative of the Galveston Bay). Hurricanes making landfall west of a bay will force water into the system, increasing the surge (Stoeten, 2013). Figure 2.2 shows how the landfall side of a hurricane influences the local wind set-up in a semi-enclosed basin. Therefore, a hurricane on the west side of the bay will increase the wind set-up. In 2017 Hurricane Harvey was on the west side of the bay, leading to a high storm surge and extreme rainfall.

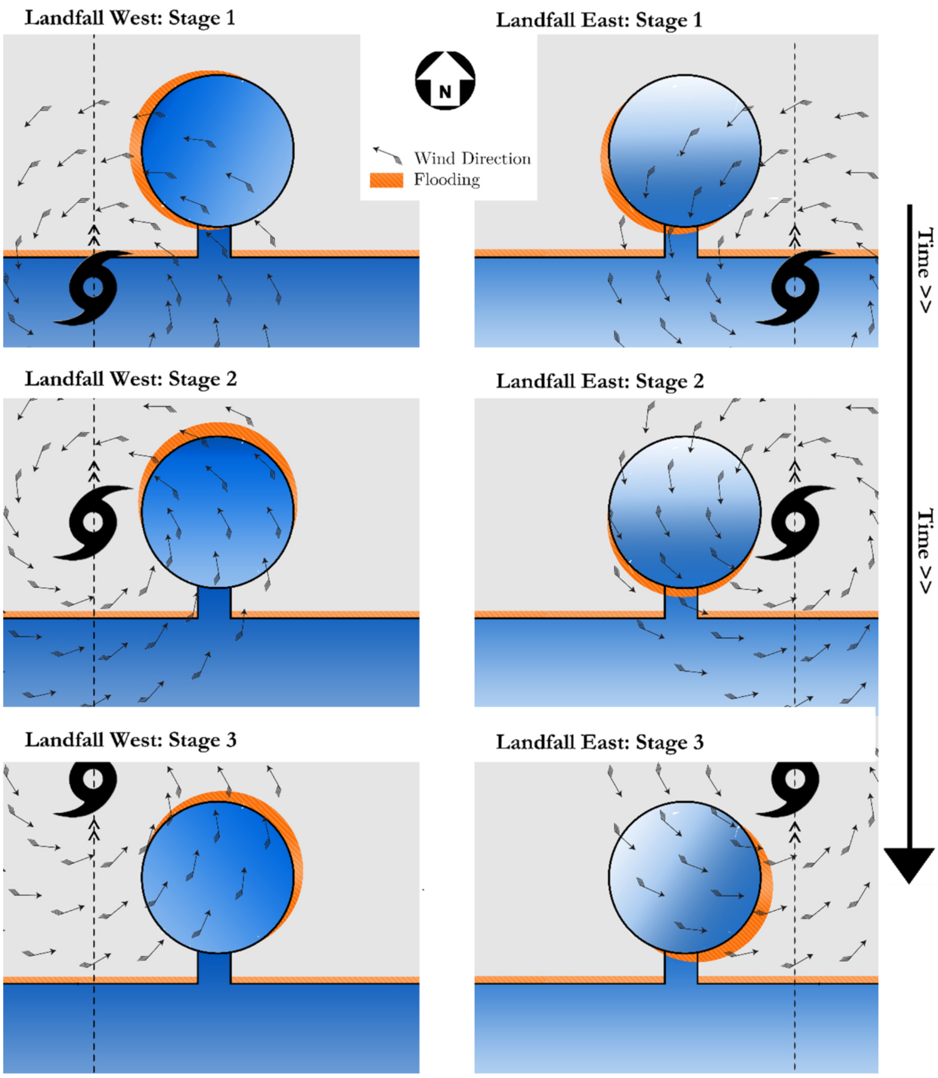

Figure 2.2: Influence landfall location with local wind set-up in semi-enclosed bays (Stoeten, 2013)

The strength and potential impact of a hurricane is categorized on a scale of 1 to 5. Table 2.1 shows the storm surge height and wind speeds corresponding with the hurricane category.
Figure 2.3 shows the area that is effected by which hurricane category. Figure 2.4 is more zoomed in at Galveston Island and the San Luis Pass. Concluding, the area behind San Luis Pass is already flooded by a category 1 surge.

Category	Wind Speed [kph]	Storm surge [m]	Damage
1	119 - 153	1.2 - 1.5	***Minimal***: No real damage to buildings. Damage to unanchored mobile homes. Several damage to poorly constructed signs. Several coastal flooding and minor pier damage. Example: Cindy and Ophelia in 2005
2	154 - 177	1.8 - 2.4	***Moderate***: Several damage to building roofs, doors, and windows. Considerable damage to mobile homes. Damage to piers from flooding. Small craft in unprotected moorings may break their moorings. Several trees blown down. Evacuation of some shoreline residences and low-lying areas required. Example: The perfect storm in 1991 and Hurricane Isabel in 2003.
3	178 - 209	3 - 4	***Extensive***: Several structural damage to small residences and utility buildings. Large trees blown down. Mobile homes and poorly built signs destroyed. Flooding near the coast destroys smaller structures with larger structures damaged by floating debris. Terrain may be flooded well inland. Evacuation of low-lying residences within several blocks of the shoreline may be required. Example: Dennis, Katerina, Rita and Wilma in 2005
4	210 - 249	4 - 5.5	***Extreme***: More extensive failure on non-bearing, exterior walls with some complete roof structure failure on small residences. Major erosion of beach areas. Terrain may be flooded well inland. Massive evacuation of residential areas as far inland as 10 km may be required. Example: Galveston Hurricane of 1900
5	>249	>5.5	***Catastrophic***: Complete roof failure on many residences and industrial buildings. Several complete building failures with small utility buildings blown over or away. Flooding causes major damage to lower floors of all structures near the shoreline. Massive evacuation of residential areas on low ground within 5 to10 mi (8 to 16 km) of the shoreline may be required. example: Andrew in 1992.

Table 2.1: Explanation of Saffir-Simpson hurricane scale

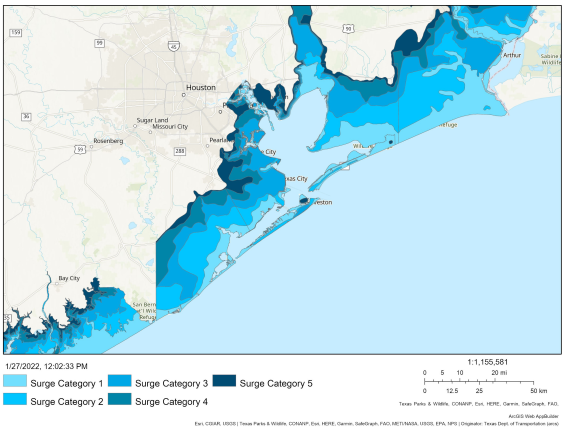

Figure 2.3: Indication of Surge Category at Houston-Galveston Area

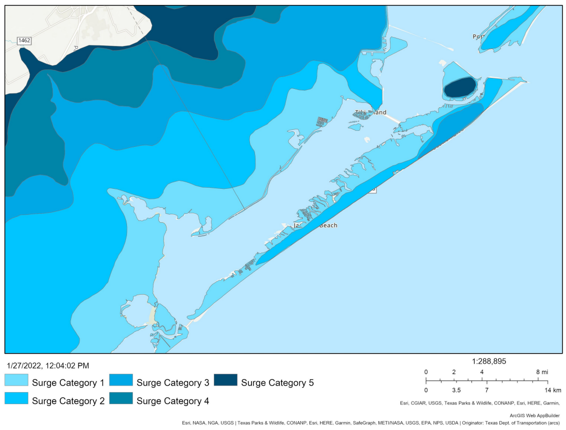

Figure 2.4: Indication of Surge Category at Galveston Island

2.2.3 San Luis Pass under Normal Conditions

Under normal conditions, the San Luis Pass is an inlet with a wide beach on the east side and residences on piles on the west side of the embankment. The four main factors that influence the San Luis Pass morphology and surroundings are briefly explained. These four components are: tides and currents, wind, sediment transport, and the bridge.

Tides and Currents

The Galveston Bay Area is a micro-tidal region, were the major diurnal tide ranges is from 0.15 to 0.5 m during non-hurricane seasons (Huang et al., 2021). The tidal influence of the San Luis Pass on Galveston Bay is around 20% (Lester and Gonzalez, 2011). Maximum current velocities vary between 0.6 and 1 m/s during a diurnal tidal cycle (Ramon-Duenas et al., 2021). A shear current dominates the San Luis Pass, resulting in a lateral sediment transport. Figure 2.5 shows tide predictions at the San Luis Pass.

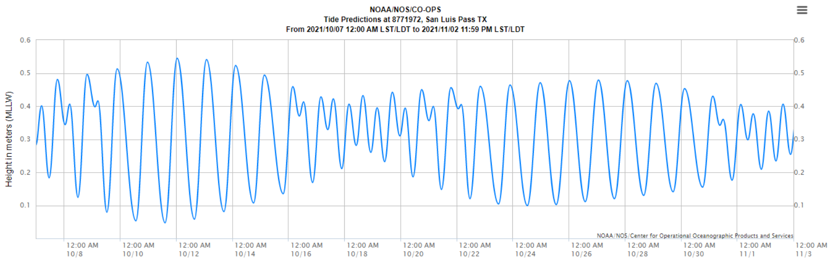

Figure 2.5: Tide predictions at San Luis Pass

Water level difference between San Luis Pass and the middle of West Bay

The way in which water levels vary in areas behind the San Luis Pass is relevant for analyzing the effectiveness of a possible storm surge barrier at the pass. An analysis of the current relation exists, comparing water levels at the San Luis Pass to those at Jamaica Beach. Figure 2.6 shows the water levels in January 2020 at San Luis Pass and Jamaica Beach in January 2020. Figure 2.7 shows the location of the measurement points in the West Bay. Figure D.9, in Appendix D.4, shows the water levels in the first semester of 2021 at the San Luis Pass.

Figure 2.6 is obtained from the data of NOAA (noaa, n.d.). This consists of the water level every 6 minutes. From these measurements, the average water level at San Luis Pass in January 2020 is 1.29 m and at Jamaica Beach 1.04 m. The time difference of the water level pattern is 180 minutes. This is estimated by comparing different time shifts.

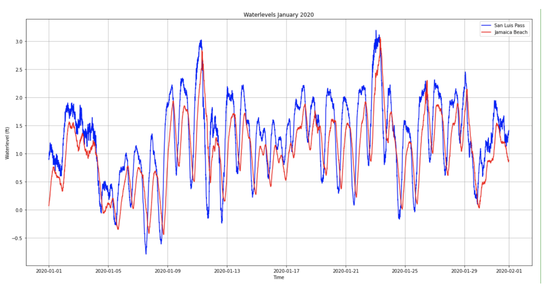

Figure 2.6: Water level at San Luis Pass and Jamaica Beach in January 2020

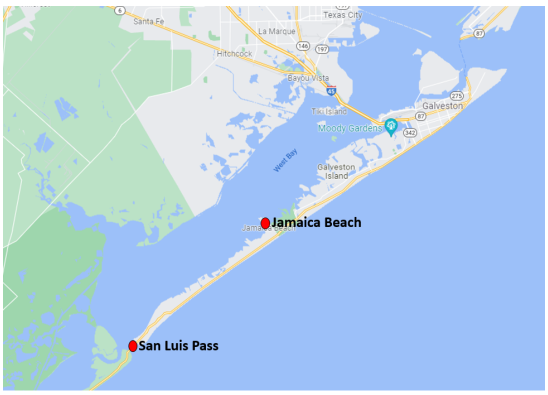

Figure 2.7: Locations of water level measurement points in the West Bay

Wind

The direction of the wind plays an important role in the flow direction through the Galveston Bay and San Luis Pass. Figure 2.8 shows the effect on the flow direction of four different wind directions though the Galveston Bay (Salas-Monreal et al., 2018). This figure shows that with north-eastern and north-western wind, there is a water outflow through the San Luis Pass. With a south-eastern and south-western wind, there is a water inflow through the San Luis Pass. A wind speed of 10 m/s is simulated in this figure.

Wind causes wind set up in the bay. Wind set up can have serious consequences for surrounding areas, such as submersion and flooding (Paugam et al., 2019). In case of a hurricane, there are strong wind speeds. Therefore, winds are expected to play an important role in the local dynamics (Salas-Monreal et al., 2018).

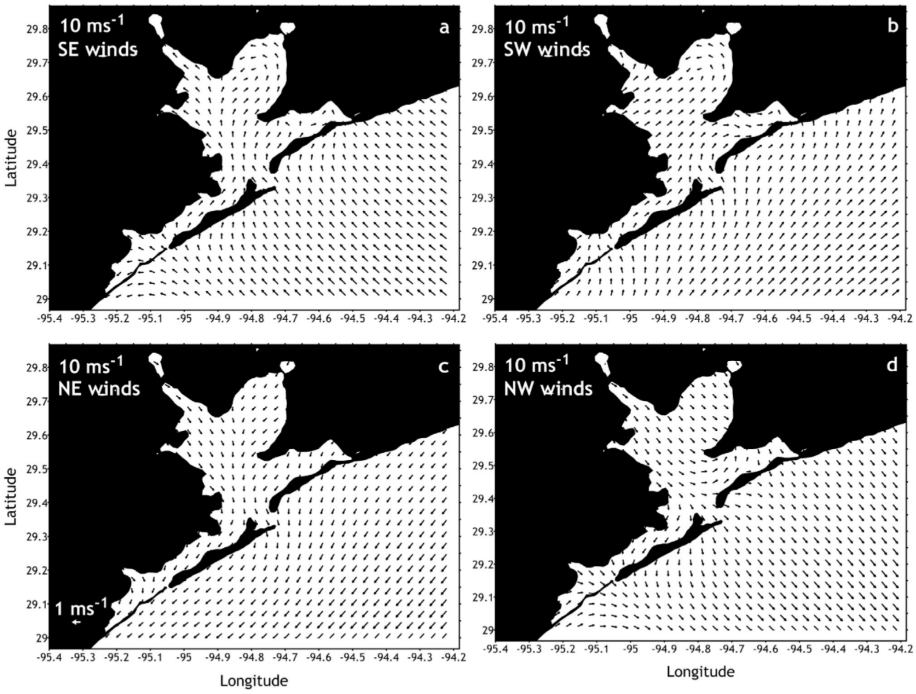

Figure 2.8: Effects of flow through Galveston Bay for different wind directions (Salas-Monreal et al., 2018)

Sediment Transport

The sediment transport in the San Luis Pass is a dynamic system. Figure 2.9 shows the sediment transport along Galveston island and at the Bolivar Roads and San Luis Pass. The beachfront along the Galveston Seawall requires beach nourishment on a regular basis and the beach west of the Seawall has deteriorated badly (Frey et al., 2015). The soil in the San Luis Pass is only poorly graded sand, Appendix D.3.1 describes this in more detail. Behind the San Luis Pass, channel-shoal systems are formed, shown in Figure 2.10. This figure shows the morphological pattern behind the San Luis Pass in December 2020. Over the last years, this pattern behind the San Luis Pass has become nearly stable. This pattern only disappeared after Hurricane Harvey. The San Luis Pass contains a lot of sediment whilst wetlands behind have been eroding in the past. In recent years, restoration projects have been undertaken. As a result of these projects, the erosion reduced. Figure D.4 in Appendix D.3 gives the exact volumes of sediment transport at Galveston Bay.

Figure 2.9: Sediment transport in Galveston Island

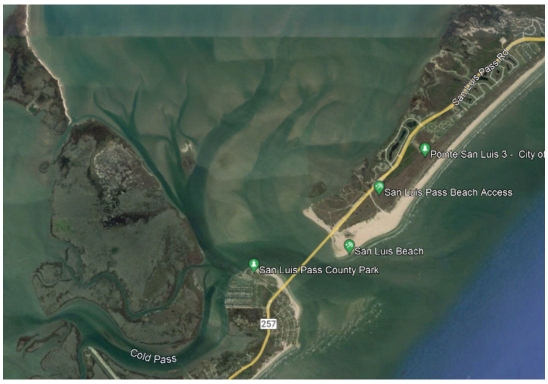

Figure 2.10: Morphological pattern behind San Luis Pass

Bridge

A bridge, doubling as an evacuation route (for example for during a hurricane) crosses the San Luis Pass. Recreational boats must be able to pass under the bridge under normal conditions. The length of the bridge is 2138.5 meters, it was constructed in 1966. The bridge requires replacement in the near future. The length of the longest span is 18.3 meters, and the width of the deck is 10.2 meters. The clearance beneath the bridge is 9.0 meters (Bridge reports, n.d.).

Brazoria National Wildlife Refuge

Brazoria National Wildlife Refuge has an incredible diversity of wild life due to it is mild temperatures, fresh and salt water estuaries, bay waters and blend of soils. Brazoria National Wildlife Refuge is for both nature and people. The area has many salt and freshwater marches, sloughs, ponds, coastal prairies. The are is home to a 12-foot alligator, more than 400 species of bird and the largest population of the Audubon Christmas bird. People can come to fish, hunt, or hike (“State of Texas Parks - Brazoria National Wildlife Refuge”, 2022).

The animals that live in the wetlands depend on the type of wetlands. The mud flats and salt water marsh are the homes for the shorebirds fishes. (Shell)fish live in the brackish wetlands and double as food source for birds that live in the area, such as the great blue herons, roseate spoonbills, and wood storks. The fresh water ponds are the home of purple gallicizes, bitterns, frogs, and crawfish. River otters frolic in the waters and alligators sun themselves on the banks (U.S. Fish & Wildlife Service, 2017).

The plants that live in the wetlands are strongly influenced by the salinity levels. In the salt environment, the smooth cord grass and sea ox-eye daisy flourish. The freshwater environment houses the Gulf cord grass and bacharis.

Salt marshes

Throughout the entire Galveston Bay, many salt marshes are present. The area of salt marshes is reducing due to subsidence, sea-level rise, wave action, sediment deficit, dredging and filling (Moulton, 1997)(Ravens et al., 2009). The rate of salt marsh loss is 0.7% yearly, on average, from 1979 to 2002 (William White et al., 2007). For the period of 2006 until 2011 this loss was 1.02% on yearly average (Entwistle et al., 2017).

2.3 Galveston Bay Future without Interfering

The predictions of the storm surge levels depend on different factors, namely on vertical land motion (VLM), sea level rise (SLR) and storm surge scenarios (Miller and Shirzaei, 2021). The mean sea level rise that is observed at Galveston Pier is 6.5 mm/year (Miller and Shirzaei, 2021). The chances of extreme flooding double approximately every 5 years (Taherkhani et al., 2020), and by 2100 over 76 km^2 of land is projected to be below sea level due to subsidence (Miller and Shirzaei, 2021). In the worst case composite scenario of an 8 m storm surge in addition to the SLR, the total affected area is 1,156 km^2 (Miller and Shirzaei, 2021). Figure 2.11 illustrates what the storm surge level is in 2100 with an SLR of 155 mm. It can be seen that much of Galveston and Texas City are already flooded with a storm surge of 0.5 m in 2100.

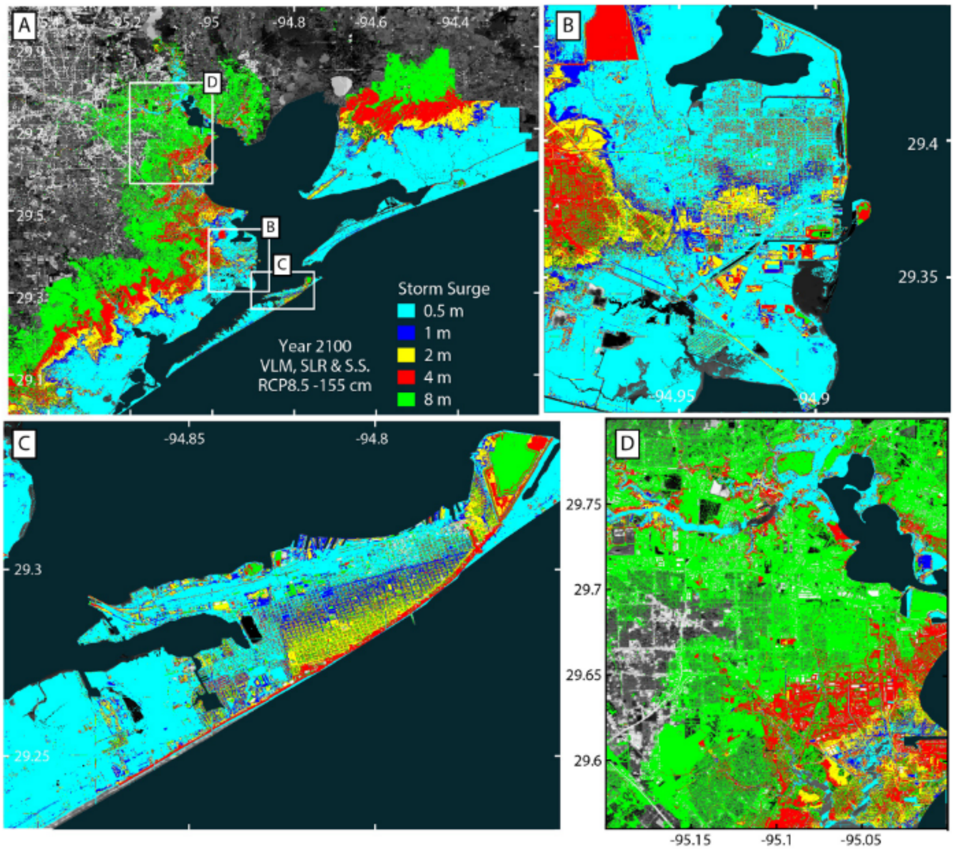

Figure 2.11: Inundation via subsidence, SLR RCP8.5 by year 2100, and storm surge flooding for (a) the Houston-Galveston region, including (b) Texas City, (c) Galveston Island, and (d) southeastern Houston (Miller and Shirzaei, 2021).

The US National Oceanic and Atmospheric Administration has recently released the report: Global and Regional Sea Level Rise Scenarios for the United States (Sweet et al., 2022). This report provides 1) sea level rise scenarios to 2150 for each decade, including estimates of vertical land motion and 2) a set of extreme water level probabilities for various heights along the U.S. coastline (Sweet et al., 2022). Figure 2.12 shows the RSLR projections for the scenarios providing the upper bound to observation-based extrapolations to 2060 for the selected tide gauges, also Galveston. The corresponding scenario for each tide gauge is shown in parentheses in the legend. Return level curves relative to the 1983–2001 MHHW tidal datum (Sweet et al., 2022). There are three types of flooding: minor, moderate and major. Sea level rise has the following effect on the types of flooding (Sweet et al., 2022):

- Minor/disruptive high tide flooding HTF (about 0.55 m above mean higher high water MHHW) is projected to increase from a U.S. average frequency of about 3 events/year in 2020 to >10 events/year by 2050.
- Moderate/typically damaging HTF (about 0.85 m above MHHW) is projected to increase from a U.S. average frequency of 0.3 events/year in 2020 to about 4 events/year in 2050.
- Major/often destructive HTF (about 1.20 m above MHHW) is projected to increase from a U.S. average frequency of 0.04 events/year in 2020 to 0.2 events/year by 2050.
- Across all severities (minor, moderate, major), HTF along the U.S. East and Gulf Coasts will largely continue to occur at or above the national average frequency.

On top of this, higher global temperatures increase the chances of higher sea level by the end of the century and beyond. The scenario projections of relative sea level along the contiguous U.S. coastline are about 0.6–2.2 m in 2100 and 0.8–3.9 m in 2150 (relative to sea level in 2000); these ranges are driven by uncertainty in future emissions pathways and the response of the underlying physical processes (Sweet et al., 2022). This is anticipated to be stronger in the Galveston Bay Area, where sea level rise is significantly greater than the national average, consequently increasing the average event frequency in the Galveston Bay Area, illustrated in Figure 2.12.

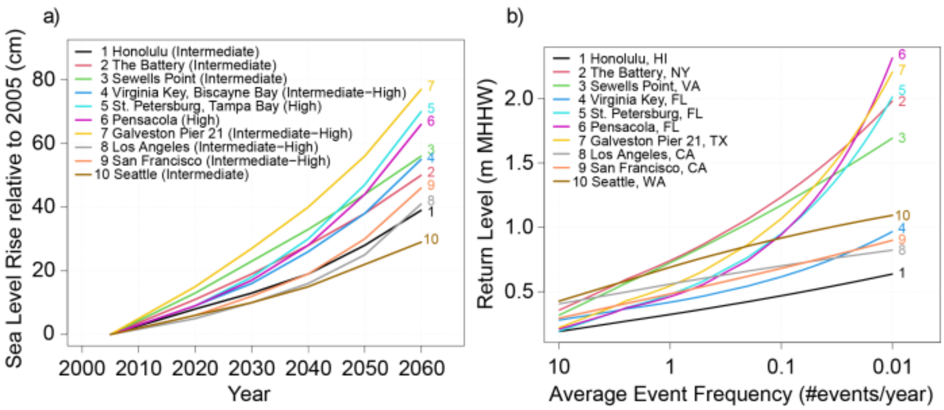

Figure 2.12: a) RSL projections for the scenarios providing the upper bound to observation-based extrapolations to 2060 for the selected tide gauges. The corresponding scenario for each tide gauge is shown in parentheses in the legend. b) Return level curves relative to the 1983–2001 MHHW tidal datum (Sweet et al., 2022)

2.4 Consequences of Leaving the San Luis Pass Open

In the aforementioned plan by USACE to form a resilient Texas coast, Bolivar Roads is closed with two double floating sector gates at the location of the shipping lane and a number of vertical lift gates, while the San Luis Pass remains open (Army Corps of Engineers - Galveston District (US), 2021). However, recent research has shown that leaving the San Luis Pass open results in a significant higher flood risk and damage to the Houston-Galveston area (Texas A&M University Galveston, 2021).

Hurricane-forced winds are extremely effective in shifting water from one side of the bay to another in very shallow bays. This is called wind set-up and leads to even higher storm surge levels on the down-wind side of the bay (Texas A&M University Galveston, 2021). Leaving the San Luis Pass open results in an increase of peak storm surge in the bay, this increases the generation of internal surge and therefore reduces the effectiveness and performance of the USACE plan. This happens through two mechanisms: 1) allowing the hurricane surge forerunner to propagate through San Luis Pass into the bay in the days leading up to hurricane landfall, and 2) allowing the main storm surge to flank the western end of the coastal barrier, initially via San Luis Pass and then via an inundated Follets Island, as the hurricane approaches and makes landfall (Texas A&M University Galveston, 2021).

The research of Texas A&M University compares two scenarios. These two scenarios are with and without a barrier at the San Luis Pass, which is referred to as with and without a western section in the research. Three different aspects increase the damage and flood risk in the area, which result from omission of a barrier at the San Luis Pass. The first is surge forerunner propagation through an ungated San Luis Pass. The second is increase in peak surge elevation and inundation in both West and Galveston Bays caused by the main storm surge that flanks the western end of the USACE coastal spine. The third is the influence of sea level rise on increased peak surge and inundation associated with flanking (Texas A&M University Galveston, 2021).

Forerunner

Forerunners result in a slow, steady rise of water surface elevation near the coast in the days before the hurricane eye make landfalls. Leaving the San Luis Pass open would, for a hurricane similar to Hurricane Ike, result in respectively 1.0 m and 0.2 m higher water surface elevation in the West and Galveston Bay 12 hours before the eye of the hurricane makes landfall (Texas A&M University Galveston, 2021).

Figure 2.13 shows the water level elevation in central Galveston Bay with and without a barrier at the San Luis Pass (referred to as with and no western dike). Figure 2.14 shows the water level elevation in central West Bay with and without a barrier at the San Luis Pass. The black line shows the difference in water level elevation in feet. In both cases there is a barrier at the Bolivar Roads and a hurricane similar to Hurricane Ike.

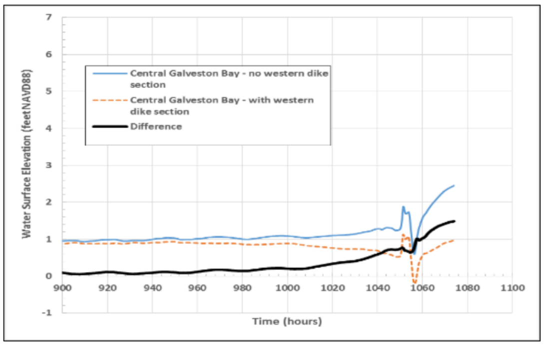

Figure 2.13: Water level elevation in central Galveston Bay with and without a barrier at the San Luis Pass (Texas A&M University Galveston, n.d.).

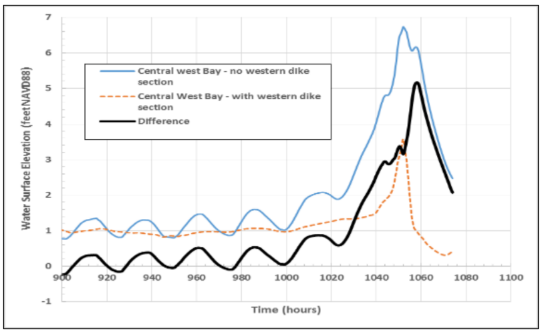

Figure 2.14: Water level elevation in central West Bay, with and without a barrier at the San Luis Pass (Texas A&M University Galveston, n.d.).

Main storm surge

The peak storm surge in the West Bay and Galveston Bay is reduced by having a barrier at the San Luis Pass. For a hurricane similar to Hurricane Ike, this results in respectively a 1.6 m and 0.4 m lower peak storm surge at the west end and throughout most of Galveston Bay (Texas A&M University Galveston, 2021).

Figure 2.15 shows the peak surge height for a hurricane similar to Hurricane Ike in the Galveston-Houston area and with a barrier at the San Luis Pass. Figure 2.16 shows the peak surge height for a hurricane similar to Hurricane Ike in the Galveston-Houston area without a barrier San Luis Pass. In both cases there is a barrier at the Bolivar Roads Pass. The elevation is given in feet.

The consequences of leaving San Luis Pass open are determined by the hurricane's path, specifically where the hurricane's eye makes landfall. The hurricane eye propagated on the eastern side of the San Luis Pass for Hurricane Ike (red line in Figure 2.16). At this moment in time, water was leaving the San Luis Pass, due to the fact that hurricane air flow (winds) moves counterclockwise in the Northern Hemisphere. This indicates that if the eye of Hurricane Ike were to shift west of the San Luis Pass, the storm surge height would be even greater.

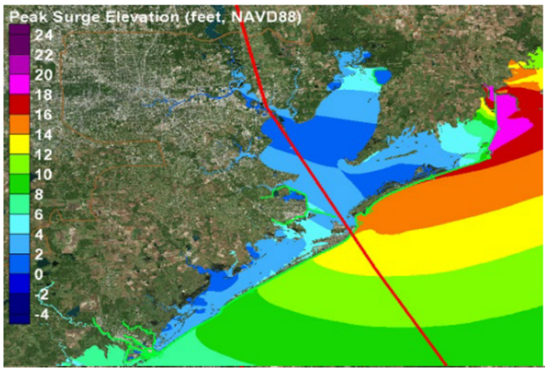

Figure 2.15: Peak surge height of Hurricane Ike, with a barrier at Bolivar Roads and San Luis Pass (Texas A&M University Galveston, n.d.).

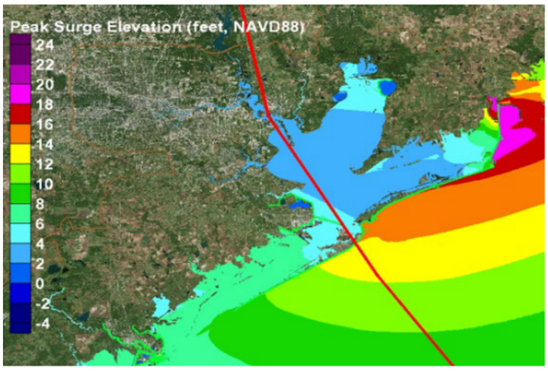

Figure 2.16: Peak surge height of Hurricane Ike, with a barrier at Bolivar Roads and without a barrier at San Luis Pass (Texas A&M University Galveston, n.d.).

Sea level rise

In general, rising sea levels will increase flood risk throughout the Houston-Galveston region, both with and without a western section. In addition to all the areas around West Bay, there also appear to be areas around the periphery of Galveston Bay where surge levels and inundation are exacerbated by leaving the San Luis Pass open. According to the report of Texas A&M University, small changes in peak surge levels that are caused by having a barrier at the San Luis Pass can reduce inundation and damage inside Galveston Bay. With sea level rise, the adverse effects are not restricted to West Bay of western side of Galveston with not having a barrier at the San Luis Pass (Texas A&M University Galveston, 2021).

Economics

This subsection describes the economical damage for the relative present (2016) and future (2080) for two levels of hurricane surge severity in Galveston Bay. The two levels of hurricane surge severity are Hurricane Ike and the modeled storm. The modeled storm is a 100-year storm, and has a probability of occurrence of 26% for the next 30 years. The present scenario is based on actual local land use and national economic conditions for the year 2016. The future scenario is based on models of future local land use and national economic development. The financial damages with and without the coastal spine system are described. The Coastal Spine System, i.e. Ike Dike, is envisioned so that the spine will be a complex system connecting seawalls and fortified dunes/levees along the coastline to retractable gates located at the mouth of Galveston Bay and San Luis Pass (The Center for Texas Beaches and Shores and Texas A&M University at Galveston, 2016).

Without Coastal Spine System

The present scenario (2016) has a total damage 1.36 billion dollar for the Hurricane Ike scenario and 1.5 billion dollar for the modeled storm scenario. The future scenario (2080) has total damage of 1.37 billion dollar for the Hurricane Ike scenario and 2.4 billion dollar for the modeled storm scenario without taking sea level rise into account. The future scenario with sea level rise taken into account results in total damage of 2.22 billion dollar for the Hurricane Ike scenario and 3.41 billion dollar for the modeled storm scenario (The Center for Texas Beaches and Shores and Texas A&M University at Galveston, 2016).

With Coastal Spine System
The present scenario (2016) has a total damage 124.21 million dollar for the Hurricane Ike scenario and 562.87 million dollar for the Modeled Storm scenario. The future scenario (2080) has a total damage of 215.96 million dollar for the Hurricane Ike scenario and 735.9 million dollar for the Modeled Storm scenario without taking sea level rise into account. The future scenario with sea level rise taken into account results in a total damage of 539.15 million dollar for the Hurricane Ike scenario and 1.2 billion dollar for the Modeled Storm scenario (The Center for Texas Beaches and Shores and Texas A&M University at Galveston, 2016).

2.5 Politics with regard to Flood Defenses in the United States of America

The flood risk management of a country depends on the geographical location and the policy of the government. In the United States of America, this policy strongly emphasizes individual responsibility (Bubeck et al., 2017). In contrast to the Netherlands, where the government is responsible for flood protection, the United States relies on private organizations. In the United States of America, the flood risk management is done by the National Flood Insurances Program (NFIP) which is administered by the Federal Emergency Management Agency (FEMA). This program imposes minimum building and flood risk zoning requirements on communities with a greater than 1/100-year flood risk. FEMA identifies flood hazard areas, makes flood risk maps, sets flood insurance premiums, covers the risk, creates design standards for constructions in floodplains and provides funds for mitigation projects (Bubeck et al., 2017). The 1/100-year is based on a storm that averages 13.2 inches (ca. 34 cm) of rain in 24 hours. In comparison, Hurricane Harvey brought 25.9 inches (0.66 m) in 24 hours (Lendering, n.d.).

In the United States of America, climate change considerations are not yet considered in flood risk management on a federal level, despite local efforts to design climate change adaptation plans. This is probably explained by an interaction effect with human behavioral factors and the still ongoing debate in the United States of America on a regional level whether climate change is an actual problem (Bubeck et al., 2017). According to the report of Sweet et al., 2022, sea level rise has a major impact on the Galveston Bay Area.

The cost for a barrier at the San Luis Pass is partly paid by the government of the United States of America and State of Texas. The government of the United States of America pays for 65% of the construction cost. The remaining 35% is paid by the state of Texas. The maintenance costs of the storm surge barrier are also for the state of Texas.

2.6 Stakeholders

Each project stakeholder has an interest in and viewpoint on the project. It is important to identify these stakeholders and get to know their preferences and motivations. In the Houston-Galveston Bay areas, several parties have conflicting interest in the development regarding flood protection. The area is an important economic area due to the port of Houston. Events near the Galveston Bay Area will have an effect on the energy prices for the rest of the US. For example, if this area is down for a few days, the energy prices on the East Coast will increase nearly immediately. The military also have their natural liquified oil deposit stored in the Galveston Bay Area. In a workshop by B. Kothuis these stakeholders were listed, including their motivation (Kothuis et al., 2014). The different stakeholders for the Houston-Galveston Bay Area could be placed in eight different interest groups, listed below (Kothuis et al., 2014). Now, 8 years later, the local and state government are the main leaders of the proposed plan for a resilient Texas. Table 2.2 presents the interest, concern, and power of the different stakeholders (de Vries, 2014).

- Federal government & US Army Corps of Engineers & Flood insurance underwriting Fed. Govt.
- American people
- Environment & Tourism interest
- State government & Local government
- Infrastructure & Emergency response
- Citizens on the Water Front
- Citizens in the Surge Zone
- Industry & Business & Ports

Stakeholder	**Interest/concern**	**Power**
Federal government & State/local government	Stimulation of the economy, Increase safety of residential areas	++
Environmentalists	Preservation of the Bay's ecosystem	++
Bay Area Houston Economic Partnership	Sustainable stimulation of the country's economy by preserving economic assets	+
Investors	High return rates, low investment risks	+
(Chemical) Industries	Protection against surges	+
Other businesses	Protection against surges	+
Citizen groups · On water front · In surge zone	Protection of personal property keep unobstructed view Protection of personal property	+/-
Contractors	Make profit	-
Operators	Accessible barrier operation	+/-
Maintenance managers	Easy to perform maintenance	+/-

Table 2.2: Stakeholder involvement (de Vries, 2014)

The Gulf Coast Community Protection and Recovery District, GCCPRD, is a local government corporation including the Brazoria, Chambers, Galveston, Harris, Jefferson, and Orange counties, shown in Figure 2.17. Several of these counties have a greater influence than others. Their goal is to develop a plan to protect the life, health, and safety of the community and provide environmental and economic resilience within the study region (GCCPRD, 2018c). The region around the San Luis Pass is strongly dependent on tourism. Galveston Bay is one of the most abundant estuaries for shrimp, oysters, crappie, and fishing. To sustain this, mud and marshes are required. Therefore, the environmental and tourist interests are represented by the Galveston Bay Foundation and the Christmas Bay Foundation. The interests of the stakeholders are taken into account in the program of requirements for the storm surge barrier at the San Luis Pass.

Figure 2.17: The Gulf Coast Community Protection and Recovery District

2.7 Result of System Analysis

The Galveston Bay is a semi-enclosed basin that contains both fresh and salt water and is a micro tidal region. The San Luis Pass is located at the east of Galveston Island. The sea level is expected to rise approximately 75 cm by 2060 (compared to the sea level in 2005), which is an intermediate-high increase compared to the rest of the United States of America. The consequences of leaving the San Luis Pass open depend on the storm/hurricane's characteristics, specifically its path and the location of the hurricane eye's landfall. In most cases however, the negative impacts of the hurricane will be worse if the San Luis Pass remains open. For a hurricane similar to Hurricane Ike, the peak surge elevation is approximately 1.6 meters higher at the west end of Galveston Bay, 0.5 meters higher in the City of Galveston, and 0.4 meters higher in Galveston Bay.

The San Luis Pass is responsible for 20% of tidal exchange for Galveston Bay. Consequently, it is crucial to investigate the impact of a storm surge barrier at San Luis Pass on the tidal range, tidal prism, flow velocity, and salinity. This determines the impact of a storm surge barrier at San Luis Pass on the local ecosystem. The San Luis Pass Bridge connects Galveston Island to Follets Island and serves as an evacuation route. Therefore, it is essential to maintain the San Luis Pass's transportation function and investigate the possibility of incorporating the bridge into the design of the storm surge barrier. Consider that the bridge is in poor condition and will need to be replaced in the near future. Behind the San Luis Pass lies Brazoria Natural Wildlife Refuge, home to various bird species, fishes, and vegetation. The San Luis Pass itself is an extremely dynamic pass, in terms of sediment, and a quicksand area. Therefore, it is prohibited to swim.

3

Program of Requirements and Boundary Conditions

This chapter describes the program of requirements and boundary conditions for the storm surge barrier at the San Luis Pass. There are three different types of boundary conditions: Functional, Environmental and Social, respectively described in Section 3.1, 3.2 and 3.3. The program of requirements for the storm surge barrier at the San Luis Pass is listed in Section 3.4. This chapter corresponds to the third step in the methodology.

3.1 Functional Boundary Conditions and Requirements

The functional boundary conditions contain the hydraulic, meteorological, geotechnical and geological conditions, as well as the structure lifetime and adaptability.

Hydraulic Boundary Conditions

The hydraulic boundary conditions for the San Luis Pass under normal conditions are shown in Table 3.1. These are based on Ruijs, 2011, Jonkman et al., 2015 and de Vries, 2014.

Variable		**Value**
Low tide	(MLLW)	0.90 m [NAVD88+m]
Mean Sea Level	(MSL)	1.15 m [NAVD88+m]
High tide	(MHHW)	1.54 m [NAVD88+m]
Significant wave height in the Gulf	(H_s)	0.5 m
Peak wave period in the Gulf	(T_p)	4.0 s

Table 3.1: Regular hydraulic boundary conditions in the Gulf of Mexico (Ruijs, 2011;Jonkman et al., 2015;de Vries, 2014)

Meteorological Boundary Conditions

The climate in the Houston-Galveston region is humid subtropical. Although Galveston receives roughly 1,104 mm of rain per year, rainfall does not increase the design storm surge level (de Vries, 2014). The water level and duration are based on the Delft University of Technology's coastal spine interim design study. These water levels do not account for sea level rise. Table 3.2 shows the hydraulic boundary condition in the Gulf of Mexico in case of three extreme events, namely a 1/100 yr^{-1}, 1/1000 $yr^{-1}$and 1/1000 yr^{-1} event. These are based on the studies by the Delft University of Technology (Jonkman et al., 2015).

		1/100 yr^{-1}	**1/1000 yr^{-1}**	**1/10000 yr^{-1}**
Maximum surge	[m]	5.2	6.1	7.0
Wave height H_s	[m]	5.0	5.7	6.3
Wave period T_p	[s]	7.2	7.7	8.2
Forerunner surge	[m]	3.0		4.2

Table 3.2: Hydraulic boundary conditions in the Gulf of Mexico for extreme events (Jonkman et al., 2015)

Relative Sea Level Rise

USACE analyzed the relative sea level rise near Galveston Island and other regions in the United States of America. The meters of sea level rise near Galveston Island depends on the category. There are three categories: low, intermediate and high. Table 3.3 shows the meters of relative sea level rise corresponding with the category for the Galveston Bay Area. The applicable category is determined by the requirements and criteria.

Relative Sea Level Rise	[m]
Low	0.52
Intermediate	0.82
High	1.77

Table 3.3: Relative Sea Level Rise (Army Corps of Engineers - Galveston District (US), 2021)

Geotechnical Boundary Conditions

The available data about the geotechnical conditions of the San Luis Pass is limited. The soil at San Luis Pass consists of poorly graded sand to a depth of -7.6 m MSL, according to the available data. The two different sediment coring data at the west side of the San Luis Pass are shown in Appendix D.3.1.

Geological Conditions

The area around the San Luis Pass consists of an inlet to the sea, the San Luis Pass, with a connecting bay, West Bay. There are no mountains near the Houston-Galveston Area. In the Houston-Galveston Area, earthquakes are rare. Previous earthquakes in the region have reached a maximum magnitude of 3 on the Richter scale. In Section 2.2 the area is described in more detail.

Hurricanes in the Houston-Galveston area occur frequently, as described in Section 2.2.2. A hurricane has a swirling character that can induce various surge directions in the basin. The direction of the wind determines the flow effect thought the inlet, shown in Figure 2.8. The wind direction is in turn determined by the landfall of the hurricane eye, illustrated in Figure 2.2. During a hurricane, the wind direction can change easily, which may result in a negative head. Negative head is the situation where the governing water level and forces on the barrier are directed from the West/Galveston Bay onto the Gulf of Mexico instead of the other way around, also known as 'back surge' effect from the West/Galveston Bay. The change in surge direction is hard to predict a long time in advance, as it depends on the landfall location and storm character of the hurricane. The barrier must be able to deal with the change in surge direction. This could be done by two different ways (de Vries, 2014):

1. Enabling the barrier to open and close within a short period of time (up to 15 minutes).
2. Constructing the barrier in such a way that it is able to deal with a negative head.

A barrier usually consists of various large structures that are hard to open and close within 15 minutes, therefore option 1 is not very likely. Consequently, option 2 is set as a requirement: the barrier must be retaining in two directions.

Structure Lifetime and Adaptability

The design lifetime of the storm surge barrier is according to the adaptive management. The lifetime of the entire structure is different from particular structural components. Adaptive management means instead of an equal lifetime for the entire structure, the lifetime is based on the lifespan of a particular structural component, resulting in different design level for each component, explained in detail in Appendix E. The design lifetime of a storm surge barrier is usually said to be 200 years, looking at the already existing worldwide storm surge barriers, described in Appendix C. As time progresses, the uncertainties regarding the sea level rise grow exponentially. Therefore, the design of the storm surge barrier realistically nears 100 years but is adaptable for future change, allowing the design to outlast the 100 years.

The foundation also has a lifetime of 100 years, but should account for a relatively conservative sea level rise scenario. The design lifetime of gates is 50 years, but should be adaptable for higher surges in the future.

3.2 Environmental Boundary Conditions and Requirements

This section describes the boundary conditions for the environment in order to design a storm surge barrier with minimum impact on the environment. The construction of a barrier that restricts flow could change the salinity, sedimentation, circulation, tidal influences, and discharge velocities (GC-CPRD, 2018a).

In order to create this design, the abiotic requirements for a good biotic conditions need to be found. Biotic factors are factors of biological origin that affect or influence ecosystems, and abiotic factors are non-biological aspects that influence an ecosystem. Abiotic factors include temperature, water and soil chemistry, water clarity and tidal range. To have good abiotic conditions, it is necessary to determine what species are required to be preserved in the area surrounding the San Luis Pass.

In previous research on the environmental impact of a barrier at Bolivar Roads is studied. They concluded that (GCCPRD, 2018a): *'The permanent presence of a barrier in a dynamic estuaries' system will have ongoing environmental effects. A barrier across Bolivar Roads, the location where Galveston Bay meets the Gulf of Mexico, not only has potential impacts on wetlands, vegetation, and wildlife, but on physical components such as salinity, circulation, sedimentation, and discharge velocity. These physical effects have the potential to impact habitats and species in Galveston Bay'*. The influence factors that are will be considered and examined in this design are tidal range, tidal prism, change in intertidal area, discharge velocities, salinity, and sediment transport.

Tidal Range

Tidal inlets are openings in the shoreline, such as between two barrier islands that connect bays or lagoons to the open sea. They are maintained by tidal currents. Essential for a tidal inlet is the tidal variation in the open sea; the tide is the engine that determines most of the occurring features of the inlet and the basin it connects to. The tidal range and the surface area of the tidal basin together determine in principle the volumes of water that have to flow in and out through the inlet during a tide (Bosboom et al., n.d.).

Behind a tidal inlet are three types of zones. These zones are the intertidal zone, shallow tidal waters and deep tidal waters and channels. The intertidal zone if defined as the area between average high water and average low water. The shallow tidal water is the region between the average high water and one meter below the average high water. The deep tidal waters and channels are areas with water depths larger than one meter below average low water. These different types of zones have different types of environmental value (van Zaal, n.d.).

San Luis Pass is a tidal inlet that is dominated by the tide (moffmat & nichol, 2010) and accounts for 20% of the tidal exchange in Galveston Bay (Gonzalez and Holligan, 2012). The residence time of water in the bay will increase as the dominance of the tide over the freshwater inflow diminishes (Ruijs, 2011). As a result of the slowed current in Galveston Bay, fine sediments may settle more quickly, which may increase light transmission through the water column (Ruijs, 2011).

Ruijs researched the closure of Bolivar Roads Pass on the tidal range in Galveston Bay. The result of his research is that the effect of closure is negligible on tidal range when the flow through area remains at least 80% of the original flow through area, shown in Figure 3.1 (Ruijs, 2011). A partial, 50% closure of the San Luis Pass would result in a 5% decrease in tidal amplitudes throughout the Galveston Bay (Ruijs, 2011). A fully closure of the San Luis Pass would result in respectively 40% and 10% less in West Bay and rest of the Bay (Ruijs, 2011). Note that there were large errors for inlet at San Luis Pass, measured max discharge was 2-3 time higher than modeled in 2011. Therefore, the effect on the tidal range could be different.

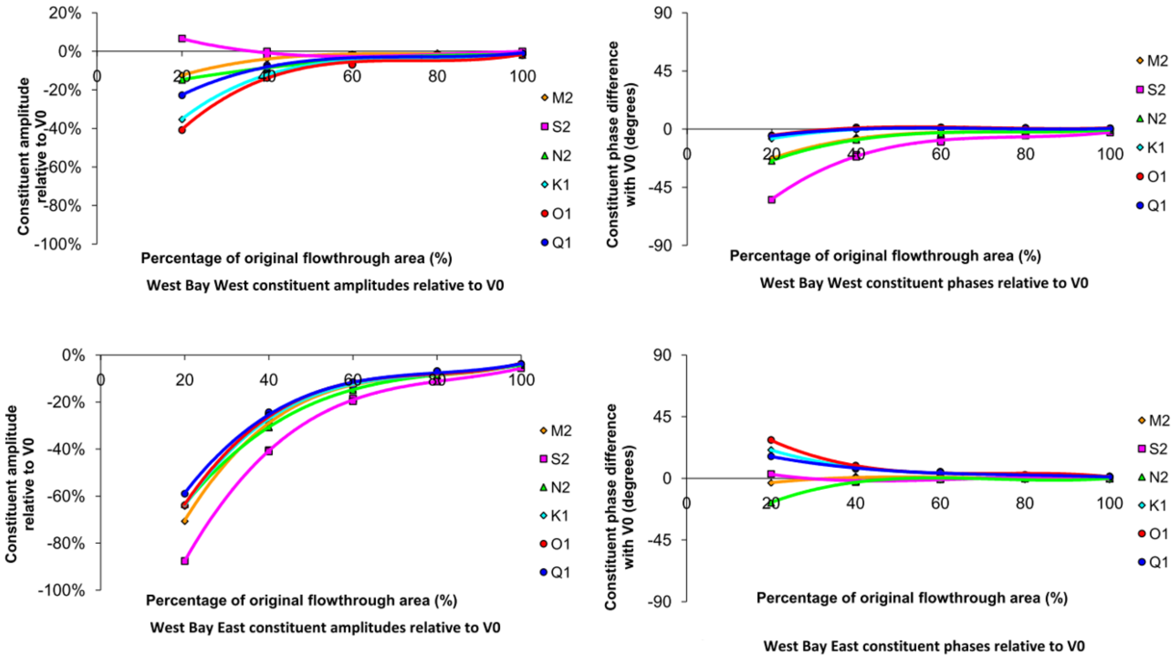

Figure 3.1: Effect of Bolivar Roads Pass barrier on tide in the West Bay (Ruijs, 2011)

The tidal basin and small basin-approximation, according to J. Battjes and R.J. Labeur (Battjes and Labeur, 2017) describes the amplitude difference between the bay and sea. This model assumes that in the West Bay, the San Luis Pass is the only inlet. The amplitude of the sea at the San Luis Pass is 0.4 m. Figure 3.2 shows the tide predictions in sea and West Bay with different reduction at opening San Luis Pass. Figure 3.3 shows the difference in tidal range for a reduction of the opening in the San Luis Pass. Appendix D.4.1 described the model.

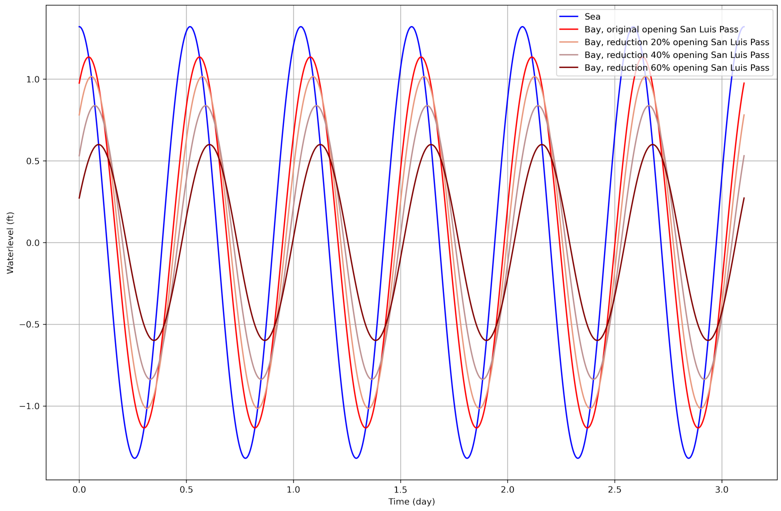

Figure 3.2: Tide predictions Sea and Bay with different reduction at opening San Luis Pass

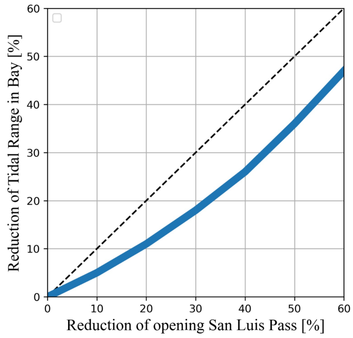

Figure 3.3: Reduction of opening San Luis Pass with corresponding reduction of tidal range in the West Bay

Tidal Prism

Under normal conditions, the water level is changing due to vertical tidal variations (Bosboom et al., n.d.). The stable equilibrium cross-section area for a tidal inlet can be calculated with equation 3.1 (Bosboom et al., n.d.). Where A_{eq} is the minimum equilibrium cross-section of the entrance channel in m^2. The P is the tidal prism, often the spring tidal prism in m^3. C and q are coefficients that are empirically found. O'Brien (O'Brien and Asce, 1969) showed that for 28 United States of America entrances, the coefficient C is $4.69 \cdot 10^{-4}$ and coefficient q is 0.85 (Bosboom et al., n.d.).

$$A_{eq} = C \cdot P^q \tag{3.1}$$

Resulting in a correction of $A_{\%\ original}{}^{1/0.85} = P_{\%\ original}$. This is in line with the environmental study of the GCCPRD, their model showed that in the that the reduction in tidal prism is proportional to the reduction in flow area (GCCPRD, 2018b).

Change in Intertidal Area

A reduction of 60% in the opening of the San Luis Pass results in a tidal range difference of 0.5 ft (15.24 cm). This corresponds to a 35% loss of intertidal area, this area will be added to the West Bay. In the original situation, the intertidal area is 15% of the total wet area of the West Bay. With a tidal reduction of 0.5 ft. the intertidal area of the West bay will decrease to 10% of the total wet area of the West Bay. The area most effected by the change in tidal range is in the area near Jamaica beach at Galveston Island. This is illustrated in Figure Shown in Figure D.17 and D.21 at Appendix D.4.1.

Discharge Velocities

The discharge velocity depends on the total discharge through the pass and the wetted cross-sectional area. The model that is used to estimate the effect of reducing the opening at San Luis Pass on the tidal range, described in Section 3.2 and explained in Appendix D.4.1. Figure 3.4 shows the maximum flow velocity in San Luis Pass.

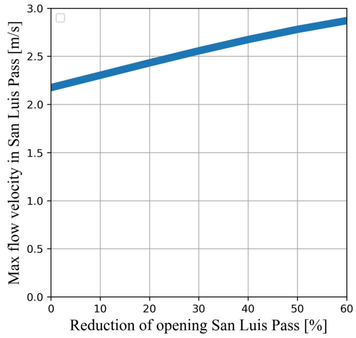

Figure 3.4: Reduction in opening San Luis Pass with corresponding maximum flow velocity

Salinity

The salinity in Galveston Bay depends on the freshwater supply from the rivers that flow into the bay. The classification of the type of estuary depends on the net freshwater supply. There are three different classifications, namely: classical estuaries, inverse estuaries and seasonally hyper saline estuaries. Classical estuaries have lower salinity than the adjacent coastal ocean, because the net freshwater supply is overwhelmingly positive, most often due to large quantities of runoff. Inverse estuaries have higher salinity than the adjacent coastal ocean as a result of overwhelmingly negative net freshwater supply, i.e., evaporation is dominant. The third type of estuary is a seasonally hypersaline estuary, where episodic hyper salinity and estuaries conditions occur at different times of the year. In seasonally hypersaline estuaries, the net freshwater supply fluctuates widely throughout the year, but is near zero on an annual basis (Kelble et al., 2007).

The GCCRPD report has investigated the effect of different barriers at Bolivar Roads Pass on the salinity levels in the mid-West Bay. The result of this research was that the salinity difference due to the barrier is negligible, shown in Figure 3.5. The salinity varies per month, this is in a range of 15-30 ppt (GCCPRD, 2018b).

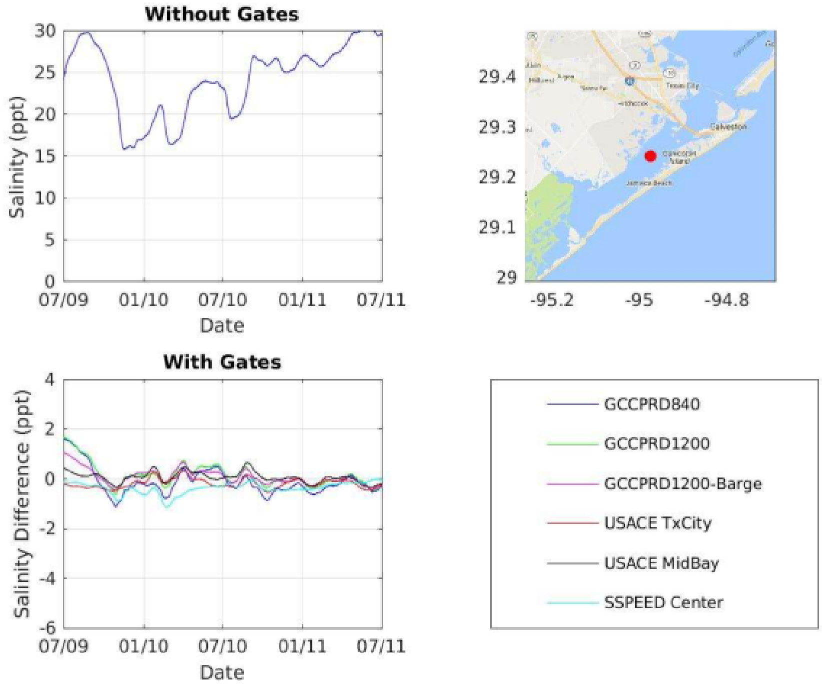

Figure 3.5: Time series of Salinity change in West Bay due to different types of barriers in Bolivar Roads Pass (GCCPRD, 2018b)

Sediment Transport

The principle of sediment transport is that the sediment is transported from places of high to low energy, resulting in erosion at high energy places and deposition in low energy places (Bosboom et al., n.d.). Galveston Bay is currently experiencing a sediment deficit caused by sea level rise and subsidence, up to 10 mm/year (Ruijs, 2011). The San Luis Pass accumulate 57,300-76,500 cubic meters of beach quality sand, mainly from the Galveston Island side (moffmat & nichol, 2010). This results in slowly retreating coastlines, marshes and tidal flats at Galveston Bay. The blocking of the sediment by the barriers and the redistribution of the sediment due to the decrease of the tidal prism, tidal range and current velocities might further enhance this problem (Ruijs, 2011).

Result Influence Factors

- Tidal range reduction in the West Bay is approximately 2/3 of the reduction in flow area at the San Luis Pass.
- Reduction in tidal prism in the West Bay is proportional, although less than linear, to the reduction in flow area at the San Luis Pass.
- Salinity in the West Bay is not effected by a barrier.
- Dynamic pass in terms of sediment transport and wave directions.

3.3 Social Boundary Conditions and Requirements

The social boundary conditions and requirements are law and regulations, operational, transformational and surrounding of the San Luis Pass.

3.3.1 Laws and Regulation

This section describes the Laws and Regulations regarding flood defenses and environment. The laws are stated in U.S. Code 701 - Flood control generally.

Safety Level

The National Flood Insurance Program establishes the safety standard for the United States of America. This program specifies that the surge protection level has a return period of 1/100 years (FEMA, 2020). Therefore, the storm surge barrier will be designed for a protection against surge levels with a return period of 1/100 yr^{-1}. Section 3.1 describes the related surge level and wave heights for this protection level.

Reliability of Barrier Closure and Opening

The reliability of the barrier depends on the type of gates of the storm surge barrier. In general, the barrier should still be able to withhold the surge sufficiently if one of the gates fails. The reliability will be defined later.

3.3.2 Operational Requirements

Similar operational requirements apply to the storm surge barrier in San Luis Pass, as well as Bolivar Roads. The Galveston Island Control/Visitor Center will be an operational center accessible via an all-weather concrete road located near Bolivar Roads. This location is constructed for the Bolivar Roads barrier, but can also be used for the San Luis Pass barrier.

The gates will be only be closed when a storm surge event threatens the Texan coast or for an annual maintenance check or inspection. The gates are intended to remain open year-round to maintain continuous navigation and existing flow characteristics (Army Corps of Engineers - Galveston District (US), 2021).

The duration of the storm surge barrier closure and opening cannot exceed that of the storm surge barrier at Bolivar Roads. A storm surge barrier protects the hinterland from high surges, but not from wind damage. In the days preceding a hurricane, the region will be evacuated (de Vries, 2014). Design must permit rapid opening after a storm, even if the primary power source is out (GCCPRD, 2018a). Therefore, a backup power source, such as a generator, is required.

3.3.3 Transportation

There are two types of transportation surrounding the San Luis Pass: the bridge across the San Luis Pass and the vessels through the San Luis Pass (Bridgehunter, n.d.).

Bridge

The capacity of the San Luis Pass bridge should be maintained or increased. Current bridge characteristics are as follows:

1. Vertical clearance of 9.0 m
2. Minimum width of 10.2 m

Vessels

The San Luis Pass is utilized primarily by fishermen. The pass should have the same design requirements as the current pass. The vertical clearance under the bridge at San Luis Pass is 9 meters, and the width between the bridge's piles is 18 meters.

3.3.4 Spatial Integration

The spatial integration is dependent on numerous factors. Only four variables are taken into account in this design. These four factors are: unique character, west end of San Luis Pass, view, and swimmer safety.

Unique Character San Luis Pass

The San Luis Pass is one of the few inlets in Texas that has natural sideways, in other words, no breakwaters. People experience an open, natural, spacious feeling when visiting the San Luis Pass area. The sediment can flow freely and generate large beaches on the east side of the San Luis Pass. A consequence of this is the eroding beach on the western side.

West End of San Luis Pass

Brazoria County has proposed to dredge approximately 376,200 cy of sand material from West Bay and San Luis Pass for beach nourishment on the north end of Follets Island. The 50 m-wide, 3600 m-long dredge area would improve vessel access through San Luis Pass and would be excavated to –9 m NAVD 88. Sand would be placed near shore, within the submerged portion of beach, to reduce wave action and allow for onshore movement of material (SWG-2015-00306) (USACE Galveston District, 2021).

View

The view of the San Luis Pass should not be blocked by a massive construction. A barrier that doesn't block more than the already existing bridge is preferred.

Swimmer Safety

At the San Luis Pass, several people die each year due to the strong and unpredictable current. The San Luis Pass is a very dangers fishing spot on the Texas coast. The currents at San Luis Pass are extremely strong, especially during tidal changes. It is forbidden to swim at the San Luis Pass. The sea floor at the San Luis Pass changes after a major storm. The maximum velocity at the San Luis Pass is around 2.2 m/s. For comparison, an Olympic swimmer could reach a maximum speed of 2.1 m/s (Olympic Games, 2020). In conclusion, it is impossible for individuals to swim across the pass at such a high maximum velocity.

3.4 Program of Requirements for Storm Surge Barrier at the San Luis Pass

The program of requirements for the storm surge barrier at San Luis Pass is derived from the boundary conditions, requirements, and system analysis. The requirements program is required as a design input for the storm surge barrier. The design input consists of requirements, criteria, and conditions. There is a difference between requirements and criteria. A requirement is a condition that needs to be satisfied irrespective of the circumstances. A criterion is an aspect of an assessment. A check to whether a concept (here a type of gate) satisfies a requirement can only deliver one of the two results: yes it does, or no it does not. The assessment with respect to a criterion can deliver any result, varying from excellent to extremely poor (Daniel and Paulus, 2019). The requirements, criteria, and desires are utilized to determine whether the concepts meet the requirements, and the concepts are compared and evaluated using the criteria. This is elaborated on in the next chapter.

Requirements

- Structural safety

  - Constructable
  - Stable
  - Strength

- The barrier must be able to be retaining in two directions or fast opening/closing
- Hold the hydraulic load
- Ability of the retaining height (safety level 1/100 yr^{-1})
- Design lifetime 100 years

Criteria

- Fast opening/closing underwater level difference
- Deal with great water level difference
- Remaining flow area (keep intertidal area)
- Structure/foundation simplicity
- Building costs
- Maintenance
- Remaining the unique sediment dynamics at the San Luis Pass
- Vessels passing under normal conditions
- Open view
- Combination storm surge barrier with bridge

4

Generation, Verification, and Evaluation of Conventional Storm Surge Barriers

This chapter describes the generation, verification, and evaluation of the concepts for the San Luis Pass. The previous chapters serve as the foundation for the design of a storm surge barrier at the San Luis Pass, considering that the San Luis Pass is a component of an integrated system. Chapter 2 describes the functioning of the San Luis Pass. Chapter 3 listed the functional specification for the San Luis Pass, regarding flood safety, ecological values, and socio-economic aspects. A storm surge barrier is preferred in this area to keep the exchange of water under normal conditions, which could lead to minimal impact on the local environment. Around the world, several storm surge barriers are in use, and can be distinct in different concepts. Section 4.1 describes the integrated system design for the San Luis Pass. Section 4.2 provides the generation of concepts within the conventional storm surge barriers. Section 4.3 compares the different types of storm surge barriers on the design input for the San Luis Pass. All input results in a conceptual design for a conventional storm surge barrier at the San Luis Pass, described and discussed in Section 4.5. This chapter corresponds to the fourth and fifth step in the methodology.

4.1 Integrated System Design

The San Luis Pass is a component of an integrated system. The integrated design for the San Luis Pass system consists of storm surge barrier, dune system, shipping lane and breakwater. The dune system prevents flooding of Galveston Island from the Gulf of Mexico. The shipping lane would allow large draft ships to enter the West Bay through the San Luis Pass. The breakwater creates a shallow area that could prevent erosion. The type of storm surge barrier depends on the different requirements, criteria, and wishes, described in further detail in this chapter. Figure 4.1 illustrates the integrated system design at the San Luis Pass. The benefits of this integrated design are:

- Economic benefits (oyster reefs and shipping lane)
- Restore and maintain the biodiversity
- Protects against erosion on west side of San Luis Pass
- Protection against 1/100 year storm surge including future sea level rise

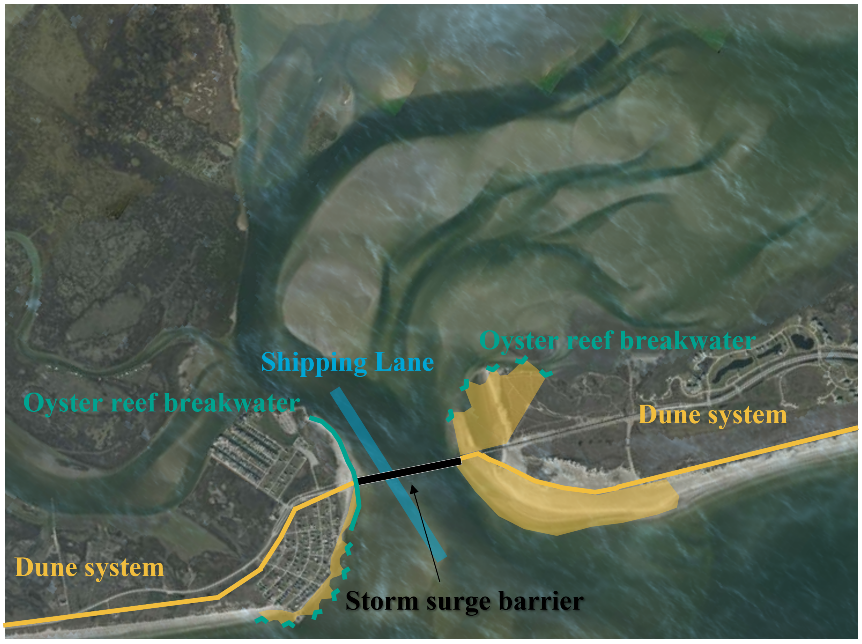

Figure 4.1: Integrated design for the San Luis Pass

The shipping lane is assumed to have a depth of 3 m. The dredged material from this shipping lane can be used for the beach nourishment on the west side of the San Luis Pass. The shipping lane would allow large draft ships to enter the West Bay through the San Luis Pass. The breakwater consists of oyster reefs at the Bay side and normal breakwaters at the Gulf of Mexico side. Oyster reef breakwaters have the advantage of increasing the biodiversity and creating a natural breakwater. Figure 4.2 show an impression of an oyster reef break water. At the west side of the San Luis Pass, the oyster reef breakwater consists of groyns that prevent this beachside for eroding. At the East side of the San Luis Pass, the beach will expand over time due to the sediment transport and deposition. The benefits of an oyster reef breakwater are (Smaal, 2019):

- Self-sustaining reef that stops coast erosion
- Enhances biodiversity
- Helps local communities to improve sustainable fishery

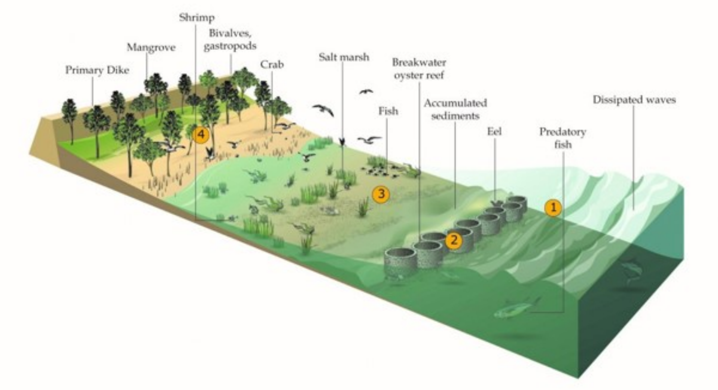

Figure 4.2: Oyster reef breakwater (Smaal, 2019)

4.2 Generation of Concepts Conventional Storm Surge Barriers

Storm surge barriers are constructed in large bays, estuaries and natural harbors as integral parts of flood risk reduction systems and be closed prior to the arrival of storms to impede storm surge and reduce the risk of flooding for the region behind the structure. The definition of a storm surge barrier is: *A storm surge barrier is a partly moveable barrier in an estuary or river branch which can be closed temporarily. Its main function during surges is to reduce or prevent the rise of inner water level and thereby sufficiently protecting the hinter lying area against inundation* (de Vries, 2014), elaborated in Appendix C. Around the world, several storm surge barriers are in use, which can be divided into seventeen concepts.

The seventeen concepts are briefly explained, the full description in given in Appendix C. The barge gate, also known as a swing gate, is a caisson stored at one side of the waterway, pivoting around a vertical axis to close. A bear trap gate is constructed of two leaves that slide over one another and seal together. The caisson structure is a concrete closure dam that is permeable in normal conditions and can be closed during surge events. Flap gates have a straight or curved retaining surface pivoted on a fixed axis that can be under or above water level. An inflatable gate is a sealed tube made of flexible material that can be inflated with air, water, or a combination. The mailbox gate is a heavy concrete flap gate hanging on two yokes, founded on inclined foundation piles. Mitre gates are double-leaf gates and the leaves form an angle pointing upstream when the gates are closed, resulting in strong gates underwater level difference. A parachute barrier is an open fabric moveable water barrier that unfolds like a parachute in horizontal direction. The principle of a reduction barrier is to reduce tidal amplitudes in a river branch, bay, or estuary by providing additional resistance near the mouth. The rolling gate is a sliding panel stored adjacent to the waterway. A rotary segment gate is similar to a segment gate, the difference is that this type of gate has a horizontal axis. A sector gate is a type of horizontally moving rotating gates. This type of gate moves over a carriageway or slideway on the sill in a river bed. The segment gate rotates around a horizontal axis through the bearing center. The gate lifts in open position and in closed position it rests on the sill. The vertical lift gates move vertically for the sill, in open position it hangs above the water. Vertical rising gates lie beneath the sill in an open position. The gate closes with vertically lifted gates and is positioned largely underwater in both open and closed situations. Finally, the visor gate is a three-hinged arc, pivoted on horizontal pins.

4.3 Verification of Conventional Storm Surge Barriers

The barrier alternatives assessment compares the several types of storm surge barriers. Seventeen different types are compared, all based on existing barriers that are already built or developed ideas. A full description of the different types of storm surge barrier is given in Appendix C.5. The score of the barrier alternatives assessment is limited to three categories: +, 0 and -, indicating favorable, neutral or unfavorable. Table 4.1 shows the barrier alternatives with their score on the different criteria. Appendix F provides reasoning of the indication for favorable, neutral or unfavorable for each storm surge barrier type.

Criteria	Barge gate	Bear-trap gate	Caisson structure	Flap gate - floating	Flap gate - hydraulic	Inflatable barrier	Mailbox gate	Mitre gate	Parachute barrier	Reduction gate	Rolling gate	Rotary segment gate	Sector gate	Segment gate	Vertical lifting gate	Vertical rising gate	Visor gate
Fast opening/closing underwater level difference	-	0	+	+	+	+	0	-	0	N/A	-	0	0	+	+	+	+
Effect on flow area (keep intertidal area favorable, normal conditions)	+	+	+	+	+	0	+	+	+	-	-	+	-	+	+	+	+
Structure/foundation simplicity	+	+	+	-	0	0	0	0	-	+	0	-	-	0	+	-	0
Building cost	+	0	+	-	0	-	-	-	+	+	0	-	-	0	+	-	+
Maintenance	+	-	+	0	-	-	0	0	+	+	-	+	0	0	+	-	0
Remain unique sediment character San Luis Pass	-	+	+	-	0	0	+	0	+	-	-	+	-	+	+	+	+
Small vessels passing under normal conditions	+	+	-	0	0	+	+	+	+	+	+	+	+	+	+	+	+
View blocking	0	+	0	+	+	0	+	-	+	-	-	+	-	-	-	+	-
Combination surge barrier with bridge	0	0	0	0	0	0	+	0	+	+	0	0	0	0	0	0	0

Table 4.1: Barrier alternatives assessment

4.4 Evaluation of Conventional Storm Surge Barriers

The evaluation of the barrier alternatives assessment reveals that there are six potential concepts for the San Luis Pass. The alternative eleven concepts did not meet the requirements or had too many disadvantages in comparison to the others. The six gates that follow from the barrier alternative assessment are: bear trap gate, caisson structure, parachute barrier, segment gate, vertical lift gate and visor gate. These six gate types can be split into two categories, depending on how they are stored under normal conditions: above or below water. The position of the storm surge barrier under normal conditions is an important aspect that determines whether or not there is an open view. The four options stored above water are: vertical lifting gate, visor gate, caisson structure, and segment gate. The main limitations of these alternatives are that they need a fixed bed and thus disrupt the view under normal circumstances. The two options stored underwater are: bear trap gate and parachute barrier. The main constraints of these alternatives are their sensitivity to sediment and maintenance difficulties. The six barriers are described in more detail below.

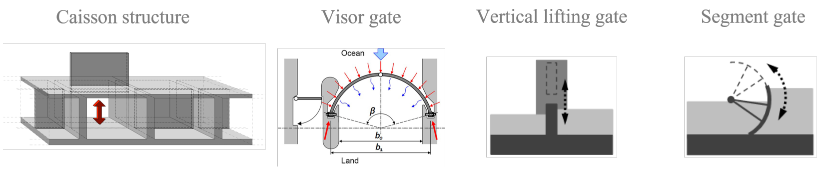

Figure 4.3: Barrier types above water under normal conditions

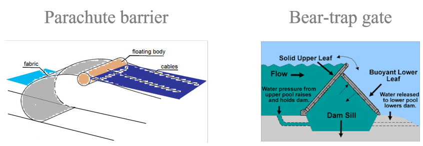

Figure 4.4: Barrier types below water under normal conditions

Caisson Structure

The caisson structure has the advantage that it is easy to construct, cheap, causes a relatively small reduction of the flow area of the San Luis Pass and doesn't require a deep foundation. On the other hand, no vessels can pass underneath during normal or extreme conditions. Figure 4.3 illustrates this barrier type.

Visor Gate

The visor gate has the advantage that relatively little material is required for production due to the curved gate. It can open/close under head difference, but can not deal with a negative head as it would then require a convex curvature on both sides. Additionally, maintenance and inspection are challenging, and dynamic stability is a concern. Figure 4.3 illustrates this barrier type.

Vertical Lifting Gate

The vertical lifting gate comes with the benefit of a large span (up to 300 m), relatively simple maintenance and inspection, and controlled operations under flow and waves. High lift forces and view obstructions are disadvantages. Figure 4.3 illustrates this barrier type.

Segment Gate

The segment gate's material efficiency and relatively simple maintenance and inspection are its primary benefits. The disadvantage is that a stiff support axis is requires and the view is blocked under normal conditions. Figure 4.3 illustrates this barrier type.

Bear-Trap Gate

The bear-trap gate is inexpensive and overflow is permitted. The drawback is that maintenance and inspection are more difficult because the structure is submerged during normal conditions. Due to the salt content of the sea, the structure needs to be replaced relatively often due to corrosion. However, the bear trap gate is kept underwater, and given the pass's dynamic nature, the construction will most likely never return to its original place. Furthermore, because the bear-trap gate's water inflow is at the bottom surface, a large amount of sediment is likely to enter the area. This can be solved or reduced by increasing the water's entrance to about 2/3 m above the bottom surface level. Figure 4.4 illustrates this barrier type.

Parachute Gate

The environmental effect of the parachute barrier is minimal, and it can be adjusted to fit different heights. The negative is that much more research is required, as well as the construction of a new bridge to support the stability cables of the parachute barrier. However, the parachute barrier is also stored underwater and due to the dynamic character of the pass the structure will probably soon or never go back to the original position. Figure 4.4 illustrates this barrier type.

4.5 Result and Discussion

The selection of conventional storm surge barrier indicates that there are six potential concepts for design of the storm surge barrier in the San Luis Pass. The six options are divided into four stored above water and two stored below. The four options stored above water (vertical lifting gate, visor gate, caisson structure and segment gate) require a fixed bottom and disrupt the view. The two options stored below water (bear trap gate and parachute barrier) are sensitive to sediment movement and difficult to maintain. From these six potential concepts, the caisson structure combined with a vertical lifting gate concept appears to fit best. The main disadvantage remains the view-blocking under normal conditions. Therefore, the advantage of this solution is limited to a minimal influence on the intertidal area. Figure 4.5 shows the proposed solution, with minimum impact on the environment. This barrier consists of vertical lifting gates. The benefits of this proposed solution are:

- Easy to construct and relatively cheap
- Minimum influence on the environment

- Bridge could be used as evacuation route due to increase height

The main goal of this thesis is to develop a conceptual design for the storm surge barrier at the San Luis Pass whilst also taking the local natural habitat into account. When limiting the aspect to minimal impact on the flow area through the San Luis Pass, this design would be successful. However, the view is disrupted under normal conditions meaning this design would most likely never be deemed applicable in this situation and thus never used. The more realistic solution would also include no disruption of the view under normal conditions, no bottom protection, whilst still having a minimum influence on the environment. This renders the conventional storm surge barrier for the San Luis Pass unsuitable as a solution. Therefore, the next chapter will introduce the shade curtain barrier as a more suitable alternative for the San Luis Pass.

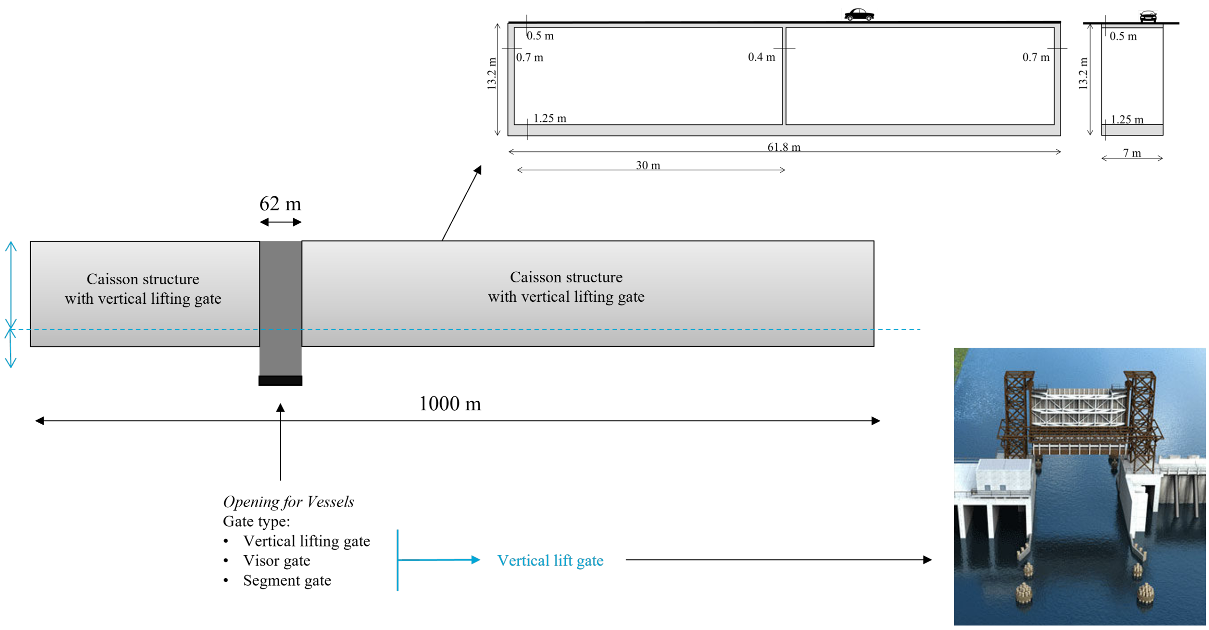

Figure 4.5: Proposed solution for the San Luis Pass, storm surge barrier, with minimum impact on the environment

5

Development of a New Concept: The Shade Curtain Barrier

This chapter introduces the development of a new concept, a shade curtain barrier. Section 5.1 introduces the concept of the shade curtain barrier, including the two different designs. Section 5.2 provides the description of the elements of these barrier designs. Section 5.3 describes the different phases of the barrier. These phases are the inactive, rolling down, retaining and rolling up phase. Section 5.4 is the structural verification of the design. This includes identification and analyzing the failure mechanisms and the load distribution under hurricane conditions. Section 5.5 describes the laboratory experiments of these designs. Section 5.6 gives the result and discussion concerning the two designs. This chapter corresponds to the fourth and fifth step in the methodology.

5.1 Introduction of the Shade Curtain Barrier

This section introduces the shade curtain barrier and describes the design process of the innovative shade curtain barrier. The previous chapter showed that no optimal solution was found with the existing storm surge barriers for the San Luis Pass. Therefore, a different barrier was needed. Understanding the system of the San Luis Pass and knowing the different gate types (proven concepts and innovative ideas) allows for taking a step back and thinking of the main aspects for the design of the storm surge barrier at the San Luis Pass. These main five aspects are:

- Protection against storm surge
- Bottom of San Luis Pass can be non-uniform
- No visual impact under normal conditions
- Connected to the bridge
- Retaining the flow area of San Luis Pass

In a brainstorm session where out-of-the-box-thinking was encouraged, the idea of a shade curtain barrier was found. The shade curtain barrier operates like a window shade curtain (roller blind); it rolls down during a hurricane, and is stored under the bridge in normal conditions. Follow-up questions like how to make it water tight, deal with the dynamics of the pass, rapidly changing water currents, force distribution and flexible bottom resulted in two types: a sinking and floating element. The method used to waterproof the structure distinguishes the sinker and floater designs. The separate elements will be discussed in further detail in Section 5.2 and illustrated in respectively Figure 5.1 and 5.2.

The material of the curtain is flexible membrane fabric. Previous research showed that membrane barriers are a good alternative for protection, costs, and effects on local view. So far, three type of membrane barriers: inflatable barrier ('Balgstuw' in Ramspol in the Netherlands and improved and scale enlargement of the inflatable barrier (van Breukelen, 2013)) and two innovative designs: the parachute barrier (van der Ziel, 2009) and tsunami barrier (Hofland et al., 2016) have already been designed. The main advantage of using membrane is that the stresses are pure tension and bending moments are absent (Marissen et al., 2013).

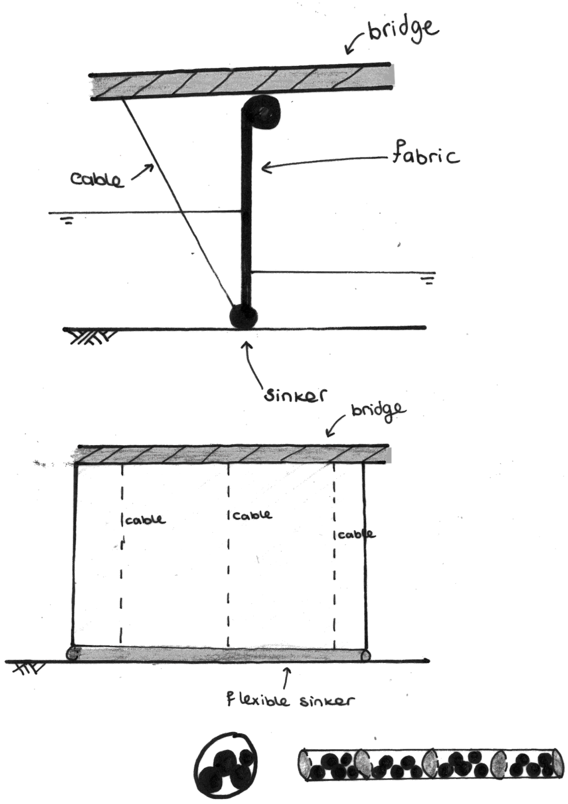

Figure 5.1: Cross-section shade curtain barrier *sinker*. Upper: side view, lower: front view

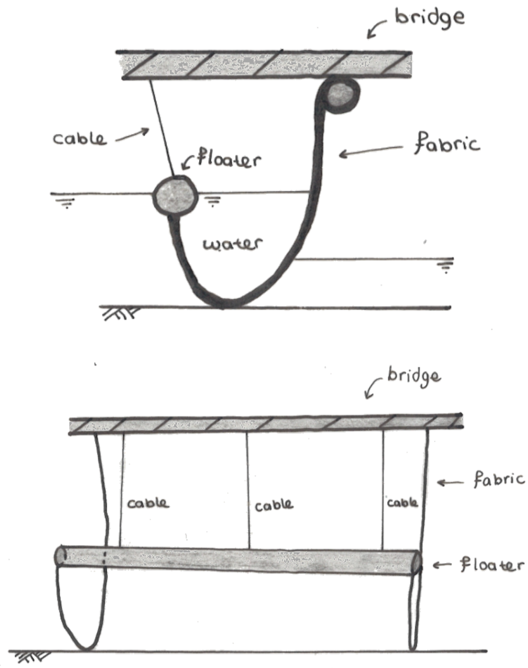

Figure 5.2: Cross-section shade curtain barrier *floater*. Upper: side view, lower: front view

5.1.1 Sinker Design

The shade curtain barrier sinker consists of flexible membrane fabric with a flexible sinker on the bottom. The sinker consists of a tube of flexible membrane fabric filled with metal balls. As the sinker is flexible, the precise water depth or bottom bumps don't matter, as gravity will compel it to close solidly at the bottom. The sinker is attached to the bridge using cables. These cables distribute the force along the bridge and prevent the curtain from moving towards the Galveston Bay side. The curtain barrier is connected to the bridge piles with a small slide and cable chain. The shade curtain is lowered when a hurricane approaches and raised after the storm has passed. The idea of the shade curtain barrier sinker is illustrated in Figure 5.1. Figure 5.3 shows the 3D impression of the barrier during hurricane conditions.

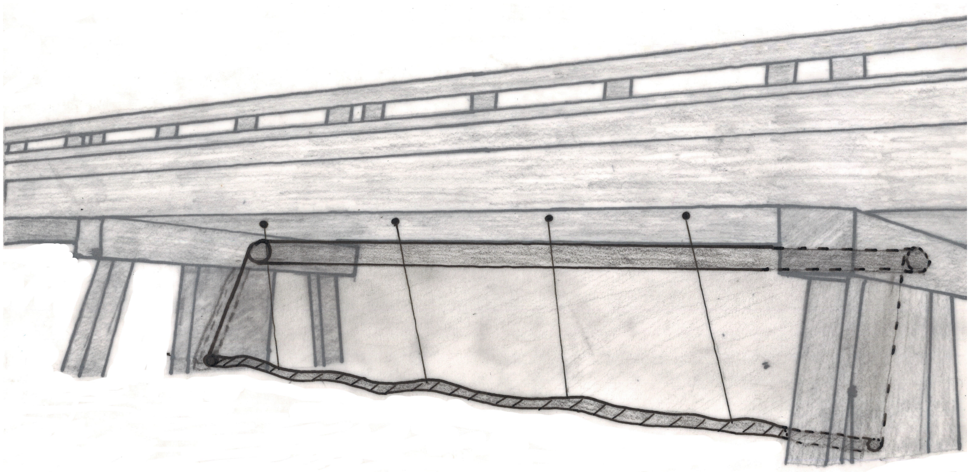

Figure 5.3: 3D impression of shade curtain barrier sinker under hurricane conditions. *Note, not to scale.*

5.1.2 Floater Design

The shade curtain barrier floater differs from the previous design in that it has a floater instead of a sinker. The flexible membrane fabric and floater combine to form a bag. When the shade curtain is lowered and water level rises, the bag automatically fills with water. The pressure provided by the water inside the bag should ensure that the bottom and sides are watertight. The floater is connected to the bridge with cables. The cables distribute the force from the floater to the bridge and guarantee that the bag has enough breadth. Figure 5.2 illustrates side and front cross-sectional views of this design. And Figure 5.4 depicts the barrier's 3D appearance under hurricane conditions. The floater design has the added benefit compared to the sinker design, that is opens automatically when there is negative head. Negative head means that the higher water level is on the opposite side of the barrier than was initially expected (in this case on the Bay side instead of the Gulf side).

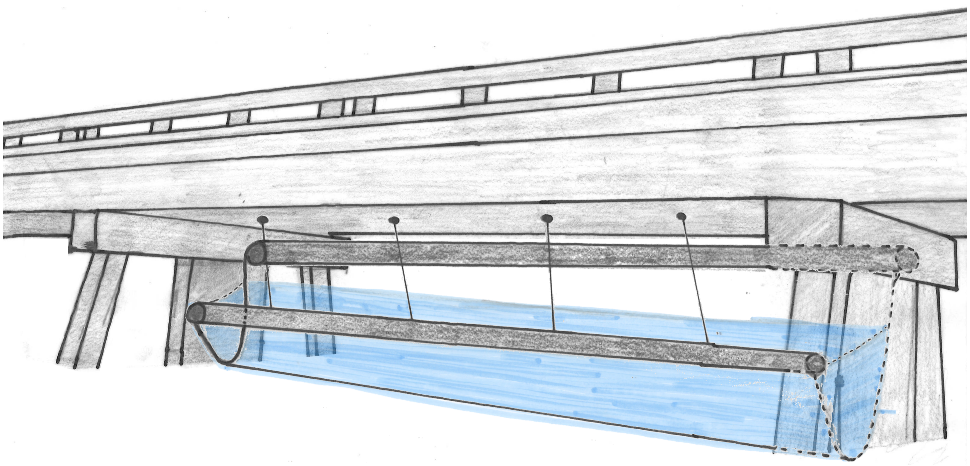

Figure 5.4: 3D impression of shade curtain barrier floater under hurricane conditions. *Note, not to scale.*

5.2 Description of Elements

The description of the elements contributes to the comprehension of the operation and functionality of this new barrier type and designs. It is essential to comprehend the function of each component of this barrier type in order to comprehend the function in the various phases and identify the various failure mechanisms. The majority of the elements of the two designs are the same; only the sinker and floater are different. The elements and their primary roles are outlined in detail below. Figure 5.1 and 5.2 illustrate the elements of the sinker and floater design, respectively.

Bridge

In the future, the San Luis Pass bridge will need to be reconstructed, hence it would be best to include a storm surge barrier. In this design, the bridge functions as a foundation of the barrier. The bridge forms the frame that the shade curtain barrier is hung on. The structure is connected by the rotating axis and cables, and transfers the load from the flexible membrane fabric to the bottom surface. In this design, it is assumed that the current bridge is capable of withstanding the barrier's loads.

Cable

The main function of the cable is to keep the sinker/floater at the required position. The cables are adjustable and placed at regular intervals along the sinker/floater. Under normal conditions, the cables hold the sinker/floater under the bridge. During a hurricane, the cable holds the tensile load from the sinker/floater.

Flexible Membrane Fabric

The flexible membrane fabric main function is to retain the water during a hurricane event. The flexible membrane fabric is made of flexible membrane fibers woven to fabric. The exact type of flexible membrane fabric depends, among other things, on the required strength, flexibility, maximum strain in fiber and machining technique. For example the Dyneema® flexible membrane fabric could be used, this is strong (up to 1 GPa) and waterproof (DSM, 2022). For the sinker design specifically, the flexible membrane fabric transfers the mainly horizontal load to the sinker and rotating axis/bridge. For the floater design specifically, the flexible membrane fabric generates a bag that fills itself with water to ensure the water tightness and transfers the load to the floater and rotating axis/bridge.

Rotating Axis

The main function of the rotating axis is to store the flexible membrane fabric under normal conditions. During hurricane conditions, hold the flexible membrane fabric at the required length and transfer the load to the bridge. The dimensions of the rotating axis depend on the load.

Connection to the Bridge

The connection between the structure and bridge is different for the two designs. For the sinker design specifically, is the connection like a cable/rails that goes down in a gutter. The line of the gutter should be a curvature. The gutter could also be used for load derivation from the flexible membrane fabric to the bridge piles. Figure 5.5 shows a drawing of how the cross-section of a connection could look like.

For the floater design specifically, there are two possibilities. One of the possibilities is a gutter in the piles of the bridge, just like the sinker design. Another possibility is creating holes in the piles of that bridge. Using suction, the bag of water can be drawn into these holes to connect it to the sides of the bridge before the hurricane arrives. Once the bag fills, the water in the bag provides an outwards pressure that ensures a water tight connection between the bridge and structure.

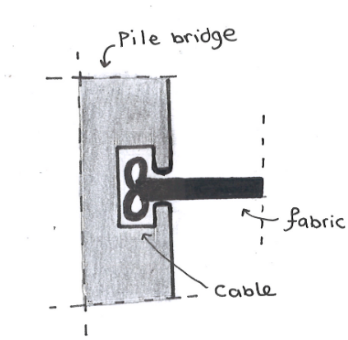

Figure 5.5: Connection of curtain barrier sinker with the bridge

Sinker

The main function of the sinker is to keep the fabric in place and ensure that the structure is watertight along the bottom surface. The sinker is made out of flexible material, so there is no hard structure bottom liner required to close the gap. The sinker consists of small compartments off for example heavy metal balls. Figure 5.6 shows an illustration of what the sinker could look like.

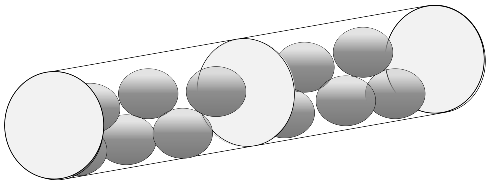

Figure 5.6: The sinker with the compartments in 3D

Floater

The main function of the floater is to maintain the water bag by holding the flexible membrane fabric up and allowing waves to overflow. The floater provides the uplift force by the buoyancy of the element. The exact design of the floater is not design yet, and should be research in-depth. It is assumed that the floater is designed to withstand the stresses due to the water force, waves, cables, and flexible membrane fabric. The function of the water inside the water bag is to create vertical water pressure that ensures a waterproof structure. The flexibility of the water and flexible membrane fabric ensures it does not matter what the bottom surface looks like, it will form around it.

5.3 Description of Phases

The description of phases contributes to the understanding of the operation and functionality of this barrier type. It is essential to comprehend the different phases of the two designs of this barrier type, in order to identify the various failure mechanisms in the different phases. The description of phases is divided into four phases of the barrier: inactive, rolling down/up and retaining phase. The sinker and floater designs are separately described below, and respectively illustrated in Figure 5.7 and 5.8. The inactive phase of the barrier is under normal conditions. The rolling down phase is just before a hurricane arrives at Galveston. The retaining phase of the barrier occurs when a hurricane is coming from the Gulf of Mexico and the eye makes landfall east of the San Luis Pass. The rolling up phase is after the hurricane has passed.

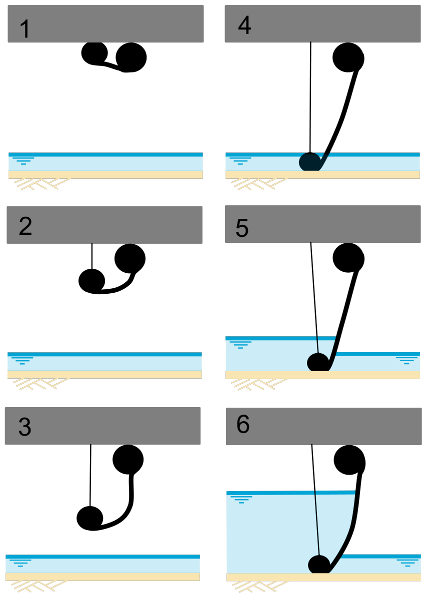

Figure 5.7: Phases shade curtain barrier sinker design. *Note, not to scale.*

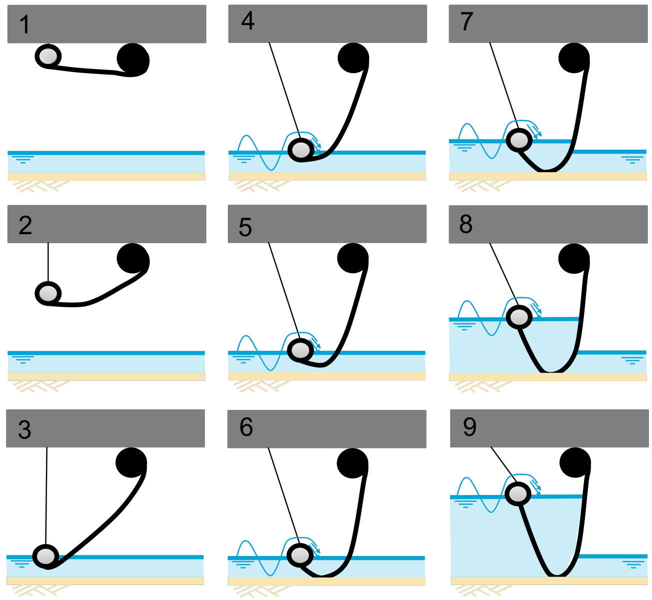

Figure 5.8: Phases shade curtain barrier floater design. *Note, not to scale.*

5.3.1 Sinker Design

Inactive phase barrier
Step 1: The barrier is inactive under normal conditions and the barrier hangs under the bridge. The cable is at its shortest and the flexible membrane fabric is fully rolled up on the rotating axis. In this phase, there is no reduction of flow area and visual impact due to the barrier.

Rolling down phase barrier
Step 2: The cable is lowered, and the rotating axis slowly gives more flexible membrane fabric.
Step 3: Continuation of previous step.
Step 4: The moment when the sinker just touches the bottom surface.
Step 5: The water level slowly rises. The sinker moves slightly towards the low waterside due to the pressure water pressure. The cable prevents the shade curtain from moving towards the low waterside.

Retaining phase barrier
Step 6: The retaining water level height is the bridge height. The flexible membrane fabric retains the water from the bay. The sinker ensures that the flexible membrane fabric is watertight with the bottom. And the cable prevent the flexible membrane fabric from moving toward the low waterside

Rolling up phase barrier
The rolling up phase is similar to the rolling down phase, only in reverse. The shade curtain is rolled up when the hurricane has passed, at this moment the water level on both sides of the barrier is the same. The rolling up phase of the barrier is illustrated in step 5-2, in Figure 5.7.

5.3.2 Floater Design

Inactive phase barrier
Step 1: The barrier is inactive under normal conditions and the barrier hangs under the bridge. The cable is shortest and the flexible membrane fabric is totally rolled up on the rotating axis. In this phase,

there is no reduction of flow area and visual impact due to the barrier.

Rolling down phase barrier
Step 2: The cable is lowered, and the rotating axis gives slowly more flexible membrane fabric.
Step 3: The moment when the floater just touches the water.
Step 4: The waves are just getting over the floater into the bag.
Step 5: The bag is filled due to overtopping waves.
Step 6: the moment when the water bag just touch the bottom surface.
Step 7: The water level keeps rising.
Step 8: The water level keeps rising.

Retaining phase barrier
Step 9: The water level is up, the cable transfers the tensile force to the bridge, and the water bag is fully filled with water. The flexible membrane fabric retains the water from the bay. The floater ensures that the flexible membrane fabric makes a bag and therefore retains the water. The cable prevents the floater from moving toward the side of lower water level.

Rolling up phase barrier
The rolling up phase is quite similar to the rolling down phase, only in reverse. The shade curtain is rolled up alongside the water level is going down, this happens after the hurricane has passed. While the water level is going down, the floater is going down as well. The moment, the water level is the same on both side of the barrier, the structure can be stored under the bridge. The rolling up phase of the barrier is illustrated in step 8-2, in Figure 5.8.

5.4 Structural Verification of Designs

The feasibility of the novel shade curtain barrier designs greatly depends on its ability to function both in normal and extreme circumstances. An important step towards recognizing it as a realistic and feasible design is the structural verification. The structural verification of the sinker and floater design consists of identifying the different failure mechanisms, and load distribution under hurricane conditions.

5.4.1 Failure Mechanisms

There are numerous failure mechanisms for storm surge barrier designs. The specific design and local environment determines whether they pose a significant risk. The failure mechanisms for the two design are quite identical, namely piping, scour, wave overtopping, failure of the bridge, damage to flexible membrane fabric, and specificity for the floater also uplift of the water bag. The different failure mechanisms are all presented in hurricane condition.

Piping

Piping is groundwater flow in a permeable soil under a structure, resulting in erosion. Groundwater flow across a hydraulic structure is caused by a water level difference. The piping paths follow the geometry of the structure. A water level difference only occurs under hurricane conditions. The maximum water level difference is 6 m at the San Luis Pass, explained in Appendix H.1. There are different design tools that describe the critical situation in which piping can occur. These design tools are all based on empirical formulas based on research. The most commonly used design tools are Bligh's method and Lane's method (Molenaar and Voorendt, 2020). However, this design tool assumes a long time water level difference. This is not the case for the San Luis Pass. The duration of a hurricane is, in order of magnitude, hours.

Rijkswaterstaat has set a maximum allowable hydraulic gradient for short time flood defenses. This design rule states that a safe permissible value for the hydraulic gradient is 0.5 (Rijkswaterstaat -

Techical Advisory Committee on Flood Defences, 2002), calculated by equation 5.1. This results in a vertical length of 12 m. Concluding, the two curtain barrier designs will probably fail due to piping under the structure. However, it is unknown whether the flexibility of the flexible membrane fabric can reduce the risk. In case of the floater design, the water bag might be made wider to get the necessary length as the flexible membrane, fabric, behaves like a geotextile.

The significance of this failure risk can therefore be determined through laboratory experiments, as described in Section 5.5.

$$i_{\mathrm{max}} = \Delta H / L \tag{5.1}$$

In which:

i_{max}	[-]	Maximum (allowed) hydraulic gradient
L	[m]	Total seepage distance, which is the distance through the soil where the water flow is impeded by the soil structure
ΔH	[m]	Differential head across structure

Scour

There are two types of scour: one caused by waves and one by currents. Scour caused by waves is generated due to the interaction of the waves and structure, which could threaten the stability of the structure. This type of scour is not a direct problem for this design. This is because the shade curtain automatically sinks down into the scour hole for both designs. Scour caused due to currents only happens when the shade curtain is not descending and results in a strong current that could cause damage to the foundation of the bridge. The flow velocity in this case depends on the water level difference. The water level difference is 6 m, resulting in a maximum flow velocity of 10.8 m/s. The corresponding maximum scour depth is 6.3 m, this is elaborated upon in Appendix H.6.

Wave Overtopping

Another potential failure mechanism is wave overtopping over the bridge. This could be solved by adding a structure on top of the bridge. However, wave overtopping does not seem an issue for the bay considering the height difference between the water surface and the bridge. Therefore, the is no significant risk of failure due to wave overtopping.

Failure of Bridge

The bridge serves as the structure's foundation, failure of the bridge causes the entire structure to collapse. In the near future, the bridge must be replaced, since determined by the system analysis. It is therefore assumed in this research that the bridge can withstand the forces and that its design is similar to the existing bridge. This failure mechanism, sufficient strength of the bridge, is therefore not elaborated upon further. However, it is possible to estimate the forces that must be considered when designing a bridge. The sinker and floater design have a different force distribution under hurricane conditions. Therefore, Section 5.4.2 provides a qualitative derivation of load for the two designs.

Damage to the Flexible Membrane Fabric

Damage to the flexible membrane fabric could result in failure of the structure. However, it is debatable how unacceptable it is deemed that one of the shade curtain may fail. For example, at the Eastern Scheldt Barrier in the Netherlands three separate gates can fail and it retains still enough water to prevent flooding of the hinterland. This failure mechanism is therefore not discussed in detail.

Uplift of Water Bag

This failure mechanism is only for the floater design. Uplift of the water bag would be disastrous for the barrier. If water flows under the water bag, it pushes the water out of the bag, consequently the structure fails. It is difficult to estimate the failure risk associated with this event. Due to the lack of research on flexible membrane fabrics as a water barrier, it is possible to conduct an experiment to determine if this poses a significant risk. This is further elaborated upon in Section 5.5.

5.4.2 Load Distribution under Hurricane Conditions

The sinker and floater each have a different load distribution. This section provides a qualitative derivation of load for the two designs. On the Gulf of Mexico side, the external forces are largely due to wave and hydrostatic load, whereas on the Galveston Bay side, solely hydrostatic pressure is present. The sinker and floater designs are described in more detail below.

Sinker Design

The sinker design has the following load distribution: horizontal external force is acting on the flexible membrane fabric. Distributing to the rotating axis/bridge deck and sinker. The sinker transfers horizontal force to the cable. Due to the angle of the cable, its vertical component must be equal to or larger than the weight of the sinker to ensure stability. Figure 5.9 depicts qualitatively the force distribution of the shade curtain barrier sinker.

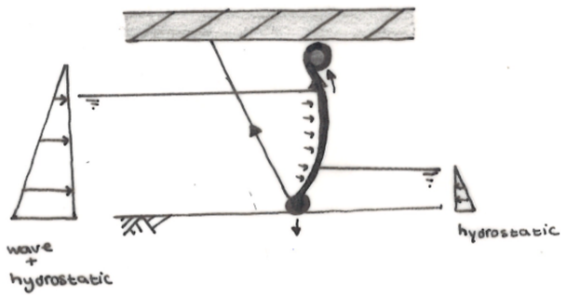

Figure 5.9: Force distribution under extreme conditions sinker curtain barrier. The left side is the Gulf of Mexico and the right side is Galveston Bay.

Floater Design

The floater design has the following load distribution: horizontal external force is acting on the flexible membrane fabric at the high waterside. The water inside the water bag provides pressure that guarantees the water tightness of the bottom and sides. The weight of the water within the bag keeps the water bag on the ground. The floater ensures that a water-retaining bag is generated. The waves can overtop the floater, therefore continuously (re-)filling the water bag with water. The cables transfer the floater's forces to the bridge. Figure 5.10 depicts the distribution of force under hurricane conditions.

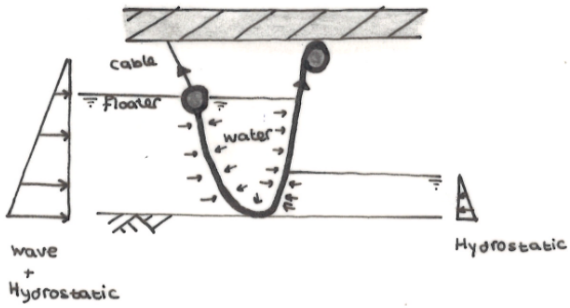

Figure 5.10: Force distribution under extreme conditions floater curtain barrier. The left side is the Gulf of Mexico and the right side is Galveston Bay.

5.4.3 Result Structural Verification

The structural verification has revealed that certain failure mechanisms are more concerning than others. The results of the structural verification indicate that the failure mechanism piping has an extremely high probability of occurring. This holds true for both sinker and floater design. The maximum flow velocity results in a maximum scour depth of 6.3 meters. Overtopping of waves is not a significant failure risk for the structure. Due to the early design stage, it is difficult to determine the probability of failure for the failure mechanisms bridge failure, damage to the flexible membrane fabric, and water bag uplift. As a result of the failure mechanism piping both of these structural designs are likely to fail.

5.5 Laboratory Experiment

The laboratory experiments provide information about the feasibility of these designs and indicate the probability of certain failure mechanisms. The laboratory experiments of the shade curtain barrier were preformed, on a sandy bottom for the sinker design and glass bottom for the floater design, in a wave flume at Delft University of Technology. The wave flume had a with of 44 cm and height of 40 cm. The flexible membrane fabric used during these experiments is tarpaulin, which is waterproof and weighs 100 gr/m^2. Not taken into account are scaling effects.

5.5.1 Sinker Design Experiments

The laboratory experiments of the sinker design essentially revealed that the structure fails immediately, due to piping. As time passes, the sinker continues to fall further into the scour hole but does not stop the process. Therefore, the experiments demonstrated what the theory had already expected, the structure fails due to piping and scour. Figure 5.11 shows a photograph during the laboratory experiment. This figure clearly illustrates that this design fails due to piping and scour. Appendix I.3 described the laboratory experiment of the sinker design shade curtain barrier in detail, including through photographs.

5.5.2 Floater Design Experiments

The laboratory experiment of the floater design demonstrates that the concept of a water bag holding water is feasible. However, it was confirmed that a flow occurs beneath the water bag. This is when the experiment was conducted over a glass bottom during the experiment. In the case of a sandy bottom, a large scour hole forms. Figure 5.12 shows a photograph during the laboratory experiment. This figure demonstrates that water is already flowing beneath the water bag, indicating that this experiment will fail immediately if conducted on a sandy bottom. Appendix I.4 described the laboratory experiment of the floater design shade curtain barrier in detail, including through photographs.

5.5.3 Conclusion Experiments

Laboratory experiments of both the floater and the sinker design revealed what the theory already indicated, the structure fails due to piping and scour. Appendix I describes the laboratory experiments of the different types of shade curtain barrier in detail.

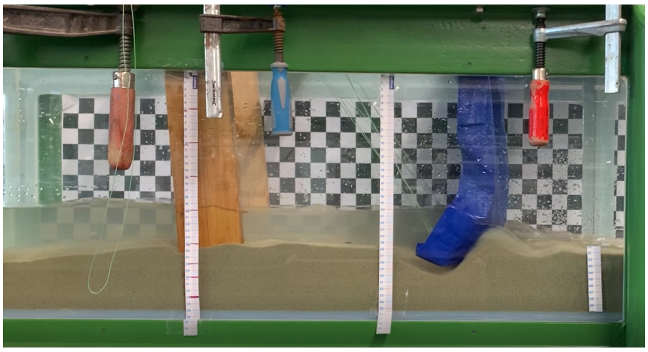

Figure 5.11: Experiment Shade Curtain Barrier sinker design. Photograph during the experiment on sandy bottom.

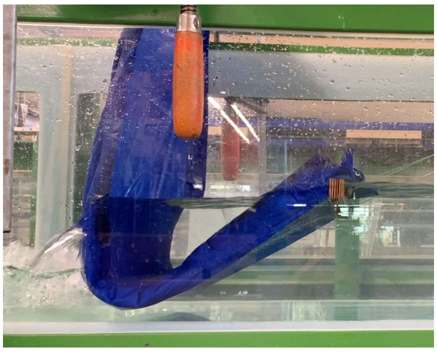

Figure 5.12: Experiment Shade Curtain Barrier floater design. Photograph during the experiment on glass bottom.

5.6 Conclusion and Discussion of New Developed Concept Designs

A storm surge barrier in the San Luis Pass should reduce the probability of flooding for the Galveston Bay Area. Currently, the conventional storm surge barrier did not fulfill not all the requirements and criteria for the San Luis Pass. Therefore, this chapter provided a new idea for a storm surge barrier, a shade curtain/roller blind. This resulted in two design types: sinker and floater. The ideas seemed promising in terms of protection against storm surge, no view disruption, no bottom protection required and flow area in San Luis Pass remains the same. However, both designs have several limitations and concerns. These are separately described below.

A corresponding discussion point is the rotating axis. What are the required dimensions of the rotating axis? Is vibration a problem for this axis? Vibration is beyond the scope of this thesis, but is also a concern and should be investigated in further research.

Sinker Design

The piping is the primary limitation of the sinker design, as demonstrated by both theory and laboratory experiments. The question arises, what happens when water flows under the sinker. Does the sinker go down due to its own weight, as expected, or will something else happen. Another uncertainty is the design of the sinker. What material should be used for the sinker compartment (for example a metal), and what will be the dimensions.

Floater Design

The main concern for the floater design is uplift of the water bag and corresponding piping. If water starts flowing under the water bag, the water inside the water bag will flow out. Resulting in failure of this design, both theory and laboratory experiment reveals that. Furthermore, a sinker is easier to construct than a floater. Piping is a failure mechanism that is likely to occur. However, the width of the water bag could be adjusted to create the required width to prevent piping. The flexible membrane fabric is waterproof and therefore behave like a geotextile.

Discussion of Result

The two designs should be combined to create a design that limited the amount of concerns in the design of the shade curtain barrier. This optimized design should have a sinker, since it is easier to construct, and a long width of flexible membrane fabric on the bottom surface to prevent the risk of piping and erosion. In the next chapter, this design is further elaborated.

6
Optimization of the Shade Curtain Barrier

This chapter provides a more optimized design of the shade curtain barrier after evaluation of the result and discussion of the sinker and floater design, described in Chapter 5. This optimized design is explained in Section 6.1. Afterwords, the optimized design will be referred to as the shade curtain barrier. Section 6.2 provides the structural verification of the shade curtain barrier, including the identification of the failure mechanisms, analysis of load under hurricane conditions. Section 6.3 described the laboratory experiments. Section 6.4 proposes the final design for the storm surge barrier at the San Luis Pass in Texas, United States of America. Lastly, Section 6.5 describes the discussion of this shade curtain barrier design concept. This chapter corresponds to the sixty and seventy step in the methodology.

6.1 Optimized Design

The understanding of the novel optimized shade curtain barrier design is crucially important for the feasibility of the design and implementation at the San Luis Pass. Therefore, this section provides a conceptual understanding of the operation and functionality of this design. First, a description of the optimized general design and a difference between the sinker and floater designs are given. Continuing with the different elements and phases of the barrier.

6.1.1 General Design and Difference with Previous Designs

The analysis of the sinker and floater design revealed various restrictions regarding their general designs, mostly due to the failure mechanisms for specific the San Luis Pass. The most concerning failure mechanism in both previous designs (sinker and floater) is piping. Another thing to take into account is that the construction of a sinker is easier than a floater. Therefore, the new optimized design consists of a sinker but in such a way that it should prevent piping. The piping is prevented by using the flexible membrane fabric as geotexile along the sand bed. The required length to prevent piping, two times the maximum water level difference (Rijkswaterstaat - Techical Advisory Committee on Flood Defences, 2002), is added to the height of the bridge above the bottom surface for the total length of the flexible membrane fabric. The new optimized design will henceforth be referred to as the shade curtain barrier. Figure 6.1 illustrates the shade curtain barrier, including the elements. The different elements are further elaborated upon in the next paragraph.

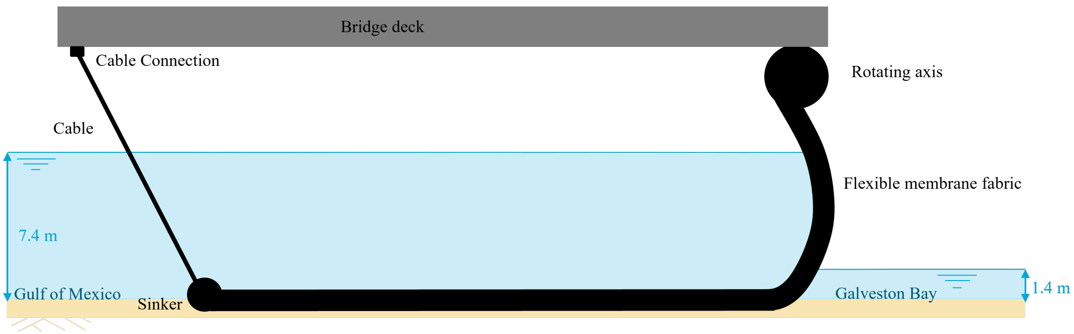

Figure 6.1: The shade curtain barrier, including the elements. *Note, not to scale.*

6.1.2 Description of Elements

This section contributes to the comprehension of the operation and functionality of this design by analyzing the shade curtain barrier's elements. It is crucial to understand the function of each component of this barrier type in order to comprehend the function in each phase and identify the various failure mechanisms for this barrier.

The design of the shade curtain barrier assumes that the barrier will hang beneath the bridge deck. Actual barrier components consist of a rotating axis, a flexible membrane material, a sinker, and a cable. The sinker is located at the end of the flexible membrane fabric on the high waterside. The sinker is connected to the bridge by a cable. Under the bridge, the rotating axis is located. It stores the flexible membrane fabric under normal conditions. Figure 6.1 illustrates the shade curtain barrier with the different elements. All the elements are already described in the previous chapter, Section 5.2. However, there are several additions for the sinker and flexible membrane fabric. Regarding the sinker, it does not need to be 100% watertight, as the flexible membrane fabric makes sure that the construction is able to hold sufficient amount of water and it is simply unrealistic to create a full, airtight closing.

Regarding the flexible membrane fabric, this has an additional function, namely to avoid piping. The flexible membrane fabric has a substantial horizontal length that rests on the ground and works as a geotextile. The primary benefit is that no rigid construction is required for bottom protection or barrier closure as the water pressure will press the membrane fabric against the bottom, no matter its structure. It will not matter whether the surface has sediment humps or erosion gaps for example. Due to its flexibility, the flexible membrane fabric will follow the bottom surface.

Another advantage of the flexible membrane fabric is that there will fewer forces carries off to the cables as they will be affected by the fabric's contact with the ground surface. This friction influences the force distribution in the barrier positively. The exact impact of this friction is unknown and must be investigated before it can be included.

6.1.3 Description of Phases

This section contributes to the comprehension of the operation and functionality of this design by analyzing the shade curtain barrier's phases. Afterwords, these phases are used to identify the different failure mechanisms. There are four phases of the barrier: inactive, rolling down, retaining, and rolling up. The phases are illustrated in different steps in Figure 6.2.

Inactive phase barrier
Step 1: The barrier is inactive under normal conditions. The elements are stored under the bridge. This minimizes flow limitation and visual impact.

Rolling down phase barrier

Step 2: The cable is slowly lowered, and the rotating axis slowly gives more flexible membrane fabric.
Step 3: The cable is lowered further and similarly the rotating axis provides more flexible membrane fabric.
Step 4: The sinker just touches the bottom surface.
Step 5: The cable attached to the sinker gets to the tensile strength.
Step 6: The flexible membrane fabric is rolled out over the bottom and the water level start rising.
Step 7: The water level continues rising.

Retaining phase barrier

Step 8: The retaining phase of the barrier occurs when a hurricane is coming that makes landfall east of the San Luis Pass. The retaining water level height is the bridge height. The flexible membrane fabric retains the water from the bay. The horizontal, long flexible membrane fabric ensures that the structure is water tight. The sinker is kept on the bottom by the weight and horizontally due to the cables and friction of the flexible membrane fabric.

Rolling up phase barrier

The rolling up phase is quite similar to the rolling down phase. The shade curtain is rolling up when the water level is equal again at the Gulf of Mexico and Galveston Bay. In the case the water level is higher at the Galveston Bay side, the water pushes the shade curtain upward and rolling it up is possible. The forces in this scenario are negligible compared to the hurricane scenario.

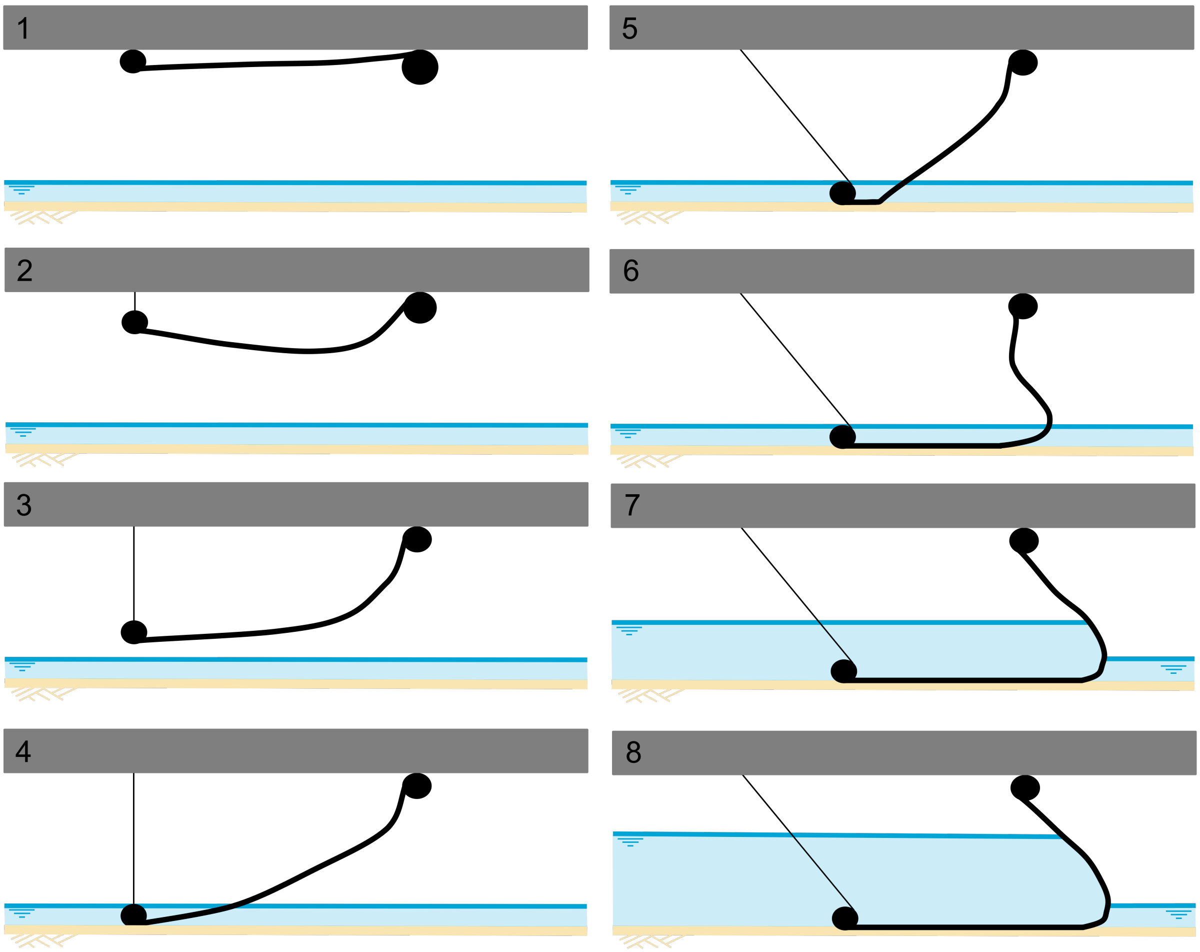

Figure 6.2: Phases of shade curtain barrier. *Note, not to scale.*

6.2 Structural Verification

The feasibility of the novel shade curtain barrier design greatly depends on its ability to function both in normal and extreme circumstances. An important step towards recognizing it as a realistic and feasible design is the structural verification. The structural verification of the shade curtain barrier design consists of identifying the different failure mechanisms and analyzing the important failure mechanisms.

6.2.1 Failure Mechanisms

There are numerous failure mechanisms for storm surge barriers. The design and local environment determines whether they pose a significant risk. The various failure mechanisms for the shade curtain barrier are described in detail below.

Piping

Piping is groundwater flow in a permeable soil under a structure, causing erosion and could result in failure of the structure. In case of the current design, this mainly occurs at the retaining phase. This failure mechanism has a significant probability of occurring and should therefore be analyzed further, elaborated upon in Section 6.2.2.

Uplift of Sinker

The uplift of the sinker means that the sinker is not on the bottom surface anymore. The sinker should have sufficient weight to remain on the bottom and ensure that the flexible membrane fabric has sufficient length to prevent piping. Therefore, this failure mechanism should be analyzed in more detail, as elaborated upon in Section 6.2.4.

Damage to the Flexible Membrane Fabric

The flexible membrane fabric could be damaged due to debris, water force, or as a result of lack of maintenance. Damage to the flexible membrane fabric can result in failure of the structure, and is a significant risk. However, the allowable amount of damage depends on the specifics of the flexible membrane fabric. Due to the fact that these characteristics are currently unknown, it is not possible to provide additional information at this stage of the design process. Therefore, this failure mechanism is not discussed in further detail.

Uplift of the Flexible Membrane Fabric

Uplift of the flexible membrane fabric could occurs under negative head, high water level on the Galveston Bay side. This is a positive development, as water can now flow from Galveston Bay to the Gulf of Mexico. It is also possible for the flexible membrane fabric to rise if water begins to flow beneath it, and it is unable to fill the area underneath itself as a result of the weight of the water on top. Due to the lack of research on flexible membrane fabrics as a water barrier, it is possible to conduct an experiment to determine whether this is a significant risk. However, this risk can also be reduced by increasing the weight of the flexible membrane fabric that lies on the bottom. The amount of additional weight can be determined by assuming the flexible membrane fabric behaves as a rigid structure and calculating the (sinker)weight required to prevent this from occurring. This is further elaborated upon in Section 6.2.4 and Appendix H.4.

Erosion under the Flexible Membrane Fabric

Erosion under the flexible membrane fabric could occur. It is uncertain whether erosion under the flexible membrane fabric poses a significant risk. A small amount of erosion is permitted, as it is anticipated that the flexible membrane fabric and the weight of the water on top will cause the fabric to fall into the erosion/scour hole. Due to the limited research on flexible membrane fabrics as a water barrier, it is impossible to determine whether this poses a significant risk. However, this hypothesis could be tested in a laboratory experiment.

Failure of the Rotational Axis

Failure of the rotational axis could result in the failure of the structure. This rotating axis holds the fabric and transfers the load on the fabric to the bridge. If this mechanism fails, the shade curtain cannot be stored again or lowered to protect the hinterland from storm surge. Failure is determined by the design of the rotating axis, in this design phase, the rotating axis has not yet been designed in detail. Consequently, this failure mechanism is not elaborated upon further.

Failure of the Bridge

Failure of the bridge results in the collapse of the entire structure, as the bridge serves as the structure's foundation. The bridge must be replaced in the near future, as determined by the system analysis. It is therefore assumed in this research that the bridge can withstand the forces and that its design is similar to the existing bridge. This failure mechanism, sufficient strength of the bridge, is therefore not elaborated upon further. Nevertheless, it is possible to estimate the forces that must be accounted for in the bridge's design. This is elaborated in Section 6.2.3.

Failure of one of the Shade Curtain Barrier Gates

One of the gates may fail under hurricane conditions, therfore this reliability should be investigated. However, it is debatable if all gates are even required to work for the entire barrier to remain effective. For example, at the Eastern Scheldt Barrier in the Netherlands, three gates can fail to close in an extreme event and the storm surge barrier is still effective. Due to the need for a more detailed design, it is currently impossible to determine the shade curtain barrier's reliability. This failure mechanism is therefore not discussed in detail. However, if one of the shade curtains does not descend, the flow velocity through this particular section is extremely high. This could result in a very deep scour, which could cause damage to the bridge's foundation. In this case, the scour depth is estimated to be 6.3 m, elaborated upon in Appendix H.6.

Failure of the Connection Cable and Anchor

Failure of the connections would result in failure of the structure. The failure of the connection between the cable and anchor would result in failure of the construction. Due to the need for a more detailed design, it is currently impossible to determine the failure of the connections. It would require additional information regarding, for example, the type of material and bridge design. Consequently, this failure mechanism is not discussed further in this research. However, it is possible to estimate the required strength of the connections under hurricane conditions. This is further detailed in Section 6.2.3.

6.2.2 Piping

Piping is groundwater flow in a permeable soil under a structure, resulting in erosion. Groundwater flow across a hydraulic structure is caused by a water level difference. The piping paths follow the geometry of the structure. A water level difference only occurs under hurricane conditions. The maximum water level difference is 6 m at the San Luis Pass, explained in Appendix H.1. There are different design tools that describe the critical situation in which piping can occur. These design tools are all based on empirical formulas based on research. The most commonly used design tools are Bligh's method and Lane's method (Molenaar and Voorendt, 2020). However, these design tools assume a long time water level difference. This is not the case for the San Luis Pass. The duration of a hurricane is, in order of magnitude, hours. Therefore, the maximum allowable hydraulic gradient for short time flood defenses of Rijkswaterstaat can be used. This design rule states that a safe permissible value for the hydraulic gradient is 0.5 (Rijkswaterstaat - Techical Advisory Committee on Flood Defences, 2002). Resulting in a required total seepage distance that is two times the water level difference. Therefore, the required seepage length is 12 m. Concluding, the failure mechanism piping is not likely to occur due to the long flexible membrane fabric on the bottom surface.

6.2.3 Load Distribution under Hurricane Conditions

The load distribution under the governing scenario, a 1/100 year hurricane event, is further elaborated upon in order to estimate the corresponding forces on the structure. Hurricane conditions cause a higher water level, wave height, and more wind compared to normal conditions. In this analysis of load distribution, wind loads are not included, but the wind generated waves and increase in water level are. The water level at the Gulf of Mexico side is significantly higher than at the Galveston Bay side. The horizontal loads under hurricane conditions are hydrostatic loads on both sides, in addition to wave load and self weight of the sinker on the Gulf of Mexico side. Figure 6.3 illustrates these forces on the shade curtain barrier.

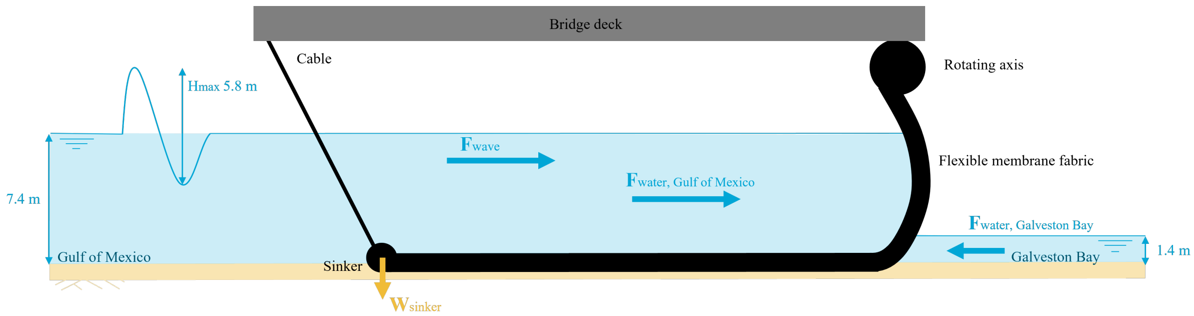

Figure 6.3: Forces on shade curtain barrier under hurricane conditions. *Note, not to scale.*

The input values for the analysis of the loads on the shade curtain barrier under hurricane conditions are given in Table 6.1. The design water depth is the cumulative of maximum water depth, high astronomic tide, sea level rise and storm surge height. For the hurricane scenario, the design water depth on the Gulf of Mexico side is 7.4 m with a maximum wave height of 5.8 m. The maximum wave height is derived from the significant wave height of a 1/100 year event, 5.0 m, as listed in Table 6.1. The design water depth at the Galveston Bay side is 1.4 m. Appendix H.1 gives a full description of the derivation of design water depth and wave height.

The external horizontal loads acting on the structure are the hydrostatic and wave load. The external vertical loads acting on the structure are the upward and downward water pressures. Figure 6.4 illustrates these loads on the shade curtain barrier under hurricane conditions for the San Luis Pass. The hydrostatic load depends on the design water depth, and the wave load on the maximum wave height.

Design height		**Water level [m]**
Sea level rise	(SLR)	0.82
Storm surge height (1/100 year)		5.2
Wave height (1/100 year)	(H_s)	5.0
High astronomic tide	(HAT)	0.4
Max water level under MSL		1
Design water depth - Gulf of Mexico	(DWD_{Gulf})	7.4
Design water depth - Galveston Bay	(DWD_{Bay})	1.4

Table 6.1: Input values for analysis loads

The hydrostatic load on the Gulf of Mexico side is 275 kN/m, and Galveston Bay side 10 kN/m. The maximum wave height is 5.8 m, part of this maximum wave will pass over the bridge. The corresponding wave load is 600 kN/m, calculated using a rule of thumb ($F_{wave}=\frac{1}{2}\ \rho g H_i^2 + d\rho g H_i$). Appendix H.2 provides a specified analysis of the loads.

The vertical equilibrium is determined by the upward and downward water pressure, illustrated in Figure 6.4. For the vertical force equilibrium, the upward water pressure is always smaller than the downwards water pressure, except for at the location of the sinker. At the location of the sinker, the water pressures are equal. Therefore, the sinker should have sufficient weight to always close off the gap and ensure the flexible membrane fabric is not 'floating' in the water. For this reason, a safety factor of 1.5 is used.

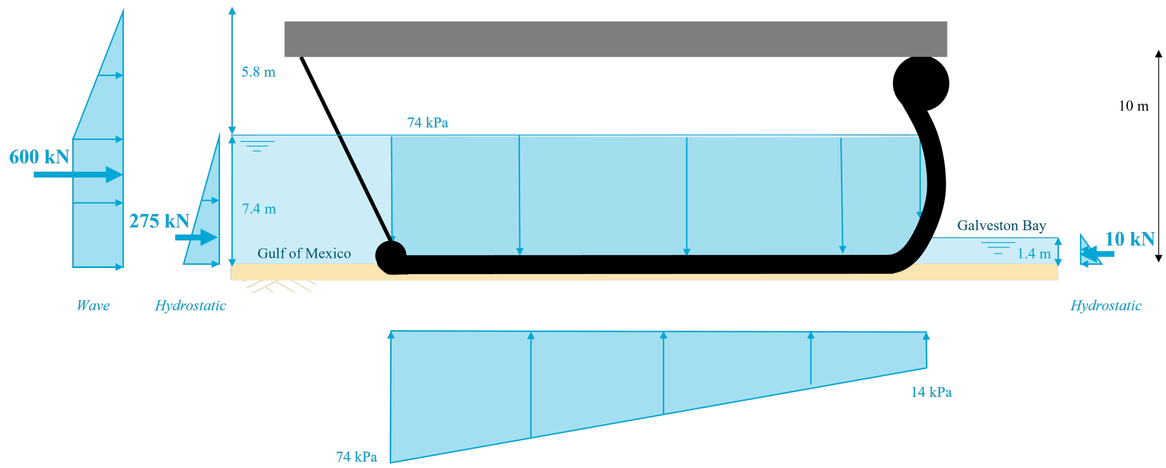

Figure 6.4: External forces on the shade curtain barrier at San Luis Pass. *Note, not to scale.*

The wave and hydrostatic loads act on the flexible membrane fabric, and transferred to the sinker and rotating axis. The total horizontal load acting on the flexible membrane fabric is roughly 800 kN/m. This results in a tensile force of 470 kN/m in the flexible membrane fabric. Appendix H.3 provides the derivation of these numbers. The tensile force in the flexible membrane fabric at the bottom is distributed to the sinker and cable, and at the top to the rotating axis. The horizontal component of the force in the cable is the force in the flexible membrane fabric. The angle of the cable determines the force in the cable, and the length. Because of the limited available horizontal width of the bridge, the angle is 75 degrees. Appendix H.3 provides analysis of the derivation of the angle. The weight of the sinker must be equal to the vertical component of the cable force. Because of the uncertainties regarding the dynamic effects of the flexible membrane fabric, a safety factor of 1.5 is used. The minimum self weight of the sinker is 2630 kN/m. As a reference, this would correspond to a solid steel pipe with a diameter of 6.5 m. This is unrealistic, but will be evaluated later. The transfer of forces between the different elements of the shade curtain barrier is illustrated in Figure 6.5. Table 6.2 gives the corresponding values of Figure 6.5. The flexible membrane fabric is flexible, and therefore it is not possible to check the structure on moment equilibrium. However, when the flexible membrane fabric behaves as a rigid structure, the moment equilibrium check results in the fabric not rotating upwards under hurricane conditions. This has been further elaborated upon in Appendix H.4. Therefore, the forces that need to be taken into account in the bridge design are 470 kN/m at the Galveston Bay side (under an angle of 45°) and 1230 kN/m at the Gulf of Mexico side (under an angle of 75°).

	Value	Symbol
F_{cable}	1230	kN/m
$T_{flexible\ membrane\ fabric}$	470	kN/m
W_{sinker}	2630	kN/m
θ	75	°
α	45	°

Table 6.2: Resulting forces on elements of shade curtain barrier under hurricane conditions

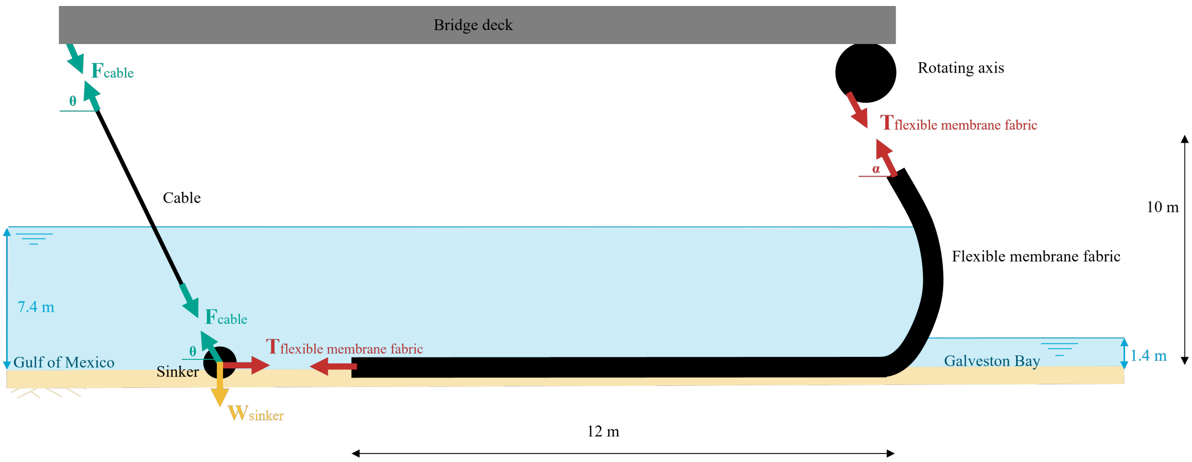

Figure 6.5: Internal load distribution between the different elements of shade curtain barrier. *Note, not to scale.*

6.2.4 Uplift Sinker

Uplift of the sinker needs to be prevented, as Section 6.2.3 showed that the required self weigh of the sinker needs be 2630 kN/m. This would correspond to a weight equal to a solid steel pipe with a diameter of 6.5 m. This is unrealistic, therefore will be evaluated in this section. This is accomplished by investigating different alternatives regarding the sinker design. In order to estimate the dimensions, it is assumed that the flexible membrane fabric behaves as a rigid structure. These alternatives investigated sinker designs are (elaborated in Appendix H.5):

- Alternative 1: Horizontal cables
- Alternative 2: Multiple sinkers
- Alternative 3: Multiple sinkers and horizontal cable
- Alternative 4: Weighted flexible membrane fabric and sinker (D=0.5 m)
- Alternative 5: Weighted flexible membrane fabric, sinker (D=0.5 m), and horizontal cable

The result of this alternative sinker design assessment is that alternative 5 (weighted flexible membrane fabric, sinker (D=0.5 m), and horizontal cable) is the most realistic one. The sinker has a weight equal to a solid steel pipe with a diameter of 0.5 m. The weighted flexible membrane fabric must have a weight equal to a solid steel plate with of thickness 0.2 m. Figure 6.6 illustrates the design of this alternative. The sinker alternatives are explained in detail in Appendix H.5.

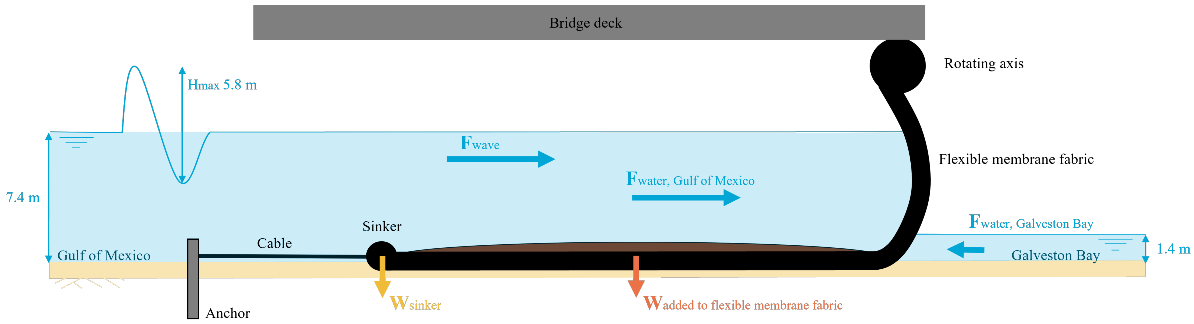

Figure 6.6: Alternative 5: Weighted flexible membrane fabric, sinker (D=0.5 m), and horizontal cable. *Note, not to scale.*

6.2.5 Result Structural Verification

The result of the structural verification is that some failure mechanisms require more concern than others. The failure mechanisms that require attention when the design phase is in further state are: damage to the flexible membrane fabric, failure of the rotational axis, failure of the bridge, failure of one of the shade curtain barrier gates, and failure of the connections. The failure mechanisms that are analyzed throughout the structural verification process, are uplift of the sinker, piping, and the estimated forces on the bridge and anchor are determined. For this purpose, simple mathematical calculations are used. The probability of the failure mechanisms, uplift of the flexible membrane fabric, erosion under the flexible membrane fabric, connection between the flexible membrane fabric and bridge piles, and feasibility of the structure, however, could be evaluated in laboratory experiments, described in Section 6.3. The result of structural verification is:

- The forces that needs to be taken into account for in the bridge design is 470 kN/m on the Galveston Bay side.
- The probability of piping is significant reduced because it meets the Rijkswaterstaat criteria for short-term water structures, since the seepage length is two time the water level difference (Rijkswaterstaat - Techical Advisory Committee on Flood Defences, 2002). However, laboratory experiment could evaluate this, as well as the importance of the connection between the flexible membrane fabric and the bridge regarding piping and scour.
- Horizontal cables can prevent the sinker from being uplifted, as the alternative of a heavier sinker is unworkable. Because the dimensions of the sinker should be unrealistic and have a large weight.

6.3 Laboratory Experiments

The laboratory experiments provide information about the feasibility of this design and indicate the probability of certain failure mechanisms. The laboratory experiments of the shade curtain barrier were preformed on a glass and a sandy bottom in a wave flume at Delft University of Technology. The wave flume had a width of 44 cm and a height of 40 cm. The flexible membrane fabric used during these experiments is tarpaulin, which is waterproof and weighs 100 gr/m^2. Note that scaling effects are not taken into account in the experiments.

6.3.1 Glass Bottom Experiments

On the glass bottom three different experiments were executed. The first experiment was a horizontal cable with small sinker, second a cable under an angle with large sinker, and third a variating cable angle with small sinker. The result of the first experiment (horizontal cable with small sinker) was that this design was able to hold a high water level difference, especially if the sidewalls are waterproofed.

Figure 6.7 left shows a photograph of this experiment. The second experiment (cable under an angle with large sinker) demonstrated that when using a large sinker (in terms of more weight), the sinker can remain on the bottom at a larger cable angle compared to the experiment when using a small sinker. Figure 6.7 right shows a photograph of this experiment. The third experiment (varying cable angle with small sinker) showed that the sinker started to uplift when force due to the weigh of the sinker and vertical component of the cable force are equal. Note that the friction between the glass bottom and flexible membrane fabric are nearly negligible. However, this has probably a larger influence when performed on a sandy bottom. The glass bottom experiments concluded that a horizontal angle of the cable is most favorable. This is inline with the theory. In addition, these experiments reveal that the idea of the shade curtain barrier design is able to retain water and therefore functions as a storm surge barrier. Appendix I.5 shows the various experiments of the shade curtain barrier on a glass bottom.

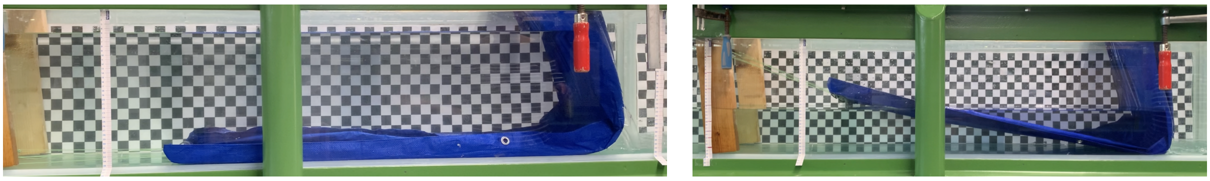

Horizontal cable Cable under an angle

Figure 6.7: Experiment Shade Curtain Barrier Glass Bottom

6.3.2 Sandy Bottom Experiments

On a sandy bottom three different experiments were executed, all with a small sinker and horizontal cables. The first experiment was without waterproofed sides. The second with partially waterproofed sides. The third with fully waterproofed sides. The first experiment, without waterproofed sides, scour, and piping occurred immediately due to the major leakage of the prototype. The second experiment, with partially waterproofed sides, showed that where the waterproofed sides began, the sour is largest and moves slowly to other parts of the construction. Figure 6.8a shows a photograph of the side view after this experiment. Figure 6.8b shows a photograph of the top view of the experiment set-up. This image was captured when water was still present on the flexible membrane fabric, at the end of the experiment. It is clear from this image that neither piping nor scouring has occurred in the center of the width of the structure. Most erosion occurred at the edge of the sides' waterproofing. At the sides that are not waterproofed, there is still sand in the middle of the width, but not near the sidewalls. The third experiment, in which the sides were completely waterproofed, revealed minimal scour at the end of the experiment. Therefore, it indicates that scour and piping do not have a significant probability of structure failure if the sides are waterproofed. Figure 6.8c shows a photograph of the side view after this experiment. Appendix I.6 shows the experiments of the shade curtain barrier on sandy bottom.

a b c

Figure 6.8: Experiment Shade Curtain Barrier Sandy Bottom. a) Photograph after the experiment, partly waterproofed sides. b) Fabric shape after experiment, partly waterproofed sides, top view. c) Photograph after the experiment, fully waterproofed sides.

6.3.3 Conclusion Experiments

The laboratory experiments of the shade curtain barrier demonstrated that this design is a more optimized design of the floater and sinker design. The experiments reveal three key points, namely:

- *Water-retaining construction.* The experiment demonstrates that the shade curtain barrier can retain water since it creates a water level difference. Resulting in the fact that the shade curtain barrier principle functions as a storm surge barrier. Consequently, protect the hinterland by decreasing the probability of flooding.
- *Uplift sinker.* The experiments demonstrated that as the cable angle increases above a curtain point, the sinker begins to rise. This indicates that it is crucial to keep the cables horizontal in order to prevent the sinker from rising.
- *Piping/erosion.* The experiments on sandy bottom revealed that piping and erosion pose a significant risk. This risk can be reduced through a relatively waterproof connection between the flexible membrane fabric and the sides. The flexible membrane fabric must be flexible enough to fall into the scour hole. As well as a slight cable angle to prevent cable entanglement when scour occurs near the sinker.

Concluding, the experiments on the various designs of the shade curtain barrier indicate that it could be used as a storm surge barrier. A storm surge barrier is *a partly moveable barrier in an estuary or river branch which can be closed temporarily. Its main function during surges is to reduce or prevent the rise of inner water level and thereby sufficiently protect the hinter lying area against inundation*, explained in Appendix C. As this design satisfies all these components, the shade curtain barrier may be recognized a storm surge barrier. Consequently, it is a promising complement to conventional storm surge barriers.

6.4 Final Design of the Storm Surge Barrier

The result of the structural verification and laboratory experiment lead to a modified design for the San Luis Pass compared to the design in illustrated in Figure 6.1. The structural verification revealed that the sinker's required heavy self-weight can be adjusted using horizontal cables. The laboratory experiments indicate that when the cables are horizontal, there is no significant failure probability associated with uplift of the flexible membrane fabric and sinker. To reduce the probability of piping, the required horizontal length of the flexible membrane fabric is 12 meters. The laboratory experiment also revealed that the flexible membrane fabric falls into the scour hole due to the weight of the water above it. The connection between the flexible membrane material and the bridge must be waterproof. The laboratory experiment revealed that without intervention, there will be a significant amount of scour in the location of this connection. This significantly increases the possibility of the bridge failing, leading to failure of the shade curtain barrier.

The final design for the storm surge barrier at the San Luis Pass consists of horizontal cables and additional horizontal length of the flexible membrane fabric on the bottom. At the end of the flexible membrane fabric is an anchor that ensure that the cables remain horizontal. A separate curtain is placed under every segment of the bridge. Note that in this design, it is assumed that the bridge can support the load of the shade curtain barrier and the design remain unchanged. The current bridge may not be able to withstand these forces, but it will be replaced in the near future, allowing the shade curtain barrier to be incorporated into the design of the new bridge. The dimensions of every segment are an inner width of 18 m and a height of 10 m. The flexible membrane fabric has a minimum length of 23 m. The benefits of this design for the San Luis Pass are:

- Lightweight construction compared to conventional storm surge barriers
- No additional influence on the environment
- Protection against 1/100 year storm

- Sediment dynamics of the pass remains
- Open view under normal conditions

Figure 6.9 illustrates the final design front view of the storm surge barrier at the San Luis Pass under normal conditions. Figure 6.10 illustrates the front view under hurricane conditions. Figure 6.11 illustrates the final design cross-sectional view of the storm surge barrier at the San Luis Pass under normal conditions. Figure 6.12 illustrates the cross-sectional view under hurricane conditions. Appendix J provides more detailed information about this design, including description of the phases and functioning under negative head.

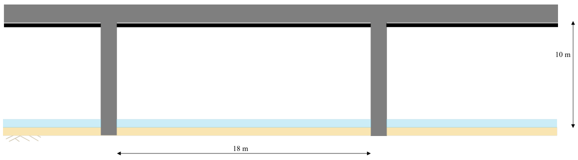

Figure 6.9: Final design shade curtain barrier, front view under normal conditions

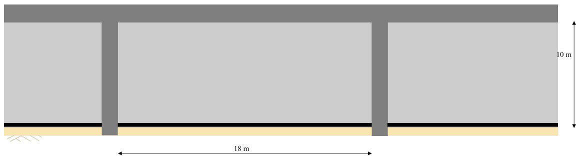

Figure 6.10: Final design shade curtain barrier, front view under hurricane conditions

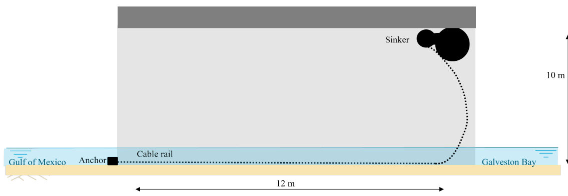

Figure 6.11: Final design shade curtain barrier, cross-sectional view under normal conditions

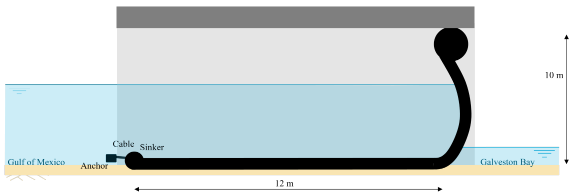

Figure 6.12: Final design shade curtain barrier, cross-sectional view under hurricane conditions

6.5 Discussion Final Barrier Design

The structural verification and laboratory experiment of the shade curtain barrier reveal that horizontal cables, additional horizontal flexible membrane on the bottom, and waterproofed sides generated a promising solution for the storm surge barrier in the San Luis Pass. However, there are still design aspects that require attention:

- *Strength of the bridge.* The bridge needs to be designed for the high tensile forces resulting from the attachment of the shade curtain barrier. In case the bridge fails, the barrier will too.
- *Rotating axis too large for attachment or production*. The dimensions of the rotating axis could be so large that the axis does not fit under the bridge or can not be built yet. However, the rotating axis could also be stored at the edge of the bridge.
- *Economical feasibility.* The costs of the shade curtain barrier is not determined.
- *Dynamic stability.* In the design and load analysis, only the static forces (water pressure and waves) are taken into account. Since there are large waves during a hurricane, the dynamic stability might be a problem, especially for the rotating axis.
- *Connection between the bridge piles and flexible membrane fabric.* This connection has not been subject to in-depth research. For now, a rail is suggested, but maybe the idea of a zipper is more suitable, or a solution that has not yet been thought of. Furthermore, the experiments showed that it is very important that this connection is at least semi-waterproof for the efficiency and thus success of the barrier.

- *Friction between flexible membrane fabric and bottom surface.* The potential beneficial friction between the flexible membrane fabric and bottom surface is not taken into consideration. This could be a beneficial for the cable force but could also have additional, still unknown, effects.
- *Wind forces.* Wind forces itself action on the barrier are not taken into account in this design. The storm surge and wave height, resulting from the wind under hurricane condition, is taken into account.
- *Maintenance.* The entire structure is above water in its neutral situation, so maintenance should be relatively simple. The gates are identical over the entire length, this simplifies the replacement and maintenance. However, it may be challenging to complete certain tasks underneath the bridge and the connection between the flexible membrane fabric and bridge piles may be able to be filled with things.
- *Sinker design.* The sinker design must have relatively high weight, which must all be supported by the rotating axis in neutral conditions.
- *Bottom anchoring.* The bottom anchor needs to be strong enough to hold the high cable force under hurricane conditions. Additionally, it should be operational and maintainable.
- *Operation.* The process of rolling down the shade curtain barrier has not yet been researched properly. This includes the exact moment of rolling down the curtain as well as the time required to complete this operation.
- *Force distribution in flexible membrane fabric.* The exact force distribution over the flexible membrane fabric is unknown. In this thesis, the assumption is made that the distribution is with respect to the geometric. However, there is not much researched about flexible membrane fabric under large water difference.

7
Discussion Design Approach

The main goal of this thesis was to develop a conceptual design for the storm surge barrier at the San Luis Pass in Texas, United States of America, whist minimizing the effects on the environment. Therefore, the methodology is in accordance to the Building with Nature philosophy en methodology. This is done in order to contribute to and elaborate on USACE's plan to form a resilient Texas coast. The results of the research conducted in this thesis showed that within the conventional designs for storm surge barriers no optimal design was found for the San Luis Pass. This was when taking into account both flood protection and value of nature on an equal footing. A new design for a storm surge barrier needed to be developed, to accomplish an optimal solution for the San Luis Pass. This was found by analyzing the integrated system, filtering out the main requirements that inspired in a customized design, and resulting in the shade curtain barrier as optimal design for the San Luis Pass.

Part of this research outlined the specific requirement of a storm surge barrier. The integrated system analysis provided the additional requirements of the storm surge barrier at the San Luis Pass. Combined, meeting all requirements provided the optimal design for this storm surge barrier. The additional requirements as a result of the system analysis were very influential regarding the final design and highlight how every specific location requires a custom design depending on the demands of the integrated area, to achieve an optimal solution for that specific location. The result of this thesis show that when looking beyond the existing solutions, a new, innovative, and more locally suitable solution can be found for a storm surge barrier. Analyzing the integrated system, and determining the main requirements for that specific storm surge barrier has the potential yield a more sustainable design solution than simply requiring a tried-and-tested design from a different system.

The main limitation of this research lies in the subjectivity of the terms building with nature, nature-friendly and optimal. The term building with nature is a very broad concept, and the definitions vary widely. Therefore, the definition for this thesis regarding building with nature is: *'The Building with Nature principle is shifting from focusing on a single object to looking at the entire system, and working to design an object that becomes a part of the system'*. This definition is formed by both literature and interviewing people, described in Appendix B.1. Thus, this definition is unique. Also, the term building with nature is subjective and personal. This research only focuses on the term building with nature in terms of the surrounding area, specifically relating to an open view and water flow through the inlet. However, building with nature and taking the local natural habitat into account could also be interpreted in terms of carbon-neutral or material (re)use instead of, or in addition to, the surrounding area. Adjusting the interpretation of these terms could have resulted in very different requirements. This in turn could result in a totally different design for the storm surge barrier at the San Luis Pass in the United States of America.

The term optimal depends on what something is referenced or compared to. This thesis defines optimal as more suitable than other, existing solutions, in terms of preserving an open view, keeping the dynamic sediment character of the pass and retaining the water flow area through the San Luis Pass. However, this supposedly optimal design is not yet tested within the Texas environment regarding the inhabitants of the area, the ecology, local weather circumstances and more. For the inhabitants of the area, this could be done with a focus group that represents the diversity of people. Regarding the ecology, it is hard to evaluate beforehand as most of the impact can only be observed once the system adapts to the presence of the barrier.

Another important limitation to discus is that the research for this storm surge barrier only focused on the specific San Luis Pass in the United States of America. The shade curtain barrier may be applicable for other locations worldwide as well, perhaps in a slightly altered form, but this should only be considered after a local system analysis and using the design approach of this thesis. This research demonstrated that the philosophy of building with nature could be applied to the design of a storm surge barrier.

8
Conclusions and Recommendations

8.1 Conclusions

This thesis has presented how the building with nature design method can be used for the design of a hydraulic structure. This lead to a new method to design a storm surge barrier at the San Luis Pass in Texas, United States of America. It was found that the shade curtain barrier has the most potential to become a well-integrated design for a storm surge barrier at the San Luis Pass and in the surrounding area.

The Building with Nature method is adjusted with the traditional civil engineering design method to incorporate flood safety and environmental aspects in the storm surge barrier requirements. This new design method is in accordance with the building with nature philosophy of this thesis, specifically: *'The Building with Nature principle is shifting from focusing on a single object to looking at the entire system, and working to design an object that becomes a part of the system'*.

The current function of the San Luis Pass within the Galveston Bay ecosystem is that it influences for 20% the tidal range inside the Galveston Bay. The San Luis Pass is a pass with unique sediment dynamics in the region and largely determines the water level in the West Bay. The Brazoria National Wildlife Refuge is located inland of the San Luis Pass. Brazoria National Wildlife Refuge is a nature reserve area, and home to various species of animals. Therefore, a storm surge barrier is preferred, due to flood risk reduction during a hurricane compared to leaving the pass open and due to decreased environmental impact under normal conditions compared to complete closure. This includes open sediment transport and water flow. The residents of the San Luis Pass area would like to keep the dynamics of the pass and an open view in normal conditions.

There are seventeen different types of storm surge barriers worldwide. Within these seventeen barrier types, six are possible at the San Luis Pass. These types could be distinguished in two categories: stored above and below water. The storm surge barriers stored above water (vertical lifting gate, visor gate, caisson structure and segment gate), require a fixed bottom and would disrupt the view. The storm surge barrier stored below water, (bear trap gate and parachute barrier), are sensitive to sedimentation and difficult in maintenance. In conclusion, within the conventional storm surge barriers, no optimal solution exists for the situation at the San Luis Pass. This is mainly due to the dynamics of sediment transport and the wish for open view under normal conditions.

In response, this research has found a new, innovative solution for the design of a storm surge barrier: the shade curtain barrier. This design requires no bottom protection, maintains an open view, and reduces hurricane-induced floods. The shade curtain barrier operates as a window shade curtain (roller blind), it rolls down during a hurricane and is stored under the bridge in normal conditions. Two possible types regarding this idea resulted in the design of the shade curtain barrier. This design would be optimal for the San Luis Pass, illustrated in Figure 8.1. The shade curtain barrier consists of a flexible membrane fabric, sinker, cable, and rotating axis. The flexible membrane fabric has two functions: it prevents the water from flowing into the Galveston Bay, and it protects against piping and scour as it functions as geotextile. The flexible membrane fabric is already available, can withstand the forces during a design storm, and can be opened under negative head. The sinker keeps the flexible membrane fabric at the bottom surface, and the cables prevent it from moving. The rotating axis stores the flexible membrane fabric under the bridge. The laboratory experiments demonstrated that the shade curtain barrier can be seen as a storm surge barrier. It can retain water and consequently protect the hinterland by decreasing the risk of flooding.

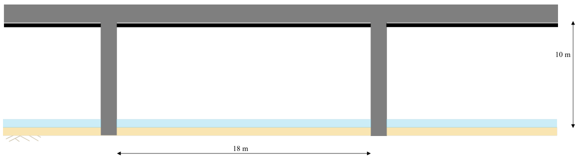

Front view under normal conditions

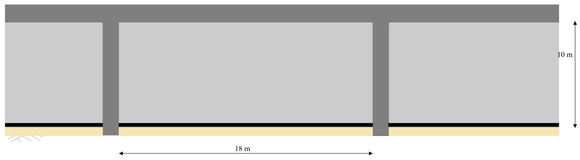

Front view under hurricane conditions

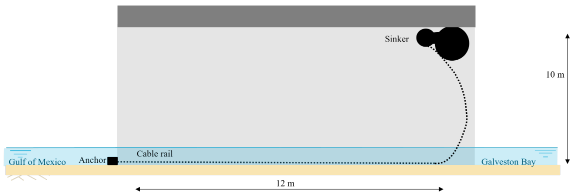

Cross-sectional view under normal conditions

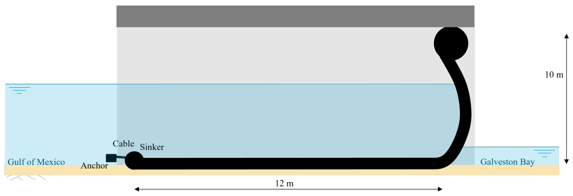

Cross-sectional view under hurricane conditions

Figure 8.1: The Shade Curtain Barrier Design for the San Luis Pass

The possible failure mechanisms of the shade curtain barrier are piping, uplift of the sinker, damage to/uplift of/erosion to the flexible membrane fabric, failure of the rotational axis, failure of the bridge, failure of one of the shade curtain barrier gates, and failure of the connection. Due to the early design phase, the failure mechanisms damage to the flexible membrane fabric, failure of the rotational axis, failure of the bridge, failure of one of the shade curtain barrier gates, and failure of the connection is not elaborated upon in further detail. However, the force of the barrier on the bridge deck that can be taken into account in the bridge design. The force on the bridge deck is 470 kN/m on the West Bay side, at an angle of 45 degrees. The anchor must be able to withstand a horizontal force of 470 kN/m under hurricane conditions. Piping is not a significant risk due to the horizontal length of the flexible membrane fabric on the bottom. However, the laboratory experiment reveals that it is important to waterproof the connection between the flexible membrane fabric and the bridge piles. Otherwise, it is likely that substantial scour and piping will occur and potentially cause failure of the structure. The cables connecting the flexible membrane fabric to the anchor should be horizontal. This significantly reduces the risk of failure of the structure due to uplift of and erosion underneath the flexible membrane fabric, as determined by the laboratory experiments. In addition, the weight of the sinker (therefore dimension) is significantly reduced in comparison to an angled cable.

In conclusion, the shade curtain barrier minimizes the unwanted effects for the San Luis Pass because, under normal conditions, it does not affect the flow area. Therefore, neither the tidal range nor the intertidal area will be effected. In addition, sediment can move freely because there is no requirement for bottom protection or a rigid closure structure. The shade curtain barrier is not visible under normal conditions because it is stored beneath the bridge and it decreases the probability of flooding during a hurricane. Therefore, this design has a minimal impact on the ecosystem, sedimentation, and landscape at the San Luis Pass. Overall, the shade curtain barrier at the San Luis Pass is a promising addition to the USACE's plan to form a resilient Texas coast in the United States of America.

8.2 Recommendations

This thesis presents a conceptual design for a storm surge barrier at the San Luis Pass in Galveston, Texas, United States of America, using the Building with Nature philosophy. However, further research is recommended on various aspects. Additional research is required on the particular San Luis Pass in terms of wave analysis, sediment dynamics and the in-depth consequences of closing this pass under hurricane conditions. At this moment, additional research is recommended regarding the exact connection between the vertical bridge piles and flexible membrane fabric, the ideal curvature, the load distribution and performance (including erosion) of the shade curtain barrier under hurricane conditions.

Wave analysis

The wave analysis is based on the Bolivar Roads and the theory of maximum wave height at certain depths. Nonetheless, the Bolivar Road is much deeper and has a large shipping lane. The maximum wave height is thus determined by the water depth and breaking parameter in this design. It is advised to examine the wave dynamics at the San Luis Pass in particular.

Sediment dynamics

The San Luis Pass is a dynamic pass. As there is no scientific study or information on sediment movement, the full meaning of this statement has not been thoroughly examined. Conversations with locals provide insight into the dynamics of this pass. Therefore, future research should include sediment type and dynamics at San Luis Pass in order to gain a clear picture of the current sediment dynamics and how this may interact with the construction of a storm surge barrier.

Impact of closing San Luis Pass

The effect of closing San Luis Pass is based on a single study that solely includes Hurricane Ike. The effect of varied hurricane paths is a topic that must be resolved in future research. The hurricane path impacts the water flow across Galveston Bay, resulting in an inflow or outflow via San Luis Pass.

The Shade Curtain Barrier

The design of the shade curtain barrier was invented during this research and implies that the shade curtain barrier is a viable substitute for storm surge barriers. However, additional research is advised regarding the global design, membrane fabric flexibility and site-specific design. Therefore, detailed below.

Global Design

- Implementation in other places/under other bridges.
- In-depth study relation of fabric/cables/sinker.
- Investigation of friction between flexible membrane fabric and bottom surface.
- Optimizes the design (angle curtain, thickness, rotational axis, cable design including space between cables, connection bridge flexible membrane fabric, reliability of the barrier, sinker design).
- Feasibility study, including costs analyzes.
- Where and exactly how to store the structure under the bridge.
- Does the flexible membrane fabric behave as a vertical wall or does is dissipate energy under waves?

- Operation, the best time to roll down the flexible membrane fabric.
- How does it behave when rolling up? When is that the best time, and how should you do it?

Flexible Membrane Fabric

- Test effect of debris on flexible membrane fabric.
- How a crack in the flexible membrane fabric develops and reacts under extreme conditions (high tensile strength in the flexible membrane fabric).
- Friction between flexible membrane fabric and surface.
- How can the added weight be realized, and is it really necessary? As indicated by laboratory experiments, this is not the case with horizontal cables.

Site Specific Design

- What would be the bridge design at the San Luis Pass for the load capacity of the shade curtain barrier under hurricane conditions.
- How would the exact connection of the structure (flexible membrane fabric) and bridge pile appear to be.
- Alternatives to prevent sinker uplift.
- Other vulnerabilities in the bridge barrier combination. This includes the effect of erosion on the bridge piles and foundation due to rolling down the barrier.

References

Aerts, J., Botzen, W., Bowman, M. J., Ward, P. J., & Dircke, P. (2012). *Climate Adaption and Flood Risk in COastal Cities*. Earthscan.

American Flood Coalition, NLNetherlands, & Arcadis. (2020). *ADAPTATION FOR ALL: HOW TO BUILD FLOOD RESILIENCE FOR COMMUNITIES OF EVERY SIZE* (tech. rep.).

Army Corps of Engineers - Galveston District (US). (2021). *COASTAL TEXAS PROTECTION AND RESTORATION FEASIBILITY STUDY COASTAL TEXAS PROTECTION AND RESTORATION FEASIBILITY STUDY - F I N A L R E P O R T* (tech. rep.).

Battjes, J., & Labeur, R. J. (2017). *Unsteady flow in open channels*. Cambrige University Press.

Bay Atlas Map. (n.d.). https://www.texascoastalatlas.com/bayatlas/index.html

Bosboom, J., Stive, M. J., & Open Textbook Library. (n.d.). *Coastal dynamics*.

Bridge reports. (n.d.). BLUEWATER HWY over SAN LUIS PASS. http://bridgereports.com/1536707

Bridgehunter. (n.d.). San Luis Pass Toll Bridge. https://bridgehunter.com/tx/galveston/bh86512/

Bridges, T., King, J., Simm, J., Beck, M., Collins, G., Lodder, Q., & Mohan, R. (2021). *Overview : International Guidelines on Natural and Nature-Based Features for Flood Risk Management* (tech. rep.). https://doi.org/10.21079/11681/41945

Bubeck, P., Kreibich, H., Penning-Rowsell, E. C., Botzen, W. J., de Moel, H., & Klijn, F. (2017). Explaining differences in flood management approaches in Europe and in the USA – a comparative analysis. *Journal of Flood Risk Management*, *10*(4), 436–445. https://doi.org/10.1111/jfr3.12151

Chen, A. (2015). Officials warn of swimming dangers in San Luis Pass.

Daniel, R., & Paulus, T. (2019). *LOCK GATES AND OTHER CLOSURES IN HYDRAULIC PROJECTS* (tech. rep.).

de Boer, R. (2015). *Building-with-Nature Solu-tions for Hurricane Flood Risk Reduction in Galveston Bay-Texas Conceptual Design Study* (tech. rep.). Delft University of Technology. http://repository.tudelft.nl/

de Boom, L. (2013). *Reduction Barrier: A cost effective solution for safety, shipping and the environment? Case Study for the Western Scheldt* (tech. rep.). Delft University of Technology.

de Kort, R. (2013). *Sketches Texas Barrier. Workshop Texas Barrier TU Delft at 20-06-2013* (tech. rep.).

de Vries, P. A. (2014). *The Bolivar Roads Surge Barrier* (Doctoral dissertation). Technical University Delft. Delft.

DSM. (2022). Dyneema® Fibre. https://www.dsm.com/dyneema/en_GB/our-products/dyneema-fiber.html

Du, J., & Park, K. (2019). Estuarine salinity recovery from an extreme precipitation event: Hurricane Harvey in Galveston Bay. *Science of the Total Environment*, *670*, 1049–1059. https://doi.org/10.1016/j.scitotenv.2019.03.265

Du, J., Park, K., Jensen, C., Dellapenna, T. M., Zhang, W. G., & Shi, Y. (2021). Massive oyster kill in Galveston Bay caused by prolonged low-salinity exposure after Hurricane Harvey. *Science of the Total Environment*, *774*. https://doi.org/10.1016/j.scitotenv.2021.145132

Duran, H., Flores, A., Jankowski, P., Gabe Martinez, R., Pherigo, J., Marc Keosayian, b., & Morgan, S. (2021). *Houston Economic Highlights* (tech. rep.). Greater Houston Partnership.

EcoShape. (2020). *Building with Nature* (E. van Eekelen & M. Bouw, Eds.). nai010 publishers.

Eelkema, M. (2013). *EASTERN SCHELDT INLET MORPHODYNAMICS* (tech. rep.). Technische Universiteit Delft.

Entwistle, C., Mora, M. A., & Knight, R. (2017). Estimating coastal wetland gain and losses in Galveston County and Cameron County, Texas, USA. *Society of Environmental Toxicology and Chemistry*.

FEMA. (2020). Laws and Regulations. https://www.fema.gov/flood-insurance/rules-legislation/laws

Frey, A. E., Morang, A., King, D. B., & Thomas, R. C. (2015). *SEDIMENT MANAGEMENT OPTIONS FOR GALVESTON ISLAND, TEXAS* (tech. rep.).

Galveston Bay Foundation. (2013). History of the Bay. https://galvbay.org/about-us/history-of-the-bay/

GCCPRD. (2018a). *Appendix D.2: Report Phase 4 Storm Surge Suppression Study Environmental Report Central Region* (tech. rep.).

GCCPRD. (2018b). *Appendix E - Galveston Bay Environmental Modeling: Daily Conditions Hydrodynamic Modeling* (tech. rep.).

GCCPRD. (2018c). *Storm Surge Suppression Study: PHASE 4 REPORT* (tech. rep.).

Gonzalez, L., & Holligan, K. (2012). State of the Bay: A Characterization of the Galveston Bay Ecosystem, Third Edition.

Greater Houston Partnership Research. (2017). Houston Metropolitan Statistical Area Profile.

GSA. (2011). *The Benefits and Challenges of Green Roofs on Public and Commercial Buildings A Report of the United States General Services Administration* (tech. rep.).

Hale, C., Gori, A., & Blackburn, J. (n.d.). *Prepared for the SSPEED Center: A review of available literature on the metrics and values of services provided by coastal ecosystems | ECOSYSTEM SERVICES OF THE MID--TEXAS COAST* (tech. rep.).

HARC. (2005). Land use/Land cover for Galveston Bay. https://www.galvbaydata.org/www.galvbaydata.org/Habitat/Wetlands/tabid/846/Default.html

Hofland, B. ; Marissen, R. ; Bergsma, O., Hofland, B., & Marissen, R. (2016). *Dynamic behaviour of a flexible membrane tsunami Barrier with Dyneema® Dynamic behaviour of a flexible membrane tsunami Barrier with Dyneema ®* (tech. rep.). Delft University of Technology. www.ascelibrary.org

Huang, W., Ye, F., Zhang, Y. J., Park, K., Du, J., Moghimi, S., Myers, E., Pe'eri, S., Calzada, J. R., Yu, H. C., Nunez, K., & Liu, Z. (2021). Compounding factors for extreme flooding around Galveston Bay during Hurricane Harvey. *Ocean Modelling*, *158*. https://doi.org/10.1016/j.ocemod.2020.101735

Irish, J. L., Song, Y. K., & Chang, K. A. (2011). Probabilistic hurricane surge forecasting using parameterized surge response functions. *Geophysical Research Letters*, *38*(3). https://doi.org/10.1029/2010GL046347

IV Group. (n.d.). Visor gates, ijsselweide. https://iv-groep.nl/en/over-iv/portfolio/inlaatkleppen-ijsselweide?returnurl=/Markten/Infra/Rijkswaterstaat

Jonkman, S. N., Van Ledden, M., Lendering, K. T., Mooyaart, L., Stoeten, K. J., De Vries, P., Willems, A., & De Kort, R. (2013). *Report Galveston Bay Bolivar Roads Flood Risk Reduction Barrier: Sketch design* (tech. rep.).

Jonkman, S., Lendering, K., Berchum, E., Nilsen, A., Mooyaart, L., de Vries, P., van Ledden, M., Willems, A., & Nooij, R. (2015). *Coastal spine system-interim design report* (tech. rep.).

Kelble, C. R., Johns, E. M., Nuttle, W. K., Lee, T. N., Smith, R. H., & Ortner, P. B. (2007). Salinity patterns of Florida Bay. *Estuarine, Coastal and Shelf Science*, *71*(1-2), 318–334. https://doi.org/10.1016/j.ecss.2006.08.006

Khaldoun, A., Eisert, E., Wegdam, G., & Bonn, D. (2005). Liquefaction of quicksand under stress. *Nature Publisching group*. https://www.nature.com/news/2005/050926/full/news050926-9.html

Kluijver, M., Dols, C., Jonkman, S. N., & Mooyaart, L. F. (2019). Advances in the Planning and Conceptual Design of Storm Surge Barriers-Application to the New York Metropolitan Area. *Henry, Hydraulic Engineering Repository - Coastal Structures*. https://doi.org/10.18451/978-3-939230-64-9{_}033

Knippels, A., & Pechtold, E. (1992). *Project Keersluis Heusdensch Kanaal* (Doctoral dissertation).

Kothuis, B. L. M., Slinger, J. H., & Cunningham, S. W. (2014). *CIGAS Workshop Houston: Report, Results & Reflection*. Delft Univeristy of Technology. http://repository.tudelft.nl

Lendering, K. (n.d.). *Related papers Hurricane Harvey Report-A fact-finding effort in t he direct aft ermat h of Hurricane Harvey in . . .* (tech. rep.). https://nyti.ms/2hqXvd5

Lester, J., & Gonzalez, L. (2011). *State of the bay: A characterization of the Galveston Bay ecosystem, Third Edition* (tech. rep.). https://www.researchgate.net/publication/261759345

Marissen, R., Mulder, J. S., Wienke, D., & Bergsma, O. (2013). Design Considerations on a Flexible Membrane Tsunami Flood Barrier. *Materials Sciences and Applications*, *04*(12), 846–855. https://doi.org/10.4236/msa.2013.412108

Matsumoto, J., Powell, G. L., Brock, D. A., & Paternostro, C. (2005). *Effects of Structures and Practices on the Circulation and Salinity Patterns of Galveston Bay, Texas* (tech. rep.).

Meyerhoof, G. (1953). *The Bearing Capacity of Foundations under Eccentric and Inclined Loads* (tech. rep.). https://www.issmge.org/publications/online-library

Miller, M. M., & Shirzaei, M. (2021). Assessment of Future Flood Hazards for Southeastern Texas: Synthesizing Subsidence, Sea-Level Rise, and Storm Surge Scenarios. *Geophysical Research Letters*, *48*(8). https://doi.org/10.1029/2021GL092544

moffmat & nichol. (2010). *GALVESTON BAY REGIONAL SEDIMENT MANAGEMENT GALVESTON, TEXAS PROGRAMMATIC SEDIMENT MANAGEMENT PLAN* (tech. rep.).

Molenaar, W., & Voorendt, M. (2020). *Hydraulic Structures General Lecture Notes* (tech. rep.).

Mooyaart, L. F., & Jonkman, S. N. (2017). Overview and Design Considerations of Storm Surge Barriers. *Journal of Waterway, Port, Coastal, and Ocean Engineering*, *143*(4), 06017001. https://doi.org/10.1061/(asce)ww.1943-5460.0000383

Mooyaart, L., Jonkman, S., De Vries, P., Van der Toorn, A., & Van Ledden, M. (2014). STORM SURGE BARRIER: OVERVIEW AND DESIGN CONSIDERATIONS. *Coastal Engineering Proceedings*, *1*(34), 45. https://doi.org/10.9753/icce.v34.structures.45

MOSE. (n.d.). MOSE System. https://www.mosevenezia.eu/project/?lang=en

Moulton, D. W. (1997). Texas Coastal Wetlands Status and Trends mid 1950s to early 1990s.

NEN. (n.d.). NEN 1991-1-2.

Ngoc Quyen, B. (2010). *MORPHOLOGY OF THE EASTERN SCHELDT EBB TIDAL DELTA* (tech. rep.). Delft University of Technology.

NOAA. (n.d.). Storm Surge Overview. https://www.nhc.noaa.gov/surge/

noaa. (n.d.). noaa. https://devgis.charttools.noaa.gov/pod/

O'Brien, M. P., & Asce, F. (1969). *EQUILIBRIUM FLOW AREAS OF INLETS ON SANDY COASTS a* (tech. rep.).

Oertel, G. (1985). The barrier island system. *Marine Geology*, 1–18.

Olympic Games. (2020). Tokyo 2020 Swimming Results.

Paugam, C., Rey, V., & Meulé, S. (2019). *FIELD STUDY OF WIND TIDE IN SEMI-ENCLOSED SHALLOW BASINS* (tech. rep.).

PIANC. (2005). *Design of Movable Weirs and Storm Surge Barriers* (tech. rep.).

Port of Houston. (2021). Port of Houston. https://porthouston.com/about-us/

Ramon-Duenas, C., Wellner, J. S., & Munoz, Y. P. (2021). Sediment transport and deposition in flood-tidal deltas: Insight from the Texas Coast. *Sedimentary Geology*, *416*. https://doi.org/10.1016/j.sedgeo.2020.105826

Ravens, T. M., Thomas, R. C., Roberts, K. A., & Santschi, P. H. (2009). Causes of salt marsh erosion in Galveston Bay, Texas. *Journal of Coastal Research*, *25*(2), 265–272. https://doi.org/10.2112/07-0942.1

Rego, J. L., & Li, C. (2010). Storm Surge propagation in Galveston bay during Hurricane Ike.

Rijkswaterstaat - Techical Advisory Committee on Flood Defences. (2002). *Technical Report on Sand Boils (Piping)* (tech. rep.). Rijkswaterstaat.

Ruijs, M. (2011). *The effects of the "Ike Dike" barriers on Galveston Bay* (tech. rep.). Delft Technical University.

Salas-Monreal, D., Anis, A., & Salas-de-Leon, D. A. (2018). Galveston Bay dynamics under different wind conditions. *Oceanologia*, *60*(2), 232–243. https://doi.org/10.1016/j.oceano.2017.10.005

Sebastian, A., Lendering, T. ; Kothuis, K. ; Brand, B. ; Jonkman, N. ; Van Gelder, B. ; Godfroij, P., Kolen, M., Comes, B., Lhermitte, T., Meesters, S., Van De Walle, K., Ebrahimi Fard, B., Cunningham, A., Khakzad, S., & Nespeca, N. (2017). *Hurricane Harvey Report A fact-finding effort in the direct aftermath of Hurricane Harvey in the Greater Houston Region* (tech. rep.). http://repository.tudelft.nl/

Skempton, A. (1951). Bearing Capacity of Clays. *Bulding Research Congress*. https://doi.org/10.4224/40000389

Smaal, A. (2019). Oyster reefs used to counter large waves.

State of Texas, & County of Brazoria. (2017). *AN ORDER OF THE COUNTY OF BRAZORIA, TEXAS TO PROHIBIT ENTERING THE WATERS OF THE SAN LUIS PASS FOR ANY ACTIVITY, INCLUDING BATHING, WADE FISHING, AND/OR SWIMMING; DESIGNATING THE AREA OF JURISDICTION; DEEMING THE VIOLATION OR FAILURE TO COMPLY WITH THIS ORDER*

TO BE A CLASS C PARKS AND WILDLIFE MISDEMEANOR; PROVIDING A PENALTY FOR VIOLATION; AND PROVIDING FOR PUBLICATION AND AN EFFECTIVE DATE (tech. rep.).

State of Texas Parks - Brazoria National Wildlife Refuge. (2022). https://www.stateparks.com/brazoria_national_wildlife_refuge_in_texas.html

Stoeten, K. J. (2013). *Hurricane surge risk reduction for Galveston Bay Tijdelijke Cover* (tech. rep.).

Sweet, W. V., Hamlington, B. D., Kopp, R. E., Weaver, C. P., Barnard, P. L., Bekaret, D., Brooks, W., Craghan, M., Dusek, G., Frederikse, T., Garner, G., Genz, A., Krasting, J. P., Larour, E., Marcy, D., Marra, J. J., Obeysekera, J., Osler, M., Pendleton, M., . . . Zuzak, C. (2022). *Global and Regional Sea Level Rise Scenarios for the United States* (tech. rep.). National Oceanic and Atmophese Administration. https://oceanservice.noaa.gov/hazards/sealevelrise/noaa-nos-

Taherkhani, M., Vitousek, S., Barnard, P. L., Frazer, N., Anderson, T. R., & Fletcher, C. H. (2020). Sea-level rise exponentially increases coastal flood frequency. *Scientific Reports*, *10*(1). https://doi.org/10.1038/s41598-020-62188-4

Texas A&M University Galveston, . (2021). *Chapter 4. Consequences of Leaving San Luis Pass Open* (tech. rep.).

Texas A&M University Galveston, . (n.d.). *Chapter 4. Consequences of Leaving San Luis Pass Open* (tech. rep.).

The Center for Texas Beaches and Shores, & Texas A&M University at Galveston. (2016). *Evaluating the Effects of a Coastal Spine: National-Level Economic Ripple Effects of Storm Surge Events* (tech. rep.).

TSHA Texas State Historical Association. (2017). Galveston Bay.

Tuin, H. G., Voortman, H. G., Bodin-Sköld, H., Andréasson, M., Schaap, G., & Moback, U. (n.d.). *Design of storm surge barriers in Gothenburg, Sweden* (tech. rep.).

U.S. Fish & Wildlife Service. (2017). Brazoria National Wildlife Refuge - Wildlife and Habitat. https://www.fws.gov/refuge/Brazoria/wildlife_and_habitat/index.html

USACE Galveston District. (2021). *COASTAL TEXAS PROTECTION AND RESTORATION FEASIBILITY STUDY FINAL ENVIRONMENTAL IMPACTSTATEMENT* (tech. rep.).

van der Ziel, F. (2009). *Movable water barrier for the 21st century* (tech. rep.). Technical University Delft.

Van Koningsveld, M., & Van Raalte, G. H. (n.d.). *INTRODUCING GUIDELINES FOR ECO-DYNAMIC DEVELOPMENT & DESIGN* (tech. rep.).

van Breukelen, M. (2013). *Improvement and scale enlargement of the inflatable rubber barrier concept* (tech. rep.). Delft University of Technology. Delft.

van Zaal, C. (n.d.). *Eco-friendly closure of tidal river systems a case study on the Hollandsche IJssel* (tech. rep.).

Voorendt, M. (2017). Design principles of multifunctional flood defences. https://doi.org/10.4233/uuid:31ec6c27-2f53-4322-ac2f-2852d58dfa05

Warren Pulich, j. (2007). *Galveston bay System* (tech. rep.).

Wetlands Communities in the Galveston Bay area. (n.d.).

William White, b. A., Tremblay, T. A., Waldinger, R. L., Calnan, T. R., Tinker, S. W., John, D. A., & Jackson, K. G. (2007). *STATUS AND TRENDS OF WETLAND AND AQUATIC HABITATS ON TEXAS BARRIERS: UPPER COAST STRANDPAIN-CHENIER SYSTEM AND SOUTHERN COAST PADRE ISLAND NATIONAL SEASHORE* (tech. rep.).

A
Design Phases for Hydraulic Structures

In this appendix, the classic design steps for a hydraulic structure is described that is based on the basic engineering design cycle (Molenaar and Voorendt, 2020). In the total design process are seven phases, the basic engineering design cycle shown in Figure A.1 and described in Section A.1. There is a relatively new integrated method of M. Voorendt (Voorendt, 2017), the integrated design process is shown in Figure A.2 and described in Section A.2. This approach is a single method that is suitable to the integrated and sustainable design of multi-functional flood defenses.

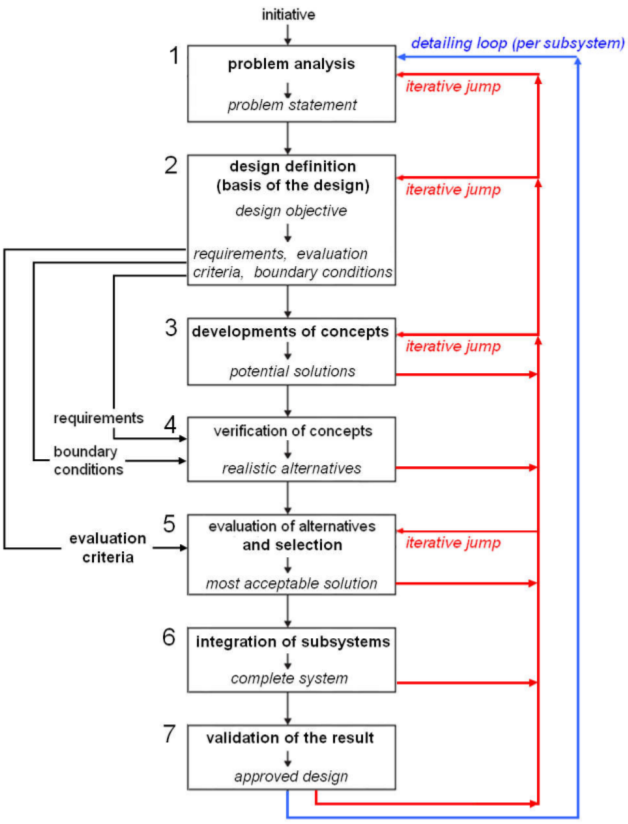

Figure A.1: The basic engineering design cycle (Molenaar and Voorendt, 2020)

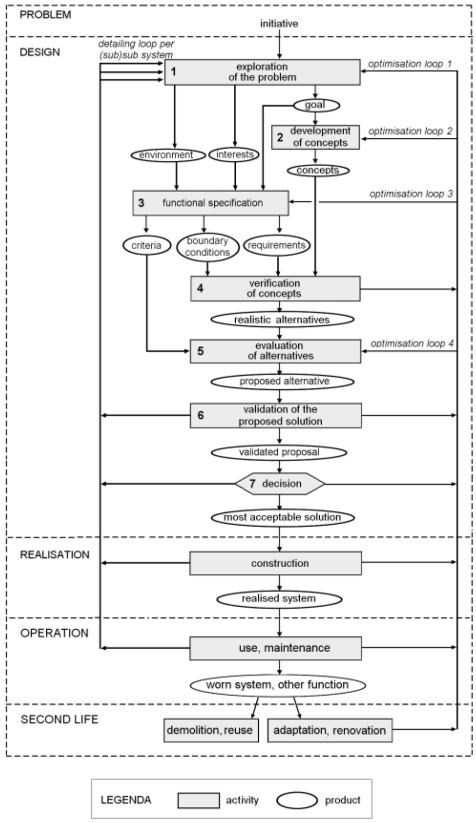

Figure A.2: The integrated design process (Voorendt, 2017)

A.1 Classic design approach

Design phases 1: Problem analysis

In this first design phase is to explore the problem. The first step in this phase is the initiation of the project and research the background. Then the stakeholders of the project, including their interest and influence, are researched. Process and function analyses give insight in the desired performance of the system or structure that has to be realized. An investigation of the environment and boundary conditions gives information on the restrictions of the solution space. A problem statement briefly summarizes the core of the problem and enables the formulation of a design objective, which is part of the following design phase.

The function of the storm surge barrier at the San Luis pass is to protect the hinterland from flooding during a hurricane.

Design phase 2: Defining the Basis of the Design

The basis of the design consists of the following five items:

1. Design objective
2. Requirements
   - Functional requirements
     Describe the desired behavior, or performance, of the system or subsystem under defined conditions
   - Aspect requirements
     Describe specific characteristics of the system that supports the primary functioning of the system
3. Evaluation criteria
4. Boundary conditions
   - Natural boundary conditions
     - Hydraulic conditions (water levels, wave heights, structural erosion or accretion)
     - Meteorological conditions (wind velocity and direction, temperature, humidity)
     - Geo-technical conditions (soil properties, layers, groundwater, ground levels, land subsidence)
     - Geological conditions (presence of hills, mountains, rivers, lakes, sea, earthquake conditions)
   - Artificial boundary conditions
     - Nautical conditions (intensity, fleet composition, max currents)
     - Road traffic (intensity, traffic composition).
   - Legal boundary conditions
     Laws, regulations and municipal plans.
5. Starting points
   Starting point are more open to discussion compared to requirements.

Design phase 3: Development of concepts

This design phase is for creating concepts that can solve the problem and a preliminary design is made.

Design phase 4: Verification of the concepts

In this design phase, the created concepts are verified to check whether they will function properly as defined in the project objective and specified in the program of requirements, defined at the detailing level of the design loop under consideration.

Design phase 5: Evaluation and Selection of the alternatives

The Evaluation design phase aims at finding a right balance between the created values and the sacrifices needed to achieve these values. It thus evaluates the feasibility and acceptability of design concepts, to enable the selection of one preferred alternative. The Evaluation phase succeeds the Verification phase, where potential design concepts are assessed against the requirements. This can be done using a Multi Criteria Analysis and Cost-Benefit Analysis.

Design phase 6: Integration of subsystems

Because this engineering design method, as described in this chapter, can be used at detailing levels where several subsystems can be developed simultaneously, the solutions for the discriminated subsystems and components will have to be integrated into a complete, functioning system

Design phase 7: Validation of the result and Decision.

It is recommended to subsequently carry out a final check on the validity of the entire design, whether the design objective has been adequately formulated and correctly translated into requirements. Validation is the confirmation, obtained through objective evidence, that the system will perform its intended functions.

A.2 Integrated design process

Design phase 1: Exploration of the problem

The first phase of the integrated design method consists of an orientation on the problem and its environment. Therefore, the 'who, when and where' questions should be explored. Then the problem statement is provisionally formulated, and the design objective is a functioning system that solves the stated problem. The design objective is primarily formulated in an abstract way.

Design phase 2: Development of concepts

In this phase, the abstract formulated objective is transforms into specific shapes and gets material properties. A properly formulated design objective aims at fulfilling the intended main function, but also specifies the intended sub-functions. In so doing, it should give sufficient direction to generate initial concepts. In this phase, reference projects are investigated.

Design phase 3: Functional specification

In this phase the design objective that describes the purpose of the system that has to be created, but it has to be specified in more detail. Therefore, the functional specification is made, in this specification is specified under what circumstance the system should function and what risks could hammer its performance. This is done by making a list of the program of requirements evaluation criteria, an inventory of boundary conditions and relevant laws regulations and risks. Optional wishes of the client are usually formulated as evaluation criteria to be used to compare alternatives in the Evaluation of Concepts phase. But interests of secondary stakeholders, other than the client, are formulated as criteria as well.

A clear distinction should therefore be made between requirements and criteria. All generated concepts have to comply with the requirements formulated for the design cycle under consideration before they can systematically be evaluated (in the multi-criteria evaluation). Therefore, requirements should not be used as criteria for the evaluation of alternatives.

Design phase 4: Verification of concepts

In this phase is verified whether the concepts created in the Development of Concepts phase will actually fulfil the desired function as defined in the project objective and specified in the program of requirements as defined at the detailing level of the design loop under consideration. A wide range of theories, formulas, tables, scale models, prototypes, drawings, and research methods from technical and behavioral science are at the disposal of the designer.

There are two types of verification: functional and structural. The functional verification checks whether a concept is able to fulfil its main functions. The structural verification succeeds a functional verification, to check whether a concept that can be realized

Design phase 5: Evaluation of alternatives

In this phase, the alternatives are evaluated. Alternatives are verified concepts, so all alternatives that survived the verification of concepts can be expected to be working solutions that can be evaluated in this phase. The feasibility of alternative solutions is evaluated by finding a right balance between the created values and the sacrifices needed to achieve these values. This can be done by a multi-criteria approach, the values, or 'qualities' of the design alternatives are determined with the help of relevant qualitative criteria. Or a cost-benefit analysis (CBA) can be used to find an optimum using formula A.1 when the added value (V_a) and costs (C) are balanced.

$$V_{\mathrm{a}} - C = 0 \tag{A.1}$$

Design phase 6: Validation of the proposed solution

In this phase the solutions for the discriminated subsystems and components will have to be integrated into a complete, functioning system and total costs, spatial aspects and planning have to be considered: technical drawings indicate how the structure has to be constructed, material quantities and equipment should be estimated, and a construction planning should be prepared.

Design phase 7: Decision

In this phase, the best alternatives are proposed to the client and the consequences are discussed. A value-cost ratio per alternative can be made to know the value for money ratio.

A.3 Building with Nature design method

The Building with Nature approach consists of five design steps (EcoShape, 2020). Building with Nature is a conceptual approach to creating, implementing, and upscaling Nature-based Solution for water-related infrastructure. This approach not only takes a look at what to do, but also how to do so. Therefore, it creates a continuation to broaden its applicability for sustainable development. Building with nature aims to embed natural processes in engineering solutions. Building with nature meets society's infrastructure demands by starting from the functioning of the natural and societal systems in which the infrastructure is to be realized. Building with Nature principle means working with rather than against nature. Building with Nature is not only green, it is the optimal combination of green and gray that best fulfills primary engineering objectives within the local physical, ecological, and societal system.

The Building with nature approach start with understanding how adjacent natural and societal systems function and creates opportunities for nature to develop. This consists of utilizes natural materials, forces, and interactions. Designing with natural materials and processes helps achieve cost-effective and resilient solutions. It encourages sustainable and innovative practices, often producing multifunctional solutions that benefit many stakeholders. The five steps of development gives the outlining of a creative process that can be followed at any phase of project realization. The five steps are described below en shown in Figure A.3.

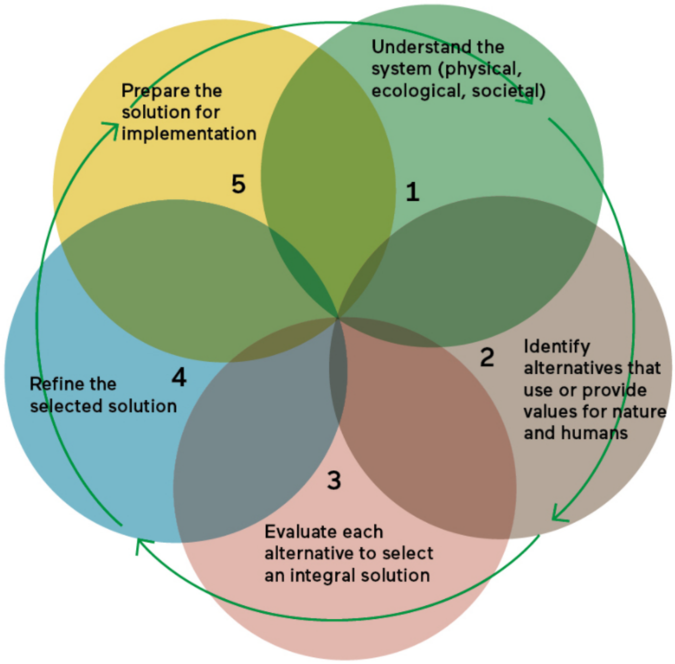

Figure A.3: The five Building with Nature design steps (EcoShape, 2020)

Step 1: Understand the system (physical, ecological, societal)

This step is to acquire a better understanding of the system in which a project is planned. In depth knowledge of the physical system (biotic and a-biotic), as well as the socio-economic system and the governance context are crucial to identify potential win-win solutions. Therefore, a map is made of the natural, physical, and social systems and the value, services, and benefits they can deliver to both nature and humans. And determines how system function influences project goals and objectives. The temporal and spatial boundaries of the systems under consideration depend on the project objectives.

- **The system to be considered depends on the project objectives**: Be clear about the primary objectives, and realize that finding win-win solutions creates room for flexibility in catering for secondary objectives. Note that looking at the primary objective alone may restrict the system to be considered. Adding secondary objectives will force consideration of other system characteristics: other temporal and spatial scales, etc.

- **Information about the system at hand can be derived from various sources**: It is important to realize is that acquiring knowledge about a system is not a prerogative of scientists. Valuable information can be found everywhere, for instance by talking to people with local knowledge (fishermen, harbormasters, waiters, elderly people, etc.). Delving into historical records to better understand the evolution of the system as a whole and to think of approaches that build on historically available expertise,

- **Think multifunctional**: Remember to look for user functions beyond those covered by the primary objective.

Step 2: Identify realistic alternatives

Identify realistic alternatives that provide true win-win solutions providing services beyond mitigation and compensation, alternatives that make maximum use of the system's potential (physical, socio-economical and governance-wise) while safeguarding or even enhancing sustainability. These alternatives that harness nature proactively to make optimal use of value-generating processes. Solutions should be transdisciplinary from the start. It should involve academic experts, practitioners, community members, business owners, decisions-makers, and other stakeholders. An open mind and involving all relevant disciplines is important during this process. Two main questions should be answered to obtain innovative inverse ideas:

- **Delivering services to the ecosystem**: How can we strengthen the functioning of the receiving system (ecology, recreation, landscape)?
  Larger scale: how can a project deliver benefits to the overall system in which it resides?
  Smaller scale: how can the project (with small adaptations) be more eco-friendly?

- **Utilizing services provided by the ecosystem**: How can better use be made of locally active (natural) resources: tide, waves, gradients, sediment availability, flora, fauna, economy, cultural values, etc.? Can available resources be utilized to lower construction and maintenance costs (more flexible solutions)? Can available resources be utilized to come to more sustainable solutions (PPP solutions: less energy, less material, multi functional)? Can the system's dynamics be used as a positive rather than a negative aspect (utilizing natural forces and expected changes as a means to achieve one's goals, use available time to achieve necessary change gradually rather than at once with associated over-engineering)?

Step 3: Valuate the qualities of alternatives and pre-select an integral solution

Assess the inherent qualities of the alternatives and combine them into one optimal integral solution. Valuate the Building with Nature alternatives and compare them with traditional designs. Dare to embrace innovative ideas, test them, and demonstrate how they work in practice. Identify uncertainties and dress them in the integral solution. Develop a business case that includes all natural and human co-benefits. Involve stakeholders in valuation and selection.

Step 4: Elaborate selected alternatives

Elaborate selected alternatives considering practical restrictions and governance context. Consider the conditions and restrictions that come from the practicability and governance of the project. Make sure that an innovative idea is elaborated in such a way, that it may actually be constructed. Recognize that implementation requires the involvement of a network of actors and stakeholders.

Step 5: Prepare the solution for implementation in the next phase on the road to realization

Handle the practical bottlenecks to get the solution included in the next phase on the road to realization: inclusion in request for proposals, inclusion in the detailed design, inclusion in the project delivery, inclusion in maintenance and monitoring scheme. Make key elements of the solution explicit to facilitate further uptake, funding, and stakeholder involvement. Prepare project documentation including actions plans, technical design, risk analyses, contingency plans, contracts, and permit applications. The development process is cyclical. Later phases will optimize the solution further.

A.4 Methodology of this research

This section describes the methodology of this research. The main goal of this thesis is to develop a conceptual design for the storm surge barrier at the San Luis Pass in Texas, United States of America that has minimum impact on the ecosystem, sedimentation, and landscape. The civil engineering method is commonly used for to design a storm surge barrier. Recently a new design method, Building with Nature, was created to design more nature based solutions for water related infrastructure, for instance dikes. However, hard structural infrastructure has not yet been built using this methodology. Therefore, the methodology of this research combines the civil engineering method, Section A.1 and the 'Building with Nature' method, Section A.3. This in an effort to design a more integrated, environmentally friendly storm surge barrier at the San Luis Pass in the United States of America. Resulting in adding an analysis of the integrated system before the functional specification, leading to flood safety, ecological values, and socio-economic aspects in the requirements of a storm surge barrier. Figure A.4 illustrates how the methodology of this research is formed. The colors indicate the order in which the design steps are combined. Below, every design step of the methodology in this research is briefly described.

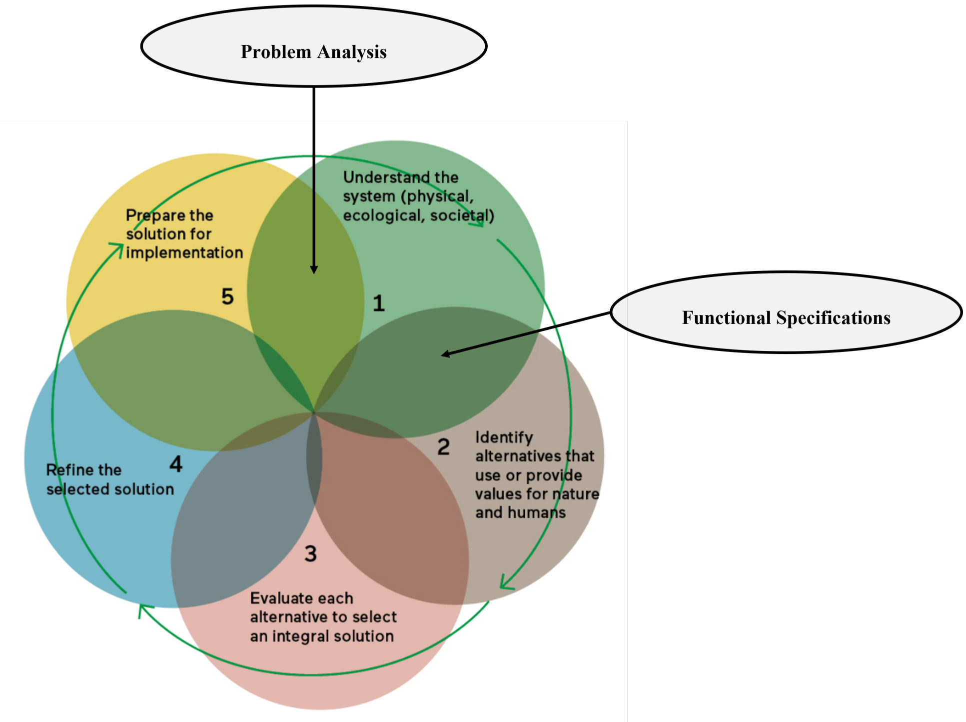

Figure A.4: Combined methodology for this research

Step 1: Problem Analyses

This step is an orientation of the problem. This step explores the 'where', 'when', 'who' questions. The result of this step is the problem statement.

Step 2: Understanding the system

This step is the understanding of the system, including physical, ecological and societal. This includes the analysis of the natural, physical, and social systems and the value, services, and benefits they deliver to both nature and humans. Also, the history of the system to understand how the system developed to the current system. Then determines how system function influences project goals and objectives. Resulting in an overview of the entire system.

Step 3: Functional specifications

In this step, a design objective that describes the purpose of the system that has to be created is described. This takes into account the functional, environmental, and social boundary conditions. The previous step leads to flood safety, ecological values, and socio-economic aspects in the requirements of a storm surge barrier. The outcome of this step states the criteria, requirement, and wishes for the design.

Step 4: Identifying alternatives that use or provide values for nature and humans

In this step, the concepts for the problem are generated. Afterwords, are verified to the criteria, requirement, and wishes for the design. This includes thinking of failure modes.

Step 5: Evaluate each alternative to select an integral solution

This step evaluates the concepts. This means the right balance between the created values and sacrifices needed to achieve these values. Ass well. in terms of practicability and governance of the project. This also includes the benefits and consequences of the concepts.

Step 6: Refine the selected solution

This step refines the best alternative for the solution, resulting in a more optimized solution for the specific problem.

Step 7: Refine the concept and prepare for implementation

This step refines the practical bottlenecks of the solution, included in the next phase on the road to realization. Consisting request for proposals, inclusion in the detailed design, inclusion in the project delivery, inclusion in maintenance and monitoring scheme.

B
Building with Nature

In this appendix, the definition for this thesis is explained and the different types of building with nature are described. There are different categories for flood protection using the building with nature philosophy. In Section B.2 is beaches and dunes described. In Section B.3 is coastal wetlands and tidal flats. Islands and reefs are respectively described in Section B.4 and B.5. In Section B.6 plant systems are described. And last in Section B.7 the use of green and blue roofs is described.

B.1 Definition

The first idea of the now known building with nature philosophy was an ecological design. In the literature ecological design is defined as (Voorendt, 2017):

Ecological design takes the environment into account as an additional factor to those that are already used, in particular using energy conservation, efficient insulation, rainwater, solar radiation, wind-power, and recycling technologies.

But an ecological design is still a static design. It is impossible in nature to have a static design, because everything is changing but could be in equilibrium. Therefore, the concept of an eco-dynamic design is not focused on living nature but on the processes. The idea behind eco-dynamic design is using the processes of nature to accomplish a water infrastructure, meanwhile preserving nature. In the literature, an eco-dynamic design is defines as (Van Koningsveld and Van Raalte, n.d.):

Eco-dynamic design is an integration of disciplines, knowledge, information and methods in the 'green-blue' development process related to wet infrastructure (decision-making, design, realization, use, maintenance). The dynamism of the natural system is optimally taken into account, whereby cost and benefits are balanced for human and society against a background of a sustainable perspective. To achieve this objective, aspects like decision-making, design, biotic, abiotic, socio-economic system knowledge, construction, monitoring and modelling should be integrated as leading research and application areas.

There are different types of ideas what the definition is of Building with Nature and Nature Based Solutions are given. Below, several of these definitions are given.

'Building with Nature is a conceptual approach to creating, implementing, and upscaling Nature-based Solution for water-related infrastructure'
Building with Nature Book (EcoShape, 2020).

'Nature-based solutions and building with nature are two terms that are alike but not the same. Nature-based solution is an overall term for finding a solution for larger and smaller problems and including a positive for nature. Several examples of topic are blue-green infrastructure and nature-including building. Blue-green infrastructure is design a city such that the increases nature and using the ecosystem services, for example to decrease the heat in the city. Nature-including building is for example building houses where birds have a breeding ground. Building with Nature is using the ecosystem services in the solution. For example, coastal protection by means of mangroves.'
Cas Dinjens, Ecologist at Arcadis

'Nature based solution is a combination between green and gray. It doesn't matter what is combination percentage of both is. Proactive using the natural process and system thinking. So natural vegetation, sediment and water flow. For barriers and dikes the goal is flood reduction with minimum interfere with the natural processes. The principle difference is system thinking instead of a single object.'
Luca Sittoni, Deltaris

'Using nature or natural (physical) processes in the realization.'
Niels Nijborg, Arcadis

Definition for this thesis
Building with Nature principle is shifting from focusing on a single object to looking at the entire system, and working to design an object that becomes a part of the system.

B.2 Beaches and Dunes

In this section, the building with nature approach regards beaches and dunes is described. Sediments are transported by winds, waves and tides, using the knowledge could result in the assistance for beach and dune building. Creating the idea that a beach and dune should be a dynamic instead of static system whenever feasible. This would result in dynamic profile with range of beach slope, volume, and width as primary design parameters. Dunes form a natural buffer against erosion of the beach. Since they temporary store necessary sediments that can be shifted towards the sea during an extreme event (Bridges et al., 2021).

B.3 Coastal Wetlands and Tidal Flats

Coastal wetlands and tidal flats have a beneficial role in the ecosystem. They stimulate fish production, reduce the pollutant from upland runoff due to filtration, have a negation role between disputing parties, carbon sequestration and are used for recreation. The coastal wetlands and tidal flats have the characteristics to dampen waves, surge and current energy, trap sediments and in specific settings self-sustaining under sea level rise. The reduction of surge water levels are increased with the size of the wetland. This is across the width of the feature and along the length of the estuary (Bridges et al., 2021).

B.4 Islands

Island can reduce the severity of hazards on the nearby habitats and shorelines. These islands can be located in estuaries, major river deltas and open-coast environments. They can reduce the erosion and flooding from wind-drive waves and extreme water levels, what happens during a hurricane (Bridges et al., 2021). Galveston Island is such an island, it protects the coast of Houston.

B.5 Reefs

Reefs provide many ecosystem services, such as fisheries, recreation, and tourism. One of the most important services is protection from coastal flooding and erosion (Bridges et al., 2021). Natural and artificial reefs provide coastal protection and risk reduction services by dissipating wind waves originating from the open ocean as the waves propagate over shallow and rough reef structures. Healthy coral reefs, for example, often dissipate most incident wave energy before the waves reach the shore. This wave-energy buffering reduces risk to coastal communities by wave-driven coastal flooding and associated losses.The effectiveness of reefs to attenuate wave energy and protect coastlines depends on their size, orientation, elevation, and location relative to shore, as well as tidal range, among other

characteristics. One of the most important characteristics that governs coastal protection is the elevation of the reef crest (i.e., the shallowest part of a reef) relative to sea level. The capacity of a reef to dissipate wave energy decreases as the elevation of the reef crest becomes deeper. Tidal variations and other sources of sea-level variability can also greatly diminish the effectiveness of reefs to dissipate wave energy when water levels are high. (Bridges et al., 2021).
Research indicates that the vertical growth rates of unharvested oyster reefs are faster than predicted rates of sea-level rise (Bridges et al., 2021), meaning that they could maintain their coastal protection benefits in the face of climate change and adapt to sea-level rise in contrast to conventional engineering structures (Bridges et al., 2021).

B.5.1 Oyster reefs

The narrow tidal range prevents many oyster reefs from growing a three-dimensional structure and instead results in large, flat, subtidal oyster beds (Hale et al., n.d.). Because oyster reefs can grow vertically with sea-level rise, they can be attributed a higher value than engineered devices because they are naturally resistant to sea level rise and are able to regenerate themselves following any damaging events (Hale et al., n.d.). The wettest tropical cyclone in the US history, causing a 1000-year flood in the Houston metropolitan area, provides an opportunity to study the response of coastal ecosystems to extreme events. Bottom low-salinity exposure time (duration of bottom salinity continuously less than 5 PSU) Oysters play an important role in the ecosystem by filtering phytoplankton, removing particles in the water column, providing food, shelter, and habitat for fish and invertebrates, and protecting the shoreline from erosion (Du et al., 2021).

Oyster reefs can also be used at the bottom protection for offshore wind turbine. Figure B.1 shows different types of vegetation near an offshore wind turbine (Arcadis, 2022). Oyster reefs could function as a natural breakwater instead of an impermeable revetment (Hynes et all., 2022).

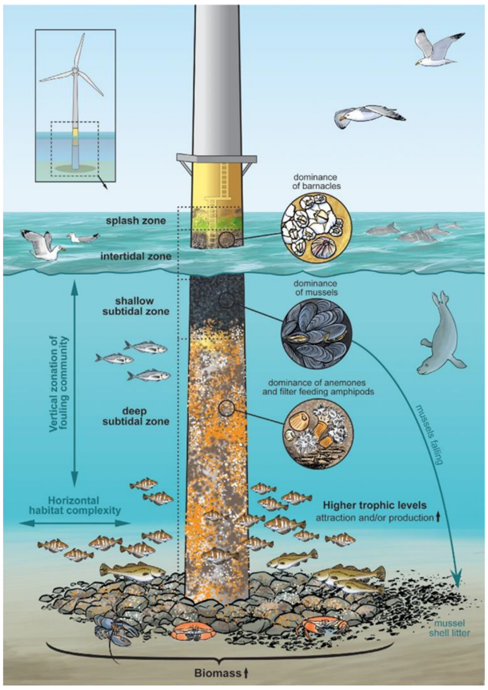

Figure B.1: Oyster reef at bottom protection near offshore wind turbine (Arcadis, 2022)

B.6 Plant Systems: Submerged Aquatic Vegetation and Kelp

SAV and kelp can play a vital role in coastal protection by attenuating wave energy and reducing the current velocity in the canopy, near the bed.The reduced hydrodynamic conditions can influence sediment transport in the canopy by increasing bed stabilization, reducing sediment resuspension, and creating an environment more conducive for suspended sediment deposition. Kelp requires available hard substrate (usually, rocky surfaces) for hold fast attachment, high-nutrient conditions, and light for growth. Since the comply height is much less than the total water-column height, the movement of the water overlying the canopy is relatively unaffected by the presence of SAV below. In this cases, SAV still provides a valuable service by trapping and stabilizing sediments. (Bridges et al., 2021).

B.7 Green and blue roofs

Green and blue roofs capture stormwater as it falls on building roofs, slowing or halting its progress to storm drains. Blue roofs use artificial structures to retain stormwater and allow it to evaporate or discharge slowly into a drainage system. Instead of using physical structures, green roofs use vegetation and soil that absorb water. Green roofs can capture up to 80% pf rainfall during rainstorms, compared to 24% typical for standard roofs (American Flood Coalition et al., 2020).

There are three potential benefits for a green and blue roof. The first benefit is that during peak flow it reduces the runoff to storm water systems up to 65% (GSA, 2011). It can catch and retain 1/2 to 3/4 inch of rainfall during a storm (GSA, 2011). Second, they have a longer lifetime than traditional roofs. Last it has a positive effect on the environment since it increases the air quality, provide wildlife habitat, reduces urban heat-island effect and reduces urban heat-island effects (American Flood Coalition et al., 2020).

There are also several considerations for the implementation of the green and blue roofs. There are two main considerations for the implementations. The first thing that need to be taken into account is that a green and blue roofs are most effective on large flat roofs. Second, when additional structural reinforcement is needed, it could result in cost-prohibitive circumstances (American Flood Coalition et al., 2020).

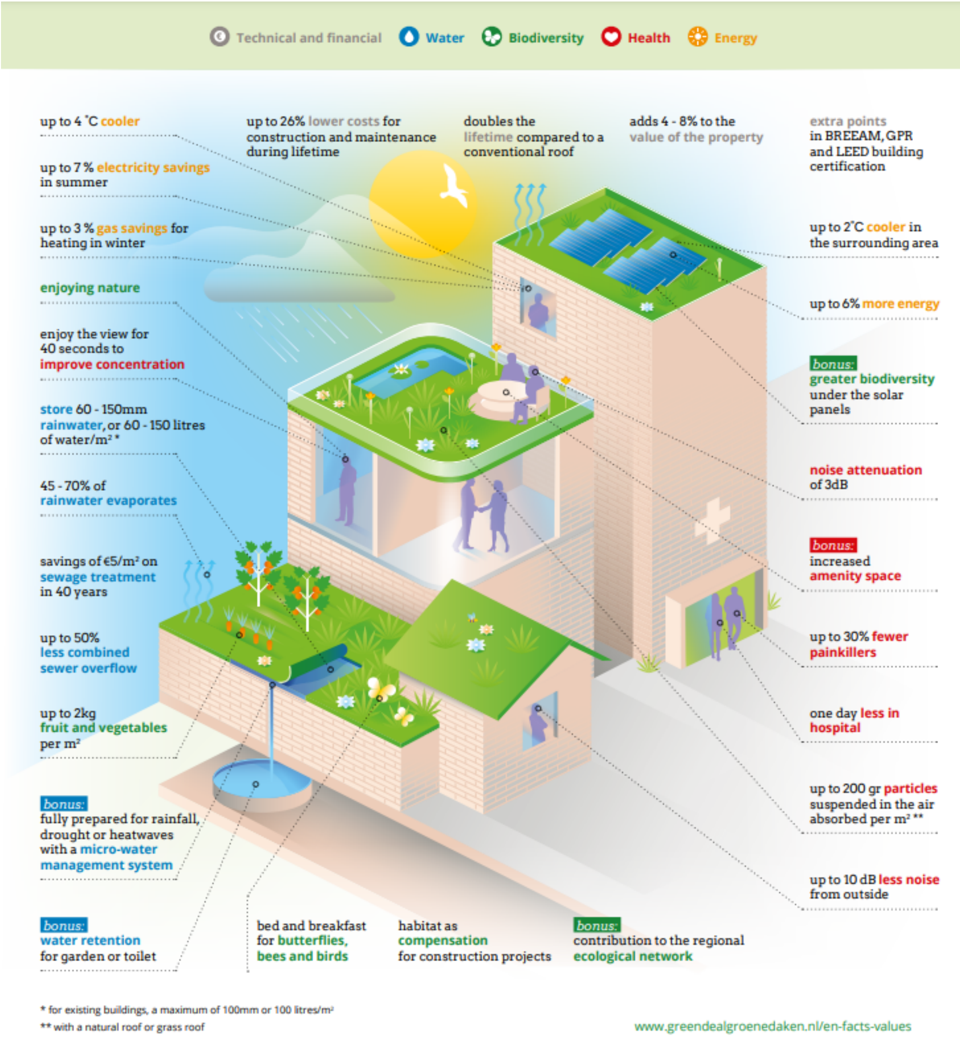

Figure B.2: Benefits of green roofs

C
Storm Surge Barriers

The purpose of this appendix is to give relevant background information about storm surge barriers. First, Section C.1 describes the definition of a storm surge barrier. Second, Section C.2 briefly explains the worldwide location and use of storm surge barrier. Section C.3 describes the requirements for a storm surge barrier. Section C.4 explained how a rough estimation of the construction cost and duration of a storm surge barrier can be given. Lastly, Section C.5 described the different gate types, including examples.

C.1 Definition

First, the definition of a storm surge barrier is set before describing the definition of a storm surge barrier. The U.S. National Hurricane Center (NHC), a department of the National Oceanic and Atmospheric Administration (NOAA), defines a storm surge as "an abnormal rise of water generated by a storm, over and above the predicted astronomical tides" (NOAA, n.d.). Water is pushed towards the shore by a force created by the cyclonically moving winds around the storm and low pressure water systems. This happens during a hurricane. This can cause extreme flooding in coastal area's, especially when a storm surge coincides with normal high tide, known as a storm tide. A storm tide is defined as 'the water level rise due to the combination of storm surge and the astronomical tide' (NOAA, n.d.). A storm surge barrier, also referred to as a flood barrier, is a structure that the hinterland, people and property, from flooding due to storm surge.

***Definition**: A storm surge barrier is a partly moveable[(i)] barrier in an estuary or river branch which can be closed temporarily[(ii)]. Its main function during surges is to reduce or prevent the rise of inner water level and thereby sufficiently[(iii)] protecting the hinter lying area against inundation. (de Vries, 2014)*

[(i)] The ratio of the cross-section that is moveable must be large enough to be able to allow sufficient circulation flow in the inner water in normal conditions. This can for example be important for inner water ecosystems.

[(ii)] A temporary closure is defined as either (INC-WG26, 2006; van der Toorn and de Gijt, 2012):

- A closure required to protect against flooding starting from the moment of closing (related to expected high water levels) until the outer water level has dropped sufficiently. Overflow and increased inner water levels are taken into account.
- A closure required to make the structure available for maintenance or repair.

[(iii)] Sufficiently regards the maximum allowable inner water level which, in turn, is influenced by river runoff and is determined by the height and safety standards of the dike ring behind the barrier.

A storm surge barrier is open under normal conditions. And the primary function of a storm surge barrier is already set by the definition. Other functions of a storm surge barrier could be for example separation of fresh and salt water, discharge regulation or fish migration.

C.2 Worldwide

Storm surge barriers are constructed in large bays, estuaries and natural harbors as integral parts of flood risk reduction systems and be closed prior to the arrival of storms to impede storm surge and reduce the risk of flooding for the region behind the structure. A storm surge barrier is a fully or partially closable barrier that is navigable and includes operable elements that can be closed temporarily to impede storm surge generated by coastal storms and limit water levels in the basin, thereby reducing flood risk for coastal areas surrounding the basin (Kluijver et al., 2019). The typical layout of a storm surge barrier consists of three elements: a gated section, a dam section and a lock (L. F. Mooyaart and Jonkman, 2017).

In the world there are 31 storm surge barriers built and 2 are in the design/construction phase, all these barriers are unique and chosen for a specific reason. Most of the gates have been operating for many years and are therefore a proven concept for flood protection systems. Since these barriers are unique, every barrier has its advantages and disadvantages. Taking into account the type of gate structures, design criteria, risk management, environmental aspects, navigation aspects, technical design details and operation and maintenance. Knowing these characteristics of the barriers increases the knowledge of the barrier at San Luis Pass, Texas.

C.3 Requirements

The classic approach to the design of a storm surge barrier starts with a function analyses in addition to the basic function of retaining a storm surge. The main components of the design are the transfer of hydraulic loads to the foundation, choice of mechanical system of the gates in relation to span and operation, foundation of the barrier (including bed and bank protection). In addition, aspects such as maintainability, reliability, durability, constructability, morphological impact and environmental impact can play an important role in determining the design (Aerts et al., 2012). In Table C.1 the requirements and impact of barrier are listed.

Requirement categories	**Requirements for storm surge barrier**	**Impact upon design**
Structure	Risk of failure should be minimized and not exceed the design probability of failure.	Reliable structure design; use of reliable materials; application of reliable driving system; careful operation.
Hydraulics	Amount of storm water overtopping or leaking past the barrier should meet the criteria.	Sufficient height of the barrier; application of seals; construction of breakwaters.
	Strong flow- or wave-induced vibrations and oscillations must be prevented.	Gate with adequate dynamic properties and favourable detailed design in view of dynamic flow forces and feedback phenomena.
	Translatory waves and different head (caused by closure) should be acceptable.	Section of suitable closing time and opening time.

Morphology	Designed to reduce/eliminate siltation impacts.	Removal of silt by gate operation; prevention of siltation by an adequate barrier design and layout.
Climate	Limited sensibility for wind loads.	Adequate dynamic properties required in view of wind loads; application of windshields.
Hydrology	Passage of tides and discharge river flow. Discharge of ice. Reverse flow conditions and reverse head.	Adequate flow opening. Adequate width of flow opening. Adequate structural design and favourable design in view of flow forces and feedback phenomena.
Navigation and transport	Passage of ships. Connection between both land sides for traffic.	Width and depth of navigational opening in relation to navigational requirements and ship clearance. Road and rail bridge.
Environment	Allow for tidal flow in view of water quality and ecology. Passage of fish.	Sill level, wet cross-section, effect of density differences. Wet cross-section, flow velocity, salinity gradient.
Maintenance	Accessible for inspection and maintenance. Proper choice of materials and techniques for minimum maintenance.	Drying possible of interior. Corrosion protection.
Other	Limited vulnerability to impact of unexpected heavy objects such as barges. Limited vulnerability to vandalism (or terrorism).	Solid construction and collision impact protection. Solid construction, safeguarding of vulnerable parts and other security-related issues.

Table C.1: Requirements and their impact upon the storm surge barrier design (Aerts et al., 2012)

C.4 Costs

The rough estimated construction cost and duration of a storm surge barrier is shown in equation C.4 and C.2 (Kluijver et al., 2019).

$$Cost =$$

€157,000 x Navigable Area + €102,000 x Auxiliary Area + €26,000 x Dam Area (C.1)

$$Duration = 2Years + \frac{33months}{100mofNavigableSpan} + \frac{23weeks}{100mofAuxiliaryFlowSpan} + \frac{16days}{100mofdam} \tag{C.2}$$

There are also cost prediction models that separate the costs in different criteria (L. Mooyaart et al., 2014). The first model makes a difference in a simple and complex structure. A complex structure is have larger spans (>50 m) and unlimited clearance (L. Mooyaart et al., 2014). The total coast for a simple structure is shown in equation C.3 and complex structure in equation C.4. Another way to calculate the cost of the barrier at San Luis Pass is a model that depends on the country of the barrier. This is shown in equation C.5. The constants c_{51}, c_{52} and c_{62} are respectively 2.1, 2.5 and 2.9 (L. Mooyaart et al., 2014).

$$Simple : f = c_{51} \cdot L \tag{C.3}$$

$$Complex : f = c_{52} \cdot L \tag{C.4}$$

$$f = c_{62} \cdot L \tag{C.5}$$

Which:

L	[m]	Length of the barrier is the distance along the axis of the barrier reaching from bank to bank

C.5 Gate types

A barrier is mainly characterized by the gate type. In the following sections the different gate types are explained. Figure C.1 gives an overview of the comparison of the different gate characteristic. Due to lack of time not all the gate types are specified. There are nine hydraulic types of gates that can be used for storm surge barriers (L. F. Mooyaart and Jonkman, 2017). These types of gates are: vertical lift gate, vertical rising gate, segment gate, rotary segment gate, sector gate, inflatable gate, flap gate, barge gate and rolling gate.

	Mitre	*Vertical lift*	*Flap*	*Horizontal*	*Vertical rotate*	*Rubber*
Span > 30m	–	+	+	+	+	+
Span > 100m	–	–	+	+	–	–
Water depth > 10m	+	+	+	+	+	–
Impact upon landscape	+	–	+	+	–/+	+
Maintenance	+	+	–	0	+	0
Currents and waves	–	+	0	0/+	0/+	0
Closure time	+	+	+	+	+	0/–
Space required	+	+	+	–	+	+
Colliding ships	0/–	+	+	0/–	+	0
Reliability	–/+	+	0/+	–/+	+	0
Clearance height	+	–	+	+	–/+	+

Note: – not favourable up to not feasible; 0/– below average/vulnerable; 0 average/possible; 0/+ above average; + favourable/proven technology; –/+ score depends on design choices and conditions.

Figure C.1: Comparison of gate type characteristics (Aerts et al., 2012)

C.5.1 Barge gate

The barge gate, also known as a swing gate, is a caisson stored at one side of the waterway, pivoting around a vertical axis to close. A barge gate may be buoyant or equipped with gated openings to reduce hinge and operating forces (L. F. Mooyaart and Jonkman, 2017). The advantage of a barge gate is that the structure is simple and therefore inexpensive. This type of barrier can be used for navigable openings and is space efficient. The disadvantage is the is rough and imprecise closing with large leakage. The movement of a barge gate is difficult and slow (Daniel and Paulus, 2019). Figure C.2 shows the cross-section of a barge gate. Application of this type of barrier is IHNC barrier in the US.

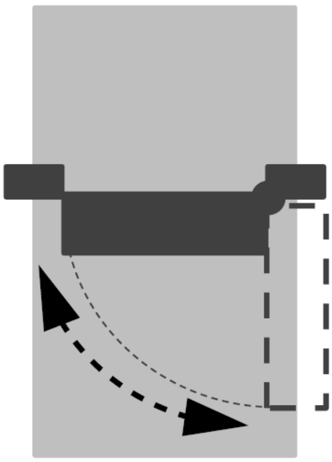

Figure C.2: Cross-section of barge gate (L. F. Mooyaart and Jonkman, 2017)

C.5.2 Bear-trap gate

Bear trap gate were frequently used in the past, not that common now anymore. A bear trap gate is constructed of two leaves that slide over one another and seal together. They are stored on the bottom of the waterway. Typically water is allowed to enter the space beneath the gate and the upstream water pressurizes the space beneath the leaves and the gate leaves rise to block the flow.

The advantage of this type of barrier it saves coast due to the elimination of a deep hydraulic chamber. The disadvantage is that the maximum height is 6 m and operation speed is very slow (PIANC, 2005).

Tees Barrage Bear Trap Gate - United Kingdom

The barrier in the United Kingdom is a bear trap gate with a width of 5.950 m. And used to control the flows for white water canoe and kayak recreation. The upstream reach is 1.598 m, center to center, and the downstream leaf 3.160 m.

C.5.3 Caisson structure

'The caisson structure is in fact a concrete closure dam that is permeable in normal conditions and can be closed during surge events. In the middle of the caissons for example a vertical lifting gate can be constructed. In normal conditions, the water is able to flow back and forth. In case a surge event approaches, the gate will be lowered, just like a regular vertical lifting gate. The disadvantage it has compared to a vertical lifting gate is that it is unlikely that that navigation will be possible through this barrier. The advantage it has compared to the vertical lifting gate is it deals better when shallow, founded on weak soils. The loads on the structure are spread out over a bigger footprint.'(de Vries, 2014)

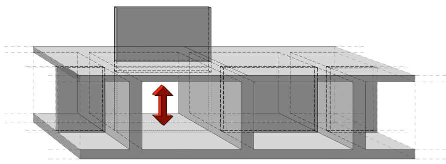

Figure C.3: Caisson structure (de Vries, 2014)

C.5.4 Flap gate

Flap gate have a straight or curved retaining surface pivoted on a fixed axis that can be under or above water level (L. F. Mooyaart and Jonkman, 2017). Flap gates are not widely applied for flood protection because the inspection, maintenance, and replacement is difficult. Flap gates are only visible when the barrier is in use. The gates are stored at the bottom recess and with one end hinged to the sill. The free end emerged above the water surface when the barrier is put in operation (Aerts et al., 2012). There are two types of flap gates, namely: hydraulic cylinders driven gates and pneumatic gates operated by air injection in flotation tanks. The advantage of flap gates are the invisibility of the barrier in the environment, distribution of load transfer to the foundation and unlimited breadth of flow opening (Aerts et al., 2012).

There are two types of flap gate, hydraulic and floating flap gate. The hydraulic flap gate has the advantage that is an applied technology, functions in both directions and has a high open and close speed. The disadvantage is maintenance and the possibility of accumulation of sand under the gate during closure. The floating flap gate had as advantage effective for relatively small water level difference and has high open and close speed. The disadvantage it is expensive, only one way functioning and the possibility of accumulation of sand under gate during closure (Daniel and Paulus, 2019).

Figure C.4 shows the cross-section of a flap gate. Figure C.5 gives an overview of the favorable and unfavorable aspects of this gate type. Application of this type of barrier is Stamford in US, Venice in Italy and Billwerder Bucht in Germany.

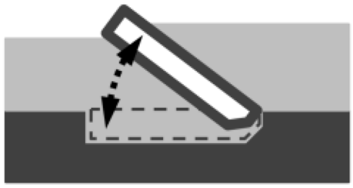

Figure C.4: Cross-section of flap gate (L. F. Mooyaart and Jonkman, 2017)

Favourable	*Unfavourable*
Structural aspects, layout and operation	
No limitation of the span	Natural frequencies low; small stiffness, great mass
Separate flaps; reduced failure risk	Pneumatic: not fully controlled
No clearance height	Hydraulic: concentration cylinders
Little space required	Underwater: corrosion, growth
Suitable for deep waters	Hinges may wear out in sand
Controlled operation flow and wave	Maintenance difficult
Not subjected to wind	
Invisible when not in use	
Hydraulic and hydrodynamic aspects	
No strong confinement of horizontal flow (gates used alternately)	Sensitivity to vibrations
Vertical closure, single flap	Small stiffness during operation
Excess water through one flap or by lowering the gate crest	Subject to down-pull flow forces and wave loads

Figure C.5: Favorable and unfavorable aspects of flap gates (Aerts et al., 2012)

Example: Stamford Hurricane Barrier - Connecticut (US)

The East Branch Barrier at Stamford comprises a 2840 foot (866m)-long earth-and-rock dike with a top elevation of more than 17 feet (5m). The structure features a 90 foot (27m)-wide channel opening protected with a single steel flap gate. The hollow steel gate rests on the bottom of the 18 foot (5.5m)-deep channel and is raised to close the opening. The gate is operated by hydraulic cylinders, which are housed in the vertical side walls. The gate is lifted in 20 minutes (Aerts et al., 2012).

Example: Venice - Italy

The MOSE barrier at Venice has a length of 370 m and a width of 48 m. Each gate has a width of 20 m and the length depends on the inlet, but varies between 18 and 30 m. When the gates are not used, they lie completely underwater. In case of a storm event, compressed air is introduced into the sluices, which empties it from the water. As the water exits the sluice gates, rotating around the axis of the hinges, they rise up to emerge and block the flow of the incoming tide in the lagoon. It has an average closing time of about 4/5 hours (MOSE, n.d.).

C.5.5 Inflatable gate

An inflatable gate is a sealed tube made of flexible material that can be inflated with air, water, or a combination. The tube is anchored with bolts and air- and watertight clamping system to the sill and wall. The material can be synthetic fiber, rubber or laminated plastic (L. F. Mooyaart and Jonkman, 2017). Figure C.6 shows the cross-section of the inflatable gate. An application of this type of barrier is the Ramspol barrier in the Netherlands.

The advantage of an inflatable barrier is that it functions in both directions and the height can be adjustable. This is because the rubber material had a durability of 25 to 50 years. The disadvantage it is expensive due to the durability of the rubber sheet, high safety factors for the rubber sheet and that the rubber material is vulnerable to punching loads (currents and waves) and UV light (Daniel and Paulus, 2019).

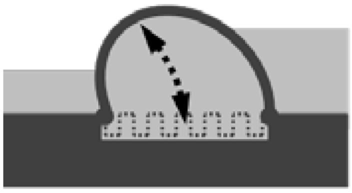

Figure C.6: Cross-section of inflatable gate (L. F. Mooyaart and Jonkman, 2017)

C.5.6 Mailbox gate

'The 'Mailbox' gate is a new type of gate. It is a heavy concrete flap gate hanging on two yokes. The yokes are founded on inclined foundation piles. In this way, an eventual soft top soil layer with poor bearing capacity is avoided. In normal conditions the flap is positioned horizontally. It can now serve as walkway while currents or tidal movement can flow underneath it. In case of surge the barrier is lowered, hanging in a somewhat diagonal position. It is a leaky system as the barrier is the combination of a top and bottom spillway. High water pressure due to surge or waves pushes the flaps open the gate. Advantage of this concept is its ability to be simply adjustable to the bathymetry. Up to now there are no examples where this gate is applied. It therefore requires thorough research in occurring internal and external forces.' (de Vries, 2014)

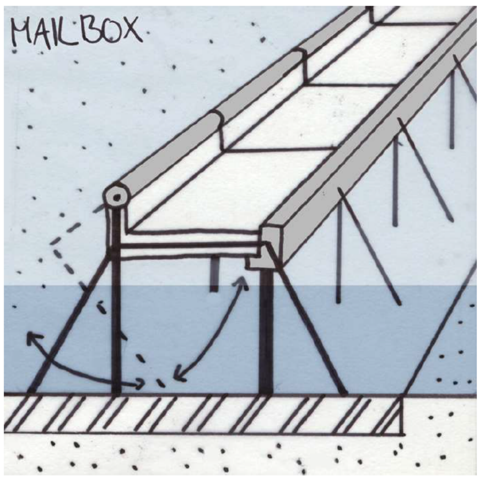

Figure C.7: Illustraction of mailbox gate (de Kort, 2013)

C.5.7 Mitre gates

Mitre gates are double-leaf gates and the leaves form an angle pointing upstream when the gates are closed, resulting in strong gates underwater level difference. Mainly used in locks (Aerts et al., 2012).

Favourable	*Unfavourable*
Structural aspects, layout and operation	
Unlimited clearance height for shipping	Very small gate span (up to 100 feet)
Little space required	Little or no controlled operation under flow and waves
Proven concept	
Not subjected to wind	
Hydraulic and hydrodynamic aspects	
Horizontal closure	Sensible to vibration as a result of flowing water
Discharge of excess water through gate	Sensible to reverse head
	Sensible to waves

Figure C.8: Favorable and unfavorable aspects of mitre gates (Aerts et al., 2012)

C.5.8 Parachute barrier

'A parachute barrier is an open fabric moveable water barrier that unfolds like a parachute in horizontal direction. Where the inflatable rubber dam is classified as closed fabric, the parachute dam is an open fabric because only one side of the rubber material is constrained. The principle is that it is opened by the water flow and kept open by the hydraulic pressure. This makes its appliance very complex in situations where a reversed head can be present. Until now, the parachute barrier has not yet been constructed. However, a structural design for a parachute barrier has been made within the context of aMaster's thesis carried out by Van der Ziel (2009).'(de Vries, 2014)

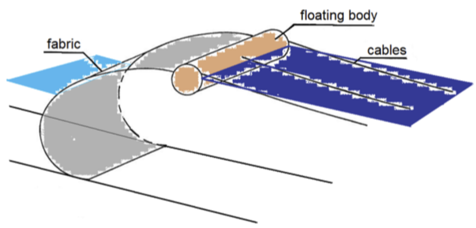

Figure C.9: Illustraction of parachute barrier (Knippels and Pechtold, 1992)

C.5.9 Reduction gate

The principle of a reduction barrier is to reduce tidal amplitudes in a river branch, bay or estuary by providing additional resistance near the mouth. The reduction barrier itself can for example be constructed as concrete caissons or rubble mound. Sections which are left open enable navigation and allow water circulation inside the estuary (de Boom, 2013). As slow changes in water level are better able to penetrate the reduction barrier the principle is most effective at fast changing water levels. Storm surges have longer time scales than tidal waves and are therefore more difficult to reduce. For locations with long storm durations (e.g. the North Sea) the reduction barrier is not that effective. For locations with shorter storm durations (e.g. hurricane prone areas like the Galveston Bay) the surges are more effectively damped increasing their applicability. The main advantages of the reduction barrier are related to the open nature of the barrier. It enables the in and outflowof water and sediments and gives migrating fish free passage. Disadvantages mainly concern the openness. The water levels inside the estuary can still rise. A sufficient retention pond behind the barrier limits this effect, but flooding will still be possible. Besides, the openness entails a feeling of being unprotected against surges. This can influence the social basis for a reduction barrier. Another downside is the high flow velocity in the openings during storm conditions. This requires a high quality bed protection to ensure the barrier's stability (de Boom, 2013).

C.5.10 Rolling gate

The rolling gate is a sliding panel stored adjacent to the waterway. They are rolled into position in case of a flood event (L. F. Mooyaart and Jonkman, 2017). Figure C.10 shows the cross-section of a rolling gate. An application of this type are the new Panama locks in Panama.

The advantage of a rolling gate is that it a strong and heavy door and proven concept. The disadvantage is that it is not possible to close under a water level difference, requires a lot of space and large part of the construction is underwater (Daniel and Paulus, 2019).

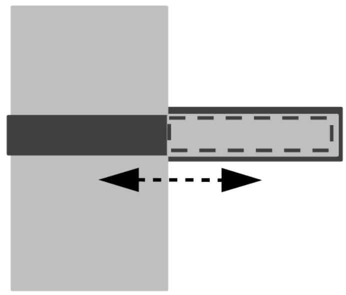

Figure C.10: Cross-section of rolling gate (L. F. Mooyaart and Jonkman, 2017)

C.5.11 Rotary segment gate

A rotary segment gate is similar to a segment gate, the difference is that this type of gate has a horizontal axis. This is located in the bed of the river and lies in a concrete sill. Therefore, it is possible to sail over the gate in opened position (L. F. Mooyaart and Jonkman, 2017). Figure C.11 shows the cross-section of a rotary segment gate.

The advantage of the rotary segment gate is the easy maintenance (inspection can be done above water), proven concept and fit for navigable opening. Disadvantage of this barrier is that is a relatively complicated structure, deep structure, expensive and potential debris can be collected in the bottom (Daniel and Paulus, 2019). An application of this type of barrier is the Thames Barrier in the United Kingdom.

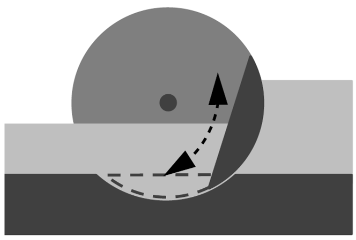

Figure C.11: Cross-section of rotary segment gate (L. F. Mooyaart and Jonkman, 2017)

C.5.12 Sector gate

A sector gate is a type of horizontally moving rotating gates. This type of gate move over a carriegeway or slideway on the sill in a river bed and not major used for floor protection. These disadvantages are the need for deep side chambers in which the gates are housed when not in use, and the risk of malfunctioning when silting occurs on the sill. When the span is limited, gates that rotate about a vertical axis can be kept free of the sill; this may reduce the risk of malfunctioning. In order to limit the forces on the slideways and in the hinges, it may be necessary to install flotation tanks in the gates. The tanks themselves, however, may not evoke dynamic wave or flow forces on the gates in a vertical direction. The side chambers and abutments with gate supports can be built within cofferdams, while the sills (concrete caissons) may be floated to the site and immersed on a gravel base or pile foundation that has been constructed underwater or built within a cofferdam (Aerts et al., 2012).

There is a special type of sector gate, the floating sector gate. Floating-sector gates have several important advantages: the gates can be stored in a relatively inexpensive, shallow dry dock in the abutments, which enables easy maintenance, and the gates can be immersed on the sill when the sill is covered with silt. A significant disadvantage of the floating gates is the sensitivity to flow-induced oscillations and dynamic wave loads, and the gates itself are expensive. The dry docks and the abutments with ball hinges can be built within cofferdams. The sill can be built underwater. The bed adjacent to the sill may be riprap protected (Aerts et al., 2012) (Daniel and Paulus, 2019).

Figure C.12 shows the cross-section of a sector gate. Figure C.14 gives an overview of the favorable and unfavorable aspects of this gate type. Application of this type of barrier is New Bedford in the US, Maeslant barrier in the Netherlands, St. Petersburg barrier in Russia, Seabrook, Harvey Canal, West Closure Complex and IHNC (Inner Harbor Navigation Canal Lake Borgne) storm barrier all in the US.

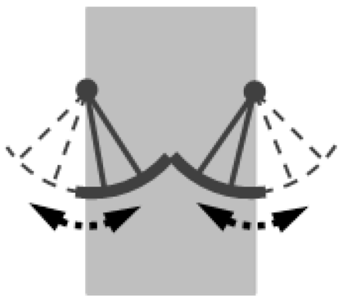

Figure C.12: Cross-section of sector gate (L. F. Mooyaart and Jonkman, 2017)

Favourable	*Unfavourable*
Structural aspects, layout and operation	
Large span feasible	Large space and deep excavation required for chambers
No clearance height limitation	Flat and smooth slideway required
Not subjected to wind	Silting may hamper operation
Suitable for deep waters	Sector gates: load transfer to hinges, maintenance, corrosion, growth
Immediately ready for operation	Straight gates: sluice gates may be required; time for dock filling
Free of sill; reduced load on sill	
Stable structure; no load concentration	
Dry docks: maintenance, no collision	
Hydraulic and hydrodynamic aspects	
Limited differential head and horizontal flow contraction in last stage of closure	Sector gates: ship collision; siltation in open chambers
Excess water: through sluice opening	
Suitable for reverse head and flow	
Not sensitive to flow vibrations	

Figure C.13: Favorable and unfavorable aspects of Horizontally moving or rotating gates (Aerts et al., 2012)

Favourable	*Unfavourable*
Structural aspects, layout and operation	
Large gate span possible	Large space required
No clearance height limitation	Operation complicated; in-flowing water may not be controlled
Shallow dry dock: easy inspection and maintenance and collision protection	A negative differential head may cause problems (pull-up forces ball hinges)
Can be immersed if sill is covered with silt	Objects on sill can cause damage
No flatness of sill required	Load concentration; forces on hinges
	Mobilization time: filling of dry docks
Hydraulic and hydrodynamic aspects	
Vertical closure of flow opening (no strong horizontal flow contraction)	Sensitivity to flow-induced oscillations
Separate sluice openings may be applied to reduce differential head and discharge excess water	Sensitive to dynamic wave forces
	Limited resistance to negative differential head

Figure C.14: Favorable and unfavorable aspects of floating-sector gates (Aerts et al., 2012)

Example: New Bedford Hurricane Barrier - Massachusetts (US)

This hurricane barrier comprises a 9100 foot (2774m)-long dam with a crest level of more than 20 feet (6m); the 150 foot (46m)-wide navigation opening can be closed with two sector gates, which are housed in side chambers in the abutments. The 60 foot (18m)-high gates roll with steel wheels on a concrete sill. The gates can be closed This hurricane barrier comprises a 9100 foot (2774m)-long dam with a crest level of more than 20 feet (6m); the 150 foot (46m)-wide navigation opening can be closed with two sector gates, which are housed in side chambers in the abutments. The 60 foot (18m)-high gates roll with steel wheels on a concrete sill. The gates can be closed (Aerts et al., 2012).

Example: Harvey Canal near New Orleans - Louisianna (US)

This hurricane barrier comprises a 9100 foot (2774m)-long dam with a crest level of more than 20 feet (6m); the 150 foot (46m)-wide navigation opening can be closed with two sector gates, which are housed in side chambers in the abutments. The 60 foot (18m)-high gates roll with steel wheels on a concrete sill. The gates can be closed (Aerts et al., 2012).

Example: Measlandkering - The Netherlands

An example of a floating-sector gate is the Rotterdam Storm Surge Barrier (Maeslantkering), The Netherlands. This well-known landmark barrier protecting the city of Rotterdam was ready for operation in 1997 and had its first and until now only successful closure under storm conditions ten years later, in November 2007. The barrier consists of two floating-sector gates, each with a radius of 807 feet (246 m) and arch length of 682 feet (208 m). The gate arm is connected to a single ball hinge on the abutments (Aerts et al., 2012).

C.5.13 Segment gate

The segment gate rotates around a horizontal axis through the bearing center. The gate lifts in open position and in closed position it rests on the sill (L. F. Mooyaart and Jonkman, 2017). And also known as a radial or tainter gate. Figure C.15 shows the cross-section of a segment gate. Application of this type of barrier is Eider Barrage and Ems Barrier in Germany, Thames Barrier in the United Kingdom and St. Petersburg barrier in Russia.

The advantage of this type of barrier is that it is material effective, relatively easy maintenance and inspection and a proven concept. The disadvantage is that a stiff support axis is requires and a disruption of the view (Daniel and Paulus, 2019).

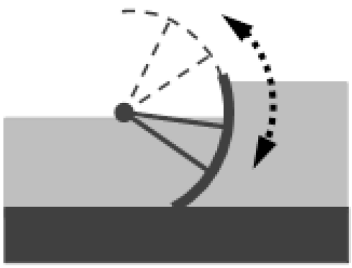

Figure C.15: Cross-section of segment gate (L. F. Mooyaart and Jonkman, 2017)

C.5.14 Vertical lift gate

Vertical lift gates move vertically for the sill. During operation, a tower supports the gate. The gate is lifted by overhead cables, sheaves, bull wheels or hydraulic cylinders. Vertical lift gates are a wildly used type of gate and therefore there is a lot of information about the construction techniques and functioning and behaviour under flow and wave conditions. Figure C.16 shows the cross-section of a vertical lift gate. Figure C.17 gives an overview of the favorable and unfavorable aspects of this gate type. Application of this type of barrier is the Hollandse IJssel, Eastern Sheldt and Hartel in The Netherlands, Ems in Germany, IHNC and Seabrook in the United States of America.

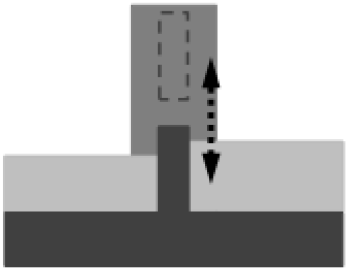

Figure C.16: Cross-section of the vertical lift gate (L. F. Mooyaart and Jonkman, 2017)

Favourable	*Unfavourable*
Structural aspects, layout and operation	
Large gate span (up to 300 feet)	Limited clearance height for shipping
Little space required	Raised gate subject to wind load
Controlled operation under flow and wave	Water depth ↔ gate height
Raised gate accessible for maintenance	Wheel gates weak spot, wearing
Proven concept	Smooth slide required ↔ growth underwater
Hydraulic and hydrodynamic aspects	
Vertical closure	Sensitivity to vibrations
Discharge of excess water	Small stiffness during operation
Overflow and reverse flow acceptable	Subject to down-pull flow forces and wave loads
Underside free of sill	
Limited vertical flow forces and wave loads	

Figure C.17: Favorable and unfavorable aspects of vertical lift gates (Aerts et al., 2012)

Example: Eastern Scheldt Storm Surge Barrier - The Netherlands

The Eastern Scheldt Storm Surge Barrier is a vertical lift gate and only closes during a storm surge. The barrier can close in one hour, during closure the gates are lowered and therefore close the flow gap (Aerts et al., 2012). It is no possible to have shipping in the Eastern Scheldt barrier. The open space of the gates can withstand heavy wave loads, a max wave height of 5.8 m and period up to 10 s (Aerts et al., 2012).

The Eastern Scheldt storm surge barrier is part of the Dutch Delta Plan. This plan consists of several back-barrier dams and storm surge barriers. Due to the dams, the tidal prism of the estuary behind the Eastern Scheldt barrier increased, resulted in larger sediment export than import. Due to the increased flow velocity, channels scoured, and the tidal flats experienced a small increased in elevation (Eelkema, 2013).

During the construction of the Delta Plan the ebb-tidal delta the sediment volume in the ebb-tidal delta increased rapidly (Eelkema, 2013). After the construction of the Delta Plan there was a strong decrease in tidal flow velocity in both the basin and ebb-tidal delta. Resulting in small clockwise rotation of the main channels and shoals. Also, the morphological activity and ebb-tidal delta sediment volume decreased (Eelkema, 2013). Due to the construction of the storm-surge barrier the tidal prism decreased by 30%, tidal range 12% and tidal current velocity by 33%. This resulted in sedimentation in channels and degradation of tidal shoals (Ngoc Quyen, 2010).

C.5.15 Vertical rising gate

Vertical rising gates lie beneath the sill in an open position. The gate closed with vertically lifted gates and positioned largely underwater in both open and closed situations. The gates can be lifted above water to allow maintenance (L. F. Mooyaart and Jonkman, 2017). Figure C.18 shows the cross-section of a vertical rising gate. Application of this type of barrier is the St. Petersburg in Russia.

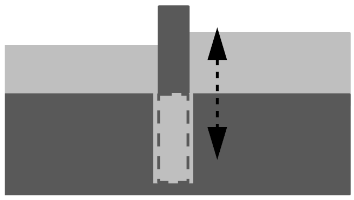

Figure C.18: Cross-section of vertical rising gate (L. F. Mooyaart and Jonkman, 2017)

C.5.16 Visor gate

'Visor gate is a three-hinged arc, pivoted on horizontal pins. In closed position, the leaf presses continuously against the sill. In open position it allows vessels to pass under the leaf, limiting the allowable air draft. The gate closure is done by gravity while opening of the gate is made by two mechanical hoists with wire ropes placed on concrete structures built on the piers. This type of gate could be applied for large spans (Erbisti, 2004).' (de Vries, 2014)

The advantage of this barrier it is material effective (relatively light and cheap due to stiffeners), proven concept, can open and close underwater level difference, strong current and standing water and no buckling possible. The disadvantage is the maintenance and inspection, spans up to 45 m, destruction of the landscape and requires though investigation to dynamic stability issues and particular vibrations (Daniel and Paulus, 2019).

IJsselweide - The Netherlands

The barrier at the south of the channel in Veessen is a 800 m long inlet that consists of a concrete bridge with 60 pans, including 60 steel visor gates. These gates seal the gap between the bridge pillars under normal circumstances and are only opened when the water is extremely high to prevent flooding. Each visor gate is 12 metres long and is opened with help from hydraulic cylinders when the water level rises. Iv-Infra designed the steel visor gates and mechanical details and performed a failure probability analysis to test the reliability of the system (IV Group, n.d.).

D Environment Study

D.1 General Galveston Bay Area

Figure D.1 shows the population density in the Galveston Bay Area. Figure D.2 shows the property values in the area.

The area that is most effected by the effect of a barrier at the San Luis Pass and Bolivar Roads Pass instead of only at Bolivar Roads Pass is the populated area at the south of Galveston Island and Texas City, and the natural area of Brazoria National Wildlife Refugee.

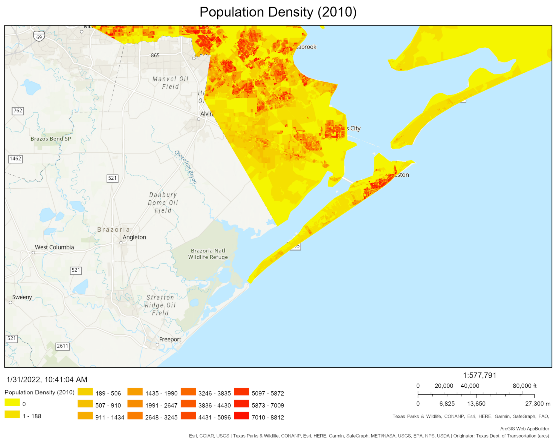

Figure D.1: Population density (2010)

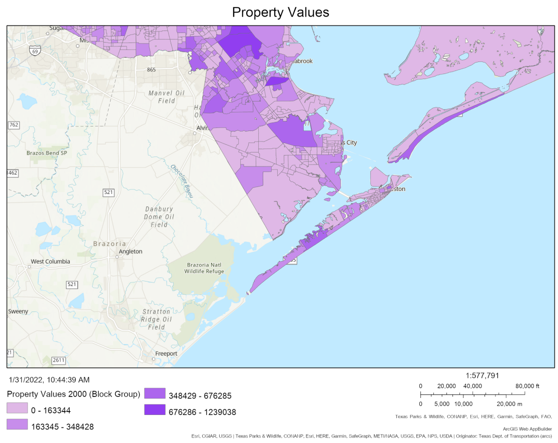

Figure D.2: Property Values

Texas City

Texas City had a population of 52 thousand people in 2020.

Brazoria National Wildlife Refugee

Brazoria National Wildlife Refugees has an incredible diversity of wild life due to it is mild temperatures, fresh and salt water estuaries, bay waters and blend of soils. Brazoria National Wildlife Refugee is for both nature and people. The area has an expanse of salt and freshwater marches, sloughs, ponds, coastal prairies, and bottom land forest represent feasting and lodging for all or part of the year. This is the home of a 12-foot alligator more than 400 species of birds, with the largest population of the Audubon Christmas bird. People can come to fish, hunt, or hike ("State of Texas Parks - Brazoria National Wildlife Refuge", 2022).

The animals that lives in the wetlands depends on the type of wetlands. The mud flats and salt water marsh are the homes for the shorebirds fishes. In the brackish wetlands' life (shell)fishes that are also the food sources for the birds. Birds that live in the area are the great blue herons, roseate spoonbills, and wood storks. The fresh water ponds are the home of purple Gallicizes, bitterns, frogs, and crawfish. River otters frolic in the tea-colored waters, and alligators sun themselves on the banks (U.S. Fish & Wildlife Service, 2017).

The type of plants that live in the wetlands depends on the salinity levels. In the salt environment, the smooth cord grass and sea ox-eye daisy. In the freshwater environment, the Gulf cord grass and bacharis.

D.2 Bathymetric of the San Luis Pass

Figure D.3 shows the bathymetric at the San Luis Pass. The San Luis Pass is a shallow area.

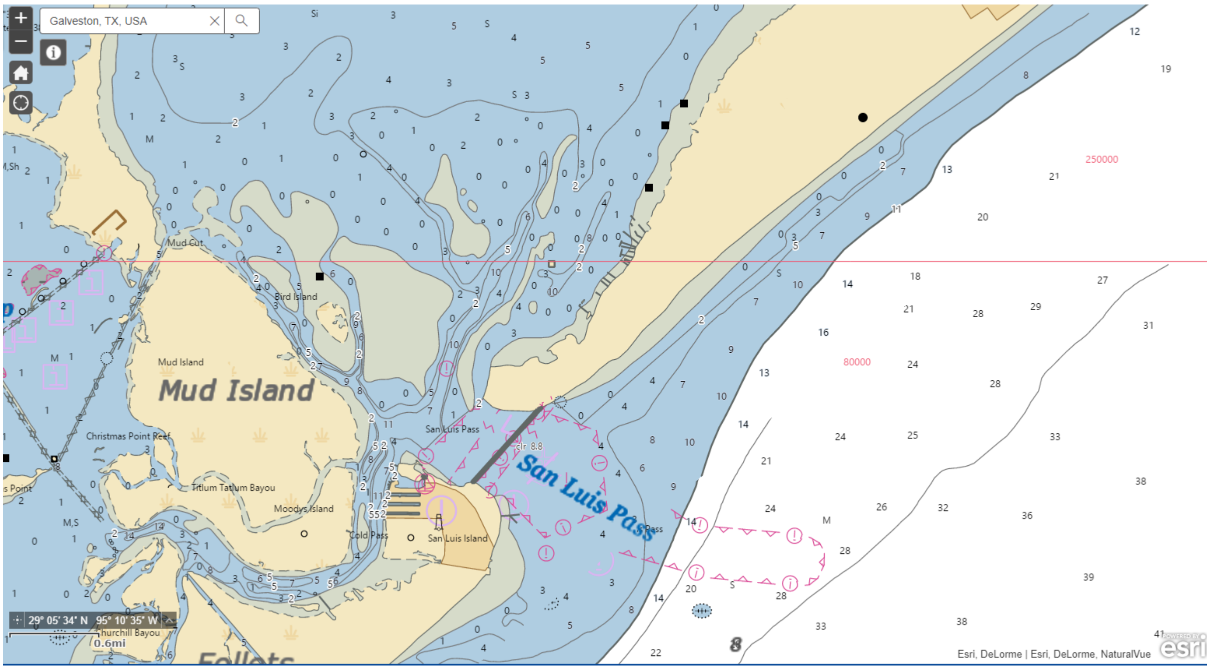

Figure D.3: Bathymetric of the San Luis Pass (noaa, n.d.)

D.3 Sediment dynamics

Figure D.4 shows the volumes of sediment around the San Luis Pass.

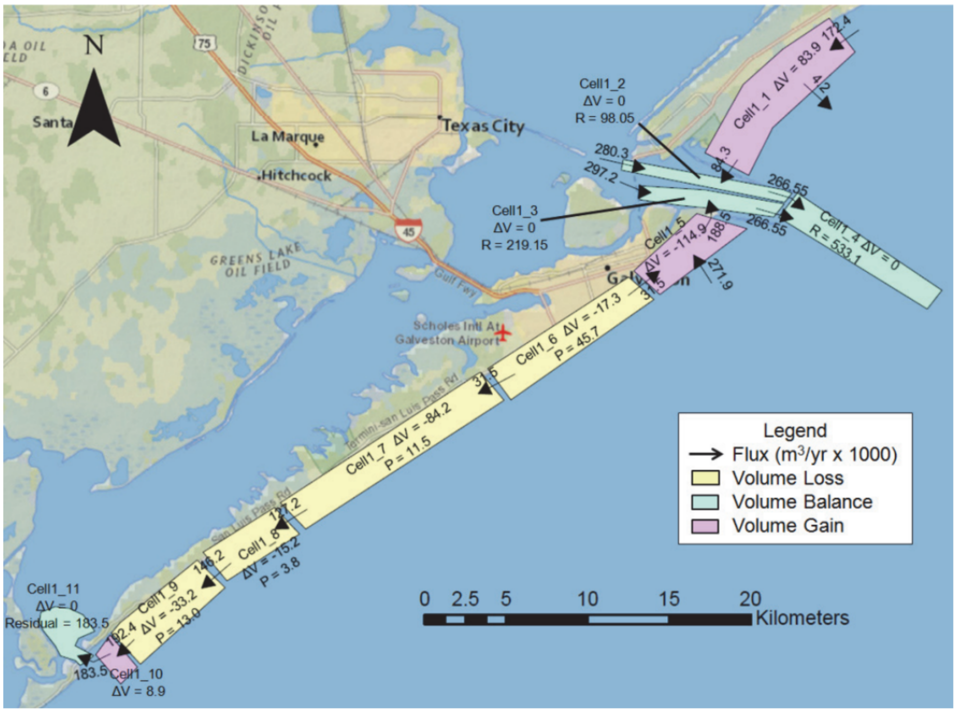

Figure D.4: Sediment transport in Galveston Island with corresponding volumes (Frey et al., 2015)

D.3.1 Soil Properties

This section describes the soil properties of the San Luis Pass. The two core samples taken at Evergreen Beach, south side of the San Luis Pass, shown in Figure D.5 and D.6. Both boring are until a depth of 7.6 m, there is only poorly graded sand.

LOG OF BORING D02 SHEET 1 of 1

ROCK

Rock Engineering & Testing Laboratory
4910 Neptune Street
Corpus Christi, TX 78405
Telephone: 361-883-4555
Fax: 361-883-4711

CLIENT: Coast and Harbor Engineering, Inc.
PROJECT: Proposed San Luis Pass Project Phase 2
LOCATION: W. Galveston Bay; Freeport, Texas
NUMBER: G106505
DATE(S) DRILLED: 9/21/06 - 9/21/06

DRILLING METHOD(S):
Disturbed Samples

GROUNDWATER INFORMATION:
Groundwater encountered at 1' during drilling.
Dry and caved at 1' upon completion of drilling operation.

SURFACE ELEVATION: N/A

FIELD DATA					LABORATORY DATA							
SOIL SYMBOL	DEPTH (FT)	SAMPLE NUMBER	SAMPLES	N: BLOWS/FT P: TONS/SQ FT T: TONS/SQ FT PERCENT RECOVERY/ ROCK QUALITY DESIGNATION	MOISTURE CONTENT (%)	ATTERBERG LIMITS: LIQUID LIMIT LL	PLASTIC LIMIT PL	PLASTICITY INDEX PI	DRY DENSITY POUNDS/CU.FT	COMPRESSIVE STRENGTH (TONS/SQ FT)	MINUS NO. 200 SIEVE (%)	DESCRIPTION OF STRATUM
		SS S-1		N = 19								POORLY GRADED SAND, 2.5Y 4/2 dark gray brown, medium.
		SS S-2		N = 25							4	Same as above, 2.5Y 5/2 brown gray.
	5											
		SS S-3		N = 21								Same as above, 2.5Y 4/2 dark gray brown.
		SS S-4		N = 11							3	POORLY GRADED SAND, 2.5Y 3/1 very dark gray, medium.
	10											
		SS S-5		N = 16								Same as above, 2.5Y 5/2 gray brown.
		SS S-6		N = 19							2	Same as above, 2.5Y 5/2 gray brown.
	15											
		SS S-7		N = 15								POORLY GRADED SAND, 2.5 4/1 dark gray, medium.
	20											
		SS S-8		N = 17							3	Same as above, 2.5 5/2 gray brown.
	25											Boring terminated at a depth of 25' below the ground surface.

N - STANDARD PENETRATION TEST RESISTANCE
P - POCKET PENETROMETER RESISTANCE
T - POCKET TORVANE SHEAR STRENGTH

REMARKS:
Soil Sampling perfomred by Envirocore, Inc, a drilling subcontractor to RETL, at N29.0785 deg W95.1248 deg.

LOG_OF_BORING G106505.GPJ ROCK_ETL.GDT 10/16/06

Figure D.5: Boring at San Luis Pass, 1

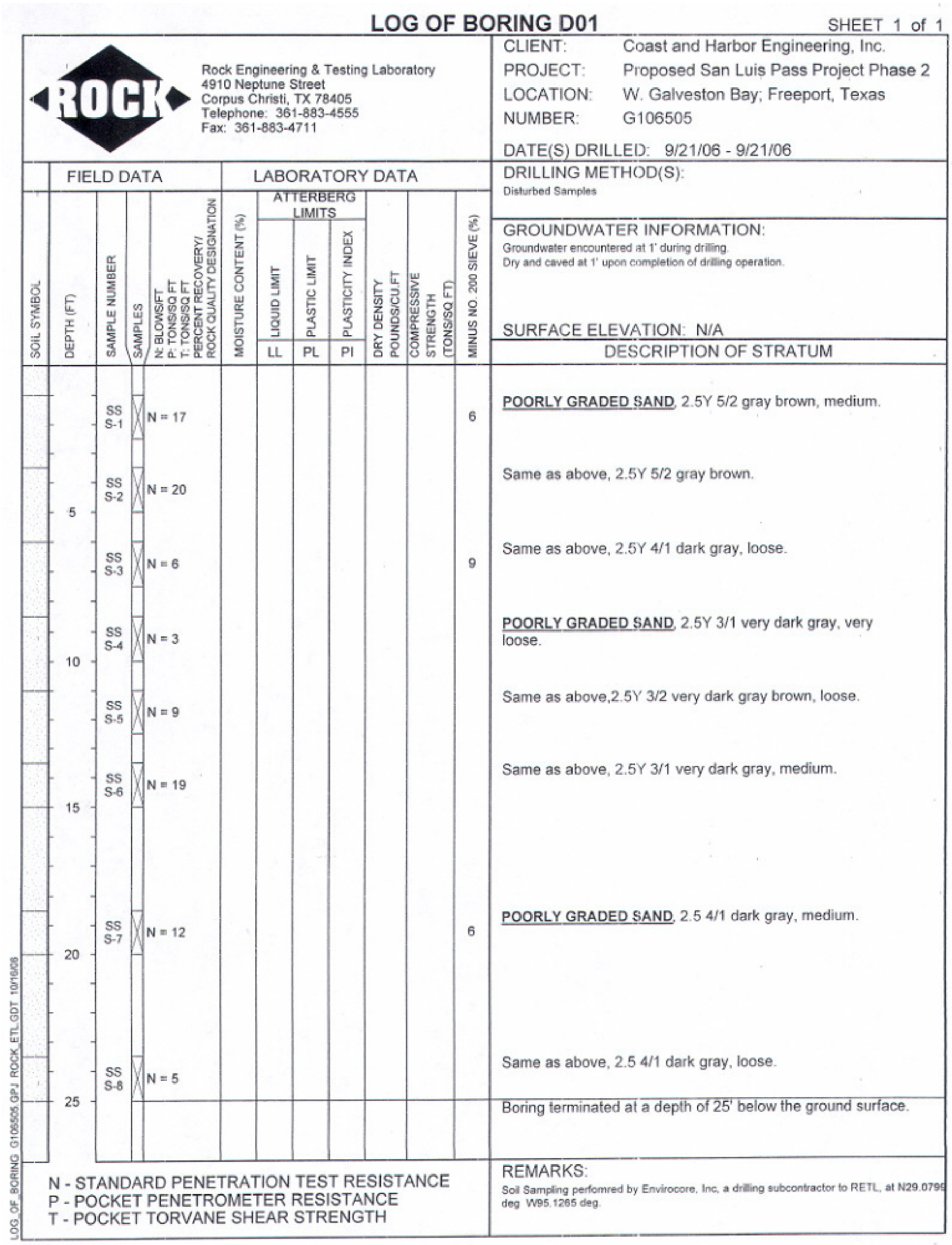

LOG OF BORING D01 SHEET 1 of 1

Rock Engineering & Testing Laboratory
4910 Neptune Street
Corpus Christi, TX 78405
Telephone: 361-883-4555
Fax: 361-883-4711

CLIENT: Coast and Harbor Engineering, Inc.
PROJECT: Proposed San Luis Pass Project Phase 2
LOCATION: W. Galveston Bay; Freeport, Texas
NUMBER: G106505
DATE(S) DRILLED: 9/21/06 - 9/21/06
DRILLING METHOD(S): Disturbed Samples
GROUNDWATER INFORMATION: Groundwater encountered at 1' during drilling. Dry and caved at 1' upon completion of drilling operation.
SURFACE ELEVATION: N/A

Depth (ft)	Sample number	N: Blows/ft	Minus No. 200 sieve (%)	Description of stratum
	SS S-1	N = 17	6	POORLY GRADED SAND, 2.5Y 5/2 gray brown, medium.
5	SS S-2	N = 20		Same as above, 2.5Y 5/2 gray brown.
	SS S-3	N = 6	9	Same as above, 2.5Y 4/1 dark gray, loose.
10	SS S-4	N = 3		POORLY GRADED SAND, 2.5Y 3/1 very dark gray, very loose.
	SS S-5	N = 9		Same as above,2.5Y 3/2 very dark gray brown, loose.
15	SS S-6	N = 19		Same as above, 2.5Y 3/1 very dark gray, medium.
20	SS S-7	N = 12	6	POORLY GRADED SAND, 2.5 4/1 dark gray, medium.
25	SS S-8	N = 5		Same as above, 2.5 4/1 dark gray, loose.
				Boring terminated at a depth of 25' below the ground surface.

N - STANDARD PENETRATION TEST RESISTANCE
P - POCKET PENETROMETER RESISTANCE
T - POCKET TORVANE SHEAR STRENGTH

REMARKS: Soil Sampling perfomred by Envirocore, Inc, a drilling subcontractor to RETL, at N29.0799 deg W95.1265 deg.

LOG OF BORING G106505.GPJ ROCK_ETL.GDT 10/16/06

Figure D.6: Boring at San Luis Pass, 2

The k-factor is a quantitative description of the inherent erodibility of a particular soil. It is a measure of the susceptibility of soil particles to detachment and transport by rainfall and runoff. For a particular soil, the soil erodibility factor is the rate of erosion per unit erosion index from a standard plot. The factor reflects the fact that different soils erode at different rates when the other factors that affect erosion (e.g., infiltration rate, permeability, total water capacity, dispersion, rain splash, and abrasion) are the same. Texture is the principal factor affecting K-factor, but structure, organic matter, and permeability also contribute. The soil erodibility factor ranges in value from 0.02 to 0.69 (Goldman et al. 1986; Mitchell and Bubenzer 1980). Author: Steven J Goldman; Taras A Bursztynsky; Katharine Jackson Publisher: New York [etc.] : McGraw-Hill, cop. 1986. Edition/Format: Print book : EnglishView all editions and formats Rating: (not yet rated) 0 with reviews - Be the first.

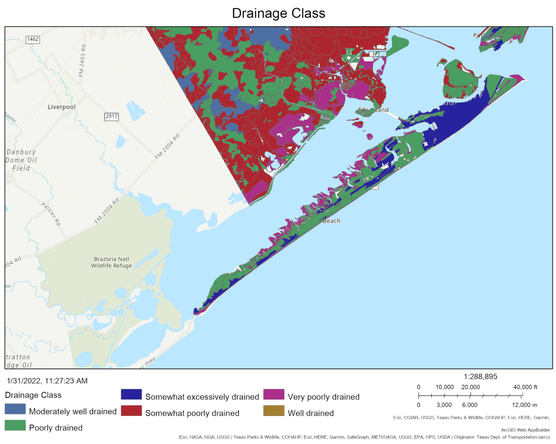

Figure D.7: Drainage class

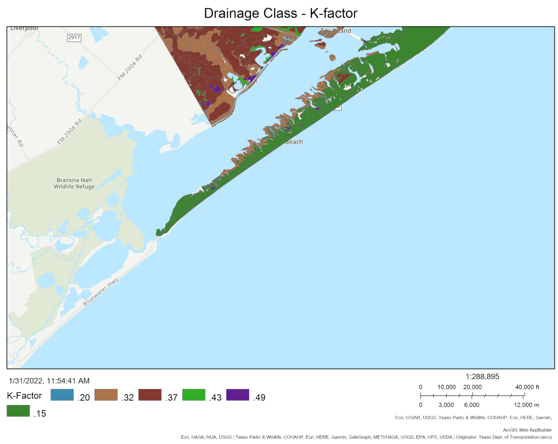

Figure D.8: Drainage class, K-factor

D.4 Tides and Currents

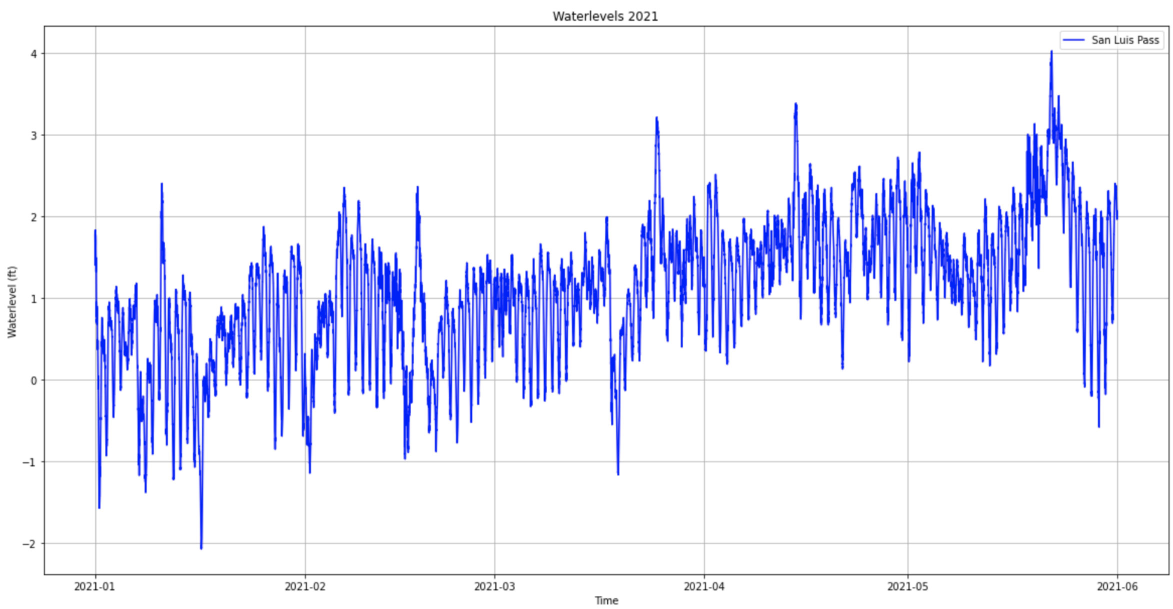

Figure D.9: Water levels 2021 San Luis Pass

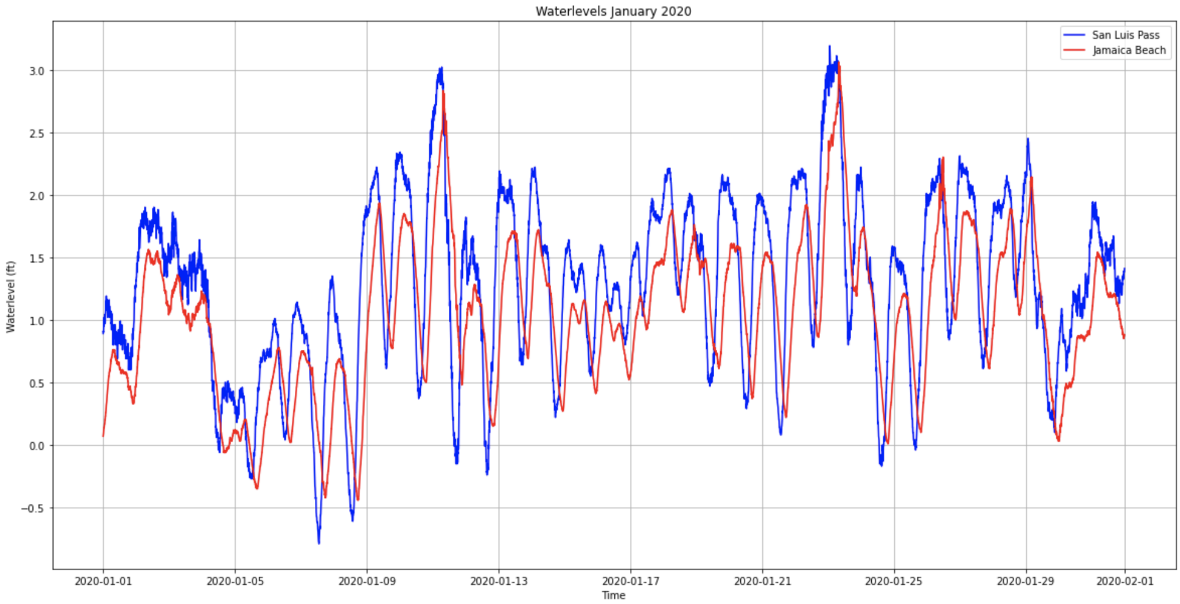

Figure D.10: Water level at San Luis Pass and Jamaica Beach in January 2020

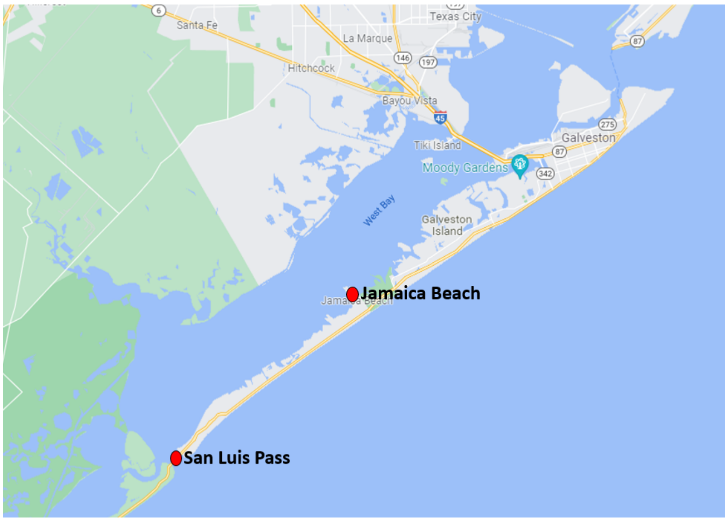

Figure D.11: Locations water level measurement points in the West Bay

D.4.1 Model tidal range predictions in San Luis Pass and West Bay

Model 1: Simplified

The effect of a reduction of the cross-sectional area at the San Luis Pass is simulated. The small basin approximation is applied. This is because the length is small compared to the tidal wave length. This model has several simplifications. The flow resistance and inertia are neglected, meaning the water level in the West Bay is always horizontal. And there is only one inlet (San Luis Pass) assumed. Therefore, a simple model can be used, shown in equation D.1 (Battjes and Labeur, 2017). With V the volume of water in the considered bay, West Bay. And Q the discharge to the bay, San Luis Pass.

$$\frac{dV}{dt} = Q \tag{D.1}$$

The velocity scales approximately with equation D.2 (Battjes and Labeur, 2017). With δh the difference in water level outside and inside the basin. It is assumed that all the kinetic energy is dissipated. The cross-sectional area (A) and bay surface (S) are constant. The differential equation, equation D.3 (Battjes and Labeur, 2017), is solved nummerically for the given outside water level in Matlab.

$$u = \sqrt{2d\delta h} \tag{D.2}$$

$$S\frac{dh_{\text{b}}}{dt} = A\sqrt{2g|(h_{\text{out}} - h_{\text{b}})|}sign(h_{\text{out}} - h_{\text{b}}) \tag{D.3}$$

The surface area of the West Bay is 195 km^3. Estimated with Google Earth The cross-section of the San Luis Pass is a length of 1 km with a width of 4 m. Figures D.12 to

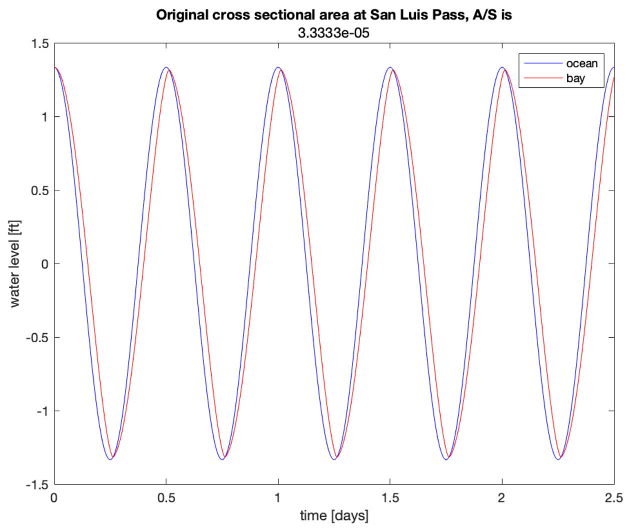

Figure D.12: Tide difference ocean and bay – original cross-section San Luis Pass

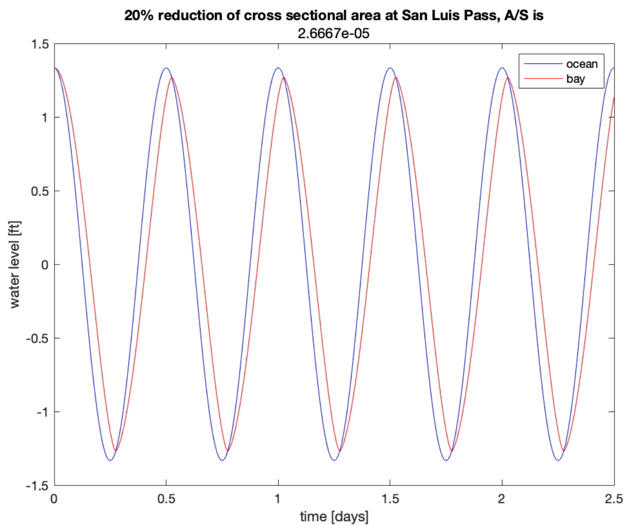

Figure D.13: Tide difference ocean and bay – 20% reduction of cross-section San Luis Pass

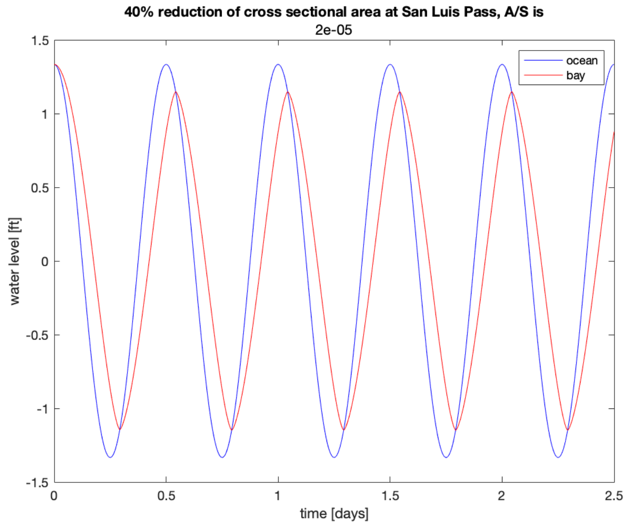

Figure D.14: Tide difference ocean and bay – 40% reduction of cross-section San Luis Pass

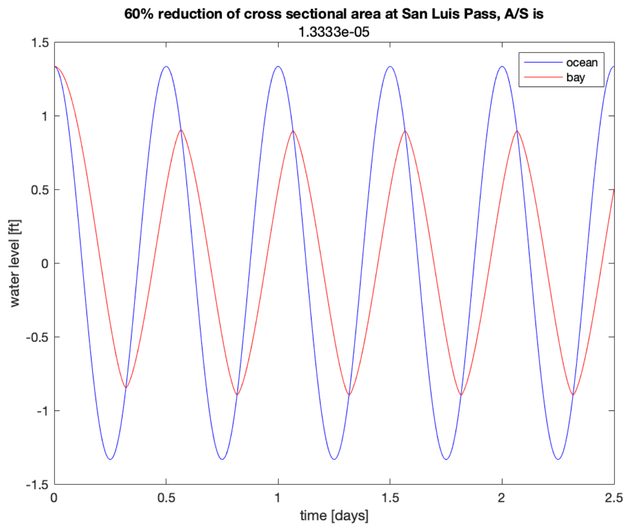

Figure D.15: Tide difference ocean and bay – 60% reduction of cross-section San Luis Pass

Model 2, according to Battjes and Labeur, 2017

The model is a discrete model that models the water levels in the bay with a reduction of the inlet at San Luis Pass. From the data of the San Luis Pass can be concluded that the amplitude of the sea is 0.4 m. The wave period is 12 hours. The area of the free surface basin in 180 km^2. And the wetted conveyance cross-section area is 4000 m^2. The San Luis Pass is a short connection, the length of the channel goes to zero. And therefore, the inertia is neglected. In the model, the assumption is made that the discharge thought the connection (San Luis Pass) responds instantaneously to the variations in the head difference across it. For a gap inlet, $\chi = 0.5$ (Battjes and Labeur, 2017)
The python model is as follows:

$$\omega = \frac{2\pi}{T} \tag{D.4}$$

$$\Gamma = \frac{8}{3\pi}\chi(\frac{A_\mathrm{b}}{A_\mathrm{c}})^2\frac{\omega^2\hat{\zeta}_\mathrm{s}}{g} \tag{D.5}$$

$$\zeta_s = \hat{\zeta}_s \cos\omega t \tag{D.6}$$

$$\zeta_b = \hat{\zeta}_b \cos(\omega t - \theta) \tag{D.7}$$

$$r = \cos\theta = \frac{1}{\sqrt{2}\Gamma}\sqrt{-1 + \sqrt{1 + 4\Gamma^2}} \tag{D.8}$$

$$tan(\theta) = \omega\tau \tag{D.9}$$

$$\hat{Q} = A_b\omega\hat{\zeta}_b \tag{D.10}$$

With:
A_b = Area of free surface basin
A_c = Area of wetted conveyance cross-section
ω = Radial frequency in harmonic motion
T = Wave period
$\hat{\zeta}_\mathrm{s}$ = Amplitude water level at sea
$\hat{\zeta}_\mathrm{b}$ = Amplitude water level in basin
ζ_s = Fluctuations of water level at sea
ζ_b = Fluctuations of level in basin
χ = Dimensionless loss coefficient
Γ = Dimensionless parameter containing all independent variables playing a role in the present problem
r= Ration between the amplitude of the sea and basin
θ = Phase lag of the water level in the basin behind the sea
τ = Relaxation time in inlet-bay system
$\hat{Q}$ = Amplitude of the discharge

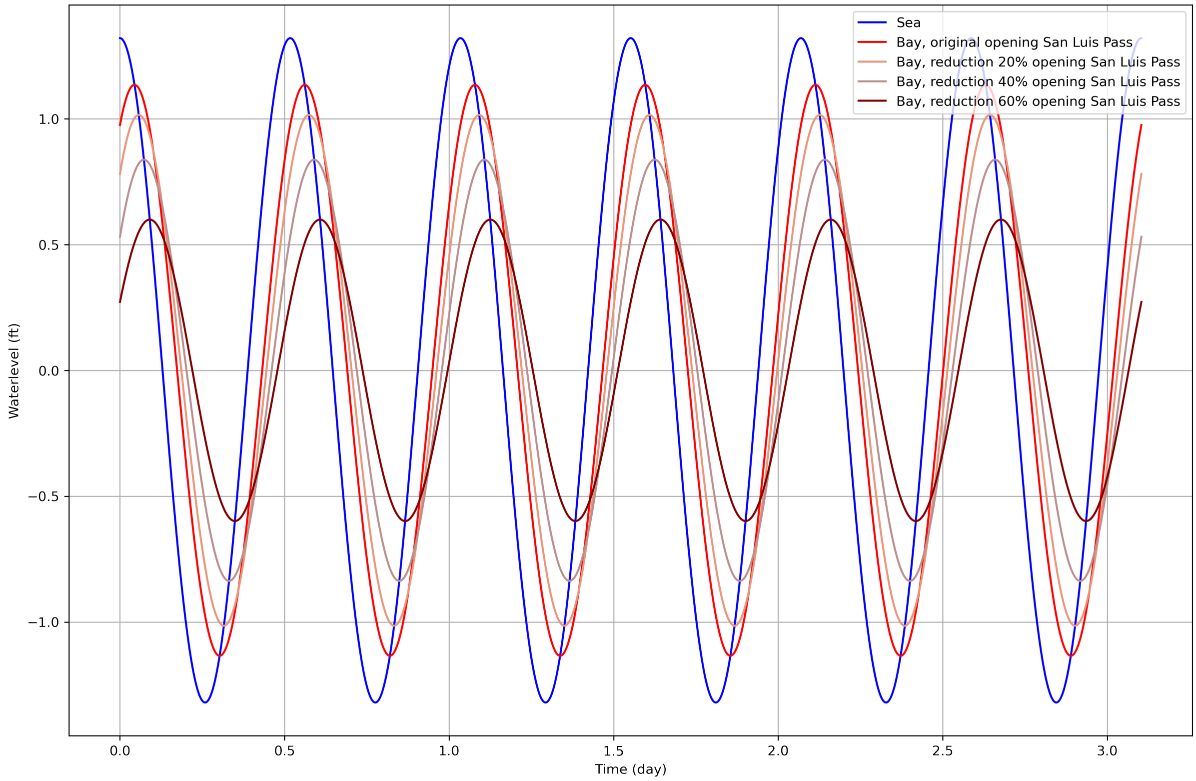

Figure D.16: Tide predictions Sea and Bay with different reduction at opening San Luis Pass

Figure D.17 shows the result of the model. The amplitude of the tide in the West Bay decreases when the opening of the San Luis Pass is reduced.

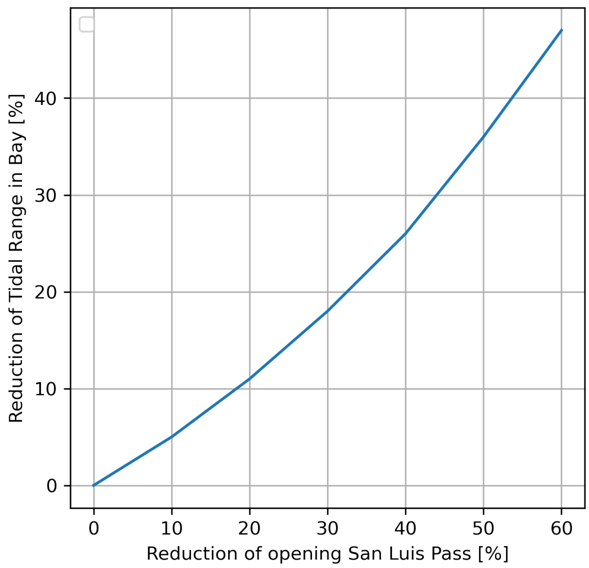

Figure D.17: Reduction of opening San Luis Pass with corresponding reduction of tidal range in the West Bay

Small values of Γ correspond with rapid and strong system response (r≃ 1) and large values show a slow and weak response (r«1). Figure D.18 shows the r with the corresponding reduction of the opening in the San Luis Pass. Without reduction of the opening, the system will respond rapid and strong. The more the opening is closed, the slower and weak the system reacts.

Equation D.9 shows the resistance of the system. Since $\omega\tau$ represents the relative magnitude of the resistance. ω is a constant since the wave period at sea doesn't change. When $\omega\tau$«1, the resistance is insignificant, so the basin level can more or less follow the relatively slowly varying water level at sea. On the other hand, when $\omega\tau$»1 the system has a timescale that is long compared with the excitation period, it can hardly follow the excitation since it variate rapidly. The response is weak, and the lag is large.

Figure D.18 shows the amplitude difference between the sea and the West Bay and the relative magnitude of the resistance. This figure concludes that a reduction of the opening in the San Luis Pass leads to a slower and weaker reaction of the system.

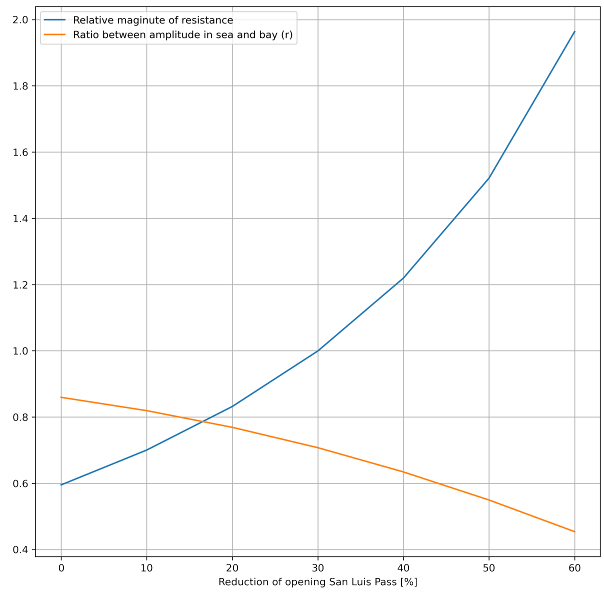

Figure D.18: Response of the system due to reduction of opening San Luis Pass

Figure D.19 shows the maximum velocity through the San Luis Pass when reducing the opening. These values, with the original opening of the San Luis Pass, are in range with the values in other studies (Matsumoto et al., 2005).

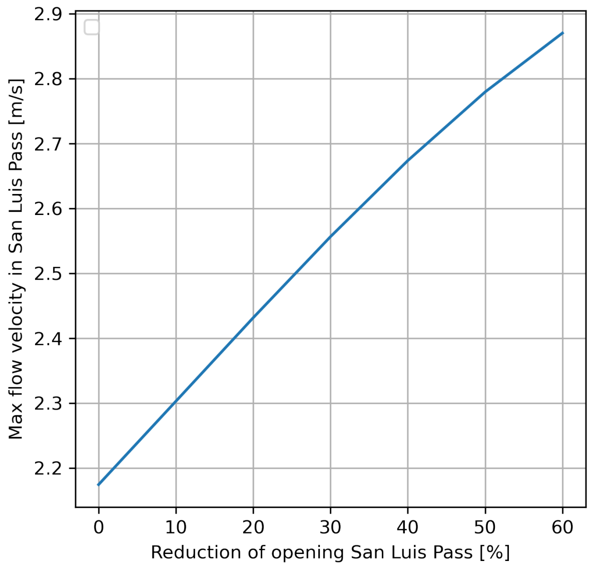

Figure D.19: Opening San Luis Pass with max flow velocity

Validation of the model

Figure D.20 shows the water level at the San Luis Pass and in the center of the West Bay (Jamaica Beach). The difference between the two water levels is approximately 0.25 ft (7.6 cm) for the current situation in January 2020. The model show a difference of 0.2 ft (6.1 cm). Therefore, it can be said that the model gives a representative of the situation in San Luis Pass and the West Bay regarding the tide amplitude differences.

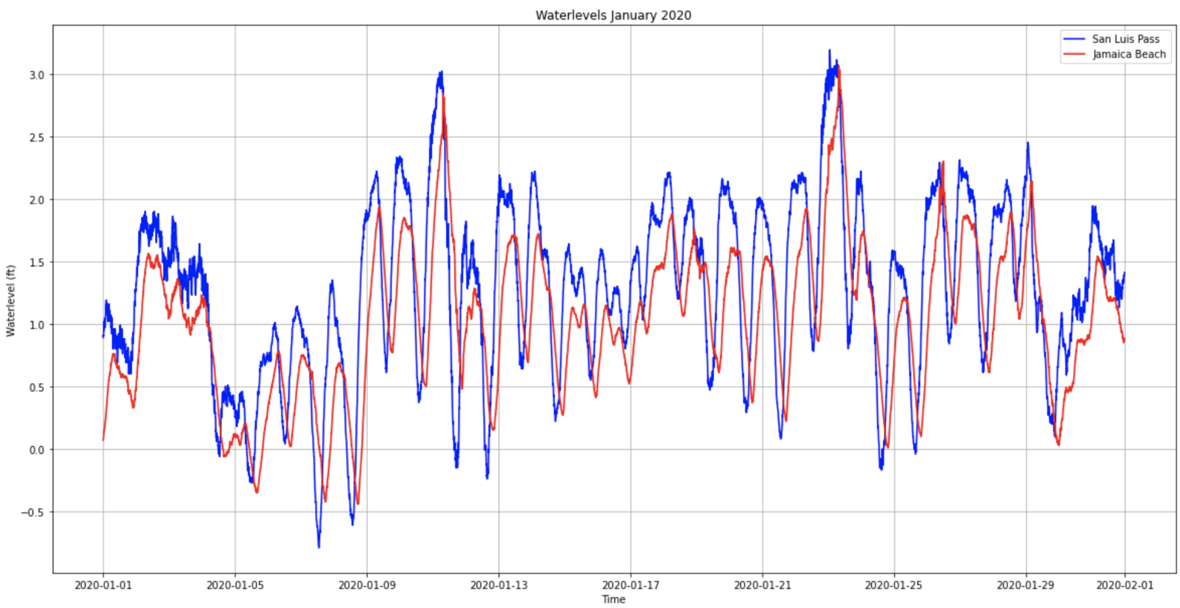

Figure D.20: Water level at San Luis Pass and Jamaica Beach in January 2020

Change in intertidal area

A reduction of 60% of the opening of the San Luis Pass result in a tidal range difference of 0.5 ft (15.24 cm). Shown in Figure D.17. The change in area of that becomes total wet instead of intertidal area due to a reduction in tidal range is 35% difference. In the original situation is the intertidal area 15% of the total wet area of the West Bay. With a tidal reduction of 0.5 ft. the intertidal area of the West bay is 10% of the total wet area of the West Bay. This is illustrated in Figure D.21. The green area is the still intertidal area with a reduction of tidal range. And the red area is the intertidal decreased area. However, most of the decreased area due to the difference in tidal range is on the east side of the West Bay. This area is close to the Bolivar Roads Pass. Therefore, it is probably more influenced by the potential barrier in this inlet than the San Luis Pass.

The area most effected by the change in tidal range is in the area near Jamaica beach at Galveston Island.

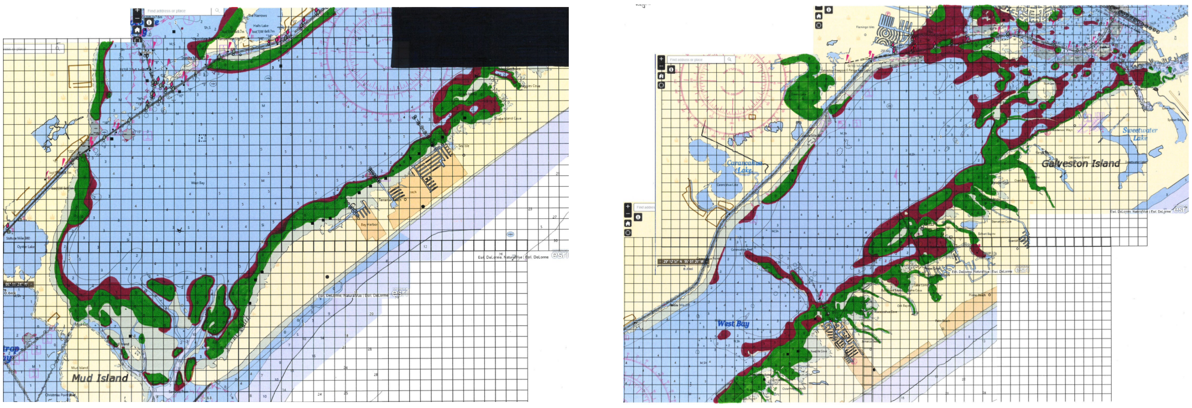

Figure D.21: Intertidal area changes for a difference of 0.5 ft (15 cm) in tidal range

D.5 Environment Species and other things

In the Galveston Bay Area are several marches. The optimum depth for fresh and intermediate marches is 80-90% of the open water area has a depth of less than 0.5 m (1.6 ft). For brackish and saline marches, the optimum is assumed to be 70-80% (GCCPRD, 2018a). For brackish marshes, this variable represents the average annual salinity conditions. Optimal conditions for brackish marshes are between 0 ppt and 10 ppt (GCCPRD, 2018a).

D.6 The land use behind the San Luis Pass

The land use around the San Luis Pass consists of mainly wetlands. The land use of Galveston Bay in 2005 is shown in Figure D.22.

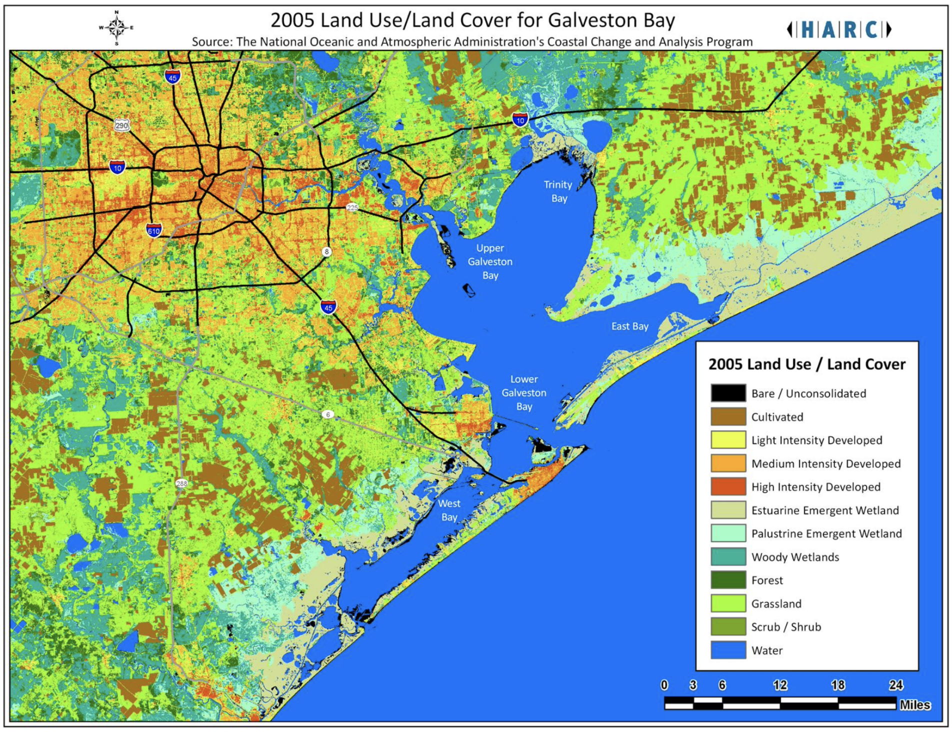

Figure D.22: Land use of Galveston Bay (HARC, 2005)

D.6.1 Definition Wetlands

The definition of wetland according to the Fish and Wildlife Service is:
Wetlands are lands transitional between terrestrial and aquatic systems where the water table is usually at or near the surface or the land is covered by shallow water ("Wetlands Communities in the Galveston Bay area", n.d.).
For purposes of this classification wetlands must have one or more of the following three attributes: (1) at least periodically, the land supports predominantly hydrophytes, (2) the substrate is predominantly undrained hydric soil, and (3) the substrate is nonsoil and is saturated with water or covered by shallow water at several time during the growing season of each year.

D.7 Other environmental details

Oil and Gas

Houston a place known for the oil and gas industry. Figure D.23 shows the location of the oil and gas units, leases and platforms.

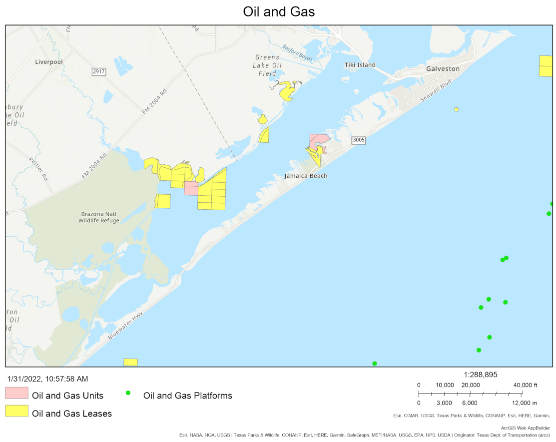

Figure D.23: Oil and Gas ("Bay Atlas Map", n.d.)

Erosion, dredged sites and ship channel

In the West Bay near the main land the intercostal highway is located. This is an important shipping channel all along the Gulf of Mexico, from Texas to Florida. Jamaica Beach is the only location that erodes in Galveston Island. Figure D.24 shows the locations of the ship channel, dredging sites, erosion sites and coastal leases.

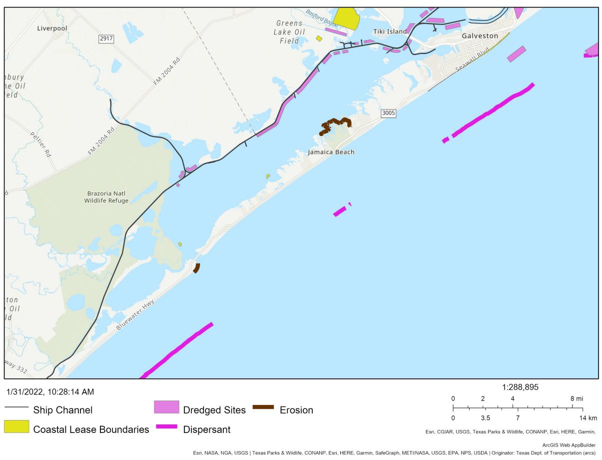

Figure D.24: Erosion, dredged sites and ship channel around the San Luis Pass ("Bay Atlas Map", n.d.)

D.8 Nature Values

Habitat priority

Figure D.25 shows the habitat priorities in the West Bay.

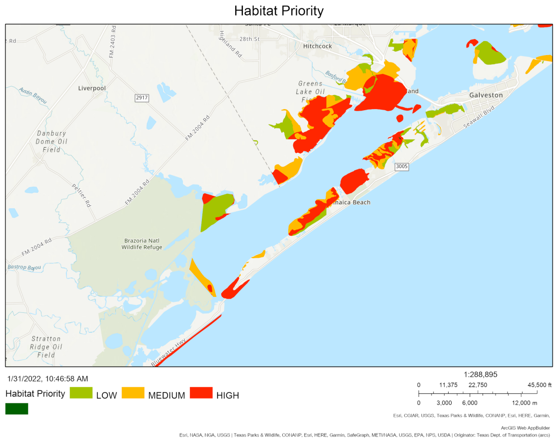

Figure D.25: Habitat Priority (“Bay Atlas Map”, n.d.)

D.9 Risks

Wind risk

Figure D.26 shows the wind risk speed on the different areas in the Galveston Bay Area. Figure D.27 shows the wind risk in the Galveston Bay Area.

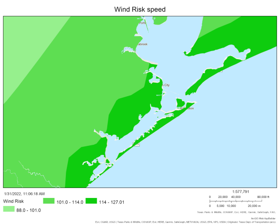

Figure D.26: Wind Risk speed (“Bay Atlas Map”, n.d.)

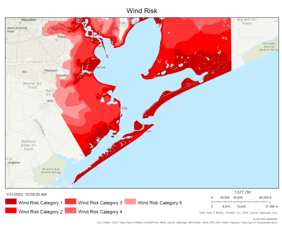

Figure D.27: Wind Risk (“Bay Atlas Map”, n.d.)

Fire Risk Zones

Figure D.28 indicated the fire risk zones.

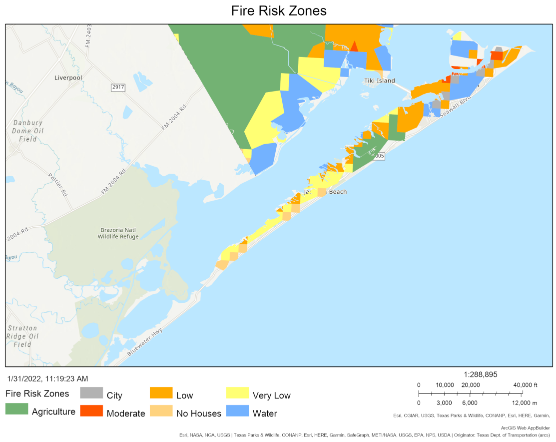

Figure D.28: Fire Risk Zones (“Bay Atlas Map”, n.d.)

Flood Frequency

Figure D.29 indicated the flood frequency, ranging from occasionally to frequent.

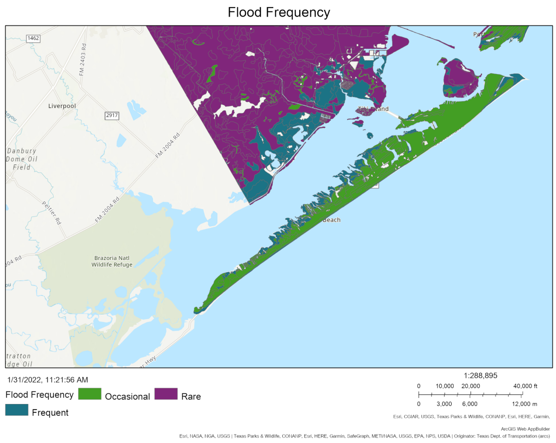

Figure D.29: Flood Frequency (“Bay Atlas Map”, n.d.)

D.10 Swimming

Swimming in the San Luis Pass is prohibited due to the unpredictable and strong current. Figure D.30 depicts the area on the western side where swimming is prohibited.

Figure D.30: Area prohibited to swim at San Luis Pass (State of Texas and County of Brazoria, 2017)

E
Adaptive Delta Management

The adaptive delta management is using system engineering to integrate and structured a set of methodologies that can be used for successfully realizing a project. This is based on the concepts of thinking in system. The system can be set up in different multilayer. Every layer is being investigated and corresponding with this layer the boundary conditions are set. The design lifetime of a foundation and superstructure is 100 years. The design lifetime of a gate is 50 years. And the design lifetime of mechanical is 25 years (Tuin et al., n.d.). The design of a storm surge barrier has a lot of uncertainties. Because the design overall design lifetime of a storm surge barrier is 100 years, the total design is made for 100 years. With a longer design life, the uncertainties are larger, and therefore the design becomes more conservative. For example the design life of a gate is 50 years, at end of 50 years gates should be replaced with new ones. Designing the gates for 50 years instead of 100 years would result in more accurate boundary conditions and a less conservative design for the gated. Since the uncertainties increase over time and there is more climate and sea level rise data available in 50 years. Resulting in a less conservative design due to the limited design lifetime of the gate, compared to the overall structure. The foundation do has a lifetime of 100 years, and therefore it is designed with the predictions of 100 years. The result of this is shown in Figure E.1 (Tuin et al., n.d.). So looking to the lifetime of the different components of the structure lead to a less over designed total structure and therefore more economically.

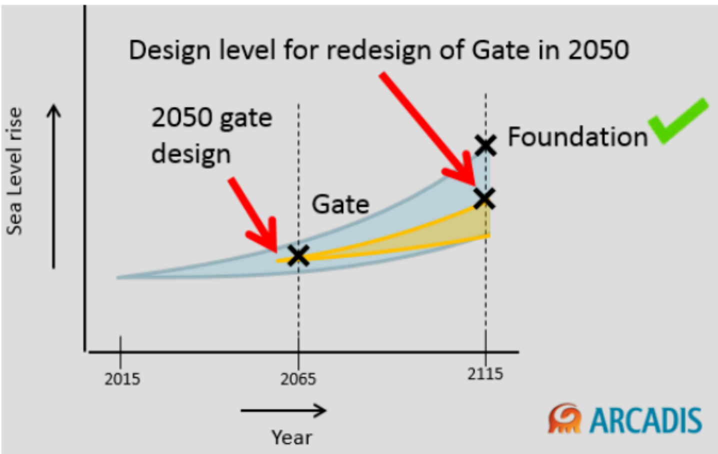

Figure E.1: Climate uncertainties with respect to barrier design

F Selection of Conventional Storm Surge Barriers

In this appendix, the barrier assessment is further explained. For the barrier assessment, 17 types of gates are investigated. Each gate type is described in appendix C. Below, every gate type is evaluated for the San Luis Pass. Table F.1 shows the result of the barrier assessment.

F.1 Barge Gate

The advantages of the barge gate are that the structure is simple and inexpensive to build, it is fit for navigable opening and free gate in space efficient. The disadvantage is that is a rough and imprecise closing with large leakage. The movement control is difficult, and the operation is slow and complex. For the San Luis Pass, this gate is not so suitable because the surface under the gate must be smooth. The San Luis Pass is a very dynamic pass with lots of sediments moving. Also, the water level at the San Luis Pass is relatively low so in the days before the hurricane, which makes the closure of a barge is extra difficult.

F.2 Bear trap gate

The advantage of the bear trap gate is that it is relatively cheap and overflow can be allowed. The disadvantage is that economically maximum height is 6 m and the inspection and maintenance is difficult. For the accumulation of sand inside the bear trap gate can be minimized with an elevated water pressure inlet.

F.3 Caisson structure

The caisson structure is simple structure that keep the intertidal area mainly the same. Therefore, it is easy to construct and relatively cheap. The only disadvantage of the caisson structure is that it is impossible for vessels to pass. This could be combined with another type of gate for vessels to pass to solve this problem. The caisson structure could be combined with vertical lifting gates. The disadvantages of this type is that the there is a lot of view blocking.

A preliminary design of the caisson structure showed that it would reduce the opening of the San Luis Pass by 3%. And that 17 caisson are needed to close the pass. Over the caissons, a bridge can be constructed. The vertical lifting gates could be steel gates with horizontal beams and vertical stiffeners.

F.4 Flap gate - Floating

The floating flap gate is for the San Luis Pass not an optimal solution because of the only one retaining height and that is can not deal great with a large head différance. The San Luis Pass is a dynamic pass with a large amount of moving sediment. A gate to come from the ground had as a large disadvantage that the sediment can accumulate behind the gate in open position. When the gate needs to be closed again, it will probably will never can go back to its original position due to the sediments.

F.5 Flap gate - Hydraulic

The hydraulic flap gate has the same main disadvantage as the floating flap gate, namely the accumulation of sand under the gate during closure. The advantage is that the gate has a fast opening and closing also under a head level différance. This is very favorable for hurricane condition due to the rapid change of winds. Site note, economically it is not feasible to construct a hydraulic flap gate in flows deeper than 6 m.

F.6 Inflatable barrier

The inflatable barrier has as advantage that is functions in both direction, but the main disadvantage is the maintenance and building cost. The barrier is stored underwater, which is favorable for the view at the San Luis Pass. But the pass is very dynamic in water depth, this makes the chose of the depth of the storage of the barrier difficult. There are high and wide piles needed for the force transfer.

F.7 Mailbox gate

The mailbox gate has a lot of potential because the gate could be stored under the bridge, so there is no view blocking. The gate could be design in different components that are place on top of each other to construct the required height of the barrier. The disadvantage of this type of barrier is that opening and closing under a water level difference requires a lot of pressure because the door opens as a garage door, so the water needs to be pushed away.

F.8 Mitre gate

The mitre gate can not deal with currents and waves and therefore is not an optimal solution as gate type for a storm surge barrier.

F.9 Parachute barrier

The advantage of the parachute barrier is that is can be adjustable for the height and has minimum impact on the environment. The disadvantage of this barrier is that there is a lot of additional research needed, and a new bridge is needed for the stability cable of the parachute barrier. Also, the parachute barrier is connected on the bottom of the surface, for the San Luis Pass this is less favorable due to its dynamical environment.

F.10 Reduction gate

The reduction is actually not really a gate type, but a more permanent structure that enables the in and outflow of water and sediment.

F.11 Rolling gate

The advantage of the rolling gate is the doors are strong and heavy. The disadvantage is that is requires a lot of space, what is not really favorable at the San Luis Pass. The gate should be close in advance of a hurricane because it can be closed and opened in water level difference.

F.12 Rotary segment gate

The rotary segment gate is stored in on the bottom of the surface. The main disadvantage at the San Luis Pass is the potential debris and sediment collection at the bottom. The building cost is relatively high because it is a quite complicated structure. The maintenance is easy because it can be done above water. Since the gate is stored underwater in normal conditions, there is no view blocking.

F.13 Sector gate

The sector gate has the advantage that it is applicable to large spans. But the gates needs to be stored on the site and therefore is not very favorable for the San Luis Pass because this would reduce the opening of the pass.

F.14 Segment gate

The advantage of the segment gate is the material effectiveness and maintenance and inspection. The disadvantage is the requirement for a stiff support axis and the view blocking.

F.15 Vertical lifting gate

The advantage is the large span (up to 100 m), the maintenance and inspection and the controlled operation under flow and waves. The disadvantage are the high lifting forces and the view blocking.

F.16 Vertical rising gate

The vertical rising gate, rises from the bottom. The advantage is that the gate is not visible under normal conditions. The disadvantage is again the sediment that could collect in the gate due to the dynamic character of the pass.

F.17 Visor gate

The main advantage of the visor gate at the San Luis Pass is that it is material effective, and it can open and close under a head difference. The disadvantage is the maintenance and inspection and the dynamic stability.

F.18 Result Barrier Alternative Assessment

The selection of conventional storm surge barrier indicates that there are six potential concepts for design of the storm surge barrier in the San Luis Pass. The six options are divided into four stored above water and two stored below. The four options stored above water (vertical lifting gate, visor gate, caisson structure and segment gate) require a fixed bottom and disrupt the view. The two options stored below water (bear trap gate and parachute barrier) are sensitive to sediment movement and difficult to maintain. From these six potential concepts, the caisson structure combined with a vertical lifting gate concept appears to fit best. The main disadvantage remains the view-blocking under normal conditions. The barrier alternative assessment is shown in Table F.1.

	Barge gate	Bear-trap gate	Caisson structure	Flap gate - floating	Flap gate - hydraulic	Inflatable barrier	Mailbox gate	Mitre gate	Parachute barrier	Reduction gate	Rolling gate	Rotary segment gate	Sector gate	Segment gate	Vertical lifting gate	Vertical rising gate	Visor gate
Criteria																	
Fast opening/closing underwater level difference	-	0	+	+	+	+	0	-	0	N/A	-	0	0	+	+	+	+
Flow area (keep intertidal area, normal conditions)	+	+	+	+	+	0	+	+	+	-	-	+	-	+	+	+	+
Structure/foundation simplicity	+	+	+	-	0	0	0	0	-	+	0	-	-	0	+	-	0
Building cost	+	0	+	-	0	-	-	-	+	+	0	-	-	0	+	-	+
Maintenance	+	-	+	0	-	-	0	0	+	+	-	+	0	0	+	-	0
Unique character San Luis Pass	-	+	+	-	0	0	+	0	+	-	-	+	-	+	+	+	+
Small vessels passing under normal conditions	+	+	-	0	0	+	+	+	+	+	+	+	+	+	+	+	+
Wishes																	
View blocking	0	+	0	+	+	0	+	-	+	-	-	+	-	-	-	+	-
Proven concept	+	+	+	+	+	+	-	-	-	+	+	+	+	+	+	+	+
Combination surge barrier with bridge	0	0	0	0	0	0	+	0	+	+	0	0	0	0	0	0	0

Table F.1: Barrier alternatives assessment

G
Verification of Concepts Conventional Storm Surge Barriers

G.1 General

The design parameters are based on the 1/100 year storm surge event. Chapter 3 described the functional specifications, including the normal and hurricane conditions. The parameters used are listed in Table H.1.

Design height		Water level [m]
Sea level rise	(SLR)	0.82
Storm surge height (1/100 year)		5.2
Wave height (1/100 year)	(H_s)	5.0
High astronomic tide	(HAT)	0.4
Max water level under MSL		1

Table G.1: Design heights for the San Luis Pass (Ruijs, 2011;Jonkman et al., 2015;de Vries, 2014)

Design water depth

The design water depth consists of mean sea level (MSL), high astronomic tide (HAT), storm surge and sea level rise (SLR). The mean sea level and height astronomic tide are from Table 3.1. The storm surge is from Table 3.2. And sea level rise, the intermediate, from Table 3.3. Resulting in design water depth of 7.4 m (1+0.4+5.2+0.8).

Maximum wave height

Waves start to break when they start feeling the bottom. Wave break when the water depth is less than 1.3 times the wave height. The significant wave height for the governing scenario is 5.0 m, shown in Table G.1. The required water depth for this wave height to occur is 6.5 m. The maximum water depth at the San Luis Pass is 7.4 m. This is a cumulative of the depth under MSL (1 m), sea level rise (0.8 m), storm surge (5.2 m), and high astronomic tide (0.4 m). The maximum wave height is 2.2 times the significant wave height. However, that is not possible due to the limited water depth. Therefore, the maximum wave height is 5.8 m.

G.2 Verification of the Hurricane Loads

This section describes the verification of the hurricane loads in order to understand the order of magnitude of these forces. The horizontal loads on the barrier that are taken into account are the hydrostatic load and wave load.

G.2.1 Horizontal loads

Hydrostatic pressure

The hydrostatic pressure is given by equation H.2 and hydrostatic force by equation H.3 (**VoorendtManualBS**).

$$P_{\text{hydro}} = \rho_w \cdot g \cdot h \tag{G.1}$$

Which:
P_{hydro} = Hydrostatic water pressure [Pa]
ρ_w = Density of water [kg/m^3]
h = Pressure head [m]
g = Gravity acceleration [m/s^3]

$$F_{\text{hydro}} = \int \rho_w \cdot dA \tag{G.2}$$

Which:
A = Total surface area [m^2] dA = A small part of area [m^2] F_{hydro}= Hydrostatic force perpendicular to plane [N]

The design water level is 7.4 m. And the density of salt water is 1025 kg/m^3 The distribution of the hydrostatic load over the height is shown in Figure G.1.

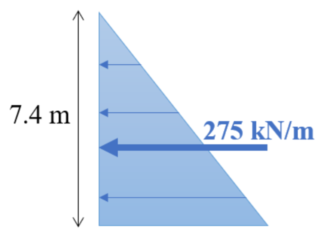

Figure G.1: Horizontal hydraulic load

Wave load

The wave load depends on the wave height and if the wave break or not. Waves start to break when the water depth is 1.3 times the wave height. The significant wave height is 5.0 meter, from Table 3.2. Resulting in a maximum wave height of 11 m, calculated with equation G.3. The maximum water depth is the design water level, 7.4 m. Therefore, the maximum wave height is 5.8 m. The larger waves are already broken before they hit the structure. The wave height of 5.8 m ware non-breaking waves on the structure.

$$H_{\text{max}} = 2.2 \cdot H_s \tag{G.3}$$

The non-breaking wave load for the rule of thumb is given in equation G.4.

$$F_{\text{max}} = \frac{1}{2} \cdot \rho \cdot g \cdot {H_i}^2 + d \cdot \rho \cdot g_i \tag{G.4}$$

Which:
H_i = Wave height incoming wave [m]
d = Depth of breakwater [m]

The maximum incoming wave height is 5.8 m. The resulting maximum wave height is 600 kN/m ($\frac{1}{2} \cdot 1025 \cdot 9.81 \cdot 5.8^2 + 7.4 \cdot 1025 \cdot 9.81 \cdot 5.8 = 600700.635$ N/m $\sim$ 600 kN/m) The distribution of the wave load over the height is shown in Figure G.2.

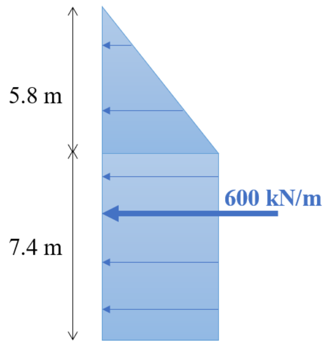

Figure G.2: Horizontal wave load

G.3 Flow under gate

This section describes the flow under the gate during closing. This is simplified by an opening of 0.5 m during hurricane conditions. There are two types of flow under a gate: free and submerged flow.

The flow under a structure due to water level difference is shown in equation G.6 (Molenaar and Voorendt, 2020). The water level difference for only hydrostatic pressure is 7.4 m and including waves is 13.2, resulting in respectively discharge of 2.7 m.

$$Q = C_d \cdot B \cdot a\sqrt{2g}z^{1/2} \tag{G.5}$$

$$Q \propto z^{1/2} \tag{G.6}$$

Which:

Q	[m^3]	Discharge
C_d		
B		
a	[m]	Vertical flow opening
z	[m]	Water level difference

G.3.1 Free flow

Free flow occurs if the condition of equation G.7 is true, the corresponding discharge is shown in equation G.8 (Molenaar and Voorendt, 2020). This resulted in no free flow for both only hydrostatic and including wave height water level.

$$\frac{h_3}{a} \leq 1,42 \cdot \sqrt{\frac{h_1}{a}} - 0,3 \tag{G.7}$$

$$Q = \mu \cdot B \cdot a \cdot \sqrt{2g\,(H_1 - \mu a)} \tag{G.8}$$

In which:

μ	[-]	Contraction coefficient (=0.6)
a	[m]	Height of flow outlet
B	[m]	Width of the structure
h_1	[m]	Water level height before the gate
h_3	[m]	Water level height after the gate

G.3.2 Submerged underflow

Submerged underflow is when there is no free flow. At the San Luis Pass this is the case. This means that there is a hydraulic jump directly behind the gate. A hydraulic jump means that this is the place energy dissipation takes place here (Molenaar and Voorendt, 2020). Equation G.9 shows the corresponding discharge. Resulting in a flow of 4.6 m^2/s for only hydrostatic pressure. And 6.3 m^2/s including wave height.

$$Q = m_{\text{suf}} \cdot b \cdot a \cdot \sqrt{2g(h_1 - h_3)} \tag{G.9}$$

Which:

m_{suf}	[-]	Discharge coefficient for submerged under flow (=0.8)
a	[m]	Height of flow outlet
b	[m]	Width of the structure
h_1	[m]	Water level height before the gate
h_3	[m]	Water level height after the gate

G.4 General Dimensions of varies Gate Types under Hurricane Conditions at the San Luis Pass.

In this section, the general dimensions of this type of gate under hurricane conditions are briefly described. Consequently, indicate the environmental impact of this gate type can be estimated. Because the environmental impact is linked to the reduction in flow area at the San Luis Pass. The gate types that are identified in this section are the inflatable dam, mailbox gate and caisson structure.

G.4.1 Inflatable dam

The section includes a very conceptual design of an inflatable dam. This is designed to investigate the dimensions of the inflatable dam barrier in the San Luis Pass. In order to say something over the remaining flow area under normal conditions.

The circumferential length (L) of an unloaded air filled dam will be minimal for the base width (B) equal to 0.9 times the crest height (H).[2] The inflatable dam has now the shape of a circle, see Figure 11.

$B = 0.9 \cdot H_{unloaded}\ [m]$
$L_{min} = 2.76 \cdot H_{unloaded}\ [m]$

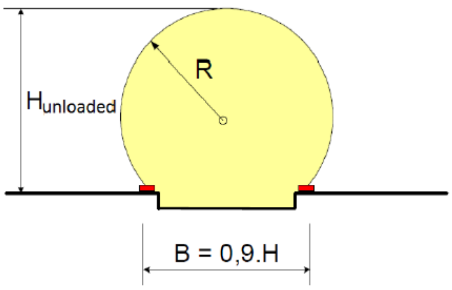

Figure 11: Two sided clamped inflatable dam (Figure: Rijkswaterstaat and WL | Delft Hydraulics).

Figure G.3: Height width relation - Inflatable barrier (van Breukelen, 2013, P.16)

In Figure 12 the force transfer of an inflatable rubber barrier with a bottom recess is given.

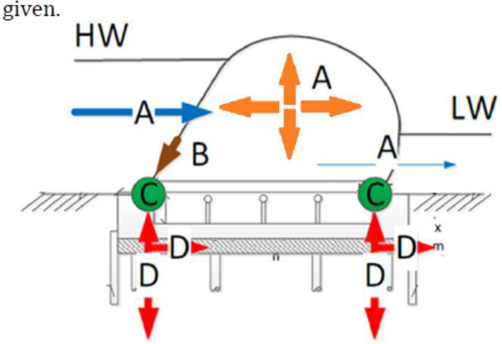

Figure 12: Force transfer inflatable rubber barrier with bottom recess.

A. Load due to the difference in water levels (head) and due to the internal pressure of the filler.
B. The load due to the pressure difference (p) is transferred to the two clamping lines as a tension force in the membrane.
C. The clamping line transfers the membrane force to the foundation.
D. The forces in the clamping lines are distributed over the construction via the foundation floor and if present transferred to the pile foundation.

Figure G.4: Force transfer - Inflatable barrier (van Breukelen, 2013, P.17)

For this concept the height of wave and hydrostatic water is simplified as a total hydrostatic force with a height of 13.2 m. The maximum force on the material of the inflatable barrier depends on the material properties. The force distribution from the material to the ground depends on the angle of the barrier under load. An angel of θ_1 and θ_2 respectively being 75 and 58 °, according to van Breukelen, 2013. This is schematized in Figure G.5.

Figure G.6 shows the total cross-section of San Luis Pass with 3 inflatable barriers with a length of 300 m each.

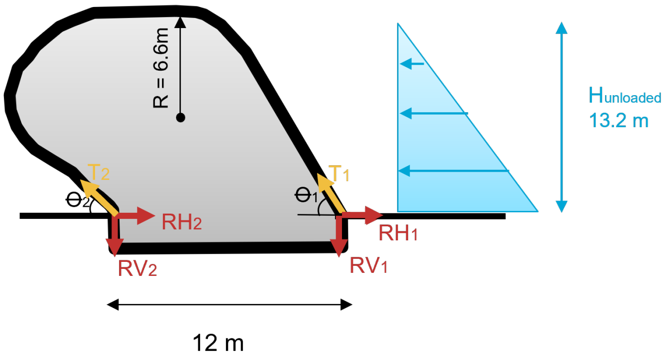

Figure G.5: Inflatable barrier force distribution

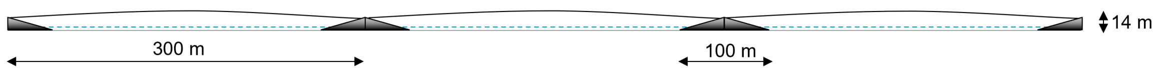

Figure G.6: Inflatable barrier cross-section San Luis Pass

G.4.2 Caisson Structure

Definition of caisson geometry

The basic definition for the dimensions of the caisson are illustrated in Figure G.7. The definition of these dimensions are given in the following equations:

$$\begin{aligned} V_c &= W_c L_c H_c && [\mathrm{m}^3] \\ V_{c,in} &= W_{c,in} L_{c,in} H_{c,\,\mathrm{in}} && [\mathrm{m}^3] \end{aligned} \tag{G.10}$$

With:

$$\begin{aligned} W_c &= n_x \cdot W_{c,\,\mathrm{in}} + 2 \cdot w_{w,out} + (n_x - 1) \cdot w_{u,in} && [\mathrm{m}] \\ H_c &= d_{local} + h_{\mathrm{sill}} && [\mathrm{m}] \\ H_{c,\,\mathrm{in}} &= H_c - w_t - w_f && [\mathrm{m}] \\ L_{c,\,\mathrm{in}} &= L_c - 2w_b && [\mathrm{m}] \end{aligned} \tag{G.11}$$

In which:

V_c	[m3]	Volume of caisson
W^c	[m]	Width caisson
L^c	[m]	Length caisson
H^c	[m]	Height caisson
$V_{c,in}$	[m3]	Volume of compartment
$W^{c,in}$	[m]	Inner width caisson
$L^{c,in}$	[m]	Inner length caisson
$H^{c,in}$	[m]	Inner height caisson
n_x	[-]	Number of compartments in x-direction
w_t	[m]	Thickness top slab
w_f	[m]	Thickness floor slab
$w_{w,out}$	[m]	Thickness outer walls
$w_{w,in}$	[m]	Thickness inner walls

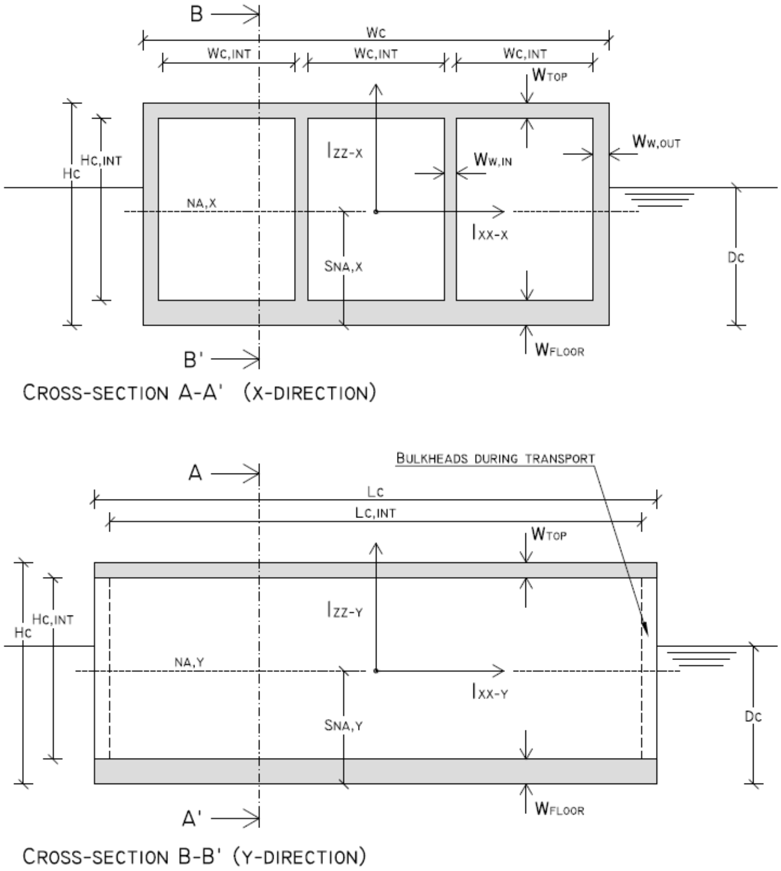

Figure G.7: Dimensions Caisson structure (de Vries, 2014)

Mass moments of inertia

The mass moments of inertia are given below.

$$\begin{aligned} I_{zz-x} =& 2 \cdot \frac{1}{12} \cdot w_{u,out} \cdot H_{c,\text{ in}}^3 + (n_x - 1)\frac{1}{12} \cdot w_{w,in} \cdot H_{c,in}^3 + \frac{1}{12} W_c \cdot w_f^3 \\ &+ \frac{1}{12} W_c \cdot w_t^3 + A_f \cdot \left(s_{na-x} - 0.5 \cdot w_f\right)^2 + A_t \cdot \left(H_c - s_{na-x} - 0.5 \cdot w_t\right)^2 \end{aligned} \tag{G.12}$$

$$\begin{aligned} I_{xx-x} =& \frac{1}{12} \cdot \left(w_f + w_t\right) \cdot W_c^3 + 2 \cdot \frac{1}{12} \cdot H_{c,\text{ in}} \cdot w_{w,\text{ out}}^3 + 2 \cdot A_{u,\text{ out}} \cdot \left(0.5 \cdot W_c - 0.5 \cdot w_{u,\text{ out}}\right)^2 \\ &+ (n_x - 1) \cdot \frac{1}{12} \cdot H_{c,\text{ in}} \cdot w_{w,\text{ in}}^3 + \left(\frac{1}{12} \cdot n_x^3 - \frac{1}{4} \cdot n_x^2 + \frac{1}{6} \cdot n_x\right) \cdot A_{w,\text{ in}} \cdot \left(W_{c,\text{ in}} + w_{w,\text{ in}}\right)^2 \end{aligned} \tag{G.13}$$

$$I_{zz-y} = \frac{1}{12} L_c \cdot w_f^3 + \frac{1}{12} L_c \cdot w_t^3 + A_f \cdot \left(s_{na-x} - 0.5 \cdot w_f\right)^2 + A_t \cdot \left(H_c - s_{na-x} - 0.5 \cdot w_t\right)^2 \tag{G.14}$$

$$I_{xx-y} = \frac{1}{12} \cdot \left(w_f + w_t\right) \cdot L_c^3 \tag{G.15}$$

$s_{na,x}$	[m]	Position of neutral axis in z-direction with respect to the bottom fiber, along the x-direction
$s_{na,y}$	[m]	Position of neutral axis in z-direction with respect to the bottom fiber, along the y-direction
$I_{zz\text{-}x}$	[m^4]	Mass moment of inertia in zz-direction along the x-direction
$I_{xx\text{-}x}$	[m^4]	Mass moment of inertia in xx-direction along the x-direction
$I_{zz\text{-}y}$	[m^4]	Mass moment of inertia in zz-direction along the y-direction
$I_{xx\text{-}y}$	[m^4]	Mass moment of inertia in xx-direction along the y-direction
A_f	[m^2]	Area of floor slab (= $w_f \cdot W_c$)
A_t	[m^2]	Area of top slab (= $w_t \cdot W_c$)
$A_{w,out}$	[m^2]	Area of outer wall (= $w_{w,out} \cdot H_{c,in}$)
$A_{w,in}$	[m^2]	Area of inner wall (= $w_{w,in} \cdot H_{c,in}$)
s_f	[m]	Distance mass center of floor slab and bottom fiber (=$0.5 \cdot w_f$)
s_t	[m]	Distance mass center of top slab and bottom fiber (=$w_f + H_{c,in} + 0.5 \cdot w_t$)
$s_{w,out}$	[m]	Distance mass center of outer wall and bottom fiber (=$w_f + 0.5 \cdot H_{c,in}$)
$s_{w,in}$	[m]	Distance mass center of inner wall and bottom fiber (=$w_f + 0.5 \cdot H_{c,in}$)
$A_{c,con\text{-}x}$	[m^2]	Area of concrete in x-direction cross-section (= $H_c \cdot W_c$ - $H_{c,in} \cdot W_{c,in}$)
$A_{c,con\text{-}y}$	[m^2]	Area of concrete in y-direction cross-section (= $H_c \cdot L_c$ - $H_{c,in} \cdot L_{c,in}$)
n_x	[-]	Number of compartments in x-direction

Checks on stability at final placement

- Check on vertical bearing capacity

$$\frac{\sigma_{\mathrm{R,vb}}}{\sigma_{\mathrm{E,vb}}} \geq 1.0 \tag{G.16}$$

$$N_c \cdot \sigma_{s,u,2} / \left(\frac{F_{V,tot}}{W_c L_c} + \frac{M_{\mathrm{tot}}}{1/6 \cdot W_c \cdot L_c^2} \right) \geq 1.0 \tag{G.17}$$

In which:

$\sigma_{R,vb}$	[kN/m^2]	Soil bearing capacity
$\sigma_{E,vb}$	[kN/m^2]	Effective vertical stress on soil
N_c	[-]	Bearing capacity factor for cohesion = 5.14 (Skempton, 1951)
$\sigma_{s,u,2}$	[kN/m^2]	Undrained shear stress below MSL
$F_{v,\ tot}$	[kN]	Total vertical load
M_{tot}	[kNm]	Sum of moments on caisson
W_c	[m]	Width caisson
L_c	[m]	Length caisson

- Check on inclined loading

$$\frac{\sigma_{R,vbi}}{\sigma_{E,vbi}} \geq 1.0 \tag{G.18}$$

$$N_{\mathrm{ci}} \cdot \sigma_{s,u,2} / \left(\frac{\sqrt{F_{V,tot}^2 + F_{V,tot}^2}}{W_c \cdot L_c} \right) \geq 1.0 \tag{G.19}$$

In which:

$\sigma_{R,vbi}$	[kN/m^2]	Soil bearing capacity under inclined loading
$\sigma_{E,vbi}$	[kN/m^2]	Effective vertical stress on soil due to inclined loading
α_{res}	[°]	Angle of resultant force with respect to vertical (=arctan($F_{H,tot}/F_{V,tot}$))
N_{ci}	[-]	Bearing capacity factor for cohesion under inclined loading = 4.2, (Meyerhoof, 1953)

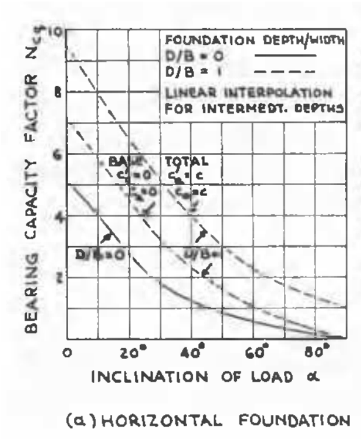

Figure G.8: Bearing capacity under inclined loading (Meyerhoof, 1953)

- Check on occurring soil tensile stresses

$$\left(\frac{F_{V,tot}}{W_c \cdot L_c}\right) / \left(\frac{M_{\text{tot}}}{1/6 \cdot W_c \cdot L_c^2}\right) \geq 1.0 \tag{G.20}$$

- Check on soil shear stresses

$$\frac{F_{V,tot} \cdot c_f}{F_{H,\text{ tot}}} \geq 1.0 \tag{G.21}$$

- Check on overturning moment

$$\frac{F_{V,tot} \cdot \frac{1}{6} \cdot L_c}{M_{\text{tot}}} \geq 1.0 \tag{G.22}$$

Resulting dimensions caisson

Figure **??** shows the final dimensions of the caisson structure. This corresponds with a 4% closing of the San Luis Pass. Resulting in nearly no change in tidal range in the West Bay.

The final caisson structure consists of 2 compartments with a tot width of 61.8 meters, length of 6 m. The inner width of the compartments is 30 m. The thickness of the top slab is 0.5 m, thickness of the floor slab is 1.25 m. Thickness of the outer wall is 0.7 m. Thickness of inner walls is 0.4 m.

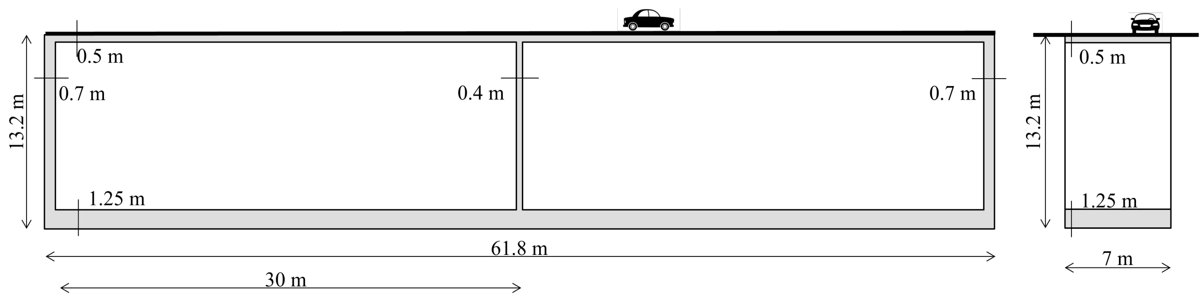

Figure G.9: Final dimensions of caisson structure

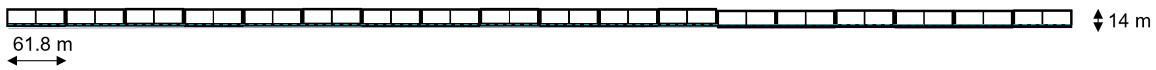

Figure G.10: Final dimensions in San Luis Pass in total 17 caisson structure

Note: Also checked for the deflection of the top slab of the caisson for traffic, the maximum allowable distributed force is 33 kN/m^2. In comparison, in the EuroCode the vertical traffic load is 9 kN/m^2 (NEN, n.d.). Maximum deflection is given in equation **??**. *And the deflection of the top slab of the caisson is given by equation G.23.*

$$w = \frac{1}{384} \cdot \frac{q \cdot L^4}{E \cdot I} \tag{G.23}$$

H Load Derivation of Shade Curtain Barrier

This appendix described in detail the load derivation of the Shade Curtain Barrier design for the San Luis Pass in Texas, United States of America. Section H.1 describes the general information, like design water level and wave height. Section H.2 described the external loads on the structure. Section H.3 described the internal load derivation between the different elements.

H.1 General

The design parameters are based on the 1/100 year storm surge event. Chapter 3 described the functional specifications, including the normal and hurricane conditions. The parameters used are listed in Table H.1.

Design height		**Water level [m]**
Sea level rise	(SLR)	0.82
Storm surge height (1/100 year)		5.2
Wave height (1/100 year)	(H_s)	5.0
High astronomic tide	(HAT)	0.4
Max water level under MSL		1

Table H.1: Design heights for the San Luis Pass (Ruijs, 2011;Jonkman et al., 2015;de Vries, 2014)

Design water depth
The design water depth is different on the Gulf of Mexico and Bay side. The design water depth is the cumulative of the maximum water depth, high astronomic tide, sea level rise and storm surge height.

Gulf of Mexico side
Design water depth (DWD) components are storm surge height (1/100 year), sea level rise, high astronomic tide, and max water level under MSL. Resulting in a design water depth of 7.4 m from bottom surface.

$$DWD_{\text{Gulf of Mexico}} = 5.2 + 0.82 + 5.2 + 0.4 + 1 = 7.4$$

Galveston Bay side
The design water depth components are sea level rise, high astronomic tide, and max water level under MSL. However, a higher design water level at the bay side has a positive influence for the design. Therefore, the sea level rise is not taken into account. Resulting in a design water depth of 1.4 m from bottom surface.

$$DWD_{\text{Bay}} = 0.4 + 1 = 1.4$$

Wave height
The wave height is different for the Gulf of Mexico and Bay side. Separately described below.

Gulf of Mexico side
The significant wave height is 5.2 m due to a 1/100 year storm. The maximum wave height is 2.2 times the significant wave height, equation H.1. Waves break when they start feeling the bottom, this occurs

when the wave height is 1.3 times the water depth. Taking with into account, the maximum wave height is 5.8 m.

$$H_{\text{max}} = 2.2 \cdot H_s \tag{H.1}$$

Galveston Bay side
In wave height at the bay side is not taken into account because of the low water level at the bay side.

H.2 External Loads under Hurricane Conditions

The external loads on the shade curtain barrier consists of the horizontal and vertical forces. The governing situation for the loads is under hurricane condition. Figure H.1 gives an overview of the external forces at the static situation under hurricane conditions

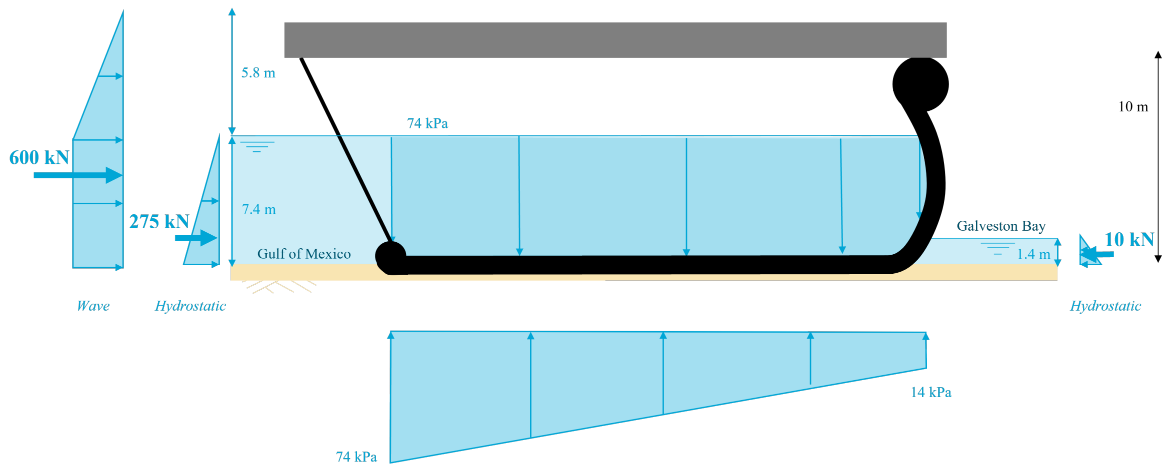

Figure H.1: Forces on the shade curtain barrier at San Luis Pass

H.2.1 Horizontal load

The horizontal loads on the storm surge barrier are due to water pressure and waves. Figure H.1 illustrates the external horizontal forces on the shade curtain barrier. The horizontal loads that are considered in this design are the hydrostatic and wave load.

Hydraulic pressure

The hydrostatic pressure is given by equation H.2 and hydrostatic force by equation H.3 (Molenaar and Voorendt, 2020).

$$P_{\text{hydro}} = \rho_w \cdot g \cdot h \tag{H.2}$$

$$F_{\text{hydro}} = \int \rho_w \cdot dA \tag{H.3}$$

$$F_{\text{hydro, resulting}} = \frac{1}{2} \cdot \rho_w \cdot g \cdot H^2 \tag{H.4}$$

In which:

P_{hydro}	[Pa]	Hydrostatic water pressure
ρ_w	[kg/m^3]	Density of water
h	[m]	Pressure head
g	[m/s^3]	Gravity acceleration
A	[m^2]	Total surface area
dA	[m^2]	A small part of area
F_{hydro}	[N]	Hydrostatic force perpendicular to plane
H	[m]	Water level height

Design values under hurricane condition for the shade curtain barrier design at the San Luis Pass are listed below.

Water level height$_{\text{Gulf of Mexico}}$	$H_{\text{Gulf of Mexico}}$	7.4	m
Water level height$_{\text{Bay}}$	H_{Bay}	1.4	m
Density of salt water	ρ	1025	kg/m^3
Gravitational constant on earth	g	9.81	m/s^2

The resulting hydrostatic force at Gulf of Mexico side is 275 kN and Bay side is 10 kN.

Wave load

The wave load depends on the incoming wave height, 5.8 m, explained in Section H.1. The resulting wave load is 600 kN.

$$F_{\text{max, wave}} = \frac{1}{2} \cdot \rho \cdot g \cdot {H_i}^2 + d \cdot \rho \cdot g \cdot H_i \tag{H.5}$$

In which:

ρ_w	[kg/m^3]	Density of water
H_i	[m]	Incoming wave height
g	[m/s^3]	Gravity acceleration
d	[m]	Design water depth

H.2.2 Vertical load

The vertical loads are due to the water pressure. Figure H.2 illustrates the external vertical forces on the shade curtain barrier. The vertical load is due to the pressure gradient of the water, calculated in equation H.2. Resting in a pressure of 74 kPa at Gulf of Mexico side and 14 kPa at Bay side. The hydrostatic pressure possesses the same curve as the flexible membrane fabric. Since the curvature is only a small area of the total length, this is neglected. The upward water pressure is always smaller than the downward water pressure, because of the water level difference and seepage length of the horizontal flexible membrane fabric. Except for the location of the sinker, the sinker diameter causes the upward water pressure to be greater than the downward water pressure (in case of an impermeable material). The difference in water level pressure is diameter[m]·10kPa. Therefore, the sinker should have sufficient weight to always close off the gap.

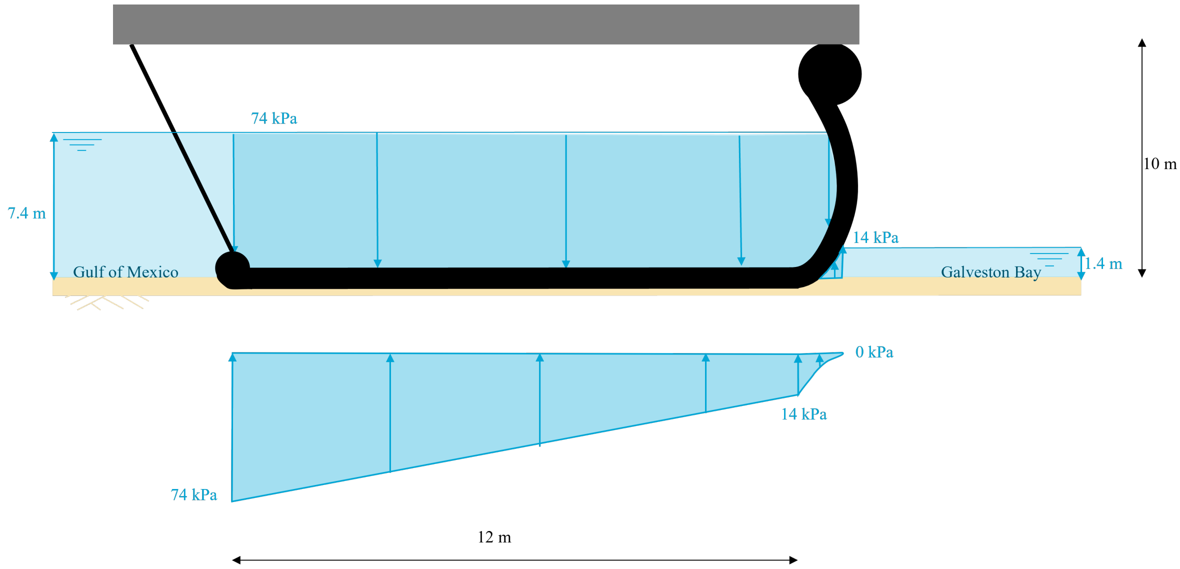

Figure H.2: External vertical forces on shade curtain barrier

H.3 Internal Load Distribution

The internal load distribution is elaborated in this section. The static situation under hurricane conditions, 1/100 year storm surge, is used. The previous section described the external loads on the shade curtain barrier. The loads from this section are distributed to the flexible membrane fabric, sinker, and cable. Finally, the bridge should withhold these forces. Figure H.3 shows the different elements with forces and afterwords the elements are described in detail.

The horizontal loads are transfers to the flexible membrane fabric. The flexible membrane fabric transfers it directly to the bridge and sinker/cable. The top and bottom forces on the flexible membrane fabric are determined by the geometry distribution of the loads on it. The top force of the flexible membrane fabric is distributed to the rotating axis and then to the bridge. The bottom force of the flexible membrane fabric is distributed to the sinker. From the sinker, the force is distributed to the ground and cable. The cable transfers the force to the bridge.

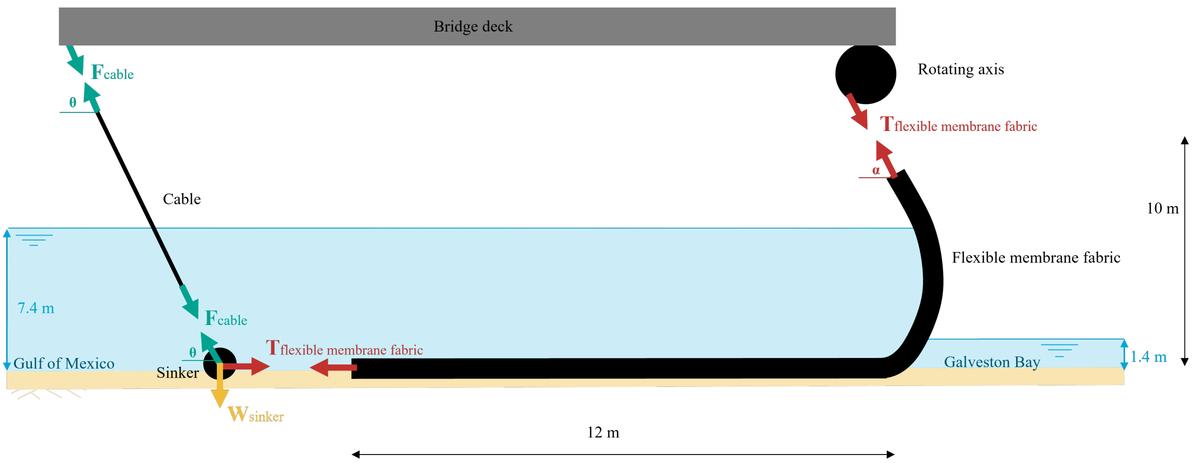

Figure H.3: Load distribution different elements of shade curtain barrier

Load on the Flexible Membrane Fabric

The flexible membrane fabric should withhold the horizontal forces and transfer these to the sinker and bridge. Previous research on vertical flexible membrane fabric and horizontal forces showed that with a hypothetical vertical membrane and water on one side, the horizontal force at the top is $\frac{1}{3}F_h$ and bottom $\frac{2}{3}F_h$, showed in Figure H.4 (Marissen et al., 2013). This is the same ratio as the geometric of the force. Note that this is only the case when the angle at the bottom of the flexible membrane fabric is very large. Concluding from this research is the force at the top and bottom of the fabric is the same as the geometric ratio of the horizontal force in the case of a vertical membrane.

The same research stated that vertical flexible membrane fabric is the least favorable scenario, since this gives the highest forces on the bottom and top side of the flexible membrane fabric. In this case, only the horizontal forces need to be taken into account at the moment of equilibrium (Marissen et al., 2013). Therefore, this scenario is used for the derivation of the load.

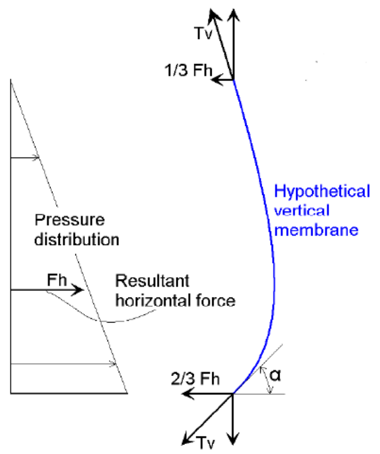

Figure H.4: Forces on the bottom and top side of a hypothetical vertical flexible membrane fabric (Marissen et al., 2013)

The tensile force in the flexible membrane fabric is the same. But the geometric determines the horizontal component of the tensile force. And therefore the angle of the flexible membrane fabric at the top and bottom. Figure H.5 shows the geometric of the horizontal forces on flexible membrane fabric. A part of the wave load goes over the bridge and therefore will not be transferred to the flexible membrane fabric, as illustrated in Figure H.5 in green. This results in a total horizontal load of 796 kN/m on the flexible membrane fabric, showed in yellow.

Figure H.5: Geometric horizontal forces on flexible membrane fabric

The resulting horizontal force on the flexible membrane fabric is at 4.1 m from the bottom surface. According to the research of Marissen on vertical flexible membrane, the force at the top and bottom of the fabric is the same as the geometric ratio of the horizontal force, the bottom horizontal force is 0.59 $F_{h,res}$ and at the top 0.41 $F_{h,res}$. The tension in the flexible membrane fabric is equal to the 0.59 $F_{h,res}$, because the horizontal force at the bottom is equal to the tension force. The tension force is 470 kN/m. The resulting angle at the top of the flexible membrane fabric can be calculated by the equation H.6. The angle at the top of the vertical membrane fabric is 46°. Because the horizontal component at the top is 326 kN/m.

$$T = \frac{F_h}{cos\alpha} \tag{H.6}$$

In which:

α	[°]	Angle of the membrane at the bottom
T	[N/m]	Tension force in membrane per meter
F_h	[N]	Horizontal force

Load on the Cable

The force in the cable is determined by the angle. The tensile force of the flexible membrane fabric is the horizontal component of the cable force. Figure H.6 shows the cable force for the different angle. Figure H.7 shows the required horizontal and total length of the cable. In this figure the horizontal required length is defined as the horizontal length between the sinker and cable anchor at the bridge deck. Concluding from these graphs is, a smaller cable angle requires a large horizontal length and result in a lower cable force, but increases the required bridge deck width.

The horizontal available length due to the inclined cable is limited. Therefore, the angle is 75 degree. Corresponding with a horizontal length of 4 m, total cable length of 11 m and force in the cable of 1230 kN/m.

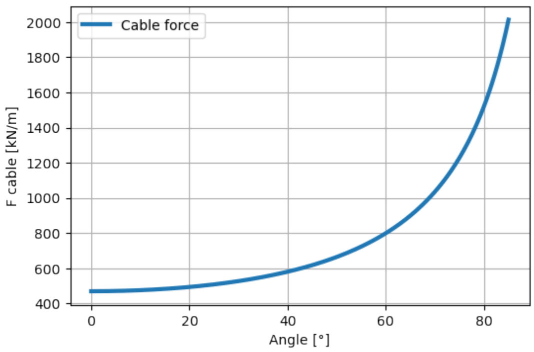

Figure H.6: Tensile force in cable with different angles

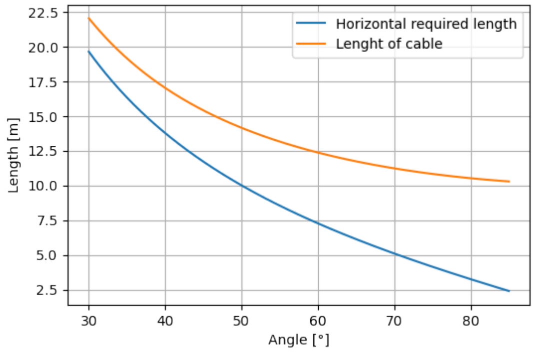

Figure H.7: Required length of cable with different angles

Load on the Sinker

The sinker transfer the tensile force of the flexible membrane fabric to the cable. The angle at of the cable determines the minimum weight of the sinker There are a lot of uncertainties regarding this design, especially the dynamic effects. Therefore, a safety factor of 1.5 is set for the self weight of the sinker. This to make sure that the self weight is large enough to close the gap. Note that the upward force due to sinker height is neglected.

The vertical component of the cable force, with an angle of 75 degrees, is 1754 kN/m. Including a safety factor of 1.5, the corresponding self weight of the sinker must be 2630 kN/m. This corresponds to a pipe of solid steel with diameter of 6.5 m. Since the mass density of steel is around 8000 kg/m^3. Therefore, this is unrealistic.

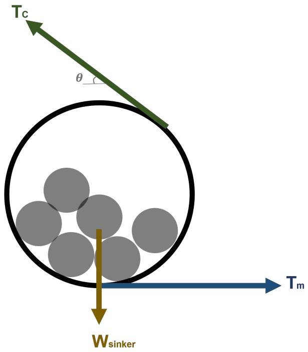

Figure H.8: Force distribution Sinker, cross-section (2D)

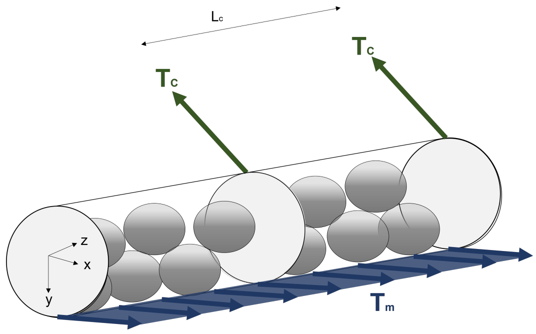

Figure H.9: Force distribution Sinker (3D)

Bridge

The bridge need to be able to hold the forces. The force on the bay side of the bridge is 470 kN/m under an angle of 46 degrees. The force on the Gulf of Mexico side depends on the angle of the cable.

H.4 Moment Equilibrium, in the case the flexible membrane fabric behaves as a rigid structure

The moment equilibrium is the taken of the flexible membrane fabric including sinker. For simplicity, the flexible membrane fabric does not have a curvature but is vertical. Figure H.10 illustrated the total forces on the shade curtain barrier design, the red arrow indicates the position of the taken moment. The corresponding forces, arms, and moments are listed in Table H.2. This results in a positive moment of, 9000 kNm/m. Therefore, the flexible membrane fabric will not rotate upwards under hurricane conditions. Even the self weight of the sinker could be reduced to 1900 kN/m and the moment equilibrium is still sufficed. Note, the self weight of the flexible membrane fabric is not taken into account. This would have a positive effect on the moment stability.

	Force [kN/m]	**Arm** [m]	**Moment** [kNm/m]
$F_{\text{cable, horizontal}}$	470	10	- 4700
$F_{\text{cable, vertical}}$	1754	12	-21048
W_{sinker}	2630	12	31560
$F_{\text{water, down}}$	888	6	5328
$F_{\text{water, up 1}}$	720	8	- 5760
$F_{\text{water, up 2}}$	168	6	- 1008
$F_{\text{h, res}}$	796	5.9	4697
		$\sum M$	9069

Table H.2: Moment equilibrium under hurricane conditions

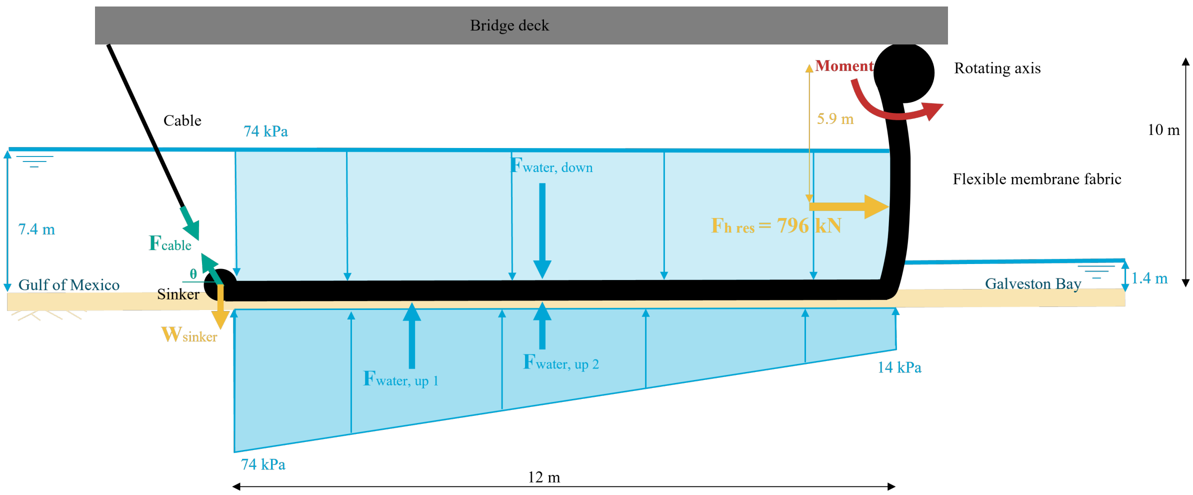

Figure H.10: Moment equilibrium under hurricane conditions

Case: cable horizontal

In the case, the cable is horizontal, the force equilibrium changes. The $F_{cable, vertical}$ becomes zero. The rest of the forces remain the same. In the case the structure behaves as a rigid structure the resulting moment is, 30117 kNm/m, rotating anti clock wise. The resulting self weight of the sinker must be minimum 121 kN/m. This would decrease the requirements weight of the sinker tremendously, decreased by 95%. This corresponds with a solid steel pipe with a diameter of 1.4 m. The mass density of steel is 8000 kg/m^3. Note, this is without the safety factor of 1.5. Including a safety factor of 1.5, result in a diameter is 1.7 m.

Another alternative would be to add mass in the flexible membrane fabric that is on the bottom surface. And take the self weigh of the flexible membrane fabric into account. For example, the self weight of the inflatable Ramspol barrier in The Netherlands is 19 kg/m^2. Therefore, the self weight of the flexible membrane fabric is negligible.

However, the diameter of the sinker could be changed by have a larger sinker at the end and smaller sinkers at the

H.5 Alternative Sinker Designs

This part describes the alternative sinker designs for the shade curtain barrier at the San Luis Pass in order to prevent uplift of the sinker. Uplift of the sinker need to be prevented because otherwise the required piping length is not sufficient. The alternatives of design to prevent uplift of the sinker are:

- Original scenario: cable under an angle of 75°
- Alternative 1: Cable horizontal
- Alternative 2: Multiple sinkers
- Alternative 3: Multiple sinkers and horizontal cable
- Alternative 4: Weighted flexible membrane fabric and sinker (D=0.5 m)
- Alternative 5: Weighted flexible membrane fabric, sinker (D=0.5 m), and horizontal cable

Original scenario: cable under an angle of 75°

The original scenario, with one sinker and a cable attached to the bridge under an angle of 75°. Figure H.11 illustrated this original scenario. This gives the follow reasoning for the sinker design:

Required force	2630 kN/m
ρ_{steel}	8000 kg/m^3
$A_{required}$	33.51 m^2
	With safety factor (1.5)
Diameter	6.5 m

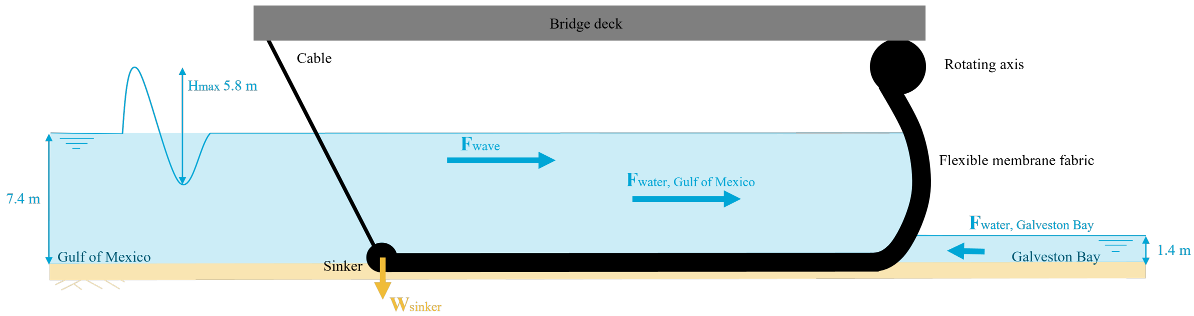

Figure H.11: Original scenario: cable under an angle of 75°

Alternative 1: Cable horizontal

In this alternative, the cable is horizontal. The required weight of the sinker depends on the moment equilibrium. Resulting in a sinker with a weight equal to solid steel pipe of diameter 1.7 m. Figure H.12 illustrated this alternative. This gives the follow reasoning for the sinker design:

Required force	121 kN/m	
ρ_{steel}	8000 kg/m^3	
	Without safety factor	*With safety factor (1.5)*
$A_{required}$	1.54 m^2	2.31 m^2
Diameter	1.4 m	1.7 m

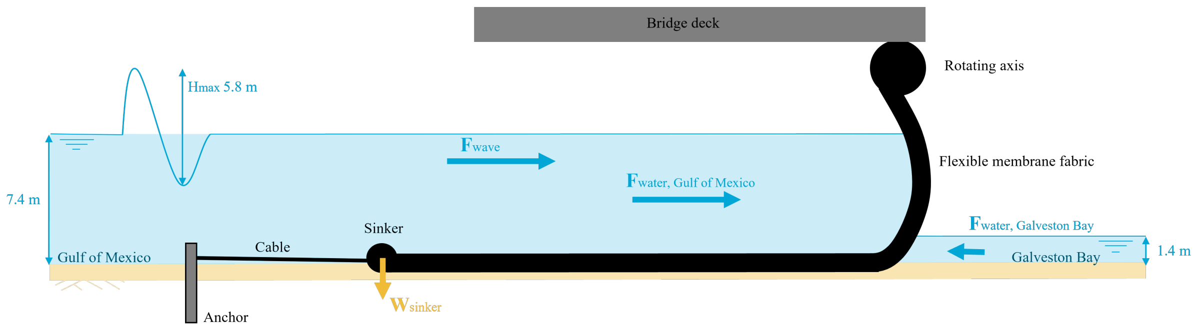

Figure H.12: Alternative 1: Cable horizontal

Alternative 2: Multiple sinkers

In this alternative, four sinkers with an equal distance between the sinkers is investigated. Resulting in four sinkers with a weight equal to solid steel pipe of diameter 4.3 m. Figure H.13 illustrated this alternative. This gives the follow reasoning for the sinker design:

Required moment	-22491 kNm/m	
W_{sinker}	749.7 kN/m	
ρ_{steel}	8000 kg/m^3	
	Without safety factor	*With safety factor (1.5)*
$A_{required}$	9.55 m^2	14.3 m^2
Diameter	3.5 m	4.3 m

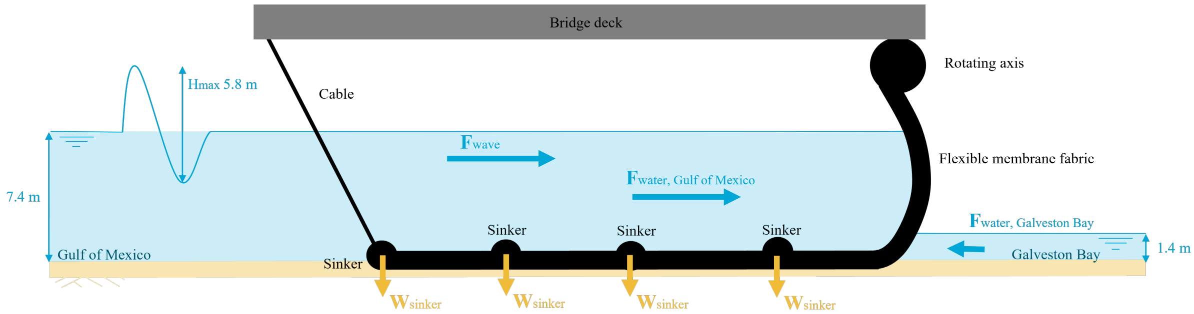

Figure H.13: Alternative 2: Multiple sinkers

Alternative 3: Multiple sinkers and horizontal cable

In this alternative, four sinkers with an equal distance between the sinkers and horizontal cable is investigated. Resulting in four sinkers with a weight equal to solid steel pipe of diameter 1.1 m. Figure H.14 illustrated this alternative. This gives the follow reasoning for the sinker design:

Required moment	-1443 kNm/m	
W_{sinker}	48.1 kN/m	
ρ_{steel}	8000 kg/m^3	
	Without safety factor	*With safety factor (1.5)*
$A_{required}$	0.61 m^2	0.92 m^2
Diameter	0.9 m	1.1 m

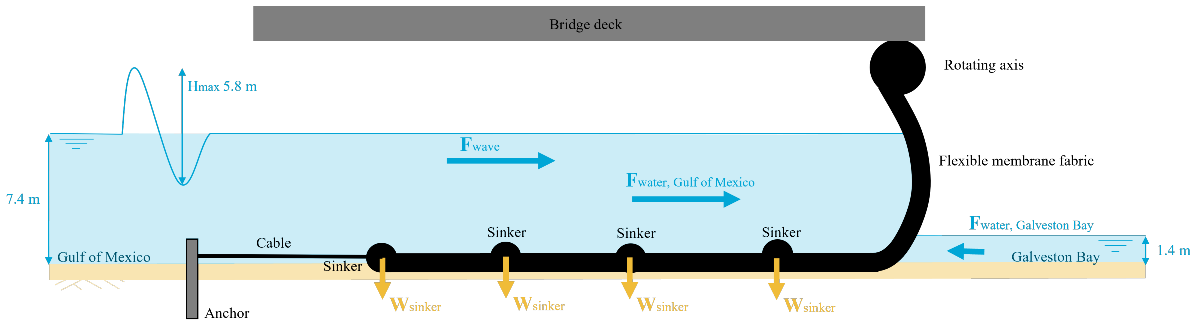

Figure H.14: Alternative 3: Multiple sinkers and horizontal cable

Alternative 4: Weighted flexible membrane fabric and sinker (D=0.5 m)

In this alternative, weighted flexible membrane fabric and sinker with diameter of 0.5 m is investigated. Resulting in weighted flexible membrane fabric with a weight equal to a solid steel plate of thickness

3.9 m. Figure H.15 illustrated this alternative. This gives the follow reasoning for the sinker design:

Required moment	-22491 kNm/m
W_{sinker}	15.4 kN/m
ρ_{steel}	8000 kg/m^3
$W_{add,\ fmf}$	78.48 x A_{steel} kN/m
$M_{Wsinker}$	158 kNm/m
$\sum M_{res,\ add,\ fmf}$	22306 kNm/m
A_{steel}	47.37 m^2
$Plate_{length\ is\ 12\ m}$	3.9 m

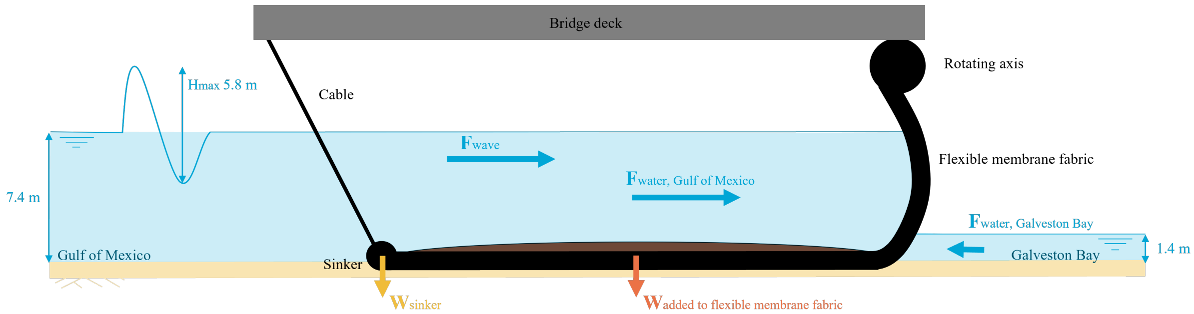

Figure H.15: Alternative 4: Weighted flexible membrane fabric and sinker (D=0.5 m)

Alternative 5: Weighted flexible membrane fabric, sinker (D=0.5 m), and horizontal cable

In this alternative, weighted flexible membrane fabric, sinker with diameter of 0.5 m, and horizontal cable is investigated. Resulting in a weighted flexible membrane fabric with weight equal to a solid steel plate of thickness 0.2 m. Figure H.16 illustrated this alternative. This gives the follow reasoning for the sinker design:

Required moment	-1443 kNm/m
W_{sinker}	15.4 kN/m
ρ_{steel}	8000 kg/m^3
$W_{add,\ fmf}$	78.48 x A_{steel} kN/m
$M_{Wsinker}$	158 kNm/m
$\sum M_{res,\ add,\ fmf}$	1258 kNm/m
A_{steel}	2.7 m^2
$Plate_{length\ is\ 12\ m}$	0.2 m

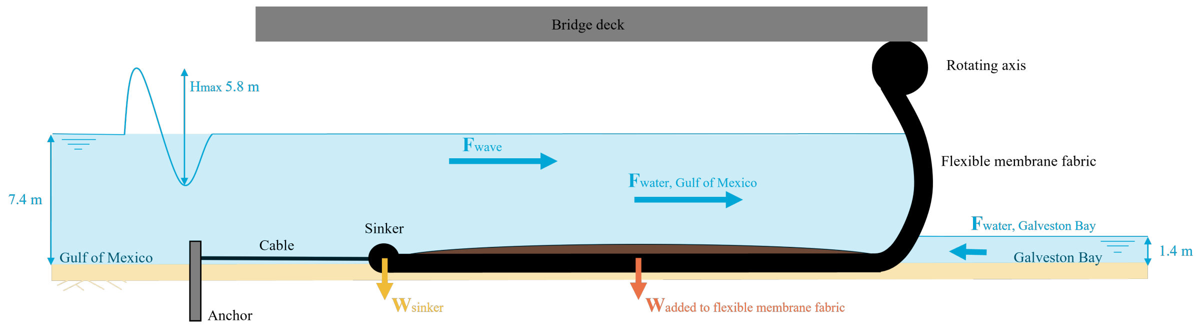

Figure H.16: Alternative 5: Weighted flexible membrane fabric, sinker (D=0.5 m), and horizontal cable

H.6 Maximum Scour Depth

This section described the scour depth when one of the shade curtains does not descend. This method is according to the Hydraulic Structures Manual (Molenaar and Voorendt, 2020). The equilibrium depth of the scour hole, while assuming that there is no sand coming from upstream (clear water scour). In that case, the maximum (= equilibrium) scour depth h_{max} is given by:

$$h_{\max} = \frac{0.5 \cdot \alpha \cdot \bar{u} - u_{cr}}{u_{cr}} \cdot h_0 \text{ for } 0.5 \cdot \alpha \cdot \bar{u} - u_{cr} > 0 \tag{H.7}$$

In which:

h_{max}	[m]	Maximum depth of the scour hole (= equilibrium depth)
h_0	[m]	Initial water depth
$\bar{u}$	[m/s]	Depth-averaged flow velocity at the end of the scour protection
u_{cr}	[m/s]	Critical velocity in regard to beginning of motion of the sand particles
α	[-]	Turbulence coefficient, depending on the upstream disturbance. Value in order of 3.

The critical velocity u_{cr} for the initiation of sand transport under uniform flow can be calculated with the Shields equation:

$$u_{cr} = C\sqrt{\Theta_{cr} \cdot \Delta \cdot D_{50}} \tag{H.8}$$

In which:

D_{50}	[m]	Mass-median nominal diameter of sand particles at the end of the sour protection
C	[$\sqrt{m}$/s]	Chézy coefficient
Θ_{cr}	[-]	Shields (stability) parameter
Δ	[-]	Relative density

The Chézy coefficient can be calculated with:

$$C = 18 \cdot \log\left(\frac{12 \cdot R}{k_r}\right) \tag{H.9}$$

In which:

k_r	[m]	Equivalent bed roughness, for sand 10-50 cm
R	[m]	Hydraulic radius of the flow channel at the end of the scour protection

The depth-averaged flow velocity depends on the water level difference, calculated with:

$$\bar{u} = \sqrt{2 \cdot g \cdot \Delta H} \tag{H.10}$$

In which:

ΔH [m] Water level difference

The water depth at the Gulf of Mexico is 7.4 m, and Galveston Bay is 1.4 m. Resulting in a flow velocity of 10.8 m/s, when one shade curtain is not descending. The bottom surface is sand, corresponding with a critical velocity of 2.2 m/s. The estimated D_{50} is 2.0 mm and shield parameter is 0.55. Resulting in a maximum scour depth of 6.3 m.

I

Shade Curtain Barrier Laboratory Experiments

This appendix describes the laboratory experiments of the shade curtain barrier. Section I.1 describes the purpose of the experiments. Section I.2 provides general information regarding the experiments. Section I.3 describes the experiment on the shade curtain barrier sinker design. Section I.4 describes the experiment on the shade curtain barrier floater design. Section I.5 describes the experiments on the shade curtain barrier optimized design on a glass bottom. Section I.6 describes the experiments on the shade curtain barrier optimized design on a sandy bottom. Section I.7 contains the conclusion of the experiments. Section I.8 provides suggestions for future shade curtain barrier experiments.

I.1 Purpose of Experiments

The purpose of these experiments was to test the hypothesis that the shade curtain barrier could function as a storm surge barrier. The definition of a storm surge barrier is: *'a partly moveable barrier in an estuary or river branch that can be closed temporarily. Its main function during surges is to reduce or prevent the rise of inner water level and thereby sufficiently protect the hinter lying area against inundation.'*, explained in Appendix C. The first part of the definition, *'a partly moveable barrier in an estuary or river branch which can be closed temporarily'*, is already proven by the design being rolled down at the start of the experiment. The second part of the definition, *'its main function during surges is to reduce or prevent the rise of inner water level'*, was to be tested. The third part of the definition, *'thereby sufficiently protect the hinter lying area against inundation'*, does not need to be proven as it has already been stated by the research of Texas A&M that closing (or partially closing through a moveable barrier) will work protectively against flood-damage for the hinterland. The experiments should thus reveal where the shade curtain barrier design is effective in preventing water flow. As well as the qualitative analyses of the performance and water relevancy capacity of the system.

I.2 Experiment General Information

The laboratory experiments were carried out in the water flume at Delft University of Technology's water lab. The cross-sectional dimensions of the water flume are 40 cm in width and 44 cm in height. The flexible membrane fabric used during these experiments is tarpaulin, which is waterproof and weighs 100 gr/m^2.

Item	**Weight** [gram]
Small sinker	627.6
Large sinker	1877.2
Floater (wood)	224.6
Steel plate	2295
Steel block	9084.8

Table I.1: Weight of items during experiment

I.3 Experiments of the Shade Curtain Barrier Sinker

The laboratory experiments for the sinker design were performed on a sand bed. Table I.2 shows the parameters of the experiment set-up. Figure I.1 shows the top and side view of the experiment set-up. Figure I.2 depicts time-lapse images of the experiment.

Experiment

When starting the experiment, water flows towards the structure. After one second, water is already flowing underneath the sinker. The scour hole grows larger over time, but the sinker falls into the formed hole. The water flows beneath the structure so quickly that there are no significant water level changes between both sides of the structure. After 23 seconds, the scour becomes so extensive that an actual pipe is formed. By the end of the experiment, 66 seconds later, the scour hole has become much larger and the structure proves unable to retain a water level difference.

	length	
Cable	46 cm	
	large/small	
Sinker type	small	
	yes/no	*height*
Sand bed	yes	8 cm
	length [cm]	*adjustable*
Fabric	53	yes

Table I.2: Test set-up Shade Curtain Barrier Sinker

Side view

Top view

Figure I.1: Experiment set-up Shade Curtain Barrier Sinker

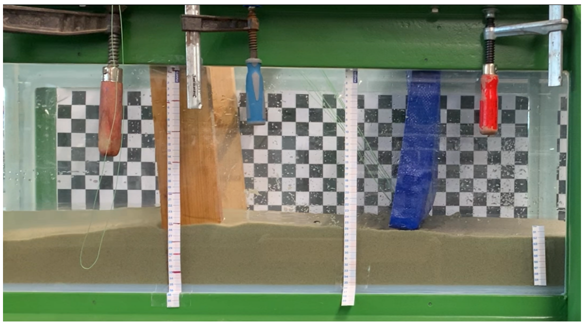

Start of experiment

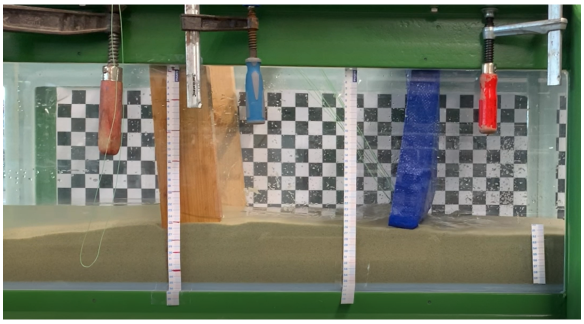

Duration 1 sec

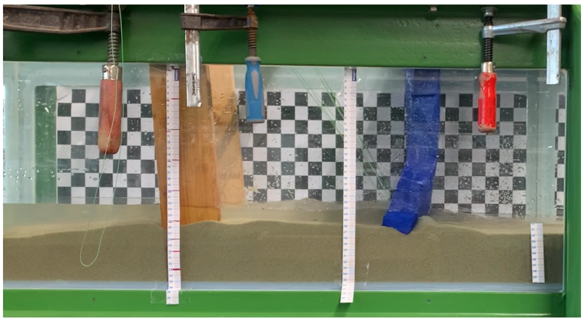

Duration 4 sec

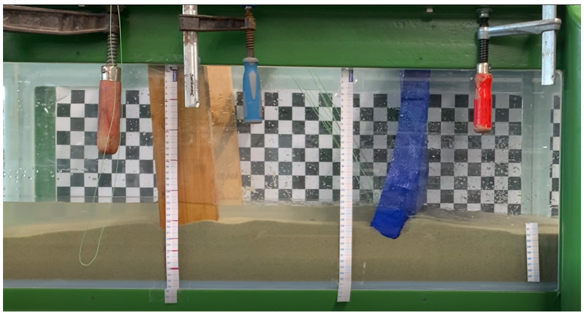

After 8 sec

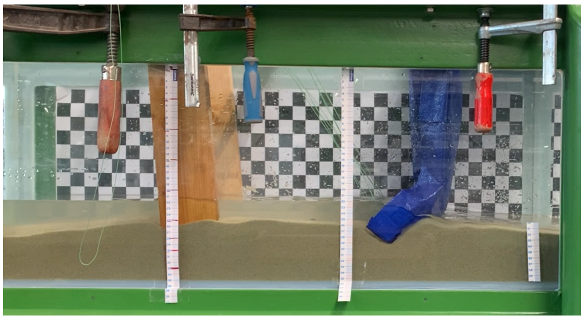

Duration 12 sec

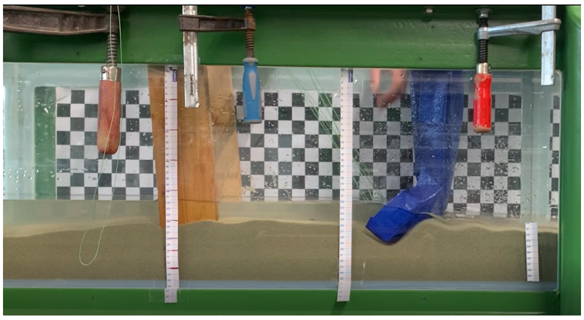

Duration 15 sec

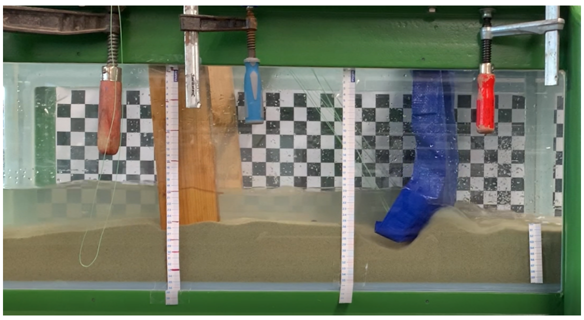

Duration 23 sec

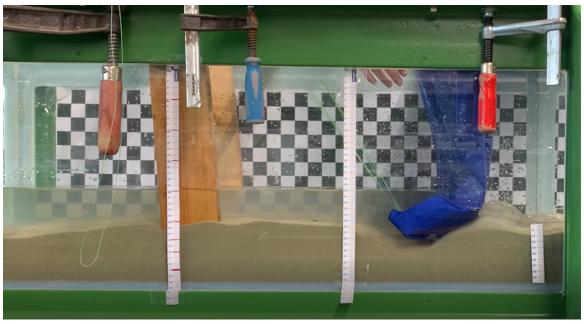

Duration 30 sec

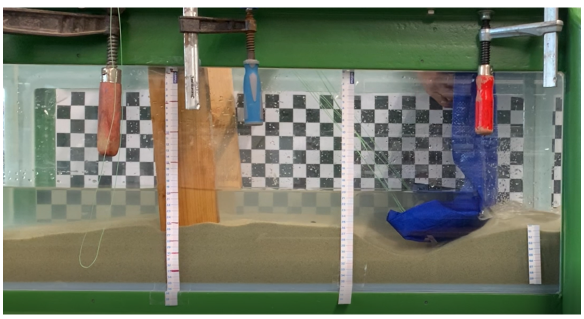

Duration 35 sec

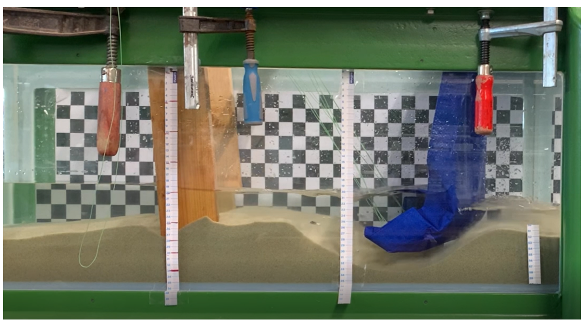

Duration 66 sec

Figure I.2: Experiment Shade Curtain Barrier Sinker Design - Sandy Bottom

Result

The result of this experiment confirmed what the theory had predicted. The design fails due to piping. This experiment proves the hypothesis that the fabric will fall into the created scour hole.

I.4 Experiments of the Shade Curtain Barrier Floater

Experiment

The experiment set-up for the shade curtain barrier floater design was as follows: the cable length is 50 cm and the length of the flexible membrane fabric is 75 cm. The floater is made of wood. Figure I.3 shows depicts images of the experiment under a difference cable angle.

Figure I.3: Experiment Shade Curtain Barrier Floater

Result

The experiment demonstrated the effectiveness of the concept of retaining water with a water bag. The experiment demonstrates that the angle of the cable connecting the bridge and floater determines whether the water bag remains on the bottom. When the water level difference became too large due to the angled cables holding up the floater, the water bag started to float. The gap created beneath the water bag experienced a very large flow velocity. This is an indication that the structure will fail when performed on a sandy bottom instead of a glass bottom as that large flow velocity will lead to high scouring rates beneath the barrier.

I.5 Experiments of the Shade Curtain Barrier - Glass Bottom

Three types of experiments were conducted on a glass bottom with the shade curtain barrier. These three types include a horizontal cable, an angled cable and a cable with a variable angle.

I.5.1 Horizontal Cable

Experiment

This experiment is performed with the small sinker, cable length of 46 cm and a fabric length of 160 cm. As a result of the sluice at the end of the wave flume, the water level behind the shade curtain barrier remains at 1 cm. Figure I.4 illustrates the experiment set-up.

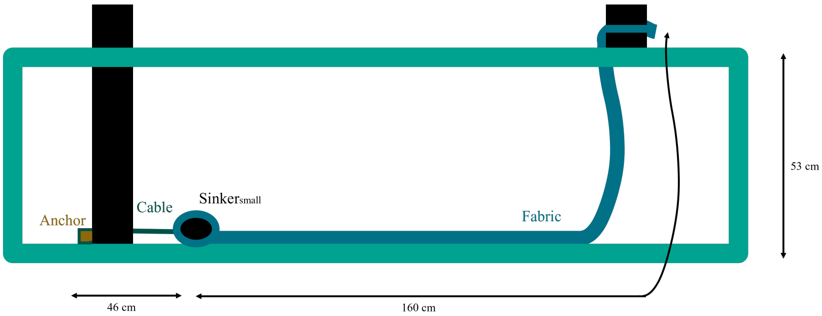

Figure I.4: Experiment Set-Up Shade Curtain Barrier - Horizontal Cables and Glass Bottom

Figure I.5 depicts time-lapse images of the experiment. The description of the different photographs are:

a) The water start flowing. The water depth is 1 cm.
b) The water enters the water bag. The outside water level is 4 cm
c) The fabric is pressed to the glass bottom. The outside water depth is 5 cm
d) The water level is rising. The outside water depth is 7 cm
e) The water level keeps rising and the cable start getting tensioned. The outside water level is 12 cm
f) The water level keeps rising. When curvature is pressed to the glass side, there is no leakage. The outside water level is 15.5 cm
g) The water level keeps rising. The outside water level is 26 cm.
h) The end of experiment. The outside water level is 30 cm.

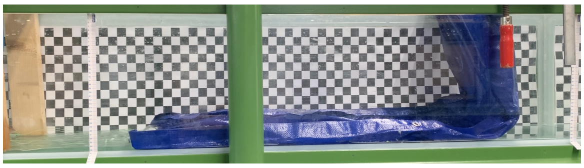

a) Start of the experiment

b) Duration 0.03

c) Duration 0.09

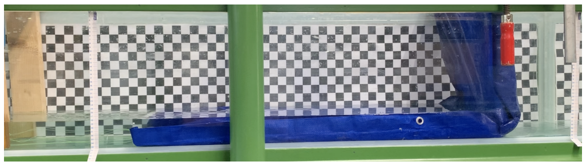

d) Duration 0.17

e) Duration 1.00

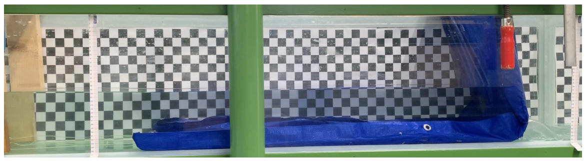

f) Duration 1.14

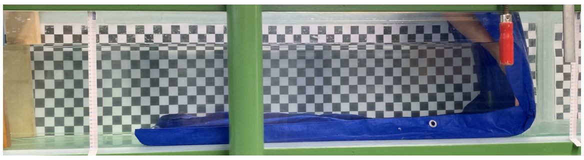

g) Duration 2.29

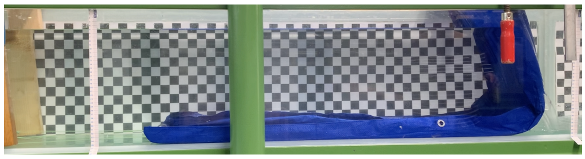

h) Duration 5.11

Figure I.5: Experiment Shade Curtain Barrier Horizontal Cable - Glass Bottom

Result

This experiment indicates that the shade curtain barrier is able to hold a high water level difference. Especially if the sidewalls are waterproofed.

I.5.2 Cable under an Angle - Large Sinker

Experiment

This experiment is performed with the large sinker, fabric length of 150 cm and cable length of 75 cm. the distance between the cable anchor and fabric is 145 cm. As a result of the sluice at the end of the wave flume, the water level behind the shade curtain barrier remains at 2 cm. Figure I.6 illustrates the experiment set-up.

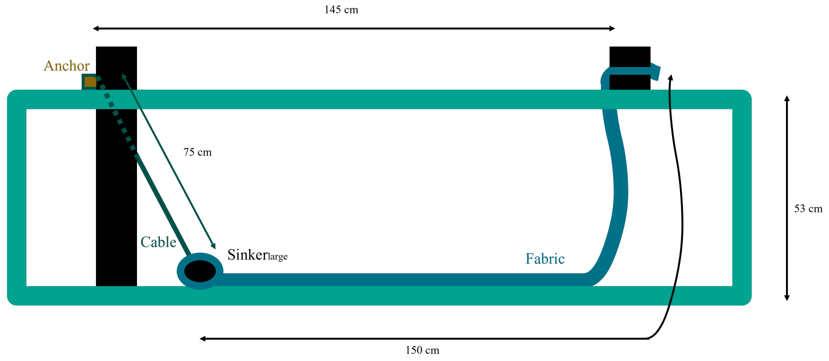

Figure I.6: Experiment Set-Up Shade Curtain Barrier - Cable under an Angle, Large Sinker and Glass Bottom

Figure I.7 depicts time-lapse images of the experiment with the large sinker. The description of the different photographs are:

a) Shade curtain Barrier is rolled out. The outside water level is 6 cm.
b) The water bag start filling.
c) Continuing filling the water bag.
d) Water level difference is generated. The sinker is still on the ground, cable are not tensioned yet. The outside water level is 8 cm.
e) Cables are getting tensioned. The outside water level difference is 9 cm.
f) The cables are tensioned and sinker is still on the ground. The outside water level is 12.5 cm.
g) Cable are still tensioned and sinker starts getting uplifted. The outside water level is 13.5 cm.
h) The sinker is uplifted. The water level is 14.5 cm.
i) The outside water level is 18 cm.
j) The outside water level is 20 cm.
k) End of experiment, the outside water level is 23 cm.

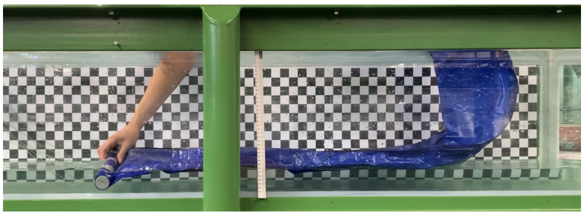

a)

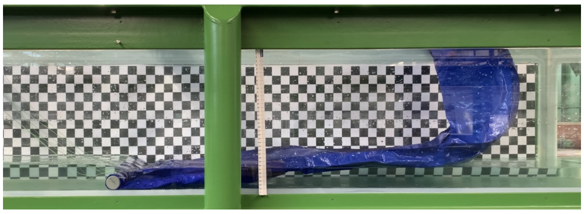

b)

c)

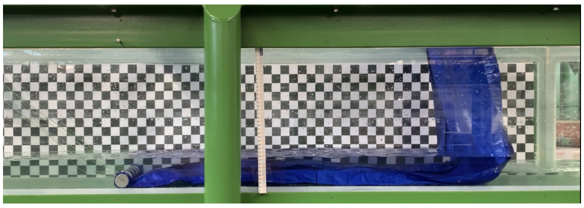

d)

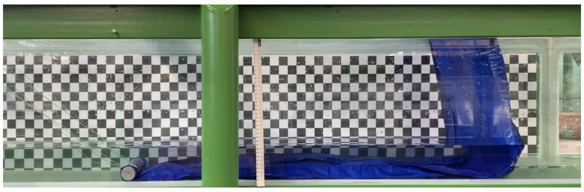

e)

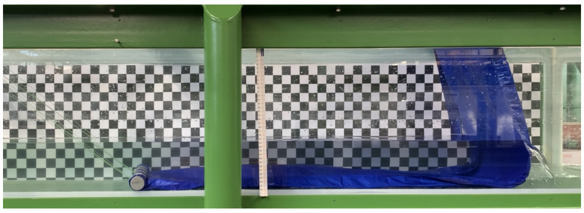

f)

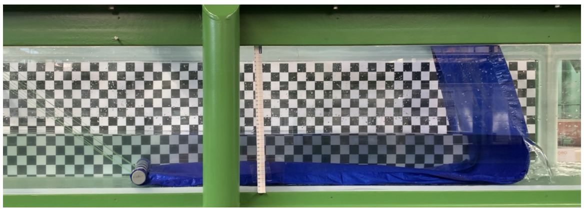

g)

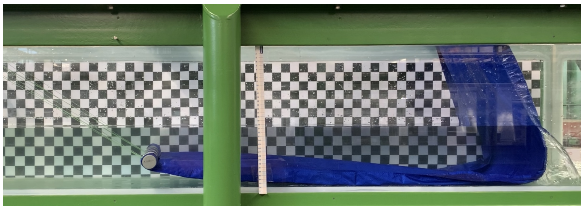

h)

i)

j)

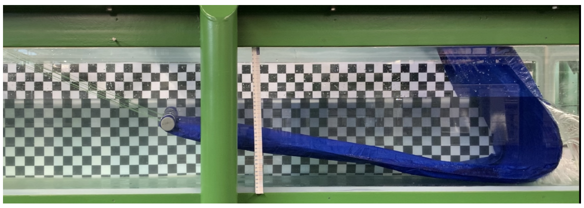

k)

Figure I.7: Experiment Shade Curtain Barrier - Large Sinker

Result

This experiment demonstrated that when using a larger sinker, the sinker can remain on the bottom at a larger cable angle compared to the experiment when using a small sinker.

I.5.3 Different Angle of Cable

Varying the height of the cables' anchors was the third test conducted on the shade curtain barrier. Following an explanation of the underlying theory, experiment results are presented. The theory and experiment results are subsequently compared.

Theory

The equilibrium of the sinker's forces is the theoretical explanation for the sinker's ascent. As a result, three such scenarios are discussed and depicted below.

Scenario 1: Cable horizontal
In this scenario, both the cable and the flexible membrane fabric are horizontal. The force in the cable is equal to the tensile force of the flexible membrane fabric. Figure I.8 depicts this scenario. F_{cable} is the cable force, $T_{flexible\ membrane\ fabric}$ is the tensile force in the fabric, and W_{sinker} is the gravitational force of the sinker. The red arrow indicates the horizontal components of the forces on the sinker.

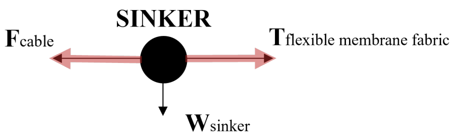

Figure I.8: Scenario 1, Cable horizontal

Scenario 2: Cable under an angle but sinker on the ground
In this scenario, the cable is under an angle and the sinker is positioned on the ground. This occurs until the vertical component of the cable force is less than or equal to the force due to the weight of the sinker. Figure I.9 depicted this scenario. The red arrow indicates the horizontal components of the forces on the sinker. The yellow arrow indicates the vertical components of the forces on the sinker. This scenario is overtaken by scenario 3 when the vertical component of the cable force is greater than the force of the sinker weight.

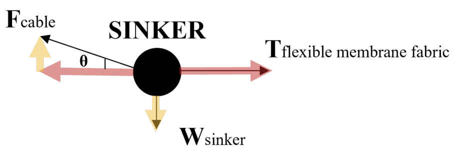

Figure I.9: Scenario 2, Cable under angle and sinker on ground

The theory predicts that the sinker will begin to rise at an angle of 3.4 degrees during the experiment. At this angle the vertical component of the cable force and self weight of the sinker are equal. The single small sinker weighs 627.6 g, but the total weight with the cable attachment is 723.6 g. Consequently, the gravitational force exerted by the sinker, W_{sinker}, is 7.1 N. $T_{flexible\ membrane\ fabric}$ represents the tensile force in the membrane fabric, which is 120 N.

Scenario 3: Cable under angle and sinker moves upwards
In this scenario, the force due to the weight of the sinker is insufficient compared to the vertical component of the cable force. The difference in vertical force is compensated by the angle in the flexible membrane fabric. Figure I.10 shows this scenario. As the angle of the cable increases, the contribution of vertical force of the flexible membrane fabric increases, illustrated in Figure I.11.

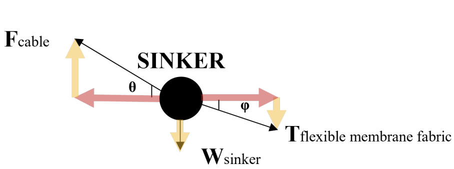

Figure I.10: Scenario 3, Cable under angle and sinker moves upwards

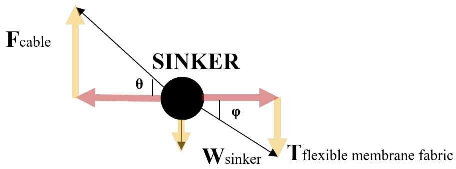

Figure I.11: Scenario 3, Cable under angle and sinker moves upwards, angle increases

Scenario 4: Cable horizontal - Taken sinker diameter into account
In this scenario, both the cable and the flexible membrane fabric are horizontal, and the sinker diameter is taken into account. The sinker diameter creates a difference in the water pressure. The difference between the up and downwards water pressure, must be equal to the sinker weight. Figure I.12 depicts this scenario. The scenario is not further elaborated upon.

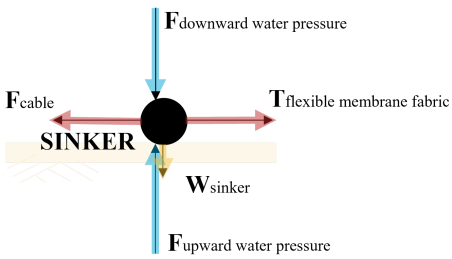

Figure I.12: Scenario 4, Cable horizontal - taken sinker diameter into account

Experiment

In this experiment, the cable anchor height is varied. The total length of the flexible membrane fabric is 160 cm. As a result of the sluice at the end of the wave flume, the water level behind the shade curtain barrier remains at 1 cm. The experiment set-up is listed in Table I.3and illustrates in Figure I.13. Note that the water level decreased over time as a result of fabric leaks on the sidewalls. This causes a change in the hydraulic load on the fabric.

	height above bottom [cm]	*length [cm]*
Cable	varies	46
	large/small	
Sinker type	small	
	yes/no	*height [cm]*
Sand bed	no	-
	length [cm]	*adjustable*
Fabric	160	no

Table I.3: Experiment set-up Shade Curtain Barrier, cable under different angles

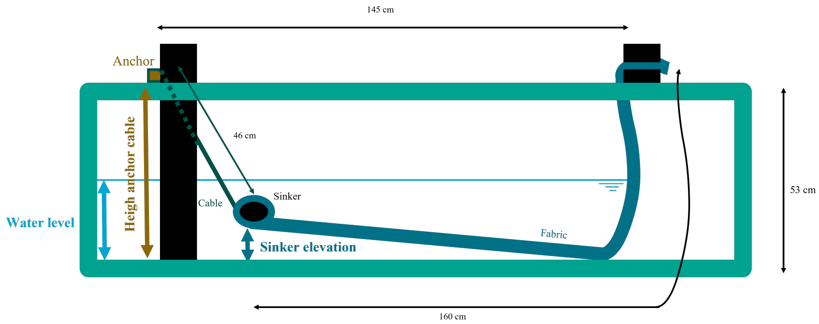

Figure I.13: Experiment Set-Up Shade Curtain Barrier - Cable under a different Angle

Figure I.14 shows the forces working on the shade curtain barrier test fabric. The F_{water} is the hydrostatic water force. This is distributed in the vertical component in geometric ratio, illustrated in the figure with smaller blue arrows. Table I.4 gives the data from the experiment, and illustrated in Figure I.3. Figure I.15 depicts time-lapse images of the experiment with the anchor of the cable at different height above the bottom.

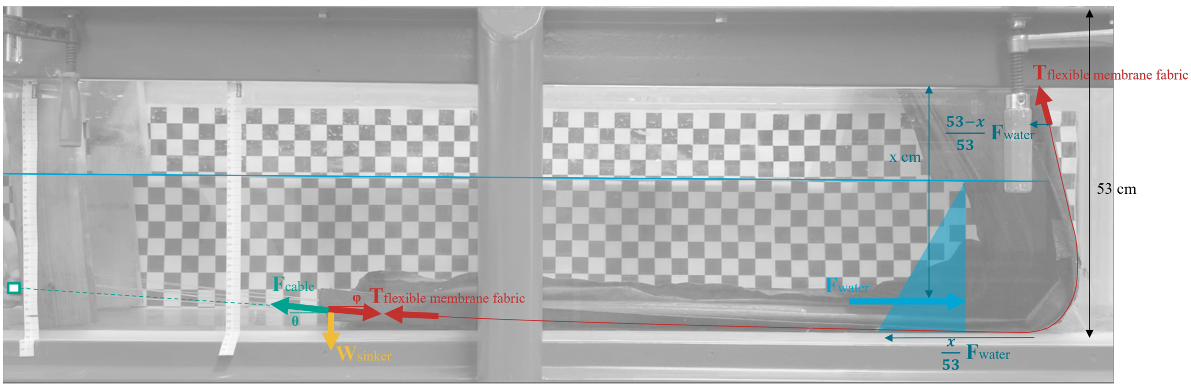

Figure I.14: Forces working on the test

Height anchor cable *from the bottom [cm]*	**Sinker elevation** *from the bottom [cm]*	**Water level** *from the bottom [cm]*	**Angle cable** *θ [degree]*	**Hydrostatic Force** *[N]*	**Tensile force** *[N]*
0	0	16.6	0	130.3	117.0
5	0	16.8	3.7	138.4	123.8
10	1.1	16	8.6	125.6	112.9
15	6.4	21	8.2	216.3	187.7
20	10.3	20	9.6	196.2	171.5
25	12	15	13.8	110.4	100.0
25	13.5	19	11.9	177.1	155.9
30	14.3	14.5	17.3	103.1	93.72
30	16.8	18	14.1	158.9	140.9
35	17.3	13.5	19.9	89.39	81.8

Table I.4: Data experiment set-up Shade Curtain Barrier, cable under different angles

On the bottom cable anchor

Cable anchor 5 cm above the bottom

Cable anchor 10 cm above the bottom

Cable anchor 15 cm above the bottom

Cable anchor 20 cm above the bottom

Cable anchor 25 cm above the bottom

Cable anchor 30 cm above the bottom

Cable anchor 35 cm above the bottom

Figure I.15: Experiment cable under different angle, top of cable anchor above the bottom surface

Result

According to the hypothesis, the sinker begins to rise at an angle of 3.4 degrees; nevertheless, the experiment revealed that the angle was 3.7 degrees when the sinker started to rise. From this, it may be concluded that both theory and experiment demonstrated the same outcome, concluding the simplified model can predict the required sinker uplift. Note that the experiment is not conducted in a very precise manner. Additionally, there is friction force between the flexible membrane fabric and the bottom. This friction has a positive influence on the required force of the sinker. However, in scenario 4, different water pressure due to the diameter of the sinker, is not taken into account.

I.6 Experiments of the Shade Curtain Barrier - Sandy Bottom

These experiments were conducted on a sandy bottom. The sand bed height was 5 cm on average. There were three distinct types of tests conducted on a sand bed: no waterproofed sides, partially waterproofed sides, and totally waterproofed sides. All variations are detailed beneath.

I.6.1 Experiment Set-Up

The experiment set-up was kept the same for the three different experiments. The total length of the flexible membrane fabric is 160 cm. The cable is horizontal and the length is 46 cm. The small sinker is used. The experiment set-up is illustrated in Figure I.16.

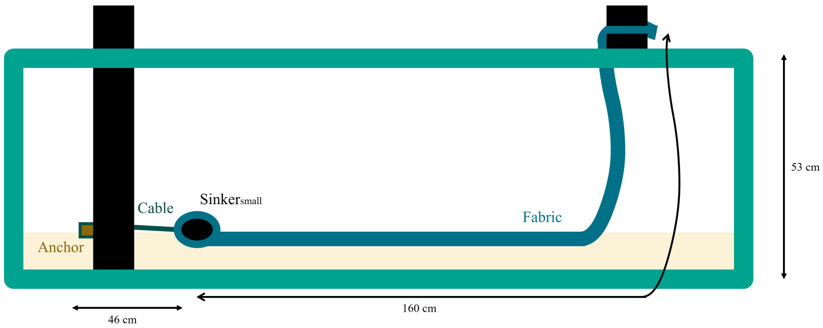

Figure I.16: Experiment Set-Up Shade Curtain Barrier - Sandy Bottom

I.6.2 Experiment no waterproofed sides

The experiment on the sandy bottom without any waterproofed sides indicated that there was scour and piping immediately. However, this was due to the major leakage of the prototype. Therefore, it is not possible to draw any conclusions about the performance of the structure.

I.6.3 Experiment partially waterproofed sides

During this experiment, the sidewall between the glass and fabric was fully waterproofed by using duct tape, only on the vertical sides. Figure I.17 depicts time-lapse images of the experiment. The description of the different photographs are:

a) Before the experiment starts.
b) The experiment start, water start flowing.
c) The water bag start filling up with water.
d) The water level starts rising.
e) The water level keeps rising and scour at the sides starts.
f) The water level keeps rising and scour at the sides growing.
g) Scour at the sides continuing and fabric fills the scour holes.
h) Scour at sides increasing.
i) Scour at sides increasing, glass bottom reached.
j) Scour at sides increasing, glass bottom nearly fully reached on non-waterproofed sides.
k) Scour at sides increasing, glass bottom fully reached on non-waterproofed sides.
l) End of the experiment.

Figure I.18 shows the top view of the shade curtain barrier after the experiment. The image on the left was captured when water was still present on the flexible membrane fabric, at the end of the experiment. It is clear from this image that neither piping nor scouring has occurred in the center of the width of the structure. The image on the right depicts the sand beneath the non-waterproofed sides. This shows that there is still sand in the middle of the width. Most erosion occurred at the edge of the sides' waterproofing.

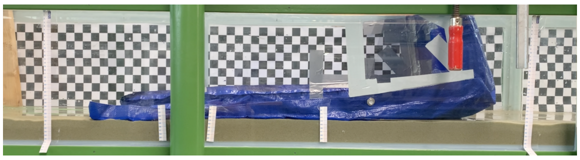

a) Before the experiment

b) Start of experiment

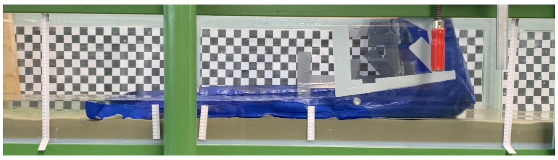

c) Duration 0.06 min

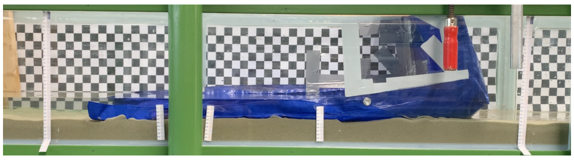

d) Duration 0.18 min

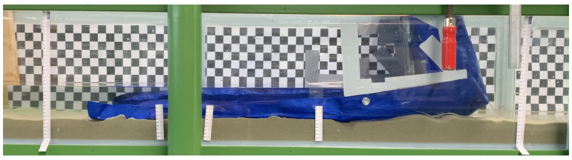

e) Duration 0.30 min

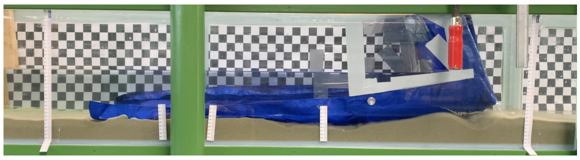

f) Duration 1.00 min

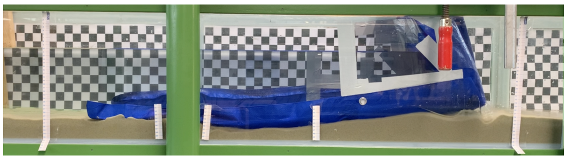

g) Duration 1.51 min

h) Duration 2.41 min

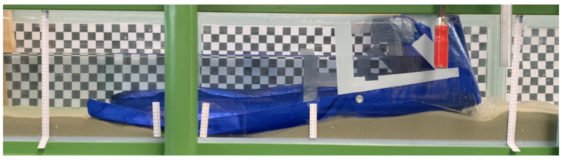

i) Duration 4.07 min

j) Duration 6.20 min

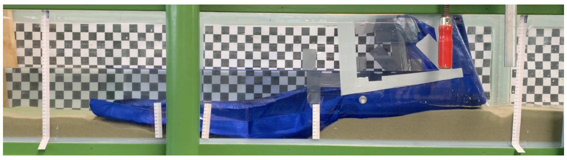

k) Duration 9.39 min

l) Duration 14.02 min

Figure I.17: Experiment Shade Curtain Barrier - Sandy Bottom, side half waterproofed

Fabric shape

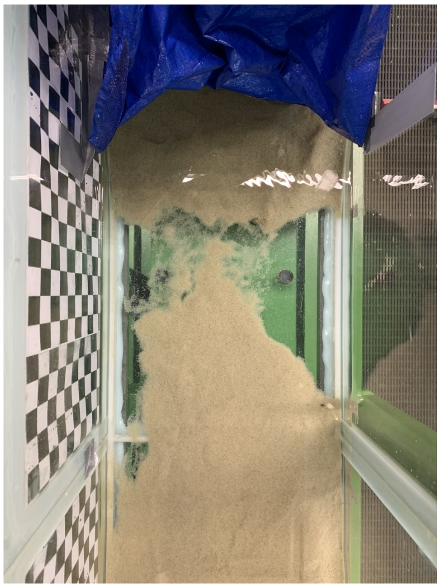

Sand under the fabric

Figure I.18: Top view after the experiment

Result

The result of this experiment is that in the location where the waterproofed sides began, the scour is largest and moves slowly to other parts of the construction. Figure I.17 shows photographs of the experiment. Figure I.18 shows the top view of the shade curtain barrier after the experiment. From these figures can be concluded that the experiment's photograph can give a distorted image. As the photograph shows very large scour holes at the end of the experiment, and the top view image shows that this is only on the sides of the structure. At this location, the sides are not waterproofed, resulting in water flowing between the fabric and glass.

I.6.4 Experiment fully waterproofed sides

During this experiment, the sidewall between the glass and fabric was fully waterproofed by using duct tape. Both on the vertical and horizontal sides. Figure I.19 depicts time-lapse images of the experiment. The description of the different images are:

a) The experiment starts, this is the situation before the water starts to rise.
b) The water is starting to rise
c) The water flowing inside the water bag
d) Water creating downwards pressure, resulting in a sealed closure between the fabric and ground
e) The water level keeps rising
f) Water level keep rising steady
g) Water level keeps rising, sinker is pushed into the ground
h) Water starts leaking at the
i) Start of failing, piping on the sides begins to start
j) Pipping occurs at the sides
k) Large scour hole developing behind the barrier due to leakage of the curved
l) Water starts flowing under the sinker. Note that this is because the sinker was taped at the top, and therefore was not able to move downwards.

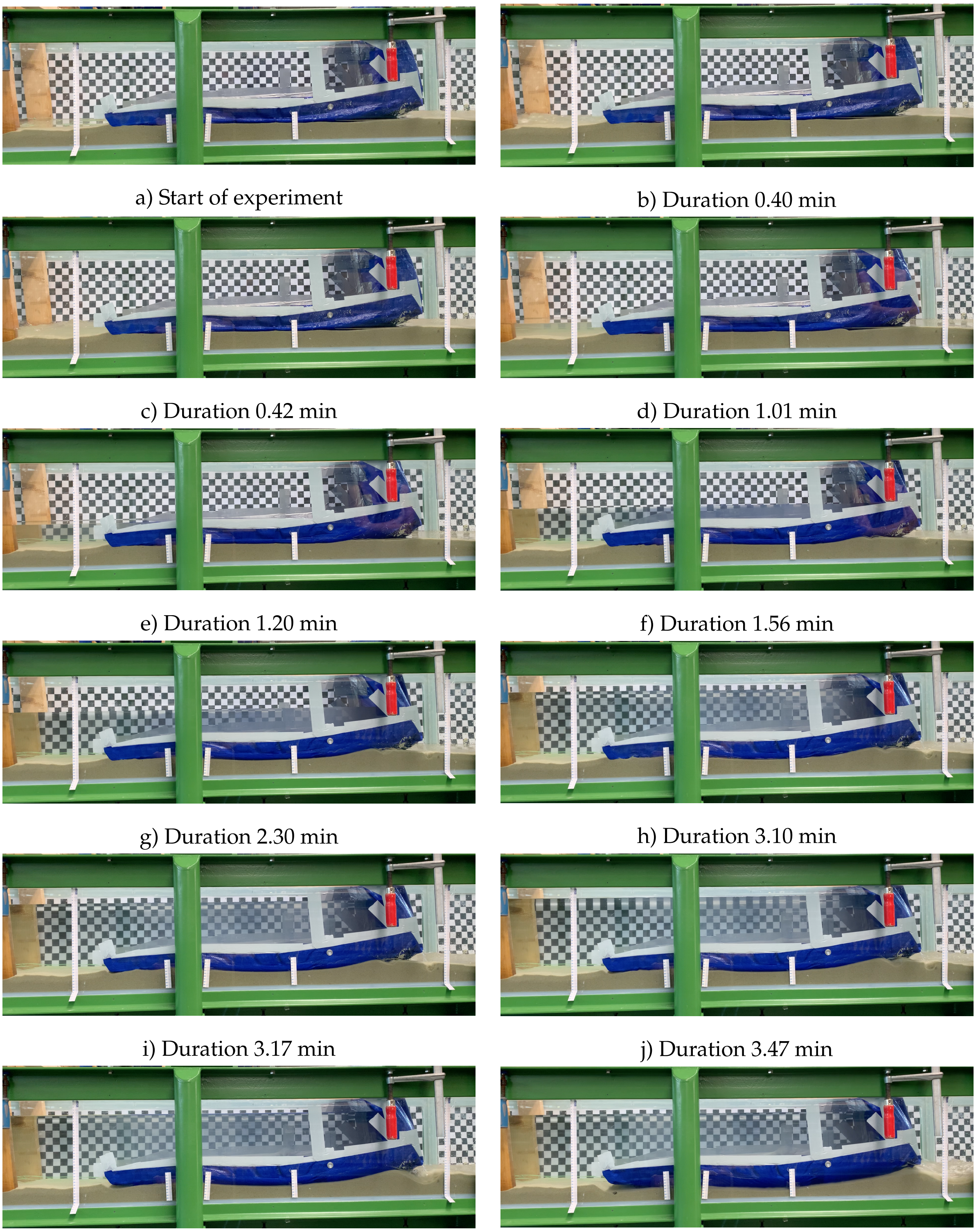

a) Start of experiment

b) Duration 0.40 min

c) Duration 0.42 min

d) Duration 1.01 min

e) Duration 1.20 min

f) Duration 1.56 min

g) Duration 2.30 min

h) Duration 3.10 min

i) Duration 3.17 min

j) Duration 3.47 min

k) Duration 4.20 min

l) Duration 4.42 min

Figure I.19: Experiment Shade Curtain Barrier - Sandy Bottom, side fully waterproofed

Result

The experiment reveals that there is an indication of piping at the ending of the experiment. As time passed during the experiment, the scour caused the fabric to descend gradually. The snapshots a and l from Figure I.19 are superimposed in Figure I.20. The red circle indicates the location of the scour, which was caused by water flowing between the glass and the fabric.

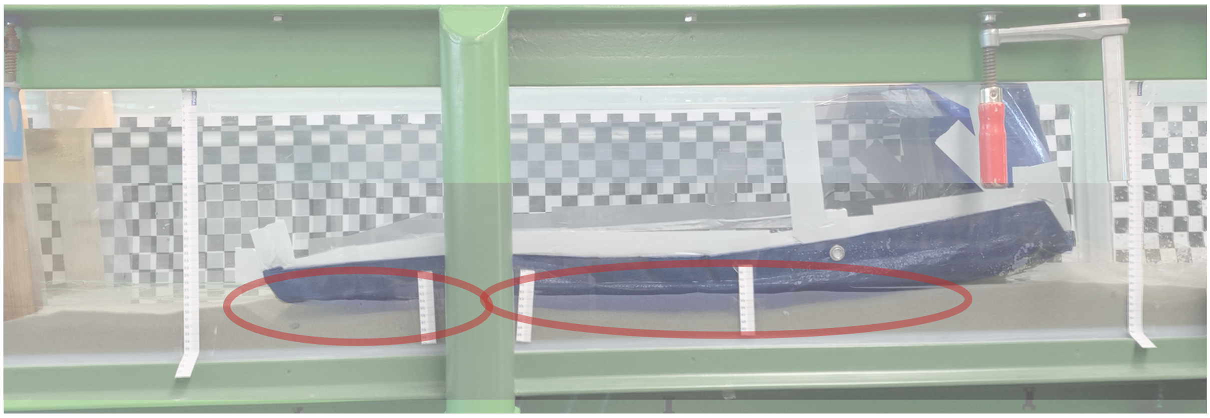

Figure I.20: Locations of scour after experiment

Note that the experiment's photographs can give a distorted image. This is due to the small gap between the glass wall and the fabric. Due to the water's slight flow here. When viewed from the top, it could be seen that in the middle, no sediments had moved.

I.6.5 Result

The laboratory experiments of the shade curtain barrier were preformed on a glass and sandy bottom. The glass bottom experiments concluded that a horizontal cable is most favorable. This is inline with the expectations resulting from theory. The sandy bottom experiment concluded that the connection between the flexible membrane fabric and bridge piles is important to create as waterproof as possible. When the sides were waterproofed, the structure had much more resilience to piping and scour. Additionally, there must be enough flexibility/additional length of the flexible membrane fabric to fill the scour hole.

I.7 Conclusion Experiments

The laboratory experiments of the shade curtain barrier sinker and floater design showed that several parts needed some adjustments in the design. The optimized design was a good combination of these two designs. Regarding the optimized design, the experiment reveals three key points. These are the three items:

- *Water-retaining construction.* The experiment demonstrates that the shade curtain barrier can retain water since it creates a water level difference.
- *Uplift sinker.* The experiments demonstrated that as the cable angle increases above a curtain point, the sinker begins to rise. This indicates that it is crucial to keep the cables horizontal in order to prevent the sinker from rising.
- *Piping/erosion.* The experiments on sandy bottom revealed that piping and erosion pose a significant risk. This risk can be reduced through a relatively waterproof connection between the flexible membrane fabric and the sides. The flexible membrane fabric must be flexible enough to fall into

the scour hole. As well as a slight cable angle to prevent cable entanglement when scour occurs near the sinker.

Concluding, the experiments on the various designs of the shade curtain barrier indicate that it could be used as a storm surge barrier. A storm surge barrier is *a partly moveable barrier in an estuary or river branch which can be closed temporarily. Its main function during surges is to reduce or prevent the rise of inner water level and thereby sufficiently protect the hinter lying area against inundation*, explained in Appendix C. As this design satisfies all these components, the shade curtain barrier may be recognized a storm surge barrier. Consequently, it is a promising complement to conventional storm surge barriers.

I.8 Future Experiments

The result and analyses of these experiments indicate that there are additional experiments needed to analyze the shade curtain barrier in more detail. Extra camera to research the top view in detail and show the scour/piping behavior over the full width of the construction. Experiments to determine the fraction coefficient between sand and flexible membrane fabric to give indication about the force. Experiment in large scale to research if there are effects that were not taken into account yet.

J
Final Design of the Storm Surge Barrier at the San Luis Pass

This appendix describes the final design of the storm surge barrier at the San Luis Pass in detail. This includes the final design, description of phases, and functioning under negative head.

J.1 Final Design

The final design for the storm surge barrier at the San Luis Pass is the shade curtain barrier. This design consists of horizontal cables, additional horizontal length of the flexible membrane fabric on the bottom and added weight. A separate curtain is placed under every segment of the bridge. The dimensions of every segment are an inner width of 18 m and height of 10 m. The flexible membrane fabric has a minimum length of 23 m. The benefits of this design for the San Luis Pass are:

- Lightweight construction compared to conventional storm surge barriers
- No additional influence on the environment
- Protection against 1/100 year storm
- Unique dynamics of the pass remains
- Open view under normal conditions

Figure J.1 illustrates the final design front view of the storm surge barrier at the San Luis Pass under normal conditions. Figure J.2 illustrates the front view under hurricane conditions. Figure J.3 illustrates the final design side view of the storm surge barrier at the San Luis Pass under normal conditions. Figure J.4 illustrates the side view under hurricane conditions.

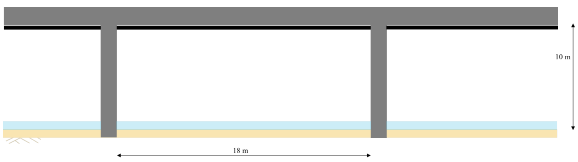

Figure J.1: Final design shade curtain barrier, front view under normal conditions

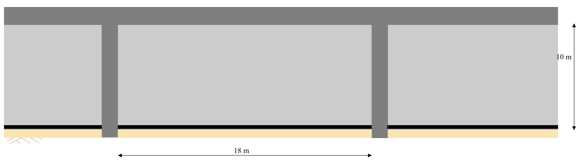

Figure J.2: Final design shade curtain barrier, front view under hurricane conditions

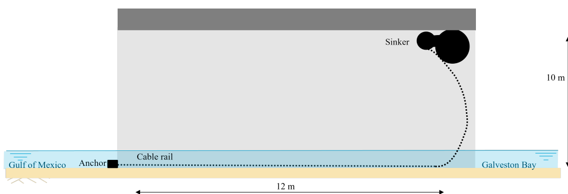

Figure J.3: Final design shade curtain barrier, side view under normal conditions

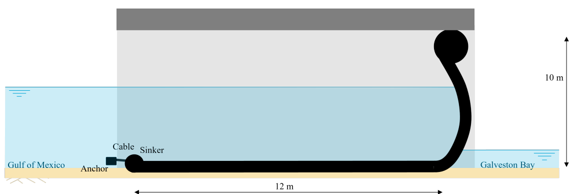

Figure J.4: Final design shade curtain barrier, Side view under hurricane conditions

J.2 Description of Phases

This section describes the phases of the final design for the storm surge barrier at the San Luis Pass. Figure J.5 illustrates the phases of the process of going down. The dashed line in Figure J.5 illustrates the cable rail in the bridge piles. This creates a waterproof connection between the flexible membrane fabric and bridge piles.

Inactive phase barrier
Step 1: The barrier is inactive under normal conditions. The elements are stored under the bridge. This minimizes flow limitation and visual impact.

Rolling down phase barrier
Step 2: The cable is pulled slowly, resulting in the sinker following the cable rail. The rotating axis slowly gives more flexible membrane fabric.
Step 3: The cable is pulled further and similarly the rotating axis provides more flexible membrane fabric.
Step 4: The sinker just touches the bottom surface.
Step 5: The sinker is pulled toward the anchor to gain the required length to prevent piping.
Step 6: Continuing of step 5.
Step 7: Continuing of step 5 and water level start to rise slowly.
Step 8: Sinker in its final position.
Step 9: The water level starts rising.

Retaining phase barrier
Step 10: The retaining phase of the barrier occurs when a hurricane is coming that makes landfall east of the San Luis Pass. The retaining water level height is the bridge height. The flexible membrane fabric retains the water from the bay. The horizontal, long flexible membrane fabric ensures that the structure is water tight. The sinker is kept on the bottom by the weight and horizontally due to the cables and friction of the flexible membrane fabric.

Rolling up phase barrier
The rolling up phase is quite similar to the rolling down phase. The shade curtain is rolling up when the water level is equal again at the Gulf of Mexico and Galveston Bay. In the case the water level is higher at the Galveston Bay side, the water pushes the shade curtain upward and rolling it up is possible. The forces in this scenario are negligible compared to the hurricane scenario.

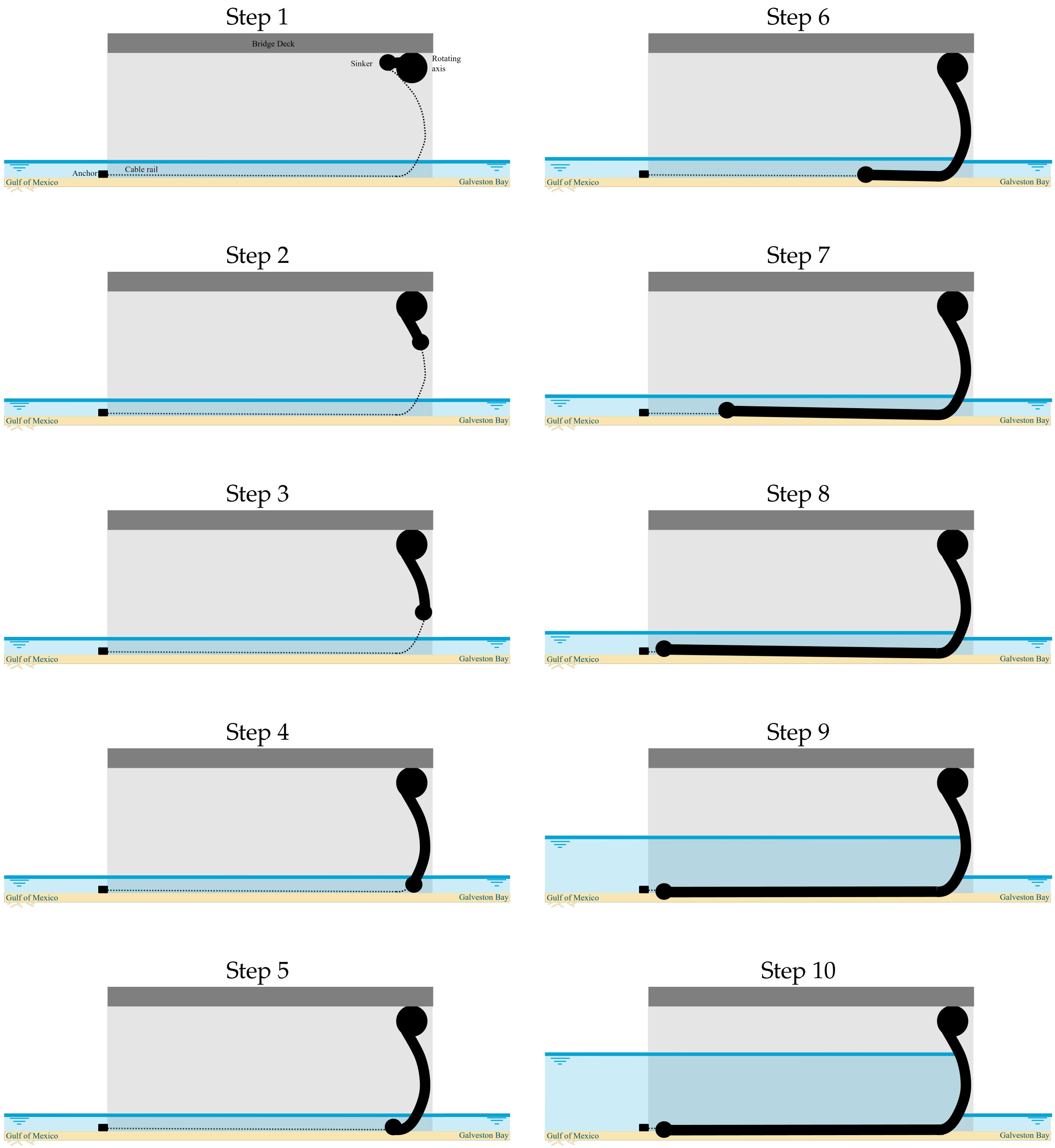

Figure J.5: Phases Final Design at San Luis Pass

J.3 Functioning under Negative Head

This section described the negative head situation for the final design. Negative head is the situation where the governing water level and forces on the barrier are directed from the West/Galveston Bay onto the Gulf of Mexico instead of the other way around, also known as 'back surge' effect from the West/Galveston Bay. Figure J.6 illustrates the negative head scenario.

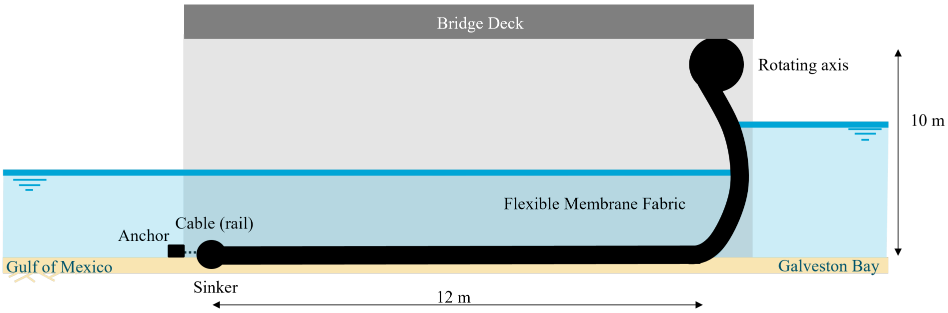

Figure J.6: Negative head on the Shade Curtain Barrier

Figure J.7 illustrates the forces of the negative head scenario. The resulting force is at the Galveston Bay side. In this scenario the cable can be loosened and due to the hydraulic resulting force the flexible membrane fabric will go out of the cable rail. The rotating axis can store the fabric under the bridge. Resulting in the water to be able to flow toward the Gulf of Mexico. Figure J.8 illustrates the curvature of the flexible membrane fabric when there is negative head. The dashed line shows curvature at the piles of the bridge and the back the curvature more in the middle of the segment.

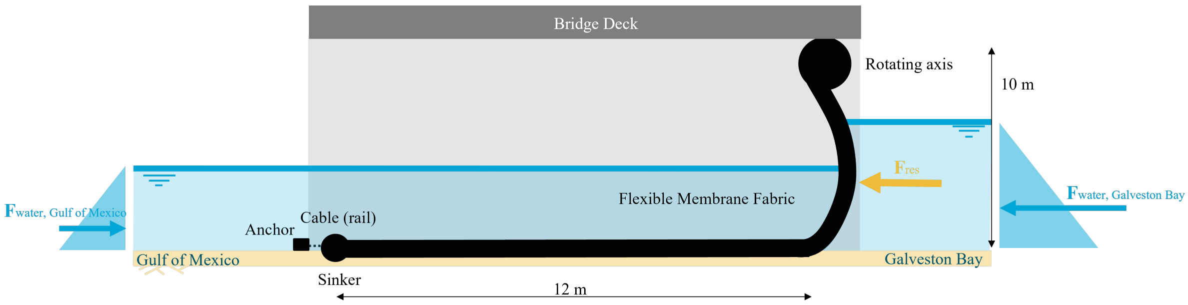

Figure J.7: Forces on the Shade Curtain Barrier in negative head situation

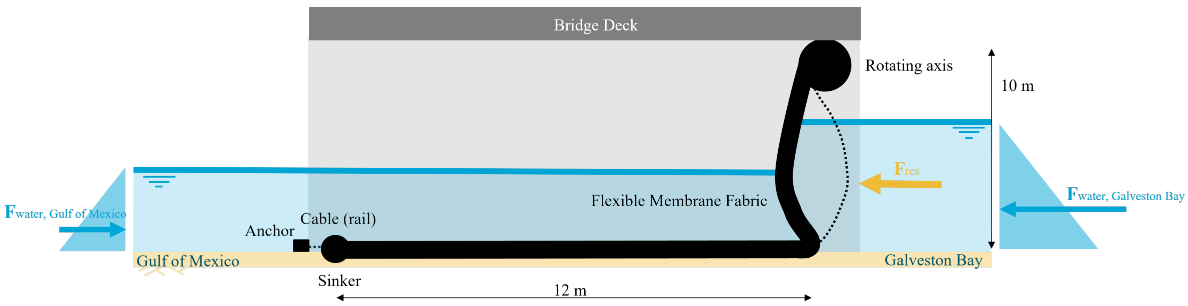

Figure J.8: The Shade Curtain Barrier in negative head situation, flexible membrane fabric